

FACOLTA' DI INGEGNERIA

CORSO DI LAUREA IN CIVIL ENGINEERING

DISTART

*Dipartimento di Ingegneria delle Strutture, dei Trasporti, delle Acque, del Rilevamento e
del Territorio*

TESI DI LAUREA

In

ADVANCED DESIGN OF STRUCTURES I.C.

**STEEL AND MACRO-SYNTHETIC SELF-COMPACTING
FIBRE REINFORCED CONCRETE,
EXPERIMENTAL STUDY ON THE LONG-TERM
DEFORMATIONS**

CANDIDATO:

Andrea Incerti

RELATORE:

Chiar.mo Prof. Ing. Claudio Mazzotti

CORRELATORE:

Prof. Ing. Nicola Buratti

Anno Accademico 2010/2011

Sessione III

“Questo studio sperimentale che sono qui a descrivervi vuole sensibilizzare il patrimonio di tecnici nazionale e non su come il calcestruzzo in Italia sia un materiale da costruzione sempre in costante e continuo sviluppo.

Il suo uso applicativo in innumerevoli campi e settori lo rende da sempre il principale elemento strutturale designato a svolgere funzioni sempre più specifiche a seconda dell'ambiente circostante in cui viene utilizzato.

Nonostante sia uno dei primi materiali adoperato fin dagli antichi, esso è in grado di adattarsi sempre più alle varie caratteristiche richieste, associandogli così una polivalenza quasi assoluta per quanto concerne ai materiali da costruzione classici.

L'utilizzo e l'aggiunta di fibre alla mistura base classica è un campo in cui necessitano molti altri studi, in ragione del quale questa tesi non vuole essere un punto d'arrivo ma bensì un punto di partenza per successive analisi, soprattutto per ciò che riguarda la resistenza a lungo termine, conoscendo infatti i limiti temporali di cui tale materiale è caratterizzato.

Ho quindi analizzato i principali parametri dettati dalla normativa vigente per visualizzare al meglio i vantaggi e gli svantaggi dei calcestruzzi con l'aggiunta di fibre, sia d'acciaio che polimeriche.

È stata poi analizzata e riassunta, nella parte finale della trattazione, la normativa americana riguardante i criteri di progetto dei calcestruzzi fibro rinforzati, in quanto negli Stati Uniti sono molto spesso utilizzati per fini strutturali.

Quest'ultima fase vuole essere uno sprono ed una base per la nostra normativa vigente, che non tiene ancora conto in maniera soddisfacente e dettagliatamente esaustiva di uno degli aspetti strutturali forse più necessari, al giorno d'oggi, dell'uso dei calcestruzzi, e cioè la durabilità di ciò che progettiamo.

Ringrazio quindi il Prof. Ing. Claudio Mazzotti ed l'Ing. Nicola Buratti per avermi consentito di lavorare a questo progetto di ricerca molto interessante ed innovativo, che mi ha reso partecipe di un'analisi evolutiva, e che mi ha dato un'ulteriore stimolo nel comprendere che fare il progettista significa anche e soprattutto saper valutare le sempre differenti condizioni in cui si opera e di conseguenza rapportarsi adoperando scelte ponderate sui materiali da costruzione da utilizzare.

Ringrazio infine la Dott.ssa Ing. Maria Carlotta Biagini, la Dott.ssa Elena Incerti e la futura Dott.ssa Carolina Incerti, oltre alla famiglia e gli amici tutti, per tutto quello che sono stati, sono e saranno sempre per me.”

Andrea Incerti

“No man stands so tall as when he stoops to help a child...”

“Non c’è uomo più alto di colui che si inginocchia per aiutare un bambino”

A. Lincoln

Contents

Contents	7
Figure	13
1. Introduction	19
2. Self-Compacting and Fiber Reinforced Concrete	21
2.1 Fiber Reinforced Concrete, FRC.....	21
2.1.1 Generalities	21
2.1.2 The Materials	22
2.1.3 The Mechanical Behavior.....	24
2.2 Self-Compacting Concrete, SCC.....	26
2.2.1 Generalities	26
2.2.2 Composition of SCC.....	27
2.2.3 Advantages on Disadvantages of SCC	27
3. Overview of the Experimental Test and Material Properties	29
3.1 Introduction	29
3.2 Fibers Types	30
3.2.1 MapeFibre ST42, called “M”	30
3.2.2 Wirand® Fibre FF3, called “S”	31
3.3 Mixture Characteristics	31
3.3.1 Aggregates	31
3.3.2 Water demand of the aggregate	32
3.3.3 Water/Cement Ratio.....	32
3.3.4 Workability, classes and slump test.....	33
3.3.5 Volumetric Mass	35
3.4 Instruments for the Packaging.....	35

3.5	Standard Packaging Operations	35
3.5.1	Particular Operation for SCC.....	36
3.6	Fresh Test Results	39
3.6.1	B Type.....	39
3.6.2	M1 Type.....	39
3.6.3	M2 Type.....	39
3.6.4	S Type	39
4.	Tests Instruments.....	41
4.1	Omega Transducers.....	41
4.1.1	Generalities	41
4.1.2	Calibration Procedure	42
4.2	LVDT Transducers.....	43
4.2.1	Generalities	43
4.2.2	Calibration Procedure	44
4.3	Strain Gauges	45
4.3.1	Generalities	45
4.3.2	Calibration Phase	46
4.3.3	Attaching Phase	46
4.4	Load Cells	52
4.5	Instruments Table.....	53
4.6	Acquisition System	54
4.6.1	SCXI System.....	54
4.6.2	LabView Software	54
4.6.3	Excel File	54
5.	Cracking and Rupture Analysis of Prismatic Samples.....	57
5.1	Generalities.....	57
5.2	Test Principle.....	57
5.3	Test Preparation.....	58
5.4	Hand Calculation.....	59
5.4.1	Maximum Bending Moment.....	59
5.4.2	Tension.....	59
5.4.3	Effective Height	59
5.4.4	Effective Resistance Modulus.....	60

5.5	Tests Results & Diagrams	60
5.6	Fibers Distribution Analysis.....	77
6.	Cracking Analysis of Beam Samples	81
6.1	Generalities.....	81
6.2	Speed Limits.....	82
6.3	Hand Calculation.....	83
6.3.1	Maximum Bending Moment.....	83
6.3.2	Tension.....	83
6.4	Tests Results & Diagrams	83
6.5	Beams VS Prismatic Samples	88
7.	Shrinkage and Creep Analysis of Cylindrical and Beam Samples.....	91
7.1	Generalities.....	91
7.2	Shrinkage Types	92
7.3	Creep	93
7.4	Viscous Deformations Computation	94
7.5	Shrinkage and Creep Tests of Cylindrical Samples	97
7.5.1	Shrinkage Test	97
7.5.2	Creep Test	103
7.6	Viscous Test of Beam Samples	110
7.6.1	Generalities	110
7.6.2	Loading Phase	114
7.6.3	Loading Phase Comparison	119
7.6.4	Absolute Viscous Deformations	121
7.6.5	Relative Viscous Deformations	125
7.6.6	Comparison with Old Test.....	129
8.	Uniaxial Tensile Test.....	133
8.1	Introduction	133
8.2	Samples and Test Device	133
8.3	Test Results	134
9.	Design Analysis.....	137
9.1	Introduction	137
9.1.1	Classical Design Theories.....	137
9.1.2	Finite Element Method	139

9.1.3	Construction Documents.....	139
9.2	Slab-On-Ground Design Criteria	140
9.2.1	Floor Flatness and Levelness Tolerance	140
9.3	Slab Types	140
9.3.1	Basic Design for Slab-On-Ground.....	141
9.3.2	General Comparison of Slab Types	143
9.3.3	Construction Variables.....	144
9.3.4	Conclusion	144
9.4	Loads	145
9.4.1	Introduction.....	145
9.4.2	Load Types.....	146
9.4.3	Environmental Factors	149
9.4.4	Safety Factors.....	150
9.5	Joints.....	152
9.5.1	Generalities	152
9.5.2	Isolation Joints	153
9.5.3	Construction Joints.....	155
9.5.4	Sawcut Contraction Joints.....	157
9.5.5	Load-Transfer Mechanism.....	159
9.6	Design of Unreinforced Concrete Slabs.....	163
9.6.1	Introduction.....	163
9.6.2	Thickness Design Methods	164
9.6.3	Portland Cement Association Design Method.....	167
9.6.4	Wire Reinforcement Institute Design Method.....	168
9.6.5	The COE Design Method.....	169
9.6.6	Shear Transfer at Joints.....	169
9.6.7	Maximum Joint Spacing	170
9.7	FRC Design	170
9.7.1	Steel Fiber Reinforcement	170
9.7.2	Synthetic Fiber Reinforcement	172
9.7.3	Thickness Design Methods	173
9.7.4	Joint Details	176
9.8	Design Example	177

**Steel and Macro-Synthetic Self-Compacting Fiber Reinforced Concrete,
Experimental Study on the Long-Term Deformations**

9.8.1	Introduction.....	177
9.8.2	Assumption and Design Criteria.....	177
9.8.3	Calculations for Concentrated Load	177
9.8.4	Calculations for Post Load.....	179
10.	Final Considerations	181
11.	Reference	183

Figure

Figure 1: Traction diagrams of FRC: low % (0.2-2) of fibers (a) and high % (2-8) of fibers (b);.....	22
Figure 2 Steel Fibers Parameters	23
Figure 3 Polymeric and Carbon Fibers Parameters	24
Figure 4: Differents Traction Behavior.....	25
Figure 5: Overview of experimental study	30
Figure 6: Polymeric fiber Mapei st42	30
Figure 7: Wirend Fibre FF3, Maccaferri.....	31
Figure 8: Abram Cone Test.....	33
Figure 9: Slump Types.....	34
Figure 10: Slump Test Measure	35
Figure 11: Slump Flow Test	36
Figure 12: J Ring Test.....	37
Figure 13: V Funnel Test	38
Figure 14: Omega Transducer Application.....	41
Figure 15: Omega 7 Calibration	42
Figure 16: Ω Constants	42
Figure 17: LVDT Section	43
Figure 18: Electromagnetic circuit of LVDT.....	43
Figure 19: LVDT Application	44
Figure 20: Calibration instrument.....	44
Figure 21: LVDT constants	44
Figure 22: Strain Gauge components.....	45
Figure 23: Strain gauge pack	45
Figure 24: Strain gauges constants	46
Figure 25: X60 and its components	47
Figure 26: Cleaning the surface	47
Figure 27: Drawing the references lines	47
Figure 28: Bonding the strain gauge.....	48
Figure 29: Application of film	48
Figure 30: Removing the film.....	49

Figure 31: Cleaning the boundary.....	49
Figure 32: Repeating the operations for all the samples.....	49
Figure 33: Insert the legs in the base connection.....	50
Figure 34: Weld the connections	50
Figure 35: Connect the cable to the base	51
Figure 36: Attach the cables for all the samples	51
Figure 37: Connect all cables into system	51
Figure 38: Load cell constants	52
Figure 39: Load cell properties	52
Figure 40: Load cell for cracking phase	52
Figure 41: Load cell for viscous test.....	53
Figure 42: Instruments test table.....	53
Figure 43: Software interface.....	54
Figure 44: Rupture scheme test.....	57
Figure 45: Wet sawing	58
Figure 46: Test preparing.....	58
Figure 47: Cut measuring.....	59
Figure 48: Excel cracking computations file	60
Figure 49: Force-CMOD for M1	61
Figure 50: Force-CTOD for M1	61
Figure 51: Tension-CMOD for M1.....	62
Figure 52: Tension CTOD for M1	62
Figure 53: Force-CMOD for M2	63
Figure 54: Force-CTOD for M2	63
Figure 55: Tension-CMOD for M2.....	64
Figure 56: Tension-CTOD for M2.....	64
Figure 57: Force-CMOD for S.....	65
Figure 58: Force-CTOD for S.....	65
Figure 59: Tension-CMOD for S	66
Figure 60: Tension-CTOD for S	66
Figure 61: Force-CMOD for all samples	67
Figure 62: Force-CTOD for all samples	67
Figure 63: Tension-CMOD for all samples	68
Figure 64: Tension-CTOD for all samples	68
Figure 65: Fibers counting table	77
Figure 66: Influence of the number of fibers in M1/M2.....	77
Figure 67: influence of the total number of fiber in M1	78
Figure 68: Influence of the total number of fiber in M2.....	78
Figure 69: Influence of fiber in middle zone of M1	79
Figure 70: Influence of fiber in middle zone of M2	79
Figure 71: Influence of the total number of fiber in S	80
Figure 72: Influence of fiber in middle zone of S.....	80
Figure 73: Cutting operation.....	81

Figure 74: Static scheme for beam analysis.....	82
Figure 75: Beam cracking test	82
Figure 76: excel file	83
Figure 77: Force-CMOD for B beam.....	84
Figure 78: Tension-CMOD for B beam.....	84
Figure 79: Force-CMOD for M1 beam.....	85
Figure 80: Tension-CMOD for M1 beam.....	85
Figure 81: Force-CMOD for M2 beam.....	86
Figure 82: Tension-CMOD for M2 beam.....	86
Figure 83: Force-CMOD for all beams.....	87
Figure 84: Tension-CMOD for all beams.....	87
Figure 85: Tension-CMOD for M1 beams and prismatic samples.....	88
Figure 86: Tension-CMOD for M2 beams and prismatic samples.....	88
Figure 87: Different deformation components	91
Figure 88: Contraction of shrinkage, creep, elastic phase and total.	94
Figure 89: Creep function behavior with different time loading	96
Figure 90: Cylindrical samples	97
Figure 91: Shrinkage test preparation	98
Figure 92: Shrinkage test of cylindrical samples	98
Figure 93: Mixture B and sample 100 mm of diameter.....	99
Figure 94: Mixture B and sample 150 mm of diameter.....	99
Figure 95: Mixture M1 and sample 100 mm of diameter.....	100
Figure 96: Mixture M1 and sample 150 mm of diameter.....	100
Figure 97: Mixture M2 and sample 100 mm of diameter.....	101
Figure 98: Mixture M2 and sample 150 mm of diameter.....	101
Figure 99: Mixture S and sample 150 mm of diameter	102
Figure 100: Generical shrinkage comparison	102
Figure 101: Creep test of cylindrical samples.....	103
Figure 102: Acquisition data system.....	104
Figure 103: Mean cubic compression resistance	104
Figure 104: Creep test comparison for cylindrical samples.....	105
Figure 105: relative creep test comparison for cylindrical samples	105
Figure 106: Creep test for samples B.....	106
Figure 107: relative creep test for samples B.....	106
Figure 108: Creep test for samples M1	107
Figure 109: Relative creep test for samples M1	107
Figure 110: Creep test for samples M2.....	108
Figure 111: Relative creep test for samples M2	108
Figure 112: Creep test for sample S.....	109
Figure 113: Relative creep test for sample S	109
Figure 114: Beam test	110
Figure 115: Beam test plan	110
Figure 116: Lateral view of beam test	111

Figure 117: Static scheme	112
Figure 118: Instruments for viscous beam testing	112
Figure 119: Viscous beam test	113
Figure 120: Beam characteristics	113
Figure 121: Critical load	114
Figure 122: Critical loads for beam test.....	114
Figure 123: Beam loads	115
Figure 124: Loading phase examples	115
Figure 125: CMOD B during loading phase.....	116
Figure 126: CMOD M1 during loading phase.....	116
Figure 127: CMOD M2 during loading phase.....	117
Figure 128: LVDT B during loading phase	117
Figure 129: LVDT M1 during loading phase	118
Figure 130: LVDT M2 during loading phase	118
Figure 131: LVDT-Force comparison during loading phase.....	119
Figure 132: CMOD-Force comparison during loading phase	120
Figure 133: Loading comparison among viscous and cracking test.....	120
Figure 134: Absolute CMOD and Mid-Span Deflection variation of B.....	121
Figure 135: Absolute CMOD and Mid-Span Deflection variation of M1.....	122
Figure 136: Absolute CMOD and Mid-Span Deflection variation of M2.....	123
Figure 137: Absolute CMOD comparison.....	124
Figure 138: Absolute Mid-Span Deflection comparison.....	124
Figure 139: Relative CMOD and Mid-Span Deflection variation of B.....	125
Figure 140: Relative CMOD and Mid-Span Deflection variation of M1	126
Figure 141: Relative CMOD and Mid-Span Deflection variation of M2.....	127
Figure 142: Relative CMOD comparison	128
Figure 143: Relative Mid-Span Deflection comparison	128
Figure 144: Old test samples comparison.....	129
Figure 145: CMOD compared with old tests	129
Figure 146: Mid-Span Deflection compared with old tests.....	130
Figure 147: Relative CMOD compared with old tests.....	130
Figure 148: Relative Mid-Span Deflection compared with old tests.....	131
Figure 149: Traction test samples	133
Figure 150: Traction test	134
Figure 151: Traction test results	135
Figure 152: Traction test failure	135
Figure 153: Traction crack failure.	136
Figure 154: Example of Designed Traffic Value.....	140
Figure 155: Table of Slab Types Comparison	144
Figure 156: Controlling Design Consideration for Various Types of Slab-On-Ground (1 in. ² = 645.2 mm ² ; 1 ft ² = 0.0929 m ²)	145
Figure 157: Joint distance in function of thickness	149
Figure 158: Load type safety factor	151

Figure 159: Stress ratio versus allowable repetitions	151
Figure 160: Appropriate locations for joints.....	152
Figure 161: Isolation joint details	155
Figure 162: Typical doweled joints	156
Figure 163: Joint details at loading dock	158
Figure 164: Sawcut contraction joint.....	159
Figure 165: Typical doweled joint.....	159
Figure 166: Indicating and movements for doweled construction joint	160
Figure 167: Dowel basket	161
Figure 168: Dowel size and spacing	162
Figure 169: Corner load	165
Figure 170: Comparative design table	174

1. Introduction

This study wants to analyze the behavior of the self-compacting fibre reinforced concrete made with different types of mixture of water, gravel, cement and fibers called B, S, M1, and M2.

In particular, I have analyzed three samples of an idealized beam $0.3 \times 0.12 \times 2.00$ m, which represent an hypothetical ground slab, eight prismatic samplers $0.15 \times 0.15 \times 0.6$ m and fourteen cylindrical samplers $h = 0.2-0.3$ m and $\varnothing = 0.1-0.15$ m.

In general, all the samplers are made and prepared with a different mixture of gravel, water, cement and fibers. The testing phase is carried out in a controlled climatic area both relative humidity 60%, and temperature 20°C are maintained constants.

Therefore, I analyzed the principal and most important effects of creep, shrinkage, flexural deflection and crack-opening displacement comparing, in function of the different mixture, the results.

The study is subdivided in:

- Self-Compacting and Fibro Reinforced Concrete;
- Overview of Experimental Test and Material Properties;
- Tests Instruments;
- Cracking and Rupture Analysis of Prismatic Samples;
- Cracking Analysis of Beam Samples;
- Shrinkage and Creep Test of Cylindrical Samples;

- Traction Analysis;
- Design Analysis;
- Final Considerations;

2. Self-Compacting and Fiber Reinforced Concrete

2.1 Fiber Reinforced Concrete, FRC

2.1.1 Generalities

The fiber reinforced concrete is a type of concrete mixture blended with a quantitative of fibers. The fibers are made with steel, polymers, inorganic materials like carbon or glass, organic materials such as wood.

Therefore, is possible to insert a steel armor, post or pre stressed.

Adding the fibers, the concrete can resist until a certain level of traction stresses, while you know that the traction resistance of normal concrete is about zero, depending on the percentage fibers, as well as mechanical and geometrical characteristics, the matrix of the concrete, the adherence among the fibers and the matrix.

Until the first cracking phase, the matrix of the concrete reacts with the initial properties, but from this level to the end of element life, the resistance will decrease quickly and at this point the fibers are very important, because when going into action, they can help to resist the structural element.

The relation that improves this behavior is:

$$V_f = \frac{\text{fiber's volume}}{\text{sampler's volume}}$$

All in all the concepts of FRC properties, you note that the fibers improve the post-crack behavior of the concrete:

- Prevent the propagation of the crack;
- Increasing the fracture energy;
- Increasing the ductility;

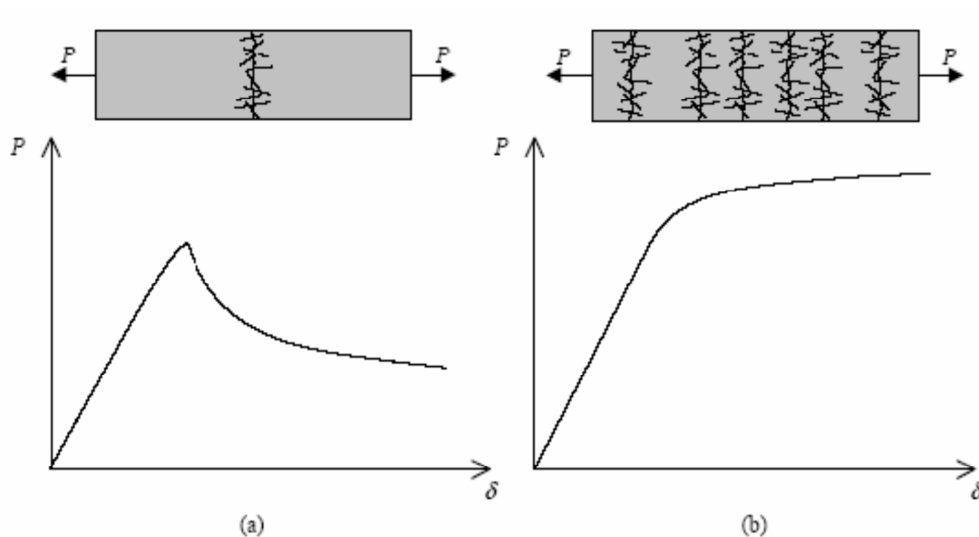


Figure 1: Traction diagrams of FRC: low % (0.2-2) of fibers (a) and high % (2-8) of fibers (b);

The main applications of this type of concrete are in:

- Bearing panels;
- Ground slabs;
- Coatings for tunnels;
- Beams;
- Structural connections;
- Roof elements;
- Structure designed to absorb shock and fatigue;
- Precast elements;

2.1.2 The Materials

The matrix of FRC elements is composed by concrete. For a better workability with the fibers and in operation phase, the granulometry of the aggregates must be design, for example, increasing the fine elements like sand, gravel etc.

Therefore, the fibers adopted in the FRC can be made of steel, polymeric, carbon, glass and natural materials. In each case, the codes impose that the length must be smaller than 60 millimeters.

▪ *Steel Fibers*

These kinds of fibers have a length, l_f , from 6 mm to 70 mm and with \varnothing , d_f , from 0.15 mm e 1.20 mm. They are classified in base of their production processes, shape and types of material:

- Considering the production:
 - Drawn wire (type A);
 - Sheet (type B);
 - Others (type C);
- Considering the shape:
 - Rectilinear;
 - Shaped (hooked, rolled, etc...);
- Considering the material:
 - Steel with low carbon content ($C \leq 0,20$, type 1);
 - Steel with high carbon content ($C > 0,20$, type 2);
 - Stainless steel (type 3);

In function of the mechanical characteristics of the fibers, we can distinguish three categories: R1, R2, and R3.

Equivalent Diameter [mm]	Traction Resistance [N/mm ²]												Alternating Bending Test
	R1				R2				R3				
	1)		2)		1)		2)		1)		2)		Without Cracks
R_m	$R_{p0.2}$	R_m	$R_{p0.2}$	R_m	$R_{p0.2}$	R_m	$R_{p0.2}$	R_m	$R_{p0.2}$	R_m	$R_{p0.2}$		
0,15 ≤ d_f < 0,50	400	320	480	400	800	720	1080	900	1700	1360	2040	1700	
0,50 ≤ d_f < 0,80	350	280	450	350	800	640	1040	800	1550	1240	2015	1550	
0,80 ≤ d_f < 1,20	300	240	390	300	700	560	910	700	1400	1120	1820	1400	
1)for Rectilinear Fibers 2)For Shaped Fibers													

Figure 2: Steel Fibers Parameters

As you can see in the table, R_m and $R_{p0.2}$ represent the traction resistance of the maximum load and the proportional deviation resistance with an extension equal to 0.2% of the base length of the extensometer.

▪ *Polymeric and Carbon Fibers*

Polymeric and carbon fibers are commercially available polymer of acrylic fibers, aramid, nylon, polyester, polyethylene, polypropylene and carbon fiber. These kinds can be used to increase:

- Short term plastic properties;
- Durability and resistance on freeze-thaw cycles;
- Impact resistance;
- Abrasion resistance;
- Post-cracking resistance of the matrix;
- Fire resistance;

Well, the fibers can be distinguished in micro-fibers, where the length is mm or macro-fibers with a length until 80 mm.

Type	Diameter [10 ⁻³ mm]	Density [g/mm ³]	Traction resistance [MPa]	Elastic modulus [MPa]	Ultimate Deformation [%]	Temperature on start [°C]	Fusion temperature [°C]	Water Absorbing [% in peso]
Acrylic	12,7 ÷ 104,14	1,16 ÷ 1,18	269÷1000	13790 ÷ 19306	7,5÷50	-	221÷235	1,0÷2,5
Aramide I	11,94	1,44	2930	62055	4,4	Alta	482	4,3
Aramide II	10,16	1,44	2344	117215	2,5	Alta	482	1,2
Carboni PAN HM	7,62	1,6÷1,7	2482 ÷ 3034	379914	0,6÷0,7	Alta	400	Nil
Carboni PAN HT	8,89	1,6÷1,7	3447 ÷ 3999	230293	1,0÷1,5	Alta	400	Nil
Carboni pitch GP	9,91 ÷ 12,95	1,6÷1,7	483÷793	27580 ÷ 34475	2,0÷2,4	Alta	400	3÷7
Carboni pitch HT	8,89 ÷ 17,78	1,80 ÷ 2,15	1517 ÷ 3103	151690 ÷ 482650	0,5÷1,1	Alta	500	Nil
Nylon	22,86	1,14	965	5171	20	-	200÷221	2,8÷5,0
Polyester	19,81	1,34 ÷ 1,39	227 ÷ 1103	17237	12÷150	593	257	0,4
polyethylene	25,4 ÷ 1016	0,92 ÷ 0,96	76 ÷ 586	4999	3÷80	-	134	Nil
Polypropyl.	-	0,90 ÷ 0,91	138 ÷ 689	3447 ÷ 4826	15	593	165	Nil
Polyvinilalc.	14 ÷ 600	1,30	880 ÷ 1600	25000 ÷ 40000	6÷10	-	-	4

Figure 3: Polymeric and Carbon Fibers Parameters

2.1.3 The Mechanical Behavior

The physical and mechanical properties of the conglomerate are determined by the doses and by the singular elements parameters. In any case the minimum dosage for structural elements must be greater than 0.3% of the volume.

The rheological properties of the FRC depend on the workability of the matrix and on the nature of the fibers, including also their geometry.

Applying the fibers with typical doses the workability decreases, in particular when the shape of the fibers are complex. One method to improve this parameter is increase the

fine fraction or decrease the maximum diameter of the aggregate and by selecting and dosing fluidizing additives.

Moreover the distribution of the fibers must be homogeneous in the conglomerate in order to avoid accumulations.

- *Compression Behavior*

The fibers in general decrease the fragility of the matrix but they don't influence much the compression behavior.

The constitutive law of the FRC and its compression resistance can be assimilated with the normal concrete without fibers. In this study will call it "B".

- *Tensile Behavior*

The fibers improve the tensile behavior of the matrix when the section of the element is cracked. As you can see in the chart, for low contents of fiber (< 2% of the volume) the behavior is degraded, while for high contents (> 2% of the volume) the traction resistance is greater because there is a hardening behavior, due to the multi-cracking phenomena.

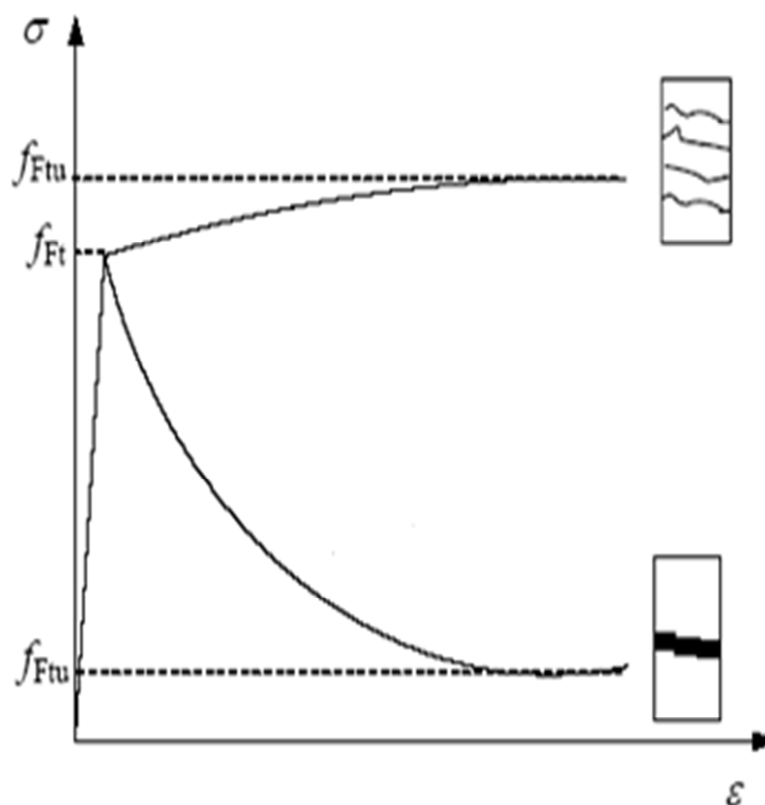


Figure 4: Different Traction Behavior

2.2 Self-Compacting Concrete, SCC

2.2.1 Generalities

Normally the concrete contains air that must be reduced by constipation. This operation is made by vibrators and can be either inside or not the conglomerate.

The vibration is necessary to reduce the negative effects of bleeding (when the water goes out) and the shrinkage of the ultimate layers, but an excessive operation would determine the segregation of the aggregates and the consequent reduction of the mechanical properties of the concrete.

The SCC, one of the most interesting new technologies in the building materials for structural purposes, constitutes a new conglomerate where the processes of vibration and constipation aren't necessary. The main use of this type of concrete is in tunnels, where considering the difficult conditions of the men at work, it represents the ideal solution to avoid the vibration in prohibitive conditions.

The SCC is developed in Japan at the beginning the 80's, where the technicians applied additives into the mix:

- New synthetic polymer that can reduce water contents and increase resistance;
- Viscosity modification agents VMA to increase cohesion for fresh concrete;
- Silicon fume, constituted by particle of few nm that increase the quality;
- Shrinkage reducing admixtures SRA for decreasing the shrinkage deformations;

The SCC has some particular rheological characteristics, physics and mechanicals, and it has high stability and small tendency to the segregation even the conditions aren't optimal.

Thanks to its innovative characteristics, the SCC can flow in all voids, avoiding the obstacles like the reinforcements. Where is possible the blocking flow, the designed volume of the SCC conglomerate must be greater than the ordinary volume usually used.

From the rheological point of view, the conglomerate is constituted by two different phases:

- Transportation Flow;
- Transported Material;

Therefore, the real possibility to make a SCC with high fluidity is associated to the needs of increase the fine material volume that constitutes the transportation flow, in favor of the minor aggregate volume that must be transported by the first.

Other parameters that SCC must have are:

- Low water/cement ratio;
- High resistance to segregation;

It must be able to conserve a uniform distribution of the ingredients (water, cement, aggregates, and additives) in the different phases.

2.2.2 Composition of SCC

Studying the composition of the SCC was noticed that there are many differences from the original concrete mixture:

- Higher quantity of material $< 150 \mu\text{m}$;
- Lower quantity of material $< 25 \text{ mm}$;

Presence of additives for fluidifying and viscosity control;

2.2.3 Advantages on Disadvantages of SCC

Advantages:

- Greater quality of the concrete;
- Better homogeneity of the product;
- Higher performances;
- Better conditions of the men at work due to the absence of vibrators (Sound intensity is decrease until 1/10);
- Reduced operating time;

Disadvantages:

- More expensive;

One interesting method to reduce the costs is that insert a normal concrete layers between SCC layers, called “sandwich panel”, where in each layer there are different properties.

This type of product can be vibrated to increase its characteristics.

Using the sandwich concept you can reduce the costs without loss in terms of SCC properties and advantages.

3. Overview of the Experimental Test and Material Properties

3.1 Introduction

The objective of this study is analyzing the viscous phenomena of different samples with different mixture of concrete. In particular we have made:

Samples Type	Samples Dimensions	Concrete Type	Test Type	Fiber Type
Beam "B"	300x120x2000	Plain SCC	Crack test; Creep test;	/
Beam "M1"	300x120x2000	FRSCC	Crack test; Creep test;	M
Beam "M2"	300x120x2000	FRSCC	Crack test; Creep test;	M
Cylinder "B Ø10"	H = 200; D = 100;	Plain SCC	Shrinkage test; Creep test;	/
Cylinder "B Ø15"	H = 300; D = 150;	Plain SCC	Shrinkage test;	/
Cylinder "M1 Ø10"	H = 200; D = 100;	FRSCC	Shrinkage test; Creep test;	M
Cylinder "M1 Ø15"	H = 300; D = 150;	FRSCC	Shrinkage test;	M
Cylinder "M2 Ø10"	H = 200; D = 100;	FRSCC	Shrinkage test; Creep test;	M
Cylinder "M2 Ø15"	H = 300; D = 150;	FRSCC	Shrinkage test;	M
Cylinder "S Ø15"	H = 300; D = 150;	FRSCC	Shrinkage test;	S

Prismatic "M1_P1"	150x150x600	FRSCC	Crack test;	M
Prismatic "M1_P2"	150x150x600	FRSCC	Crack test;	M
Prismatic "M1_P3"	150x150x600	FRSCC	Crack test;	M
Prismatic "M2_P1"	150x150x600	FRSCC	Crack test;	M
Prismatic "M2_P2"	150x150x600	FRSCC	Crack test;	M
Prismatic "M2_P3"	150x150x600	FRSCC	Crack test;	M
Prismatic "S_P1"	150x150x600	FRSCC	Crack test;	S
Prismatic "S_P2"	150x150x600	FRSCC	Crack test;	S

Figure 5: Overview of experimental study

3.2 Fibers Types

3.2.1 MapeFibre ST42, called "M"

ST42 are structural polymer fibers with a length of 42 mm respectively, developed to improve the performance characteristic of conventional concrete, pre-fabricated concrete and shot-concrete.

Represent a valid alternative to steel fibers when used to distribute loads, limit crack phenomena and to produce high-ductility concrete.

- Length of Fiber: 42 mm;
- Equivalent Diameter: 0.9 mm;
- Density: 1 g/cm³;
- Number of Fibers in 1 kg: >50,000;
- Melting Point: 150-160°C;
- Water Absorption: <0.01%;
- Resistance to alkalis, acids or salts: high;
- Tensile Strength: 700 MPa;
- Young Modulus: 2.1 GPa;

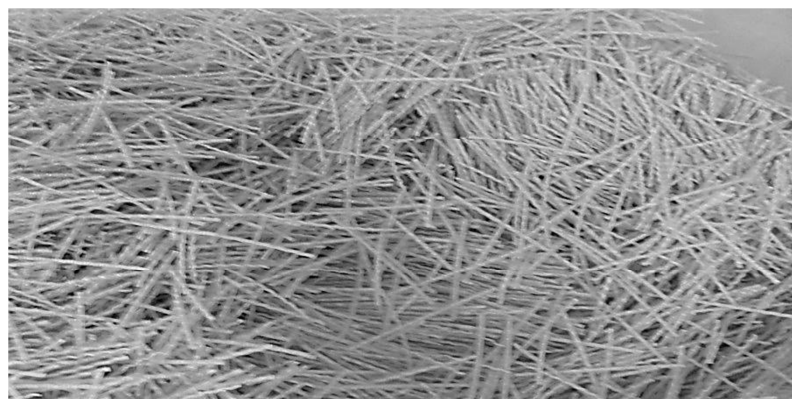


Figure 6: Polymeric fiber Mapei st42

3.2.2 Wirand® Fibre FF3, called “S”

It's a cold drawn wire of steel for the structural concrete reinforcement.

- Length: 50 mm;
- Diameter: 0.75 mm;
- Number of fibers for 1 kg: 5700;
- Tensile strength: > 1100 MPa;

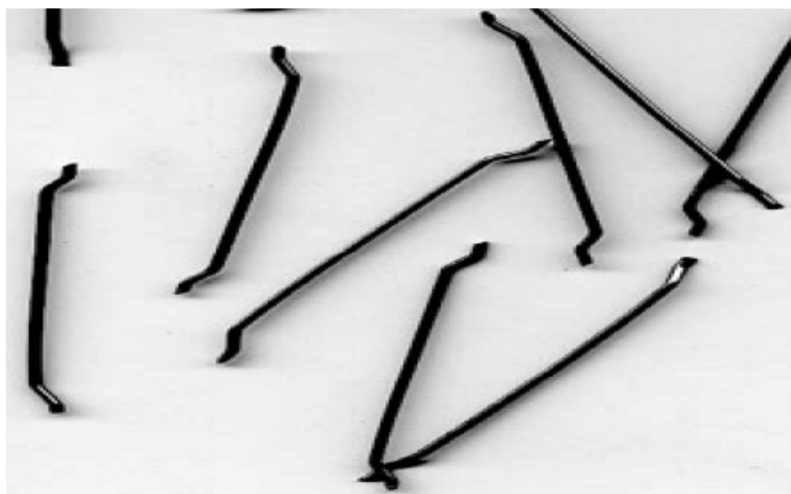


Figure 7: Wirend Fibre FF3, Maccaferri

3.3 Mixture Characteristics

This paragraph lists and describes all parameters that characterized and identified the matrix of the fibro reinforced concrete used.

3.3.1 Aggregates

The granulometric analysis is made by series of screens.

After the vibrating operations, it is measured the weight and the percentage of material in each screen, the progressive percentage of the material and the cumulative sum.

Then, the granulometric curve of the aggregate it is a graphically represented with the progressive percentage in function of the screen's diameter.

The choice of the aggregate is very important to obtain a sufficiently workable conglomerate, compactable and at the same time durable. If there are many big size aggregates, the water content could be lower, but the workability will become lower and there could be the segregation. Vice versa if there are many small size aggregates, the water content will be higher but the properties will become insufficient. For minimizing the air content in the mixture, usually are used different aggregates with different measures.

From the literature, the theory curve called “Fuller curve” it is a better compromise between resistance, workability and density. The theoretical properties are impossible to achieve, for each screen is imposed tolerance range and with it, are found two new boundaries curves of the granulometric zone. The mixture is acceptable if it is inside of this zone.

The characteristic equation of the Fuller curve is:

$$p = 100 \cdot \sqrt{\frac{d}{D}}$$

Where:

- p is the percentage of volume that cross the screen;
- d is the diameter of the screen;
- D is the maximum diameter of the aggregate;

3.3.2 Water demand of the aggregate

The below expression indicates the demand of the water for the aggregate:

$$AA\% = \frac{m_{sat} - m_s}{m_s} \cdot 100$$

Where:

- m_{sat} is the mass of the aggregate filled of water;
- m_s is the mass of the dry aggregate;

The knowledge of the water demand is a fundamental parameter for the computing of the mixture dosage. The total water content necessary for the conglomerate is equal to the sum of sufficient water for the hydration of the aggregate plus the presumed quantity for the absorbing phase.

There are three types of aggregate:

- Dry, after cooking at 110°C;
- Humid;
- Wet, after washing or raining on it;
- Wet with dry boundary layer, after short drying;

3.3.3 Water/Cement Ratio

The water of the conglomerate is important for hydration and fluidity. In theory, for the first topic the ratio of w/c is about 0.25 but also, for obtaining a best result, this ratio is increased until 0.4.

The w/c ratio is an important parameter because it modifies the workability of the concrete and the mechanical/viscosity properties.

Decreasing the water content, at first time you can determine a better mechanical resistance but then, because the workability goes down and does not guaranty the correct adhesion between mortar and aggregate, this initial increment decreases. Vice versa high water content increases the workability of the conglomerate but also increases the segregation or the viscos deformations and reduces the mechanical resistance.

The fluage phenomena are conduced only with cement: therefore the cement content and the w/c content are strategic: low content of cement and low w/c reduce the viscos effects.

Then the best approach is using specified additives for the workability without compromise the w/c ratio.

3.3.4 Workability, classes and slump test

The workability is an index of the properties in the interval time that passes from the production to the compaction of the mixture.

The connected properties are:

- Stability, capacity to maintain the uniform distribution under external loads;
- Mobility, propensity of the concrete to go to all point;
- Compactability, capacity to avoid the internal air;

The workability depends on:

- w/c content;
- temperature;
- time history;
- additives used;
- cement quality;

In function of the workability, valued by the consistency, the mixtures are divided into 4 classes. The best method to do this is the Abrams cone:

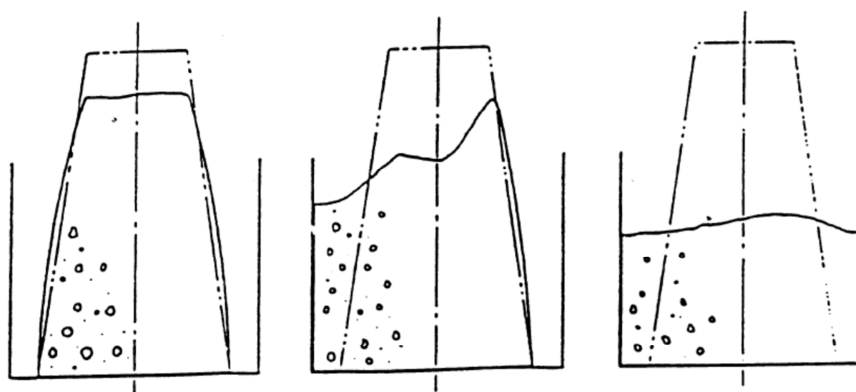


Figure 8: Abram Cone Test

This cone is made on steel, perfectly planned inside, opened in the upper part, with a high about 30 ± 2 cm and base diameter about 20 ± 2 cm. The diameter of the upper part is about 10 ± 2 cm. the cone must be placed on one plane cleaned surface.

The mixture, selected in order to represent the principal properties type, is placed in the cone in 3 different compacted layers with the same thickness. When the cone is full, the upper surface must be flat and after that the cone is removed. At this time the mixture collapses by a quantity inverse proportional to the consistency.

The slump of the conglomerate respect to the original shape is assumed as the measure of the consistency.



a) True slump

b) Shear slump

c) Collapse slump

Figure 9: Slump Types

Showing the figure above, there are three different behaviors:

- uniform slump, that indicates normal result;
- asymmetric slump, that indicates less cohesion of the conglomerate;
- generalized slump, that indicates wet mixture or mixture with low cement content;

Regarding the code UNI EN 206 – 2006 and UNI 11104:2004, there are individuated 5 classes of consistency:

- S1: slump from 10 to 40 mm, humid consistency;
- S2: slump from 50 to 90 mm, plastic consistency;
- S3: slump from 100 to 150 mm, semi-fluid consistency;
- S4: slump from 160 to 210 mm, fluid consistency;
- S5: slump from 220 to other mm, super-fluid consistency;



Figure 10: Slump Test Measure

3.3.5 Volumetric Mass

Generally this measure is expressed in kg/m^3 , and it's obtained by using a steel cylinder and a balance. The cylinder, supported by one vibrant table, is filled with concrete. After that, the volumetric mass is identified by the ratio: weight of the system minus weight of the cylinder over the volume.

3.4 Instruments for the Packaging

In this paragraph are listed the principal instruments that are used for the packaging of the samples:

- Balance: used for weighing the aggregates and the water of the mixture and then, in the last passage, for computing the volumetric mass;
- Mixer: for obtain the complete mixing of the components;
- Digital Thermometer: used for measuring the temperature;
- Cone: for measuring the slump;
- Formwork: covered by disarming for avoiding the attachment of the concrete at the sides;
- Vibrators: for standardize the mixture;

3.5 Standard Packaging Operations

The sequence is the same for all the samples that are made and includes all the passages of the process to produce them, from the mixture to the curing.

- Weigh the aggregates;
- Insert the aggregates in the mixer;

- Weigh the total water;
- Insert $\frac{1}{2}$ of the necessary water content;
- Start the mixer;
- Weigh the total quantity of cement;
- Insert the cement, water and additives continuing the mixing;
- Complete the mix;
- Measuring the slump;
- Measuring the temperature;
- Measuring the volumetric mass;
- Insert the fibers;
- Insert the mixture into the formwork with vibration operations;
- Regulation of the upper surface of the samples;
- Bring and keep the beam into controlled room;

3.5.1 Particular Operation for SCC

In addition to the other characteristics explained in the paragraph 3.3 it is necessary to impose some relative details for the SC concrete because it's very fluid and it's impossible to verify the behavior with the slump test due to their low consistency.

There are other tests for these types of concrete:

- Slump flow;
 - J ring;
 - V funnel;
- *Slump flow*

This test is made with the same instruments of the normal slump test but measuring the expansion instead of the height and computing the time travel to obtain an expansion of 500 mm that must be lower than 12 seconds.



Figure 11: Slump Flow Test

- *J ring*

It's a test finalized to determine the capacity of the SCC when passing through obstacles constituted by the reinforcement normally placed inside on the concrete element. The concrete is posed into the Abram's cone and inserted it in one ring sustained by steel bars. When the cone is uplifted, the concrete starts its expansion and crosses the bars. The diameter of the ring is lower than 300 mm the height lower than 100 mm and the diameter of the bars must be 10 mm. The bar length is 100 mm and its spacing within one another is 48 ± 2 mm. The property of the SCC is evaluated by the difference between the free expansion and the ring constrained expansion: there are measured two diameters and is computed their average value. This value must be lower than 50 mm.

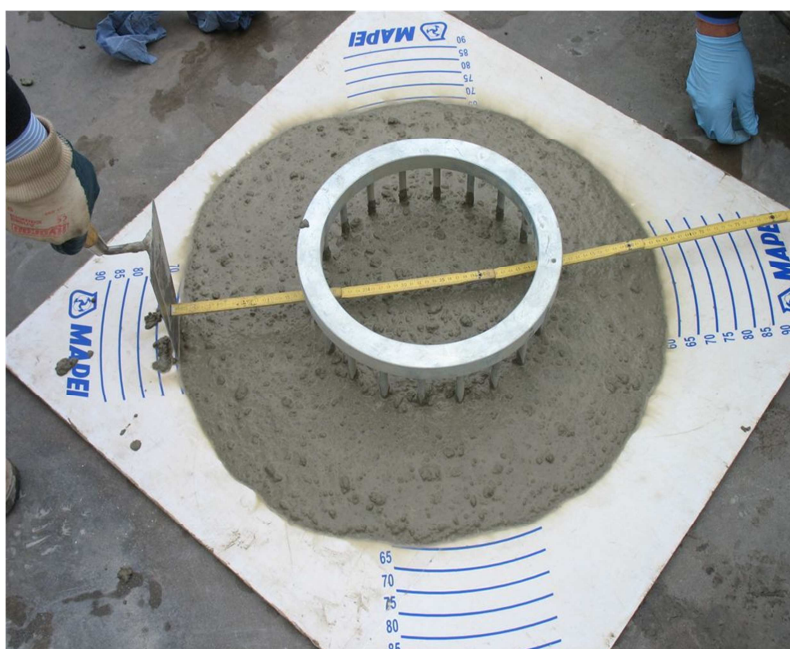


Figure 12: J Ring Test

- *V Funnel*

This test is used to determine the time that the concrete needs to come out from one V steel funnel. The time represents a deformability index that must be included between 4 to 12 seconds. Then, another test measures the time after 5 minutes the concrete has stopped inside the funnel. This second time measure must be higher or lower than the first of about 3 seconds.



Figure 13: V Funnel Test

3.6 Fresh Test Results

In 9th November 2011, at “Lombarda Calcestruzzi” near Milan, the conglomerates are made. In particular, the main characteristics of the three types of concrete are:

3.6.1 B Type

- Slump Flow I: 83 cm in the first phase;
- Slum Flow II: 75 cm with a viscosity additive about 0.6%;
- V-Tunnel Test: 4.28 s;
- Volumetric Mass: 2310 kg/m³;
- Incorporated Air: 2.4%;
- Fiber Type: /
- Fiber Dosage: / kg/m³.

3.6.2 M1 Type

- Slump Flow: 80 cm;
- Additive: 1 l/m³;
- V-Tunnel Test: 3.82 s;
- Volumetric Mass: 2355 kg/m³;
- Incorporated Air: 1.2%;
- Fiber Type: M;
- Fiber Dosage: 4 kg/m³.

3.6.3 M2 Type

- Slump Flow: 65 cm;
- Additive: 0.5 l/m³;
- V-Tunnel Test: /;
- Volumetric Mass: 2302 kg/m³;
- Incorporated Air: 1.9%;
- Fiber Type: M
- Fiber Dosage: 7 kg/m³.

3.6.4 S Type

We haven't done fresh test for this type.

- Fiber Type: S;
- Fiber Dosage: 25 kg/m³.

4. Tests Instruments

4.1 Omega Transducers

4.1.1 Generalities

The transducer used in the test is called “omega” from its shape. This kind of instrument measures the relative distance between two points (max 50 mm). We adopted it to control the cracking phase for all the samples, the width of the cracks of the beam and the viscosity of the compressed cylinders. The fixing operation consists into pasting two threaded bases with special glue called “X60”. The instrument is composed by 4 strain gauges full bridge connected positioned in the arc of the support, and the optimal positioning is over the crack in a normal direction. The omega measures a curvature variation, the strain gauge receives a signal in terms of potential difference, and from an amplifier we send it to software that converts this signal into a displacement variation.

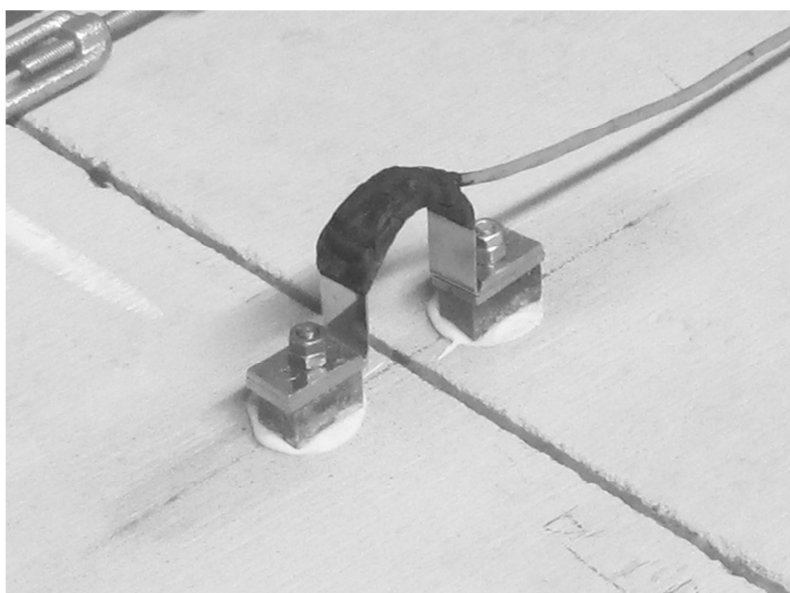


Figure 14: Omega Transducer Application

4.1.2 Calibration Procedure

The calibration of the instrument consists into assign cyclic know displacements and measuring the potential difference. Then, we interpolated the data for building the graph that represents the proportionality between these two quantities:

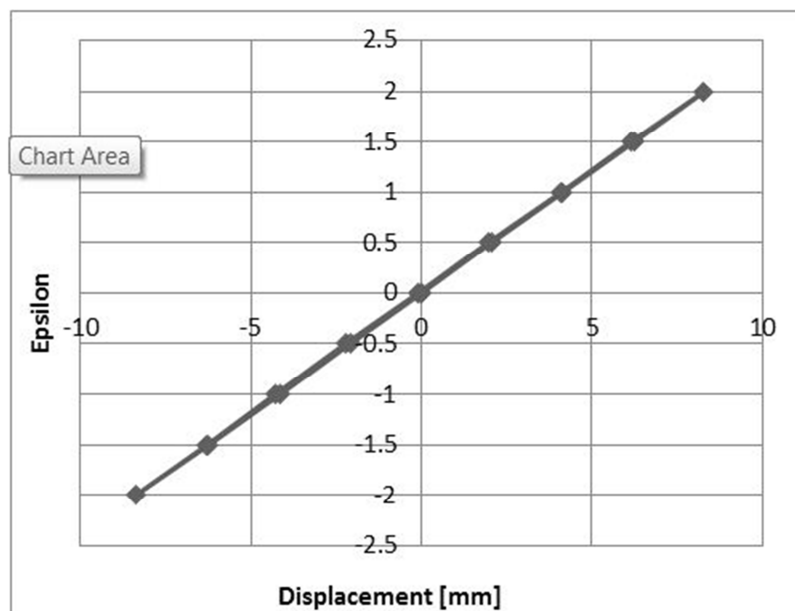


Figure 15: Omega 7 Calibration

Ω	Gain Factor	PC	Amplifier	Calibration Voltage	Excitation	Constant factor	Test Type
7	8.06	Yashi	2120	2V	2.5V	0.24045	Short Term
5	8.02	Yashi	2120	2V	2.5V	0.22367	Short Term
Big	6.02	Yashi	2120	2V	2.5V	0.63209	Short Term
6	7.95	Yashi	2120	2V	2.5V	0.23766	Short Term

Ω	Gain Factor	PC	Amplifier	Excitation	Constant factor	Test Type
8	1812	Yashi	1520 (ch. n.6)	2.5V	$0.003997 \cdot 10^6 \cdot 0.4754$	Long Term
1	1756	Yashi	1520 (ch. n.5)	2.5V	$0.001889 \cdot 10^6$	Long Term
9	1704	Yashi	1520 (ch. n.7)	2.5V	$0.001862 \cdot 10^6$	Long Term
6	1924	Yashi	1520 (ch. n.8)	2.5V	$0.001867 \cdot 10^6$	Long Term
5	2184	Yashi	1520 (ch. n.8)	2.5V	$0.001792 \cdot 10^6$	Long Term
7	1848	Yashi	1520 (ch. n.8)	2.5V	$0.001931 \cdot 10^6$	Long Term

Figure 16: Ω Constants

During the test the constant factor of Ω 8 was modified to avoid an error of the cable.

4.2 LVDT Transducers

4.2.1 Generalities

The LVDT, Linear Variable Differential Transformer, is an instrument that measures the displacement of one fixed point. It's based on the electromagnetic induction and depends only on alternating electric quantities.

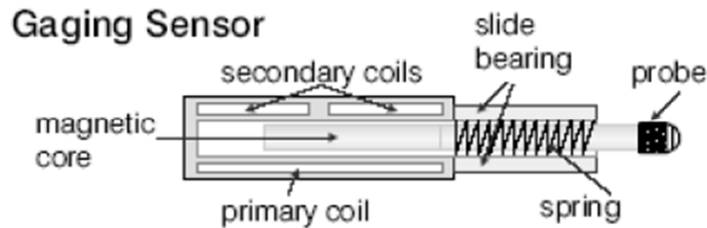


Figure 17: LVDT Section

The fixing operation consists into putting the probe in a vertical direction with direct contact on steel base in the exact point that we want analyze. When the sample is loaded the LVDT measures the displacements in time with an elastic spring.

The probe displacement is transformed in an electrical potential variation and analyzed by the software. The circuit is constituted by one principal and two secondary coils and their axis coincide with the core axis. The potential tension between the ends of the secondary circuit is null at the initial time. If the core is moved, the voltage changes and this quantity represent the displacement of the probe Δx .

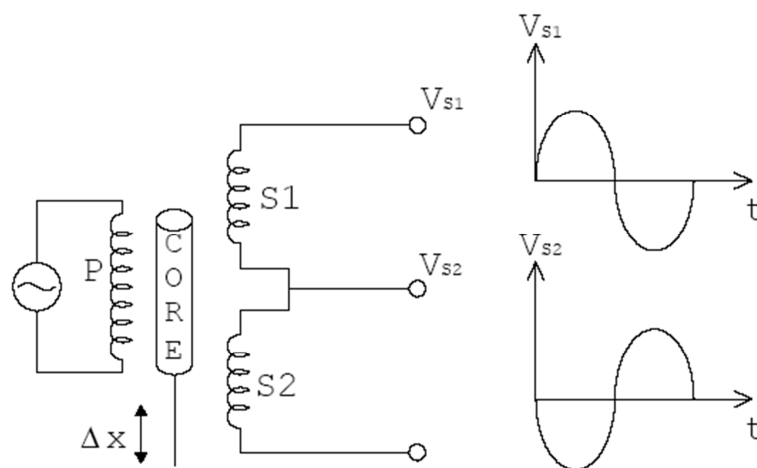


Figure 18: Electromagnetic circuit of LVDT



Figure 19: LVDT Application

4.2.2 Calibration Procedure

Before using these instruments we have to do the calibration, just like we have done for the omega.

When we have obtained the constants, we can use the instruments. In order to find the value of the slope of the line, we apply a series of cyclic displacements and read the exact quantity of movements.



Figure 20: Calibration of the instrument

LVDT	MAX (m)	MIN(m)	Sensibility [mV/V/mm]	L	Constant
WA 10-4	0.01	0.00	8.00	3.74	1000
WA 10-5	0.01	0.00	8.00	5.62	1000
WA 10-1	0.01	0.00	8.00	5.30	1000
WA 10-3	0.01	0.00	8.00	5.42	1000
WA 10-2	0.01	0.00	8.00	5.71	1000
WA 10-6	0.01	0.00	8.00	5.10	1000

Figure 21: LVDT constants

4.3 Strain Gauges

4.3.1 Generalities

A strain gauge is an instrument to measure the local surface deformation of one body.

Its functioning is based on the piezo-resistive effect. It is a transducer, which transforms a quantity like deformation in an electrical signal.

All the common strain gauges are made with steel, with a special element of (84% Cu, 12% Mn, 4% Ni) or (60% Cu, 40% Ni), with a known electrical resistance and the diameter (da 0.01 a 0.03mm). They can be longer from 5 mm up to 15 cm, depending on the material that are applied. Generally, if we want apply them on a steel element the length must be shorter while for concrete element must be higher.

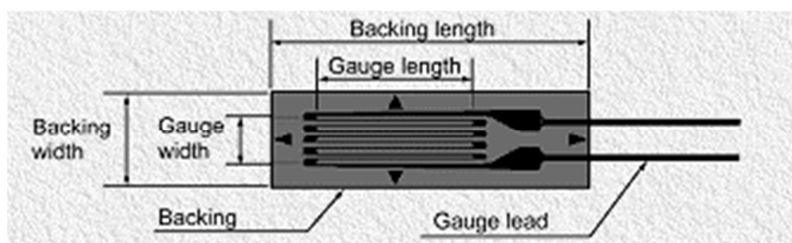


Figure 22: Strain Gauge components

The choice of the type of the strain gauge depends on the precision of the measure that we want to find because the deformation measured before is a mean value along the backing length.

The fixing operations are the same of the omega or LVDT transducer, therefore is used the “X60” as usual glue.

The common value of the resistance varies from 120 to 1000Ω, but it usually depends on the production.



Figure 23: Strain gauge pack

From the measure of the deformation is possible to find some other physical quantities as tension, force, displacement, acceleration.

The electrical resistance of the conductor cable can be expressed as:

$$R_{\text{Cable}} = \rho \cdot \frac{L}{A}$$

Where:

- R_{Cable} is the resistance;
- ρ is the electrical resistivity;
- L is the cable length;
- A is the cable section;

4.3.2 Calibration Phase

Strain Gauge	MAX [eps]	MIN [eps]	Excitation [V]	Resistance [Ω]	Gauge Factor [2.00]	Constant
E 13	0.0005	-0.002	2.50	1.20	2.11	1E+6
E 14	0.0005	-0.002	2.50	1.20	2.11	1E+6
E 11	0.0005	-0.002	2.50	1.20	2.11	1E+6
E 12	0.0005	-0.002	2.50	1.20	2.11	1E+6
E 9	0.0005	-0.002	2.50	1.20	2.11	1E+6
E 10	0.0005	-0.002	2.50	1.20	2.11	1E+6
E 8	0.0005	-0.002	2.50	1.20	2.11	1E+6
E 7	0.0005	-0.002	2.50	1.20	2.11	1E+6
E 2	0.0005	-0.002	2.50	1.20	2.11	1E+6
E 1	0.0005	-0.002	2.50	1.20	2.11	1E+6
E 3	0.0005	-0.002	2.50	1.20	2.11	1E+6
E 4	0.0005	-0.002	2.50	1.20	2.11	1E+6
E 5	0.0005	-0.002	2.50	1.20	2.11	1E+6
E 6	0.0005	-0.002	2.50	1.20	2.11	1E+6
E 23	0.01	-0.01	2.50	1.20	2.11	1E+6
E 24	0.01	-0.01	2.50	1.20	2.11	1E+6
E 21	0.01	-0.01	2.50	1.20	2.11	1E+6
E 22	0.01	-0.01	2.50	1.20	2.11	1E+6
E 27	0.01	-0.01	2.50	1.20	2.11	1E+6
E 28	0.01	-0.01	2.50	1.20	2.11	1E+6
E 26	0.01	-0.01	2.50	1.20	2.11	1E+6
E 25	0.01	-0.01	2.50	1.20	2.11	1E+6
E17/18	0.01	-0.01	2.50	1.20	2.11	1E+6
E15/16	0.01	-0.01	2.50	1.20	2.11	1E+6
E19/20	0.01	-0.01	2.50	1.20	2.11	1E+6

Figure 24: Strain gauges constants

4.3.3 Attaching Phase

- Preparation of the surface;
- Drawing the references lines on the sample;
- Bonding the strain gauge;
- Application of the transparent film;
- Connection of the cables;
- Connection to the system;



Figure 25: X60 and its components

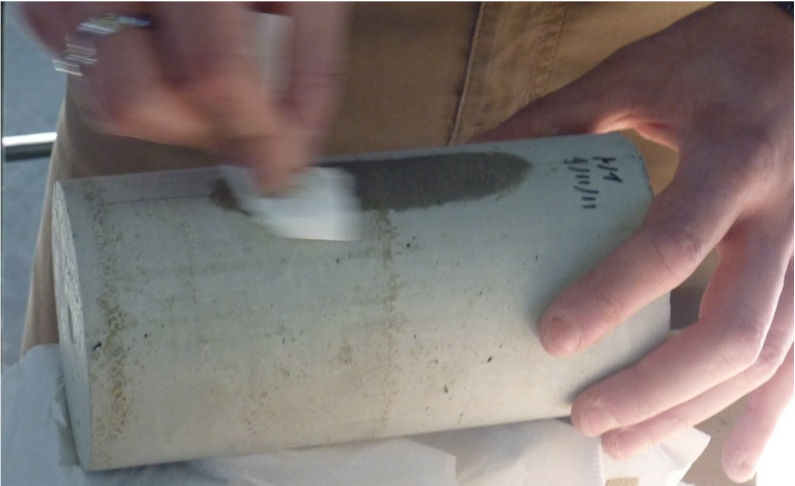


Figure 26: Cleaning the surface

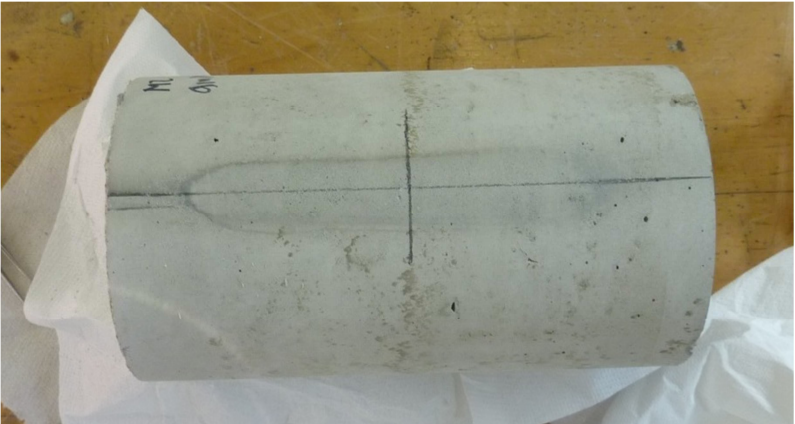


Figure 27: Drawing the reference lines



Figure 28: Bonding the strain gauge



Figure 29: Application of film

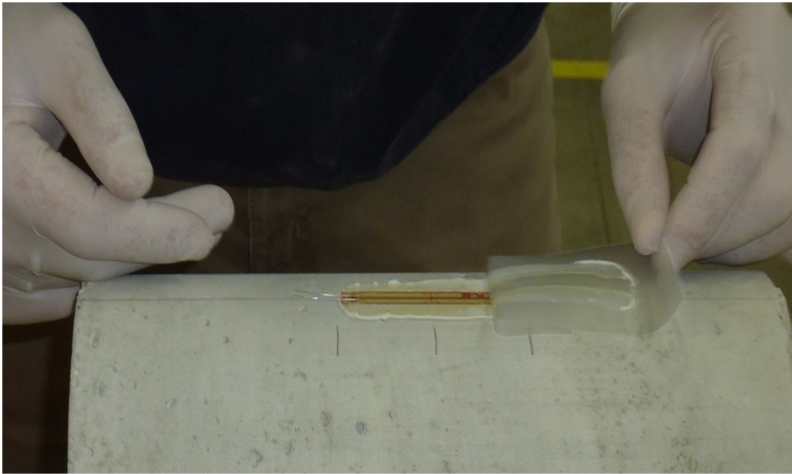


Figure 30: Removing the film

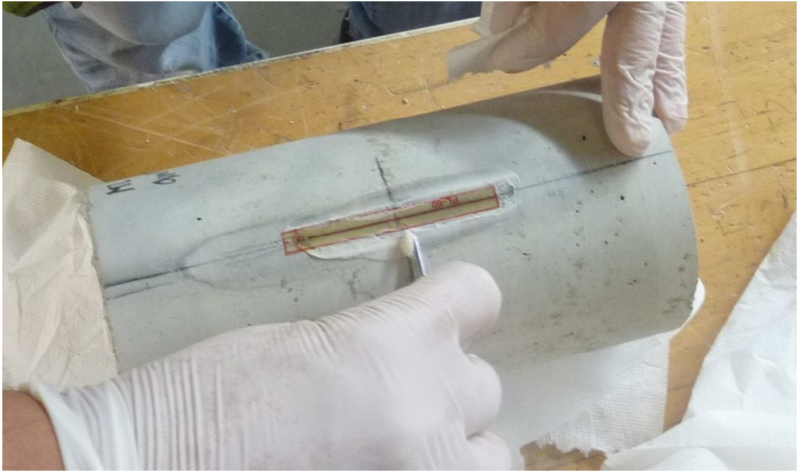


Figure 31: Cleaning the boundary

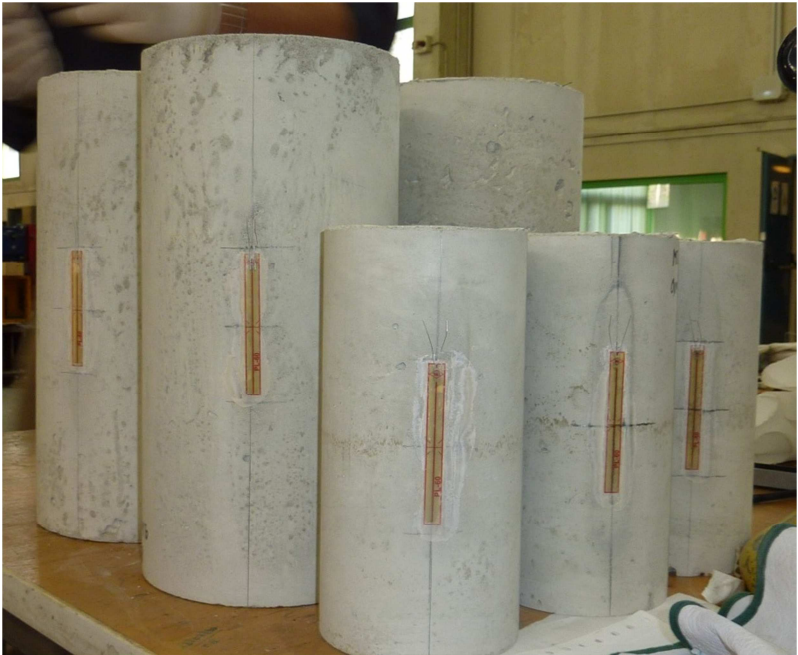


Figure 32: Repeating the operations for all the samples

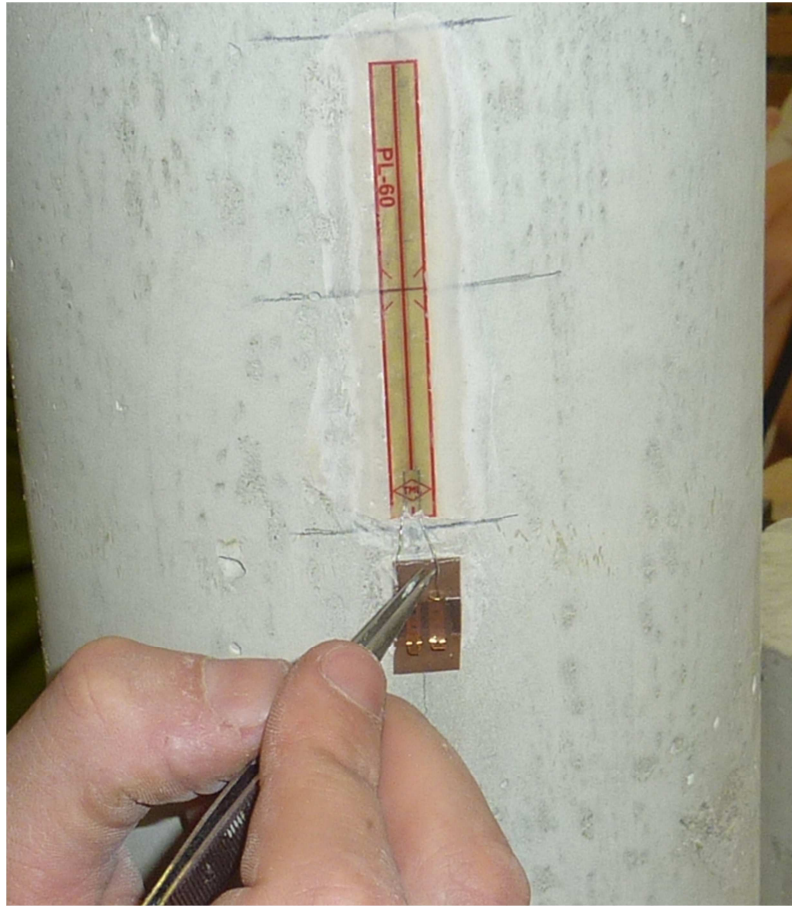


Figure 33: Insert the legs in the base connection

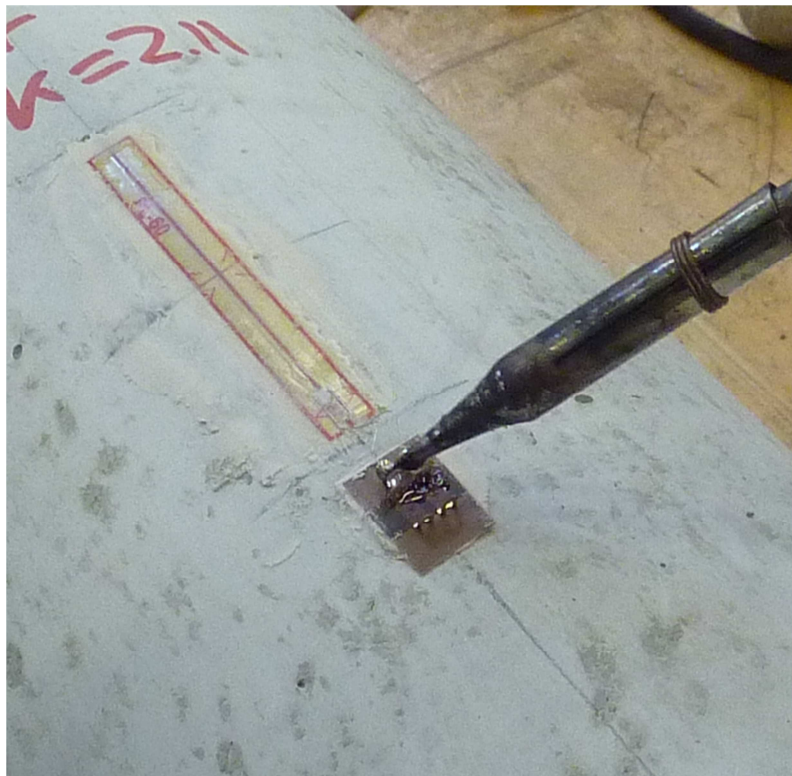


Figure 34: Weld the connections

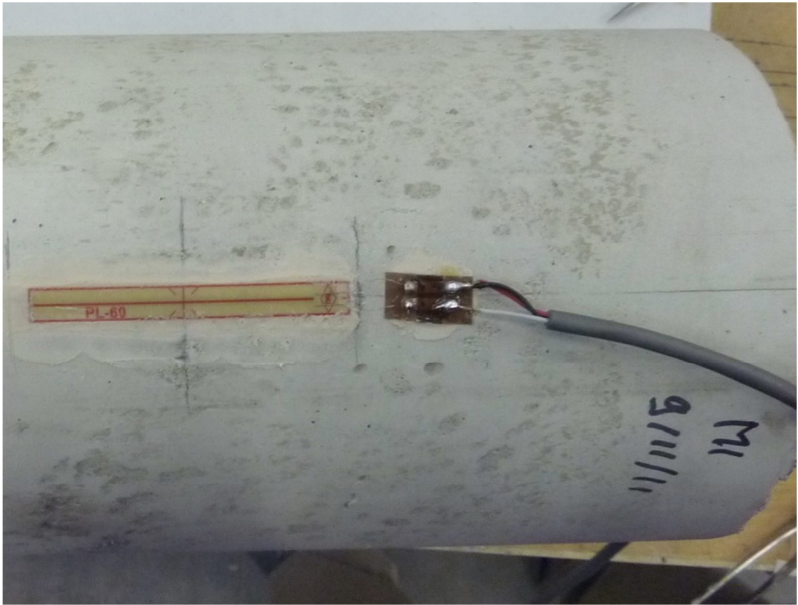


Figure 35: Connect the cable to the base



Figure 36: Attach the cables for all the samples



Figure 37: Connect all cables into system

4.4 Load Cells

The TCLP-NB Tension/Compression Universal Load Cell is a load cell widely used in applications such as measuring crane and jack loads because it offers excellent consistency.

Cell	MAX [eps]	MIN [eps]	Excitation [V]	Resistance [Ω]	Gauge Factor [2.00]	Constant
1	0.0005	-0.0005	5.00	350	2.00	496500
2	0.0005	-0.0005	5.00	350	2.00	496500

Figure 38: Load cell constants

For cracking procedure we have used the TCLP-50KNB.

Type	TCLP-10KNB	TCLP-20KNB	TCLP-30KNB	TCLP-50KNB	TCLP-100KNB	TCLP-200KNB	TCLP-300KNB	TCLP-500KNB	TCLP-1MNB	TCLP-1.5MNB	TCLP-2MNB
Capacity	10kN	20kN	30kN	50kN	100kN	200kN	300kN	500kN	1MN	1.5MN	2MN
Rated Output	1mV/V (2000 $\times 10^{-6}$ strain) $\pm 0.5\%$										
Non-linearity	0.1%RO									0.3%RO	
Hysteresis	0.1%RO									0.3%RO	
Temperature effect on zero						0.01%RO/ $^{\circ}$ C					
Temperature effect on span						0.005%/ $^{\circ}$ C					
Compensated temperature range						-10 \sim +60 $^{\circ}$ C					
Temperature range						-20 \sim +70 $^{\circ}$ C					
Over load	200%										
Input/output resistance						350 $\Omega \pm 1\%$					
Recommended exciting voltage	Less than 10V										
Allowable exciting voltage	20V										
Zero balance	5%RO										
Weight	1.5kg	1.5kg	2kg	2kg	2.5kg	5kg	8kg	15kg	50kg	85kg	110kg

Figure 39: Load cell properties



Figure 40: Load cell for cracking phase

For the viscous test we have used:

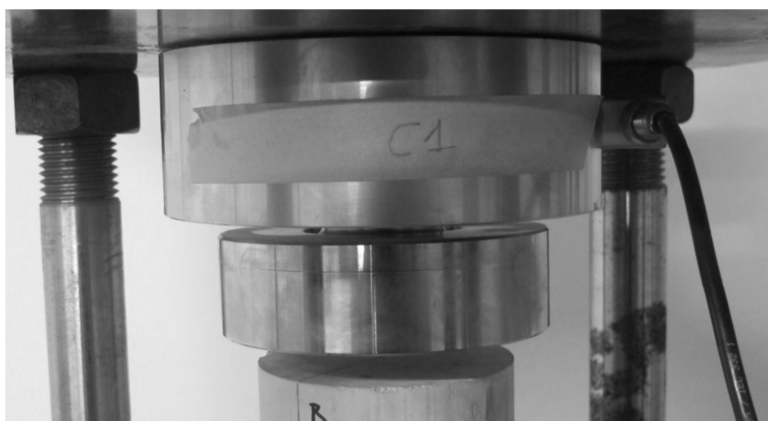


Figure 41: Load cell for viscous test

4.5 Instruments Table

Sample	Instrument	Test type	Test Conditions
Beam "B"	Ω 8; LVDT 10-4/10-5;	Creep test;	Climatic conditions controlled
Beam "M1"	Ω 1; LVDT 10-1/10-3;	Creep test;	Climatic conditions controlled
Beam "M2"	Ω 9; LVDT 10-2/10-6;	Creep test;	Climatic conditions controlled
Cylinder "B \varnothing 10"	E 13/14; E 17/18;	Shrinkage test; Creep test;	Climatic conditions controlled
Cylinder "B \varnothing 15"	E 3/4;	Shrinkage test;	Climatic conditions controlled
Cylinder "M1 \varnothing 10"	E 9/10; E 25/26/27/28; Cell 1/2;	Shrinkage test; Creep test;	Climatic conditions controlled
Cylinder "M1 \varnothing 15"	E 7/8;	Shrinkage test;	Climatic conditions controlled
Cylinder "M2 \varnothing 10"	E 11/12; E 21/22/23/24; Cell 1/2;	Shrinkage test; Creep test;	Climatic conditions controlled
Cylinder "M2 \varnothing 15"	E 1/2;	Shrinkage test;	Climatic conditions controlled
Cylinder "S \varnothing 15"	E 5/6;	Shrinkage test;	Climatic conditions controlled
Prismatic "M1_P1"	Ω 5/6/7;	Crack test;	Ambient conditions
Prismatic "M1_P2"	Ω 5/6/7;	Crack test;	Ambient conditions
Prismatic "M1_P3"	Ω 5/6/7;	Crack test;	Ambient conditions
Prismatic "M2_P1"	Ω 5/6/7;	Crack test;	Ambient conditions
Prismatic "M2_P2"	Ω 5/6/7;	Crack test;	Ambient conditions
Prismatic "M2_P3"	Ω 5/6/7;	Crack test;	Ambient conditions
Prismatic "S_P1"	Ω 5/6/7;	Crack test;	Ambient conditions
Prismatic "S_P2"	Ω 5/6/7;	Crack test;	Ambient conditions

Figure 42: Instruments test table

Well, in the table below you can see for each sample which instrument are used during all test.

In particular you can observe the climatic conditions for every test type.

4.6 Acquisition System

The various instruments described above are connected to the system for analyzing the long term data during the tests.

The measure acquisitions of Omega, LVDT and Strain Gauges are made with software called “LabView” to monitoring in time the quantities. The signals are amplified from two amplifiers called “2120” and “1520/1521/1540” and connected to PC.

4.6.1 SCXI System

It is one chassis, of National Instruments, that connect all the modulus to a plug-in scheme for the data acquisition (DAQ). This system is programmed by the same software LabView. One singular modulus can observe up to 8 channels.

4.6.2 LabView Software

The programming language used in this software is different from others because it is graphic. The definition of the data and the algorithm is made by graphical objects, connected by a wire. This language is defined as dataflow and can be treated in multithreading mode.

The extension of the output file is .dat and can be used by some software like Excel.

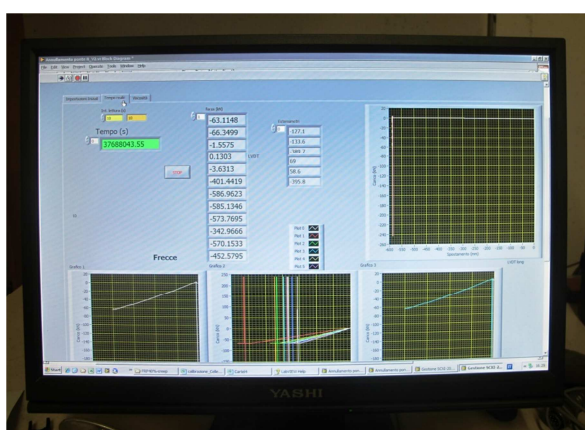


Figure 43: Software interface

4.6.3 Excel File

The output file can be imported in Excel to make data elaborations and their representations.

Steel and Macro-Synthetic Self-Compacting Fiber Reinforced Concrete, Experimental Study on the Long-Term Deformations

The image shows a screenshot of an Excel spreadsheet with a large data table. The table has columns labeled with various parameters and rows labeled with IDs like 'P1000001'. The data is color-coded according to the legend provided below. The spreadsheet interface includes the ribbon (File, Home, Insert, Page Layout, Formulas, Data, Review, View) and the status bar at the bottom.

Yellow: Time;
 Purple: Load Cells for viscosity tests of cylinders;
 Green: Omega for deflection measuring of beams;
 Blue: Strain Gauges for compression tests of cylinders;
 Pink: Strain Gauges for shrinkage tests of cylinders;
 Brown: LDVT for deflection measuring of beams;

5. Cracking and Rupture Analysis of Prismatic Samples

5.1 Generalities

In this paragraph there are showed the results found during the rupture of the prismatic samples. The dimensions of the sample are 150 x 150 x 550 mm. Three samples are made for the M1 mixture, three samples for the M2 and two samples for the S. The samples are loaded according to the center, at 500 mm of distance, according to the code DS/EN 11039. This method can be used only if the length of the fibers is less than 60 mm. The width of the cut must be less than 5 mm while the height of the samples ≥ 125 mm.

5.2 Test Principle

The tensional behavior for the fiber reinforced concrete is evaluated in terms of residual traction resistance due to flexure, determined by Tension-CMOD curve applying concentrated loads on the mid-span of a simply supported scheme.

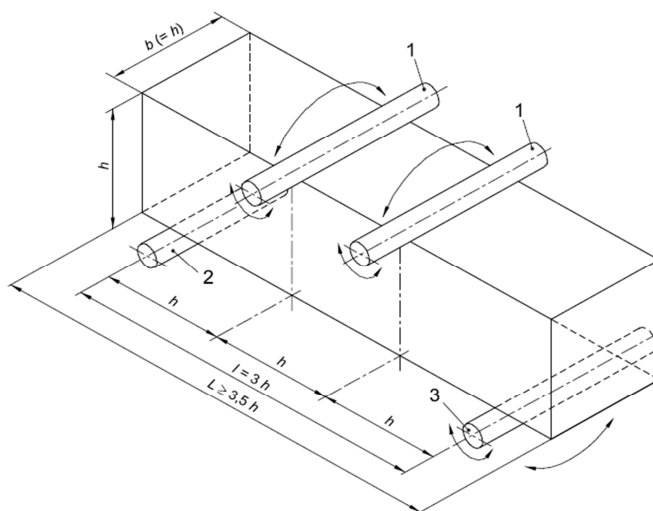


Figure 44: Rupture scheme test

5.3 Test Preparation

A wet sawing is used for cutting the sample, as you can see in the picture.



Figure 45: Wet sawing

Before testing we have to draw on the samples the reference lines, to put and load the prisms in the exact position. After that, we apply the transducer Omega in three points: over, on the left and on the right of the cut. Then, the machine is verified in all components and the sample is put in the centered position.

The speed limits of the load increment are that:

$$\begin{cases} 0.05 \text{ mm/min of CMOD} \leq 0.1 \text{ mm} \\ 0.1 < 0.2 \text{ mm/min of CMOD} \geq 4 \text{ mm} \end{cases}$$

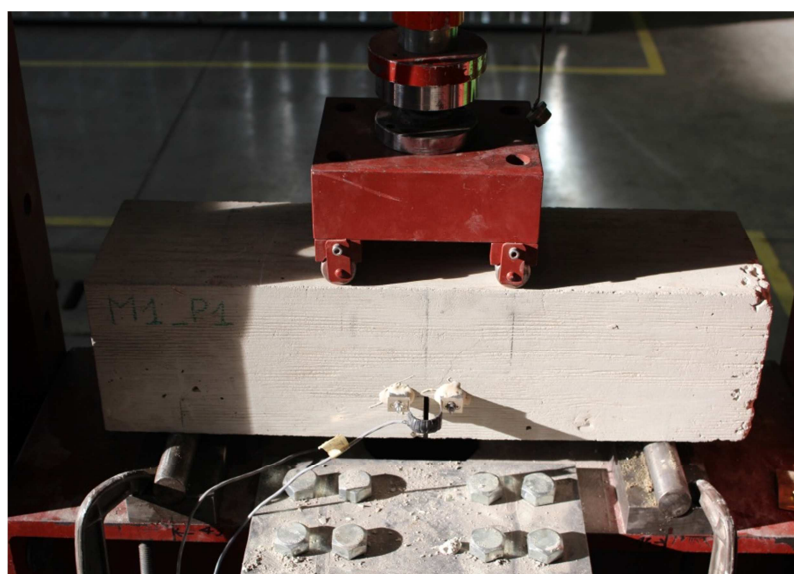


Figure 46: Test preparing

5.4 Hand Calculation

5.4.1 Maximum Bending Moment

From the theoretical scheme the maximum bending moment is:

$$M = \frac{F * h}{2}$$

Where:

- F is the concentrated load;
- h is 150 mm;

5.4.2 Tension

The tension is computed by the ratio between the moment and the resistance modulus:

$$\sigma = \frac{M}{W} = \frac{\frac{F * l}{2}}{\frac{b * h^2}{6}}$$

Where:

- b is the base of the sample = 150 mm;
- h is the height of the sample = 150 mm;

5.4.3 Effective Height

Because the cut is not exactly the same in all sides all samples, we have done the mean value:



Figure 47: Cut measuring

Sample	Hcut sx [mm]	Hcut dx [mm]	Hcut mean [mm]	H eff [mm]
M1_P1	47.42	45.02	46.22	103.78
M1_P2	45.05	43.73	44.38	105.62
M1_P3	45.53	48.25	46.89	103.11
M2_P1	48.34	45.18	46.76	103.24
M2_P2	44.53	44.62	44.58	105.42
M2_P3	46.80	47.07	46.94	103.06
S_P1	45.32	44.67	44.99	105.01
S_P2	45.01	45.03	45.02	104.98

5.4.4 Effective Resistance Modulus

Sample	W [mm^3]
M1_P1	269257.21
M1_P2	278916.02
M1_P3	265791.80
M2_P1	266462.44
M2_P2	277860.77
M2_P3	265559.86
S_P1	275651.25
S_P2	275520.01

5.5 Tests Results & Diagrams

In this paragraph we have represented the behaviors of all samples referred to the code limits of crack opening.

The force is expressed in Kg, the Crack Opening in mm and the Nominal Tension in MPa.

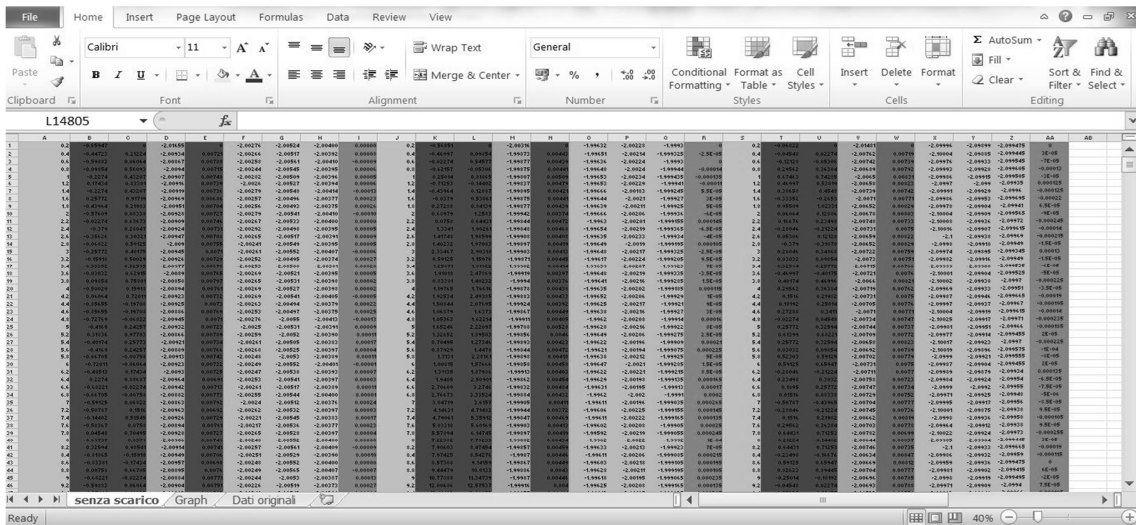


Figure 48: Excel cracking computations file

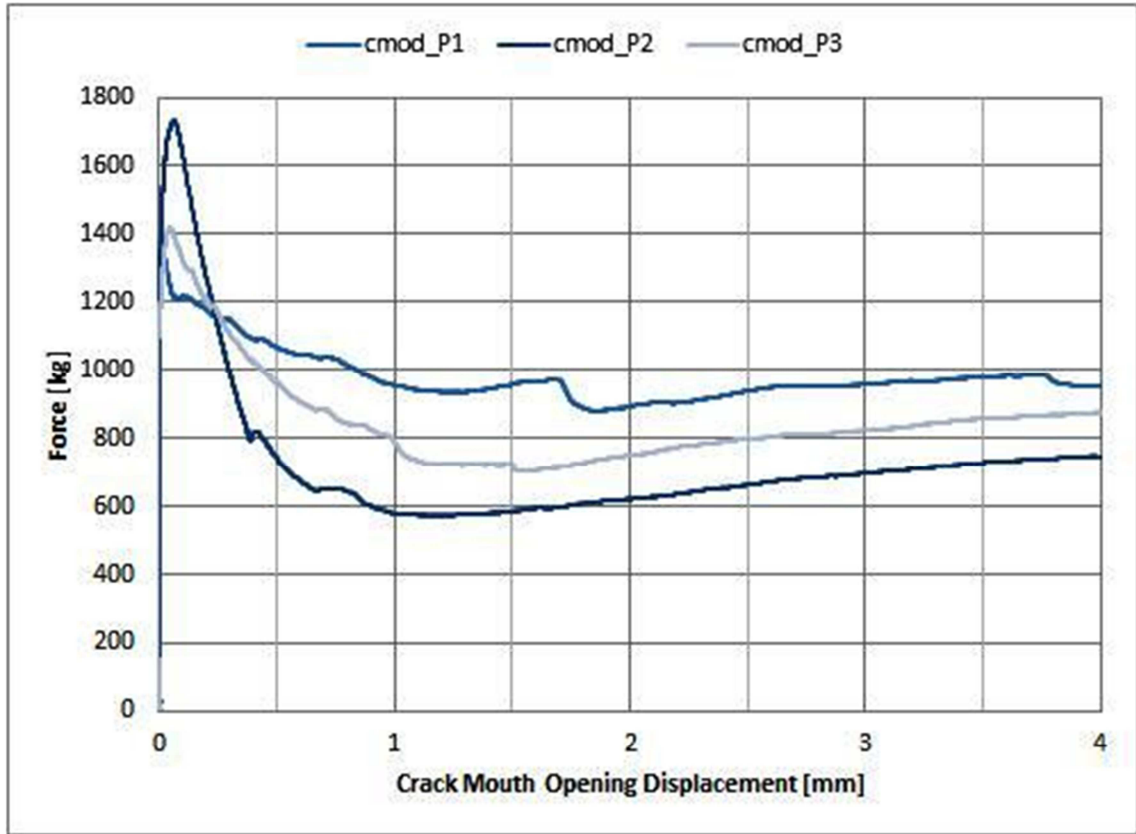


Figure 49: Force-CMOD for M1

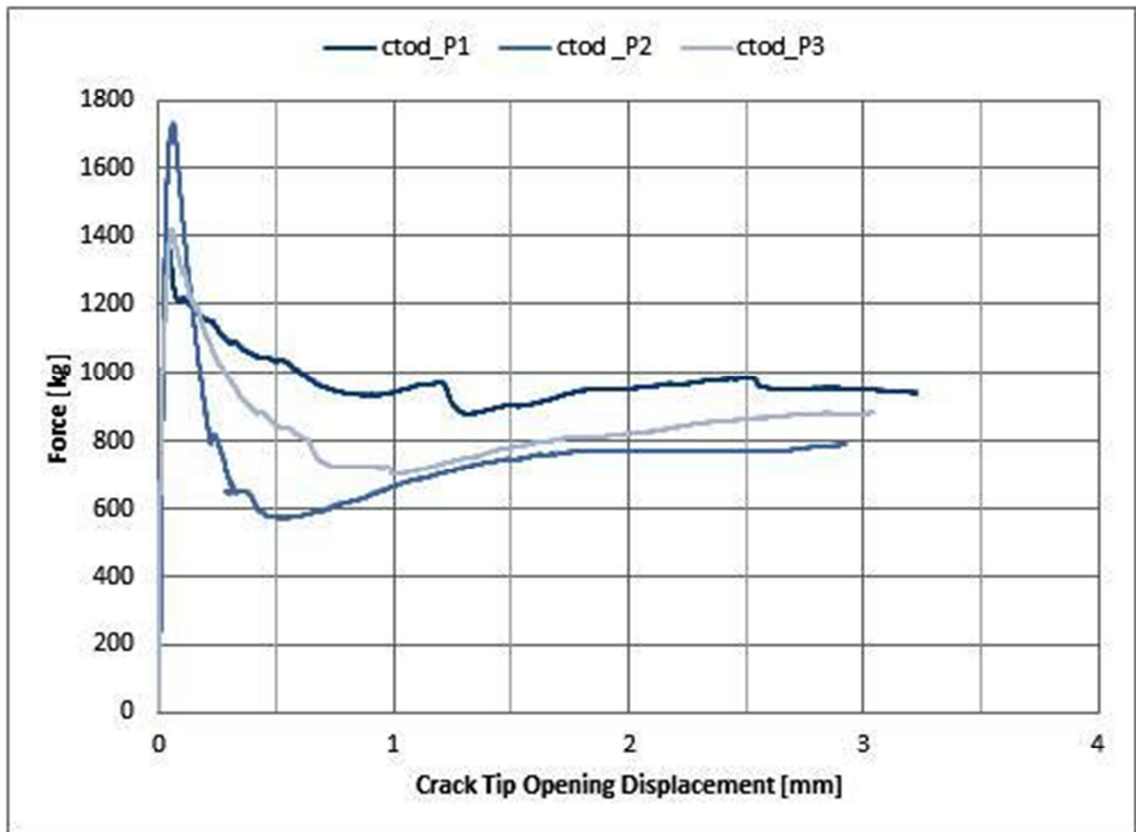


Figure 50: Force-CTOD for M1

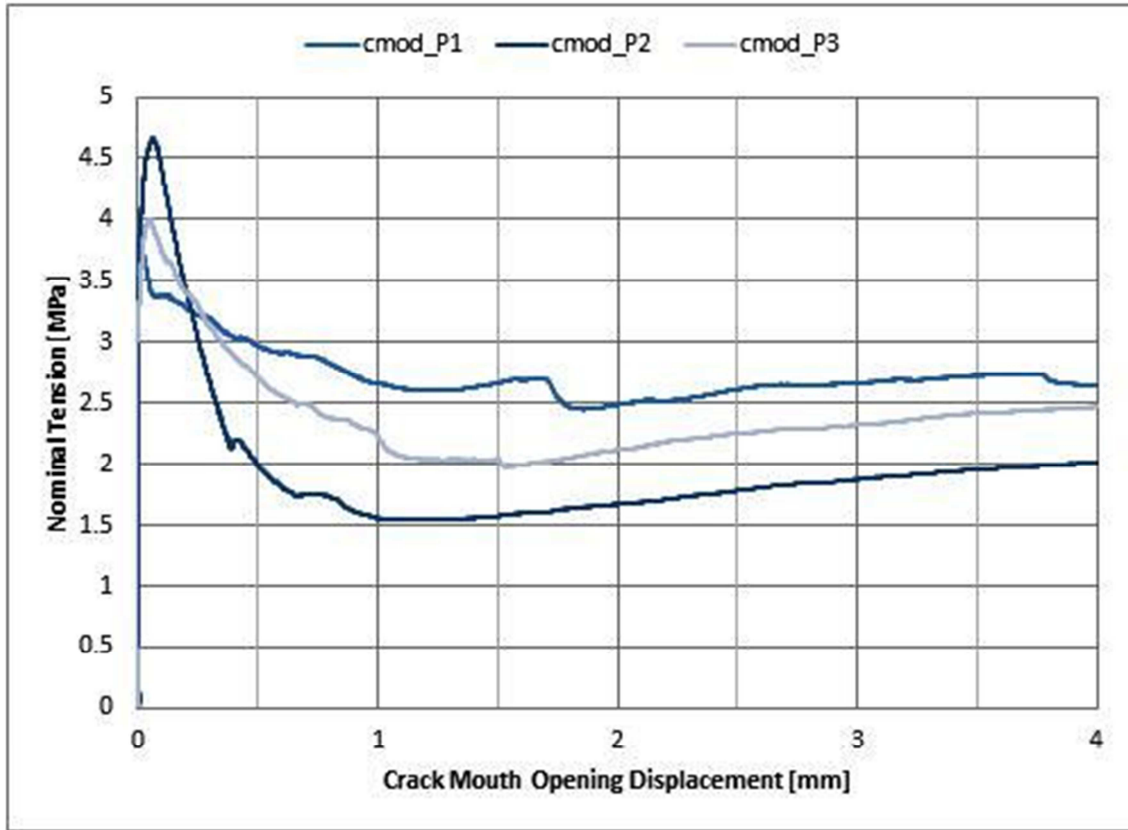


Figure 51: Tension-CMOD for M1

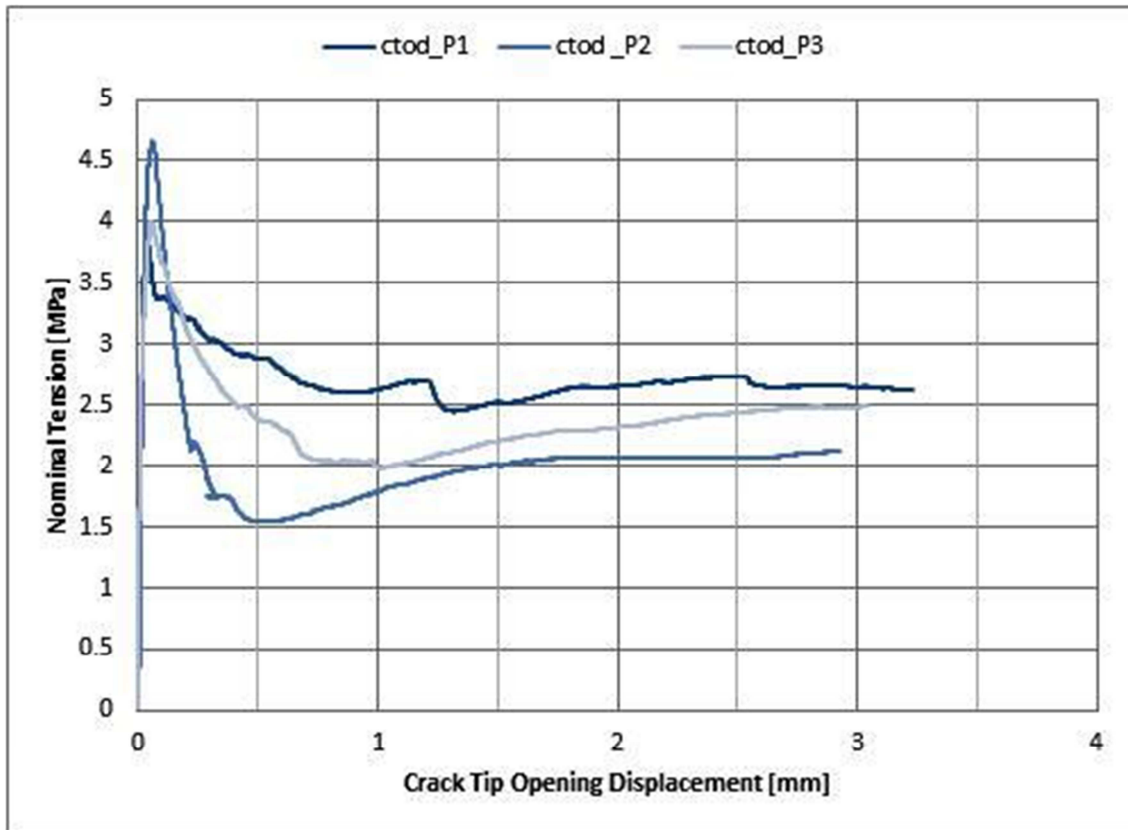


Figure 52: Tension CTOD for M1

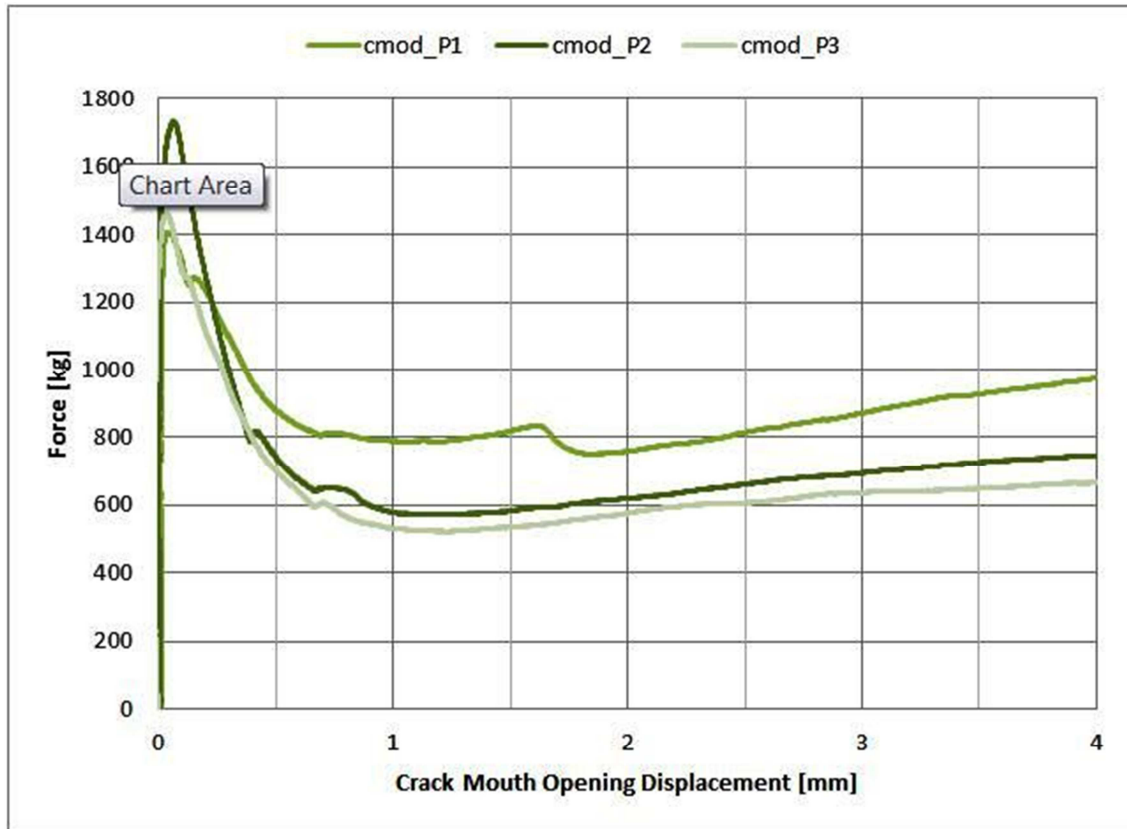


Figure 53: Force-CMOD for M2

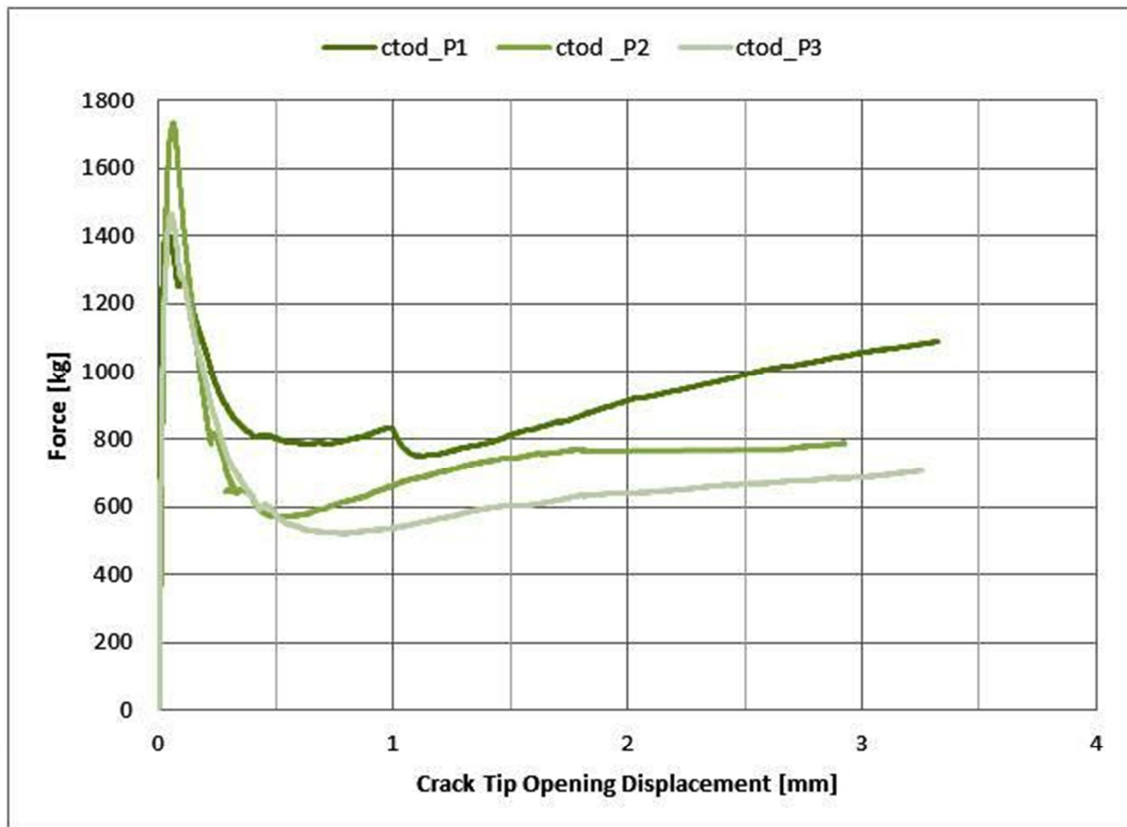


Figure 54: Force-CTOD for M2

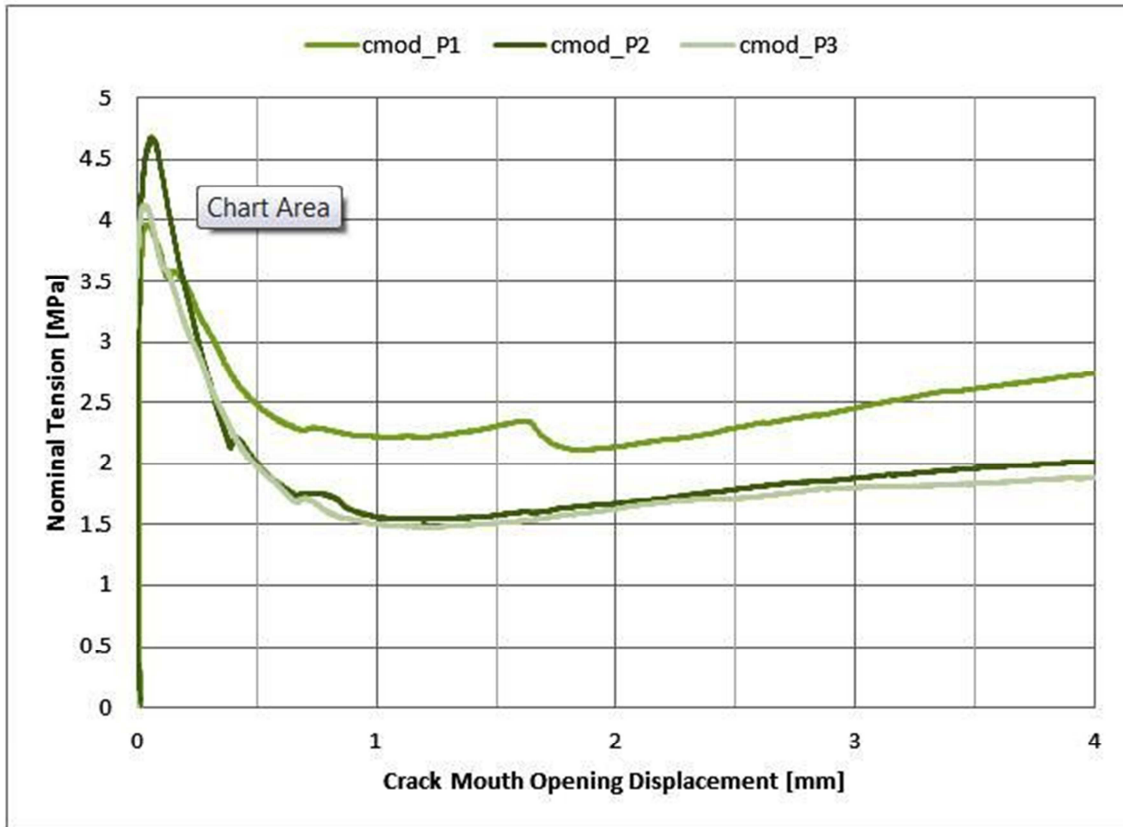


Figure 55: Tension-CMOD for M2

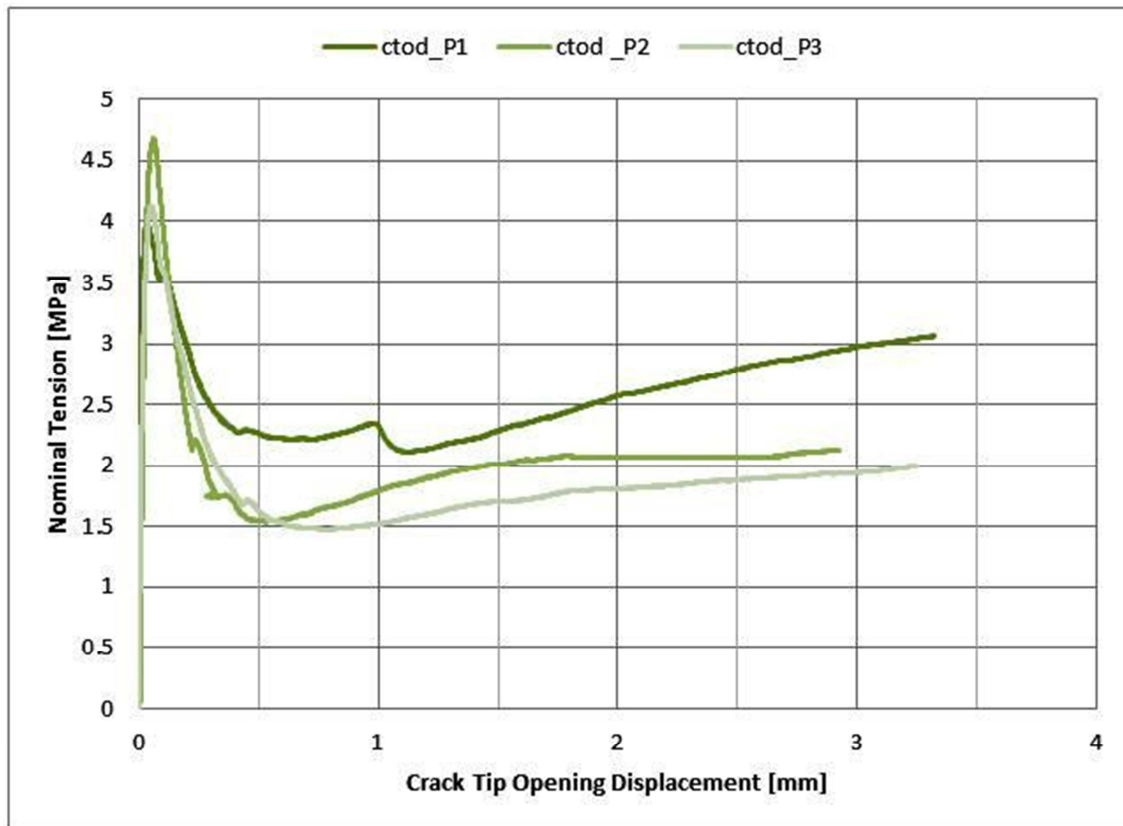


Figure 56: Tension-CTOD for M2

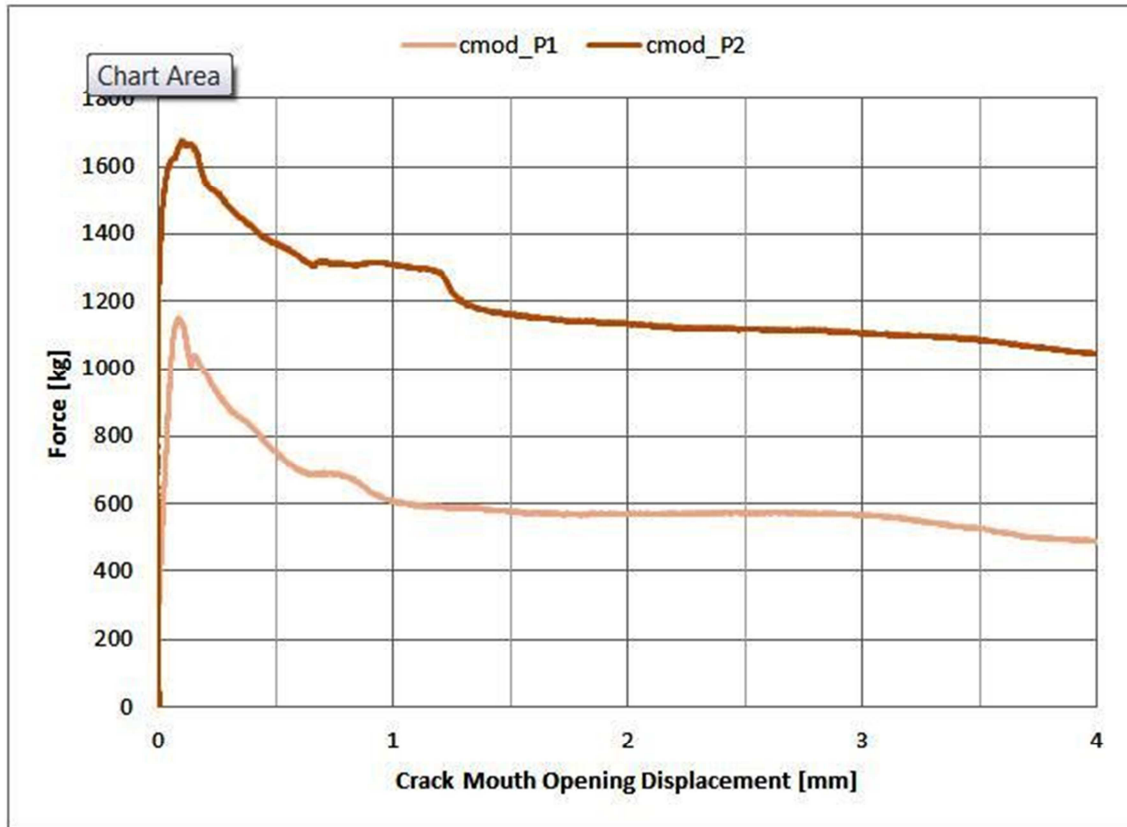


Figure 57: Force-CMOD for S

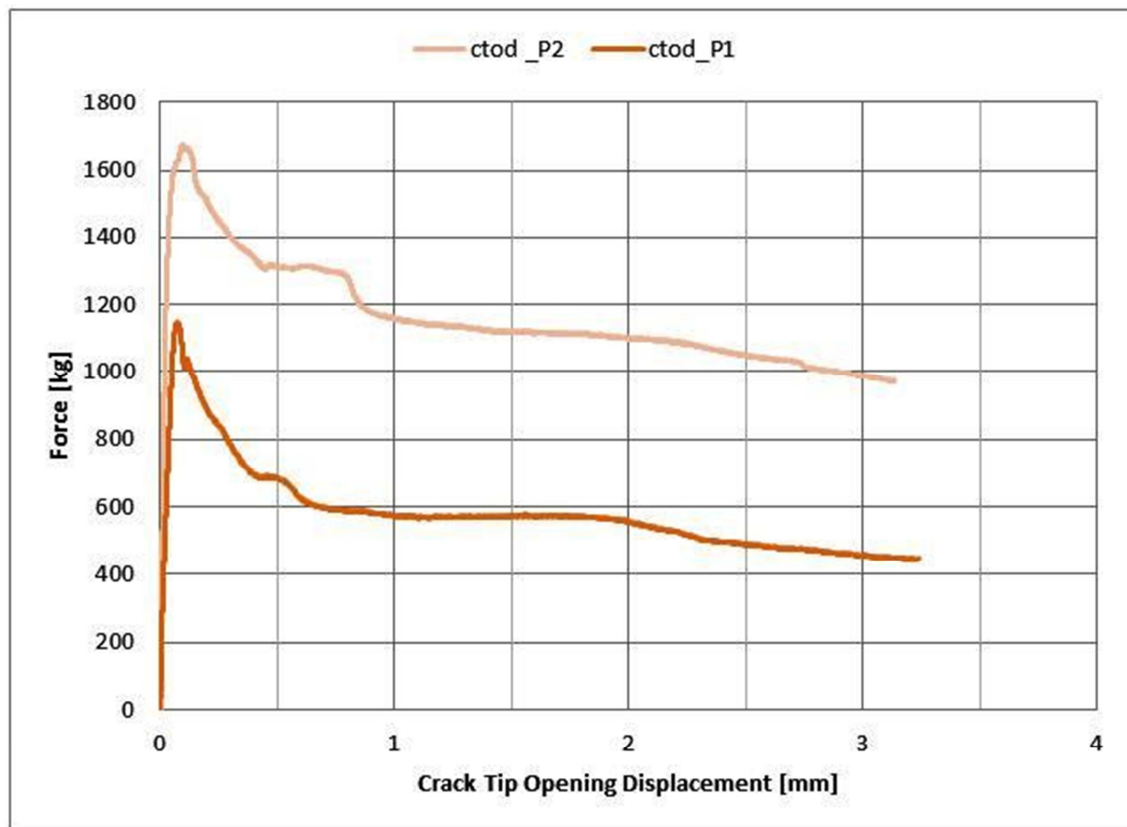


Figure 58: Force-CTOD for S

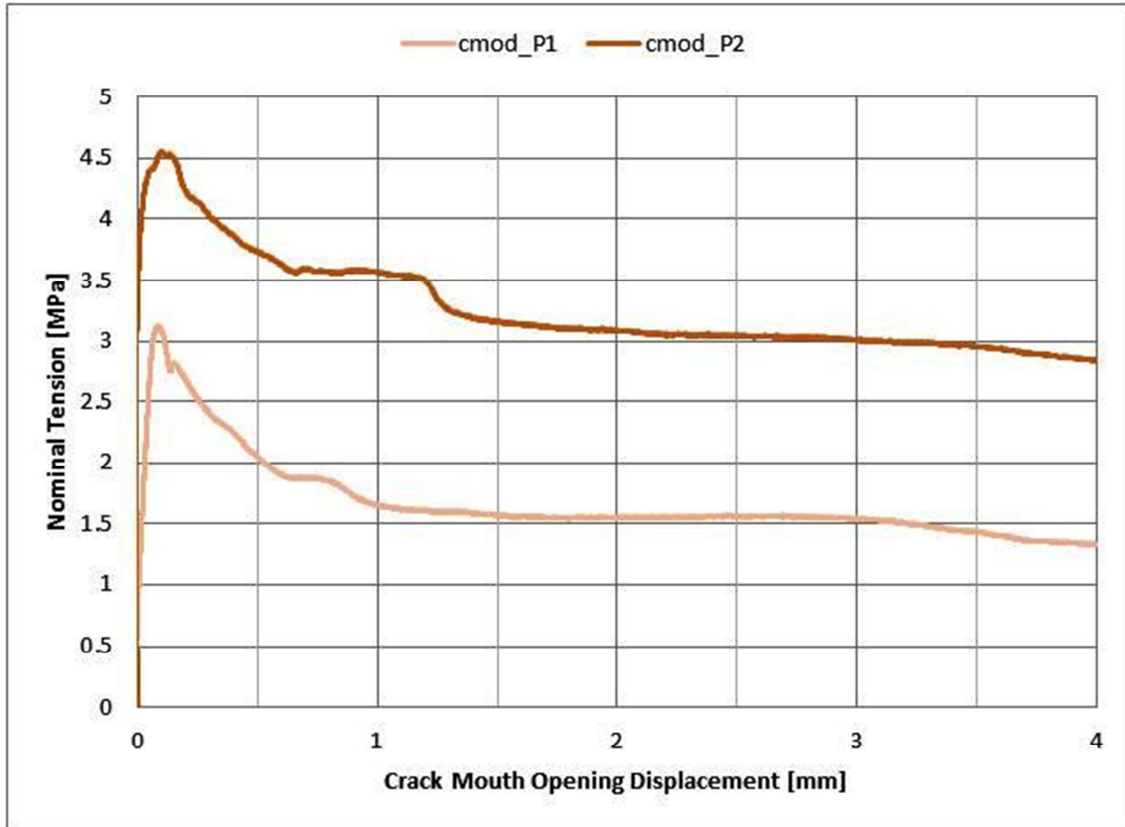


Figure 59: Tension-CMOD for S

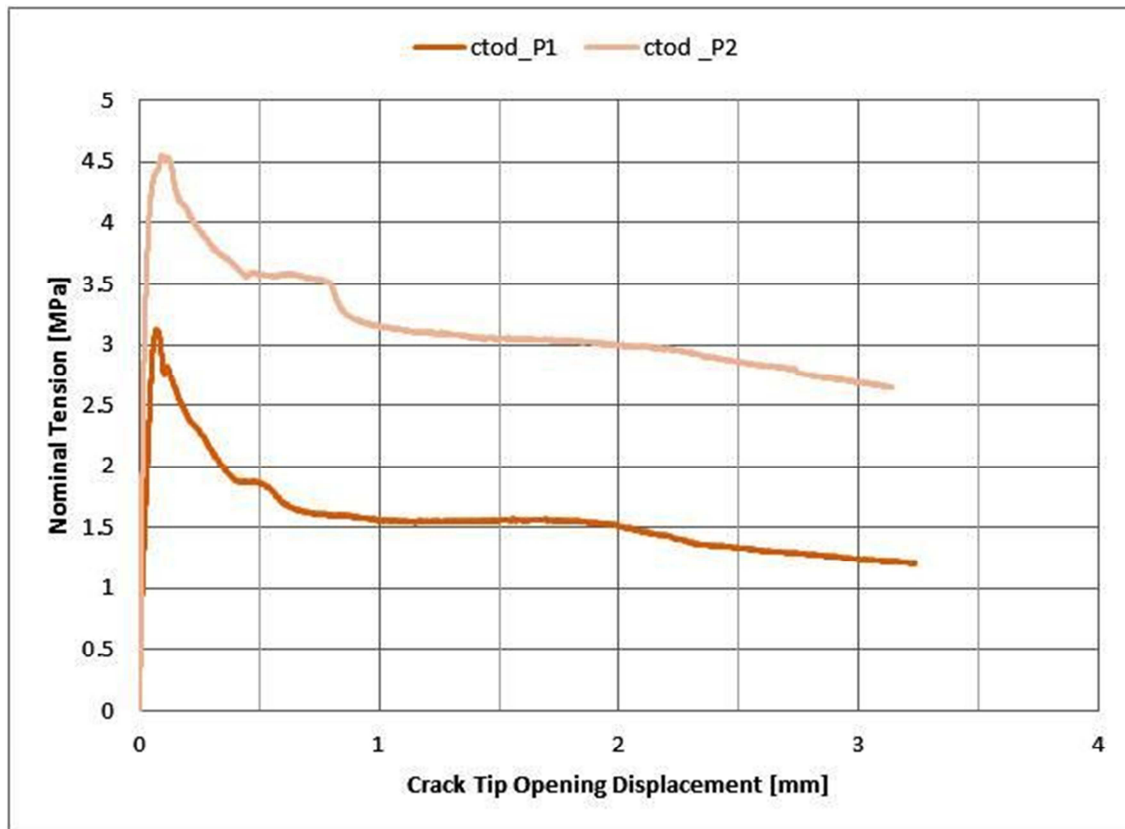


Figure 60: Tension-CTOD for S

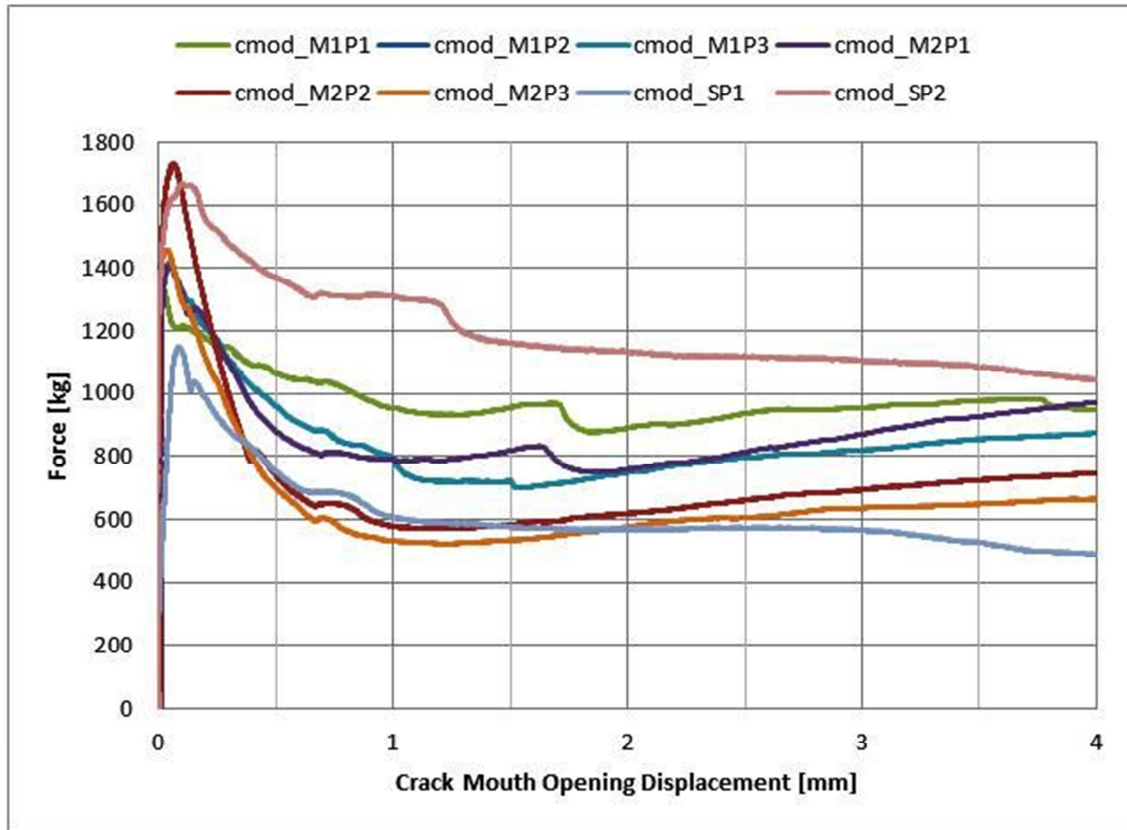


Figure 61: Force-CMOD for all samples

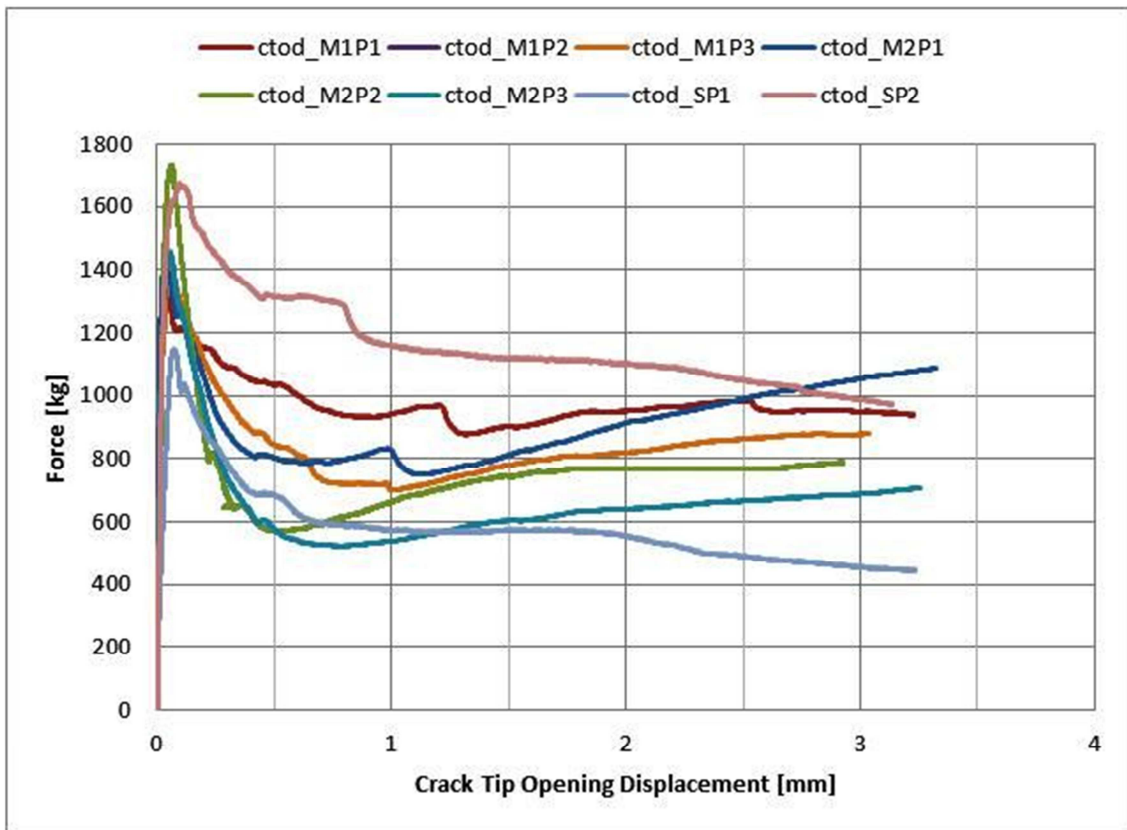


Figure 62: Force-CTOD for all samples

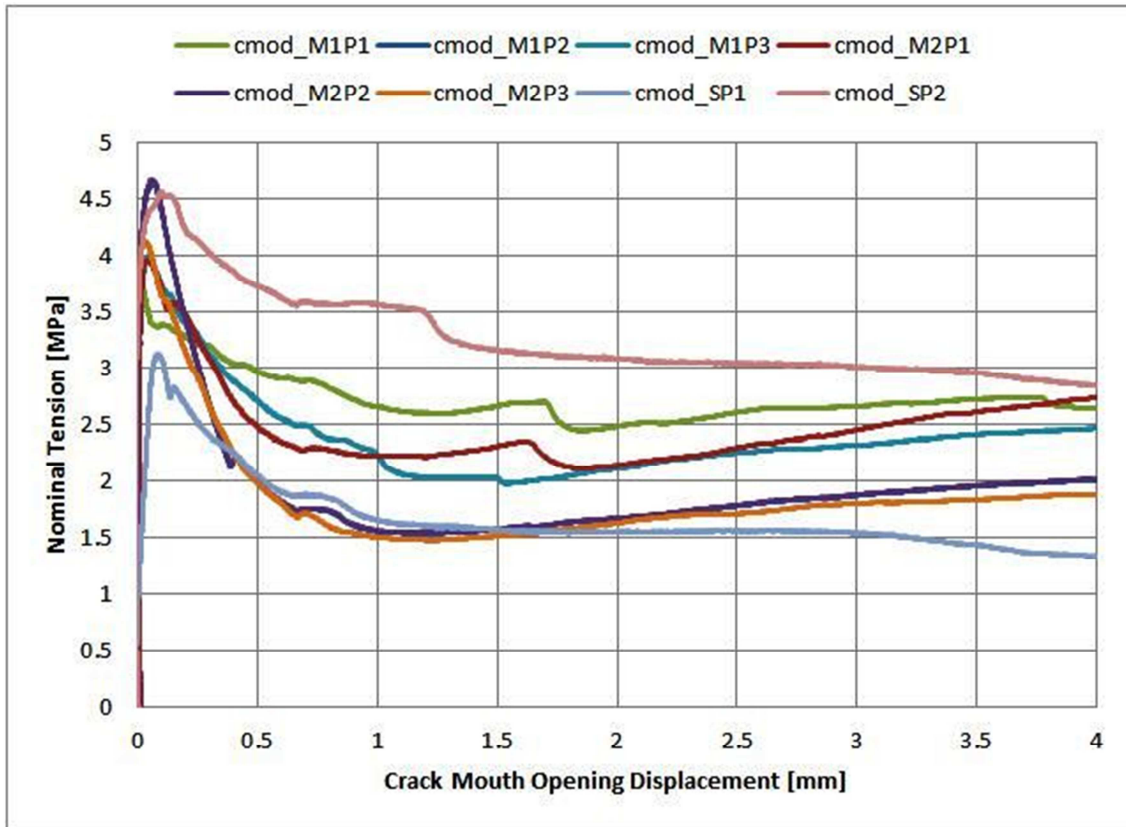


Figure 63: Tension-CMOD for all samples

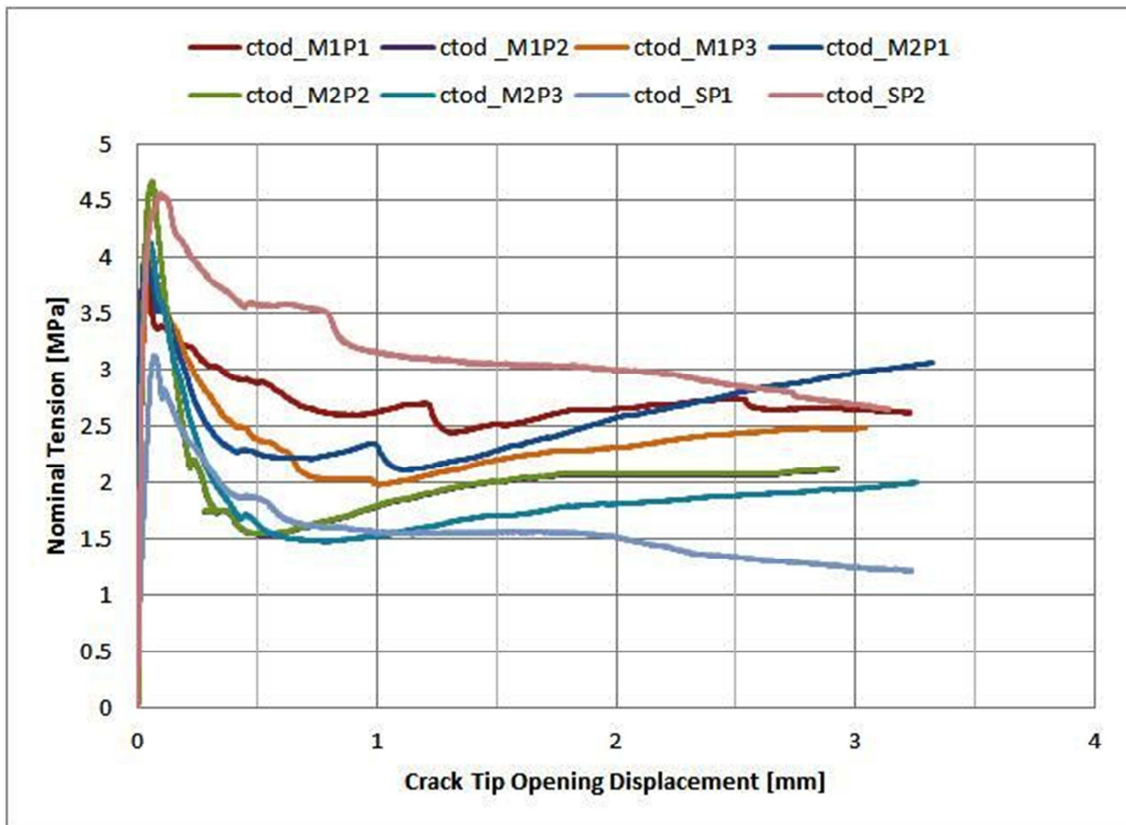
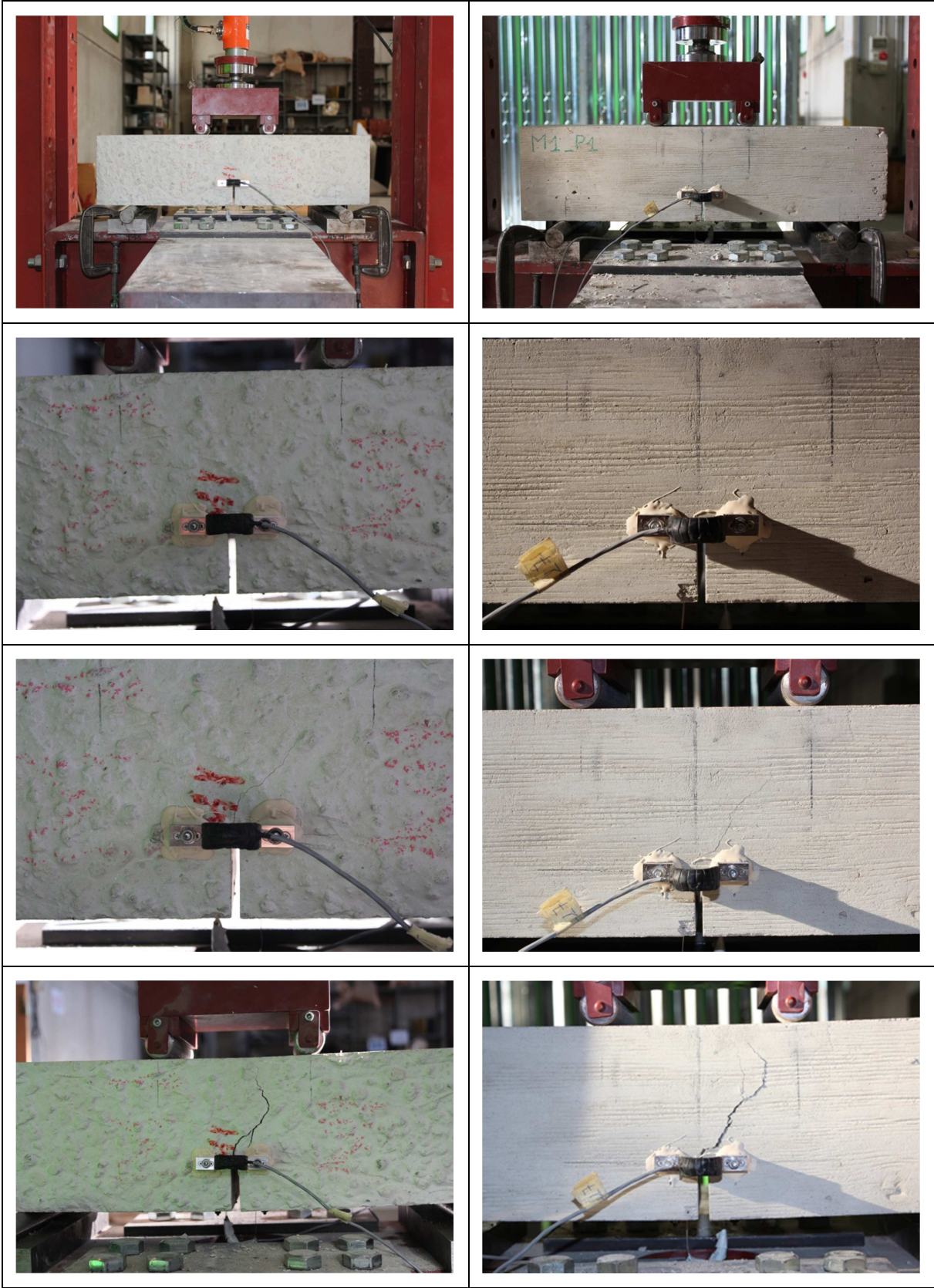


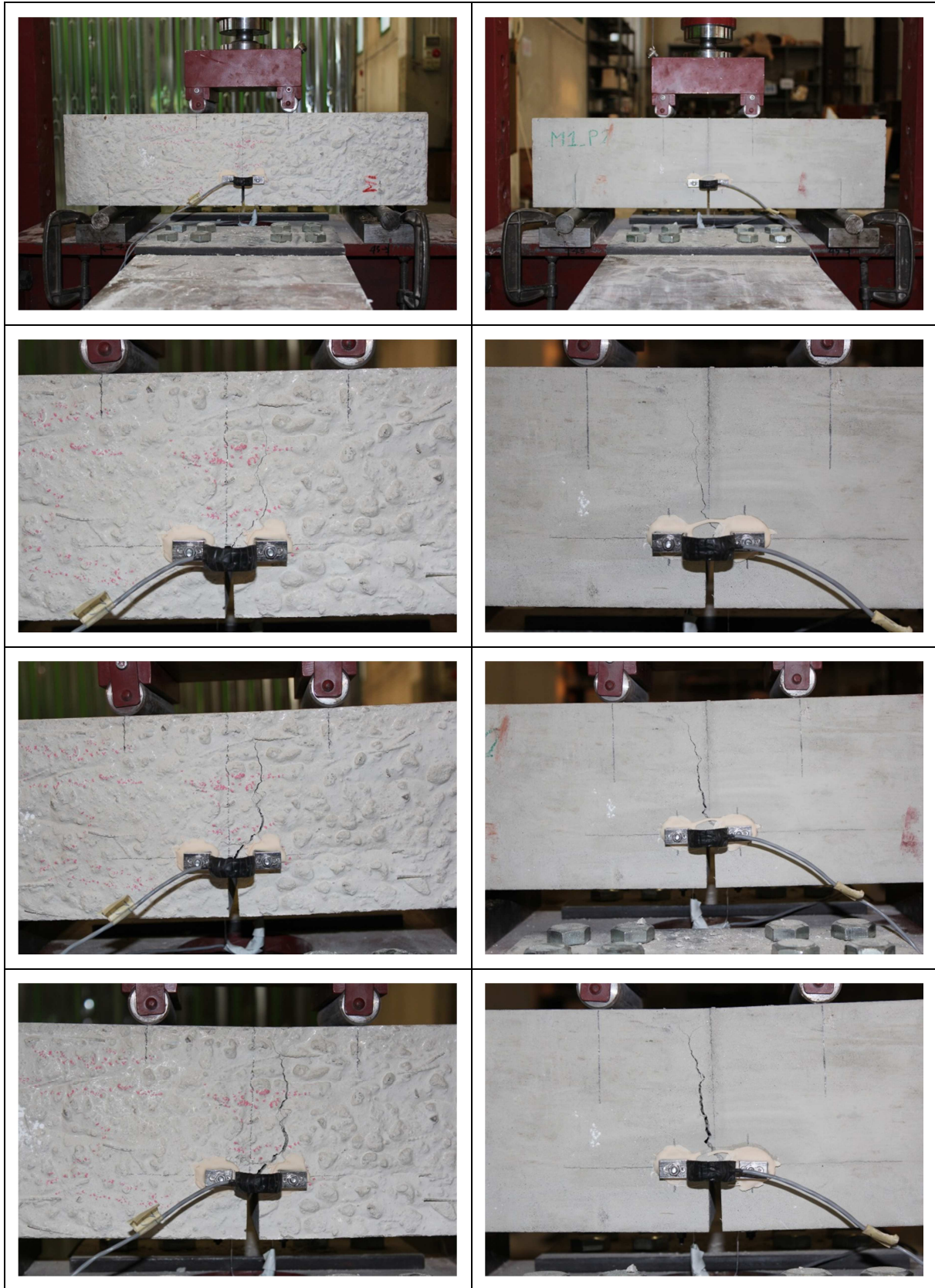
Figure 64: Tension-CTOD for all samples

Steel and Macro-Synthetic Self-Compacting Fiber Reinforced Concrete,
Experimental Study on the Long-Term Deformations

▪ Pictures of MIP1 sample test

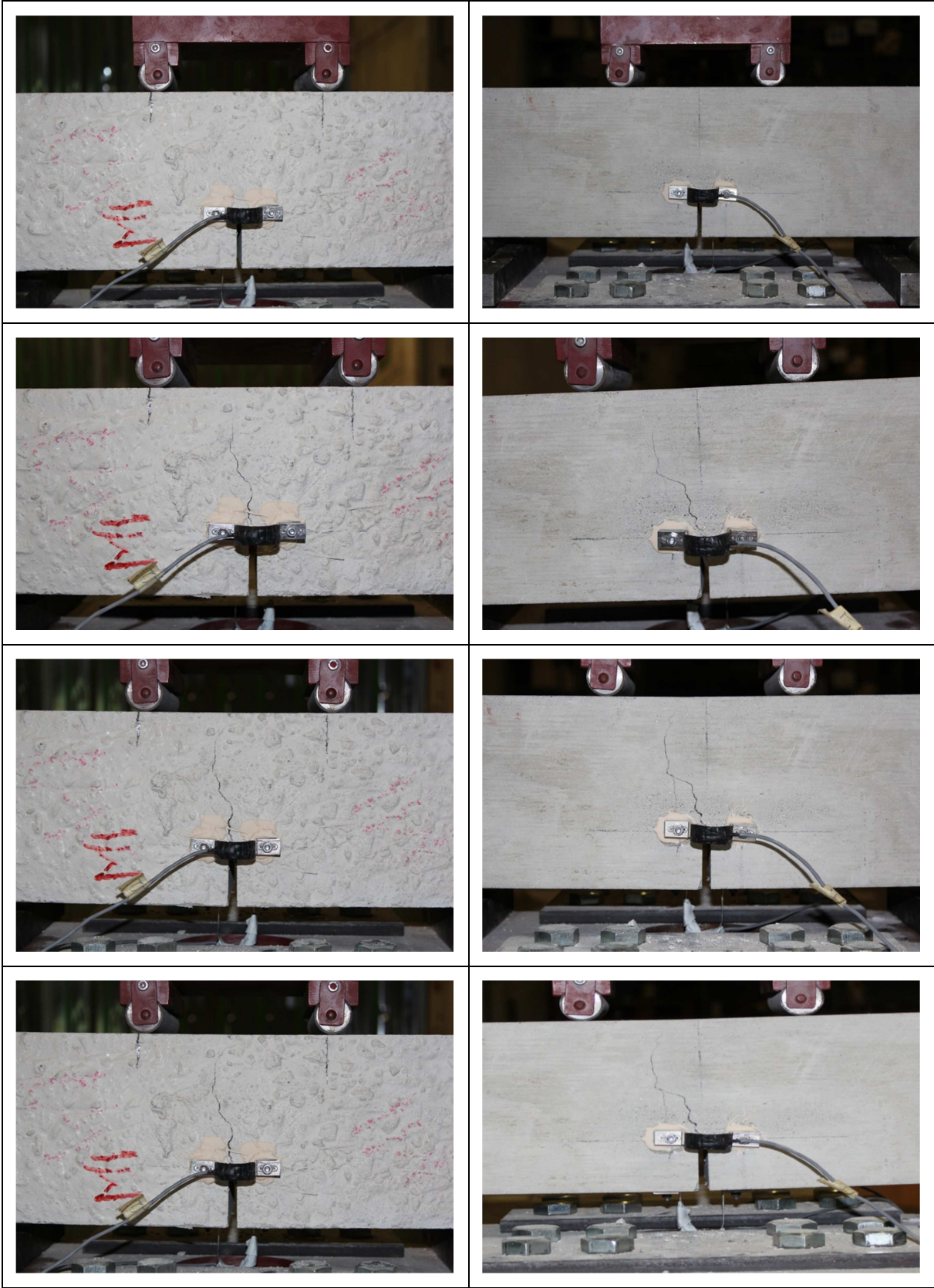


▪ *Picture of M1P2 sample test*

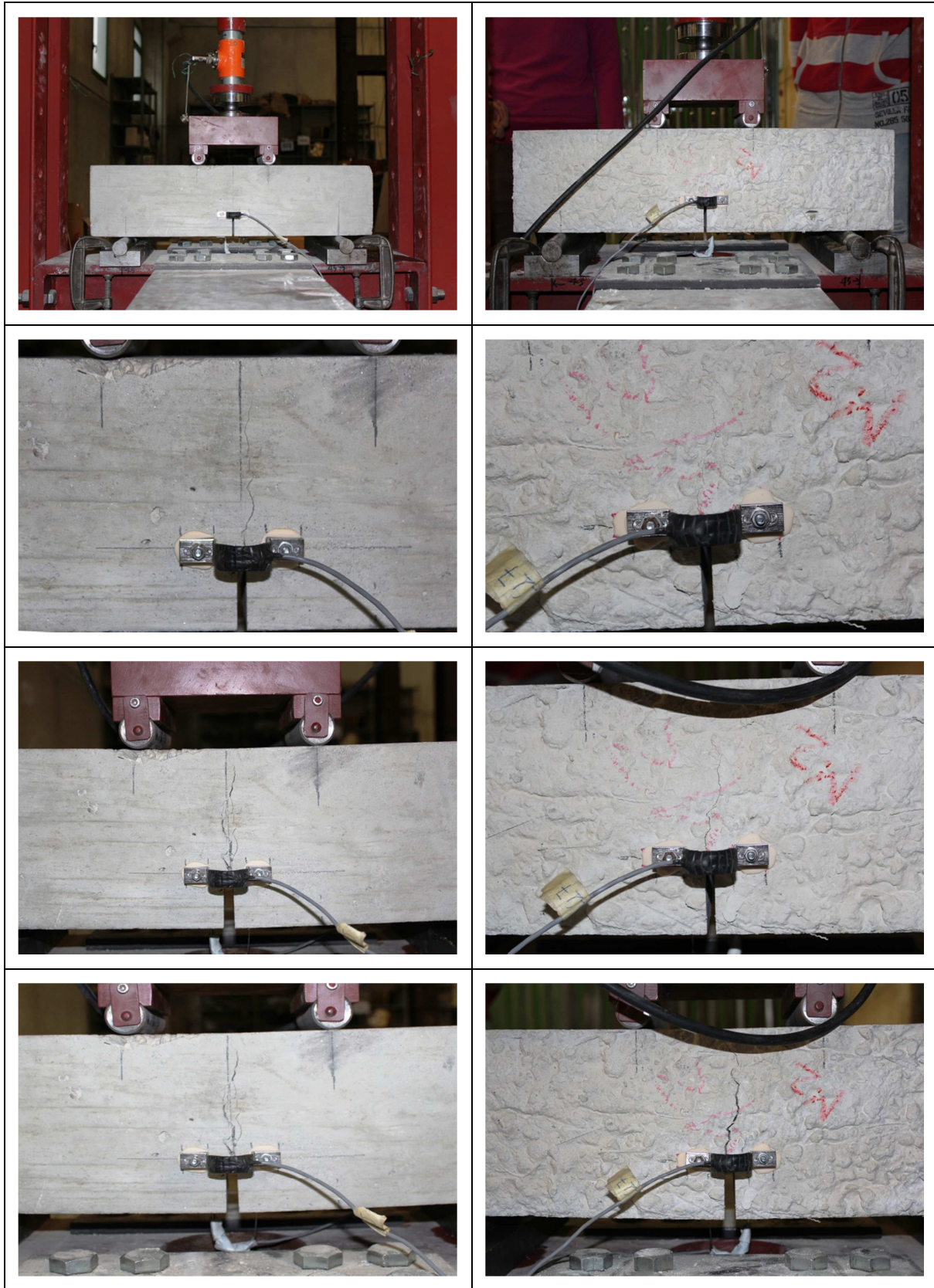


Steel and Macro-Synthetic Self-Compacting Fiber Reinforced Concrete,
Experimental Study on the Long-Term Deformations

▪ *Picture of MIP3 sample test*

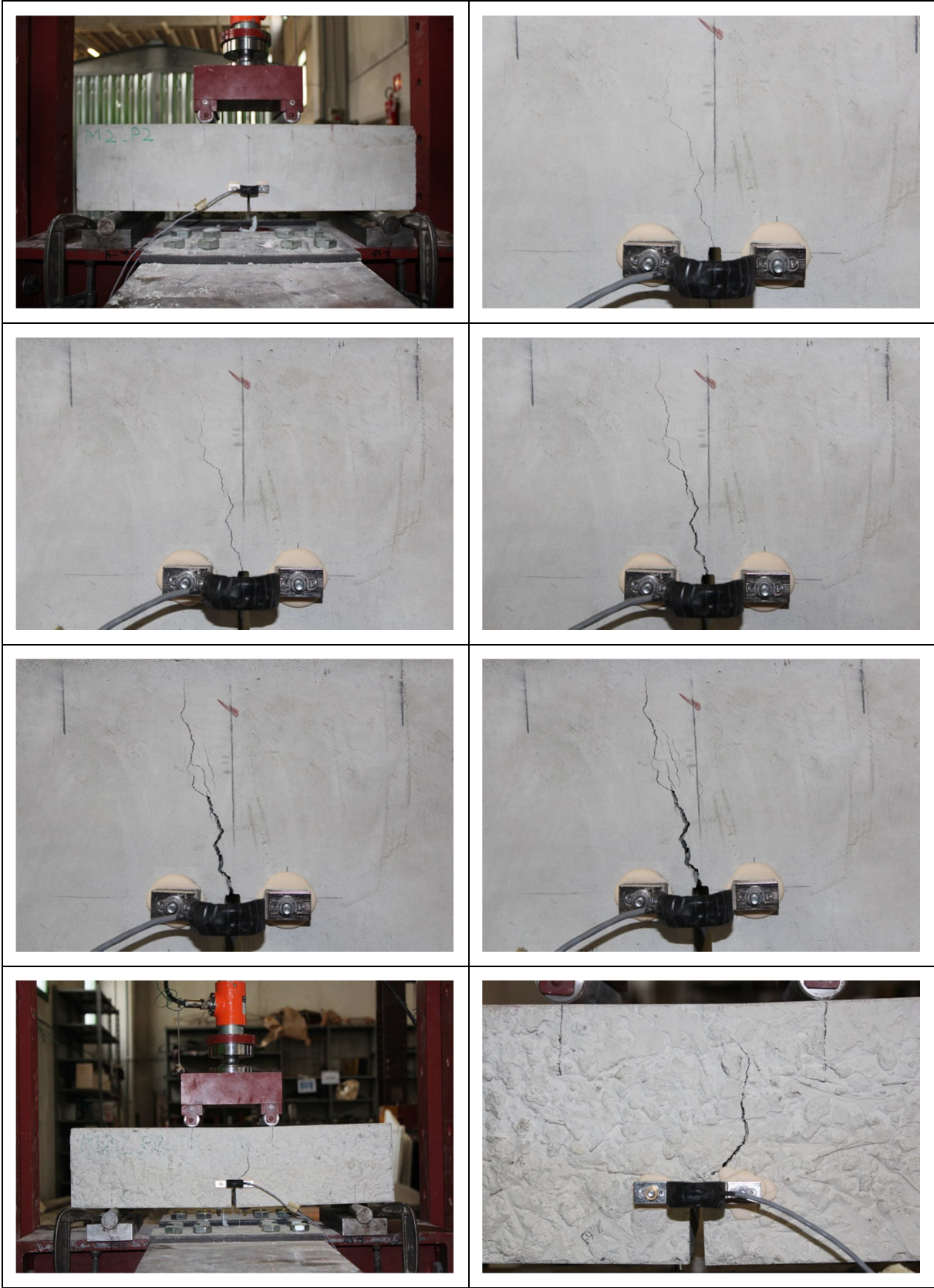


▪ *Pictures of M2P1 sample test*



Steel and Macro-Synthetic Self-Compacting Fiber Reinforced Concrete,
Experimental Study on the Long-Term Deformations

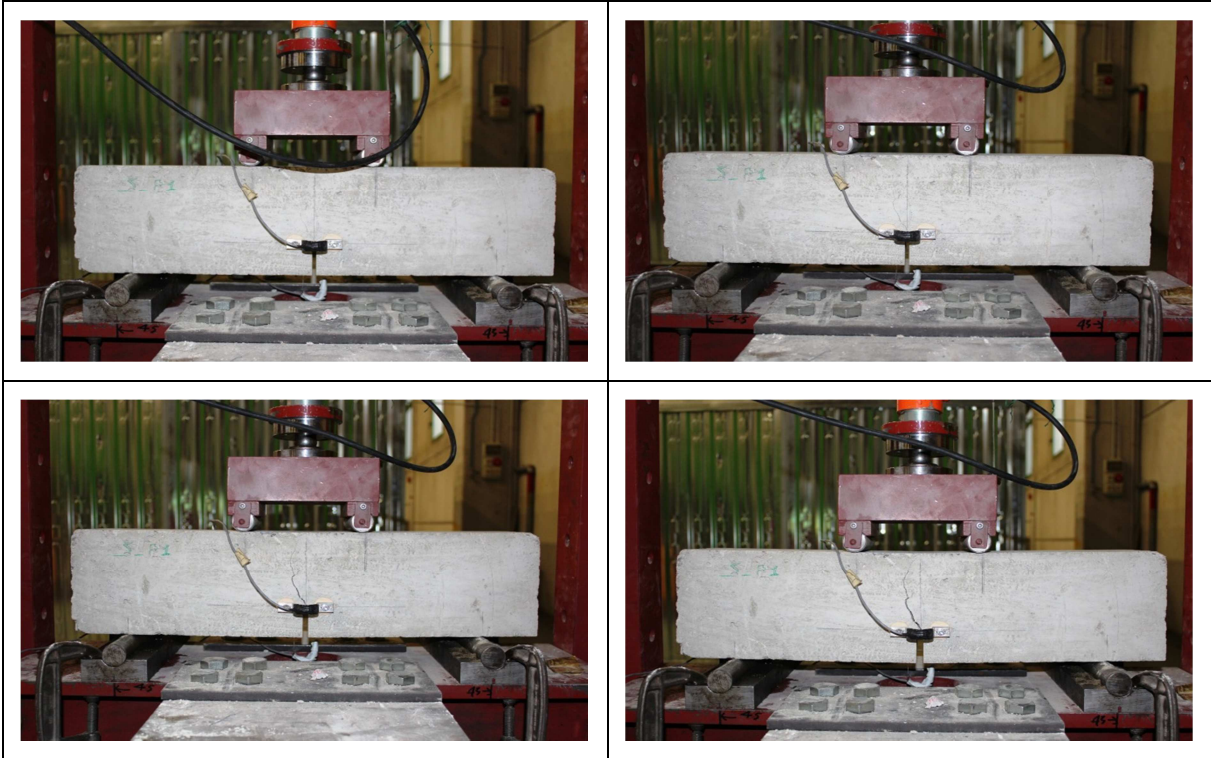
▪ Pictures of M2P2 sample test



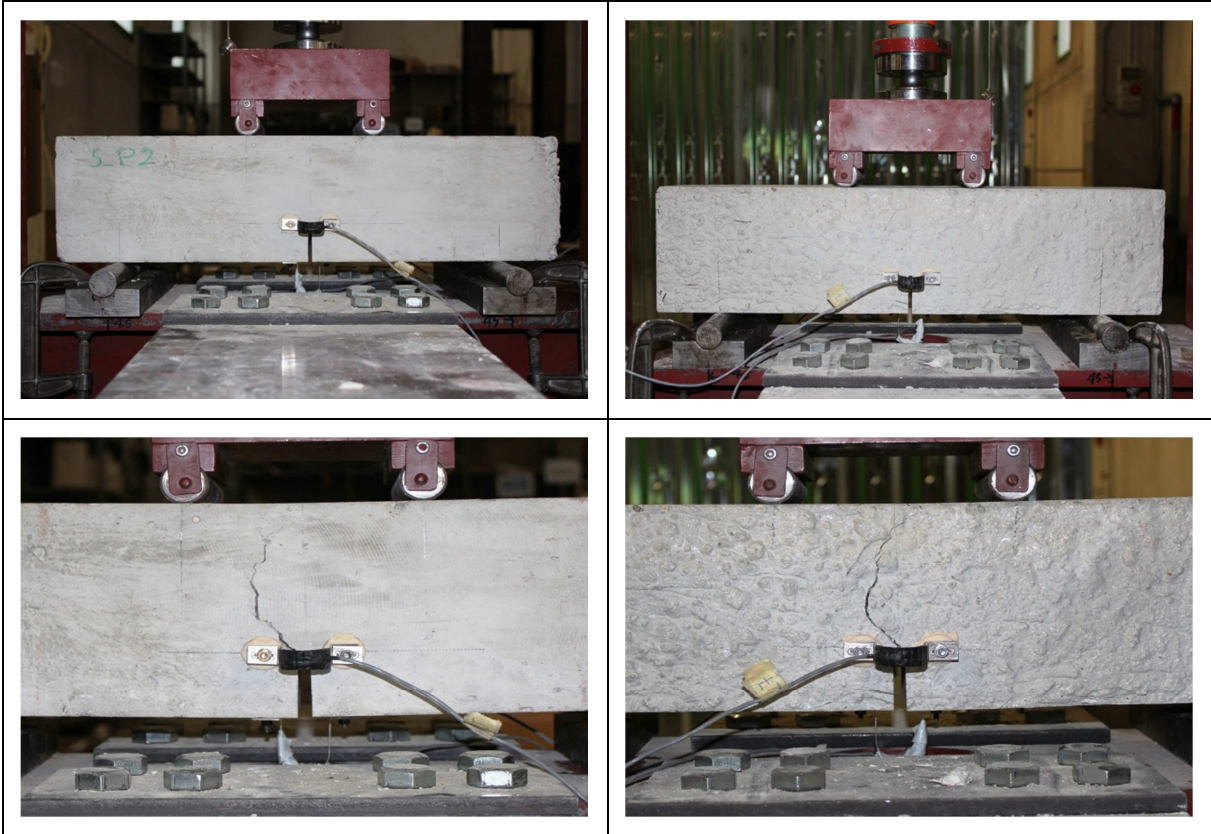
▪ *Pictures of M2P3 sample test*



▪ Pictures of SP1 sample test

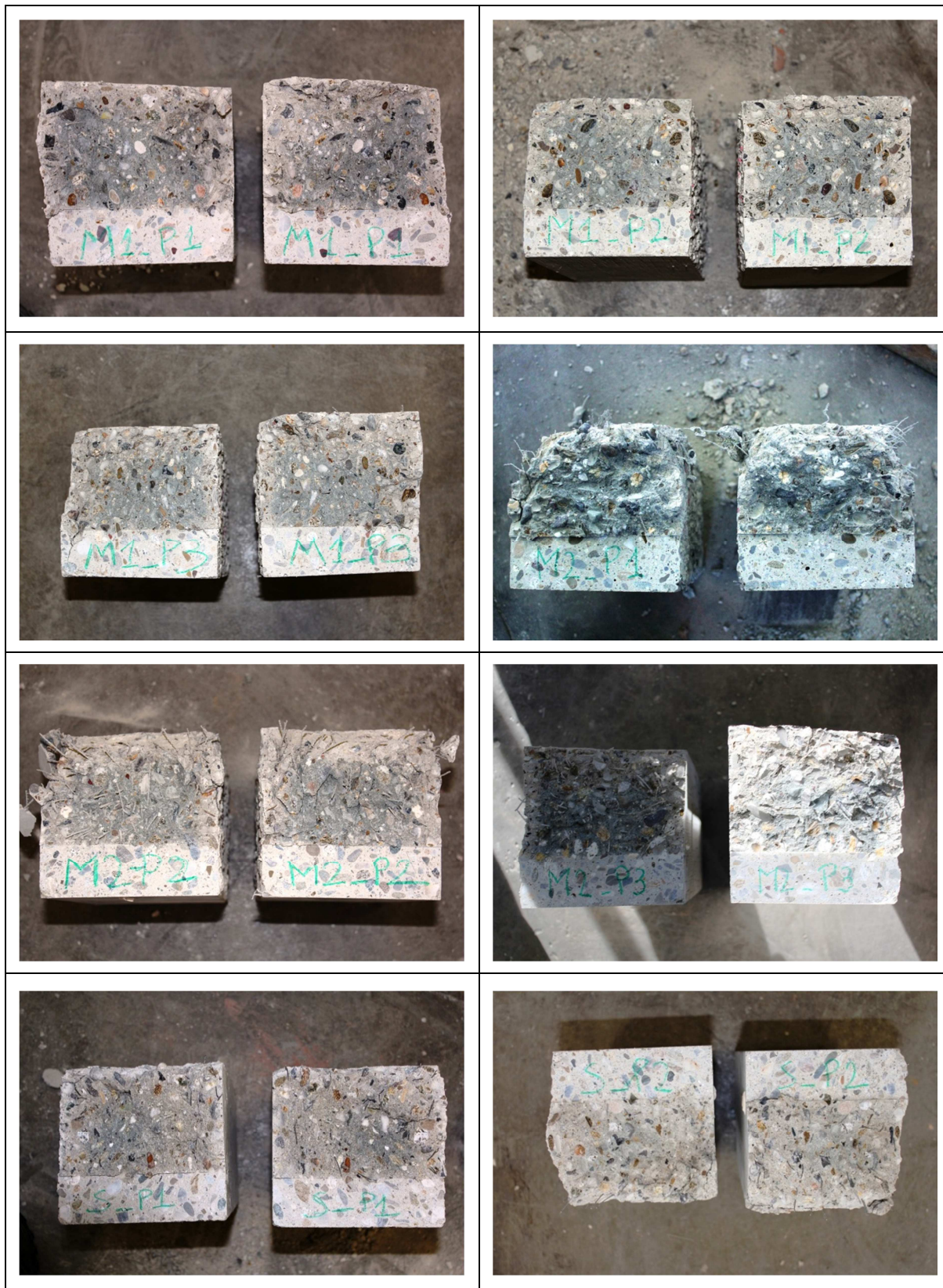


▪ Pictures of SP2 sample test



▪ *Rupture samples*

At the end of the test phase the samples are broken to evaluate in a better mode the behavior of the fibers and their influence inside the concrete.



5.6 Fibers Distribution Analysis

After the rupture of all the samples we have counted how many fibers there was in a cracked face and in particular we have subdivided in two zones these surfaces in order to analyze the fiber distribution and their influence on the resistance.

In the table below you can see all the results.

Samples	Fibers Upper Part	Fibers Middle Part	Total Fibers
M1_P1	34	26	60
M1_P2	34	18	52
M1_P3	29	27	56
M2_P1	81	41	122
M2_P2	80	55	135
M2_P3	59	45	104
S_P1	37	17	54
S_P2	45	35	80

Figure 65: Fibers counting table

In the chart below are represent all types of prismatic samples in function of the Nominal Tension evaluated during the cracking test at three certain points:

- 1 mm of CTOD;
- 2 mm of CTOD;
- 3 mm of CTOD;

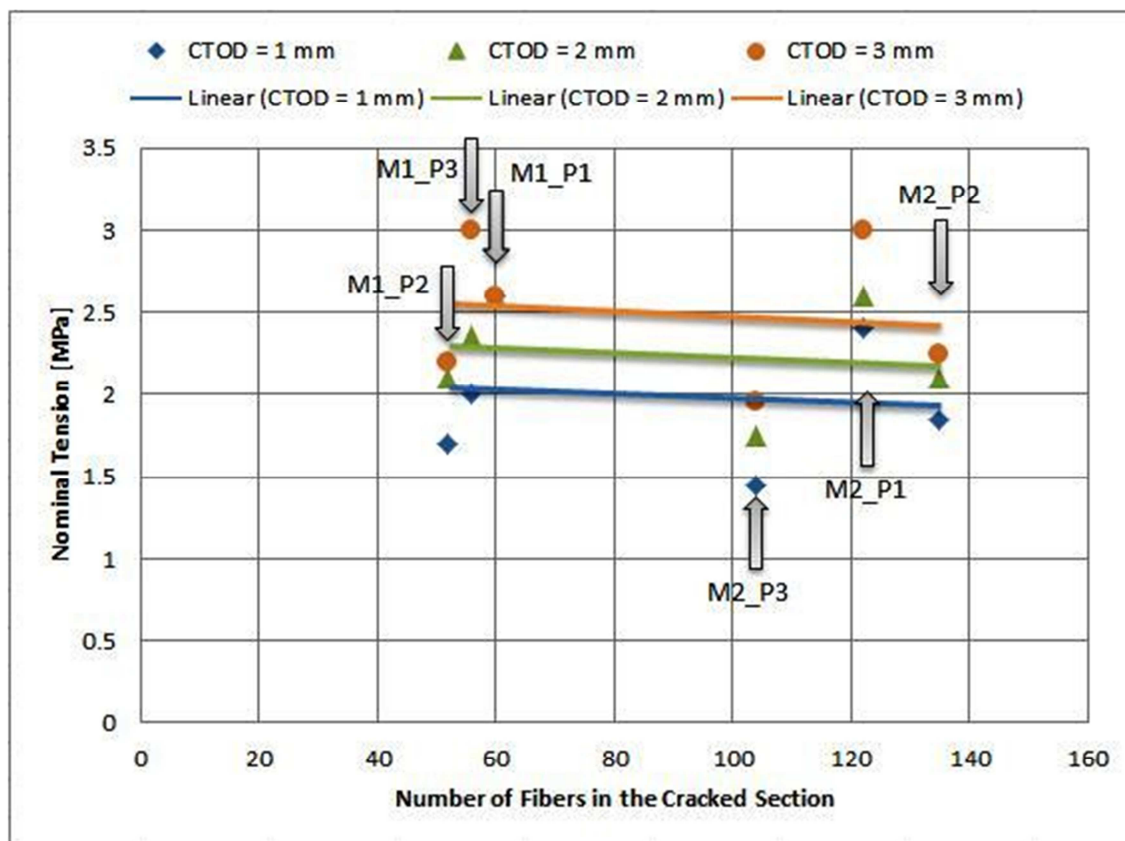


Figure 66: Influence of the number of fibers in M1/M2

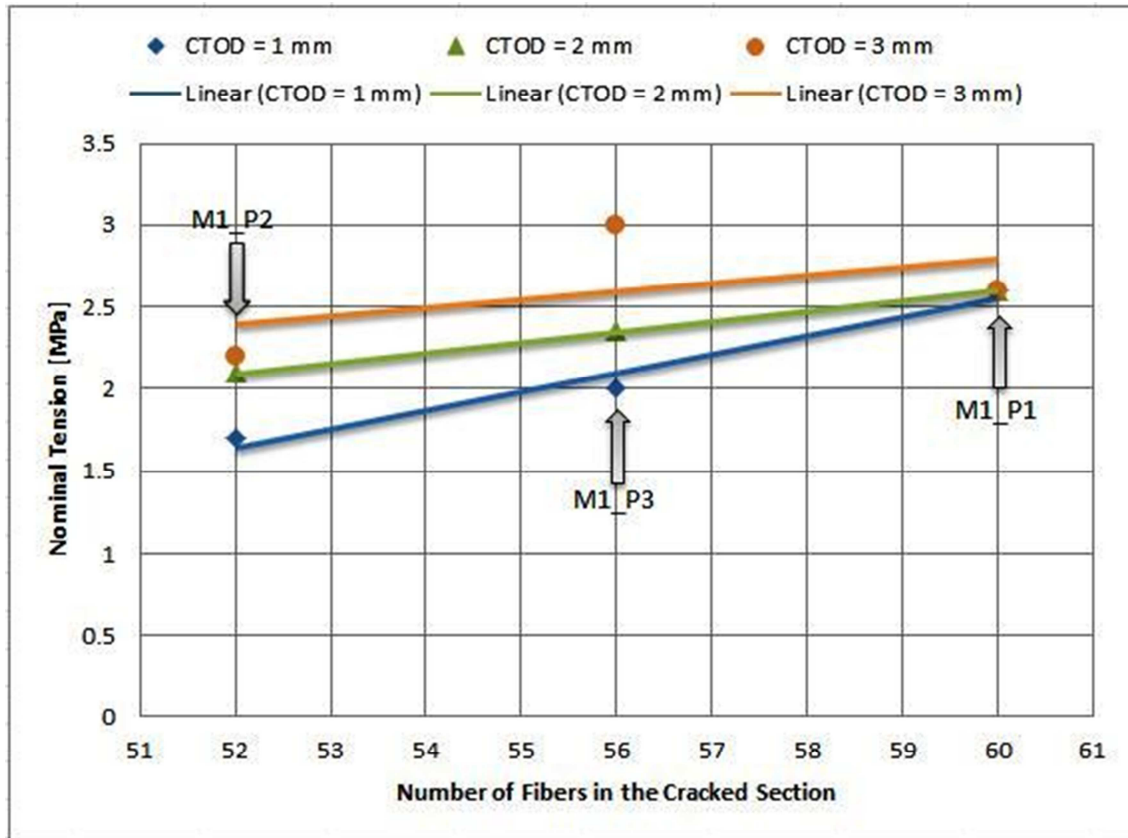


Figure 67: influence of the total number of fiber in M1

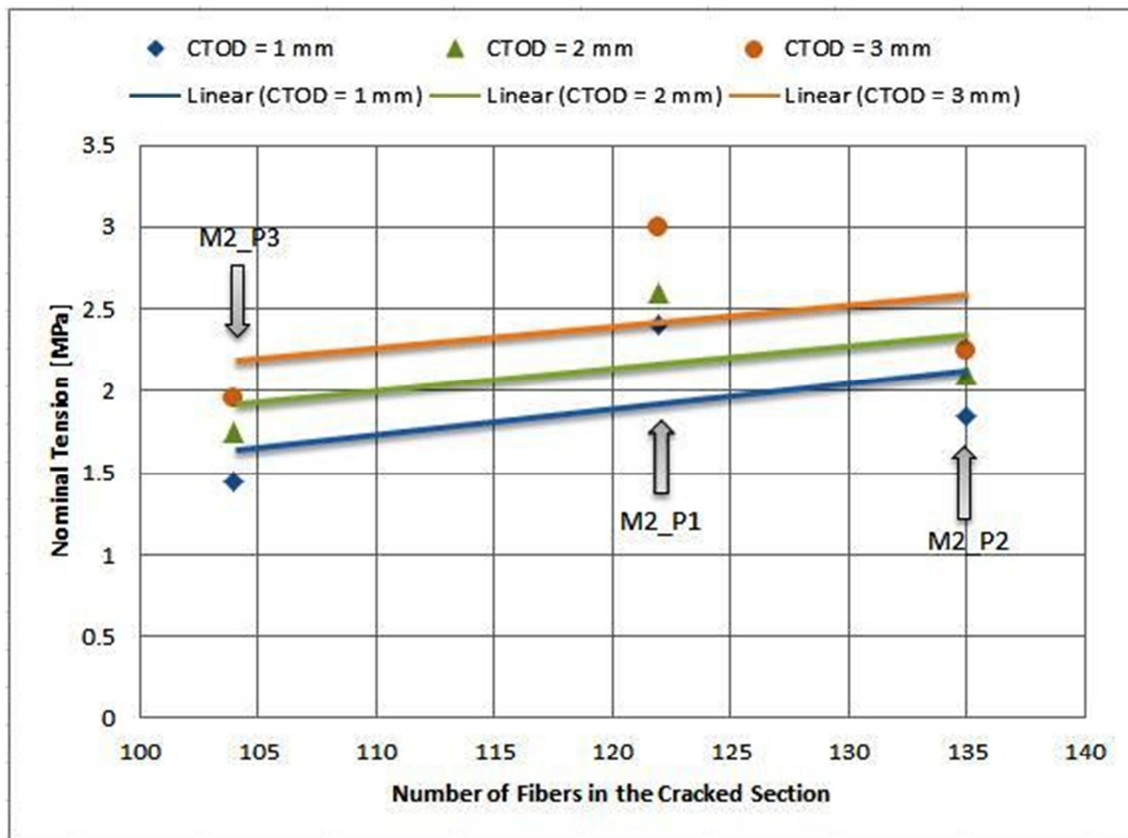


Figure 68: Influence of the total number of fiber in M2

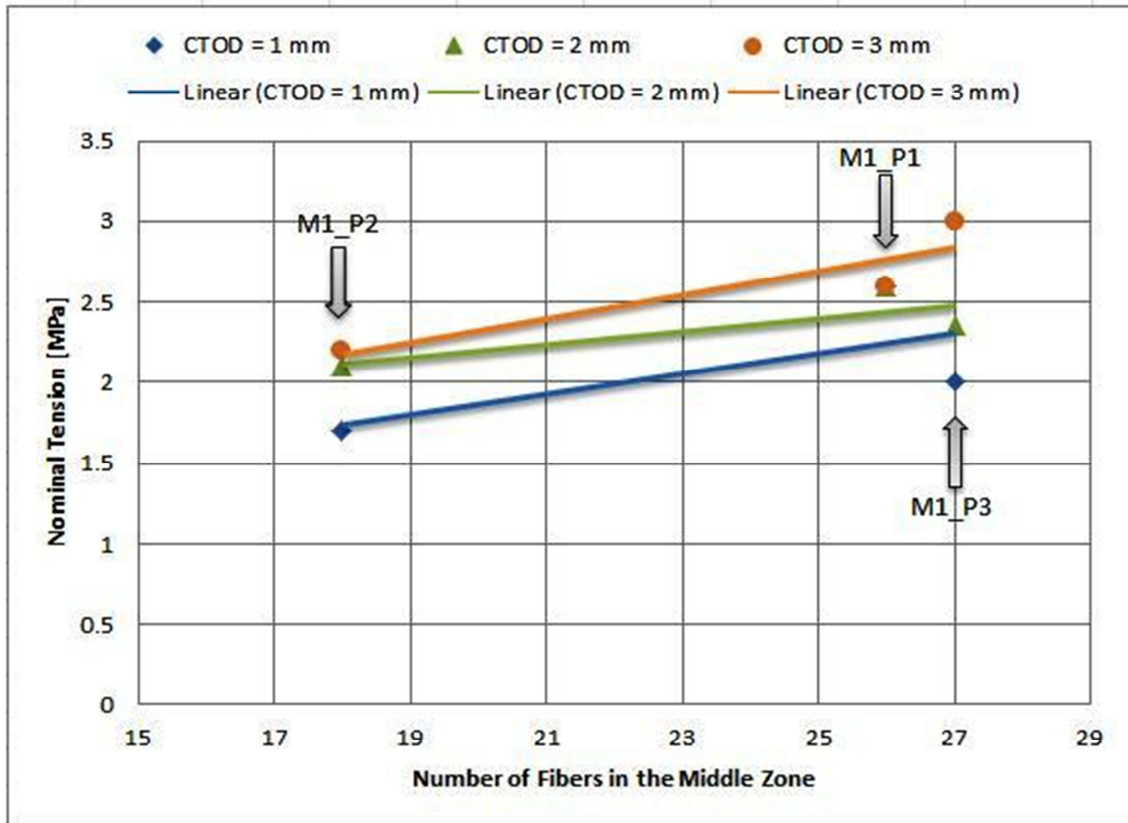


Figure 69: Influence of fiber in middle zone of M1

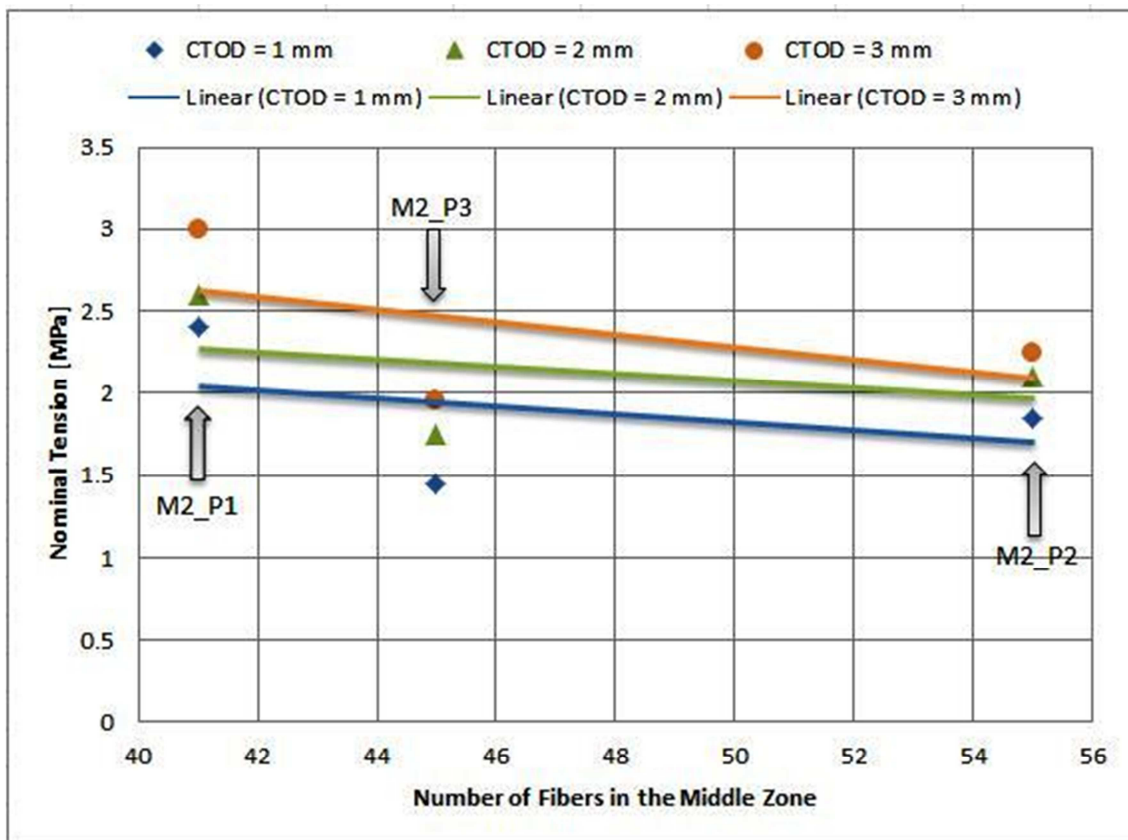


Figure 70: Influence of fiber in middle zone of M2

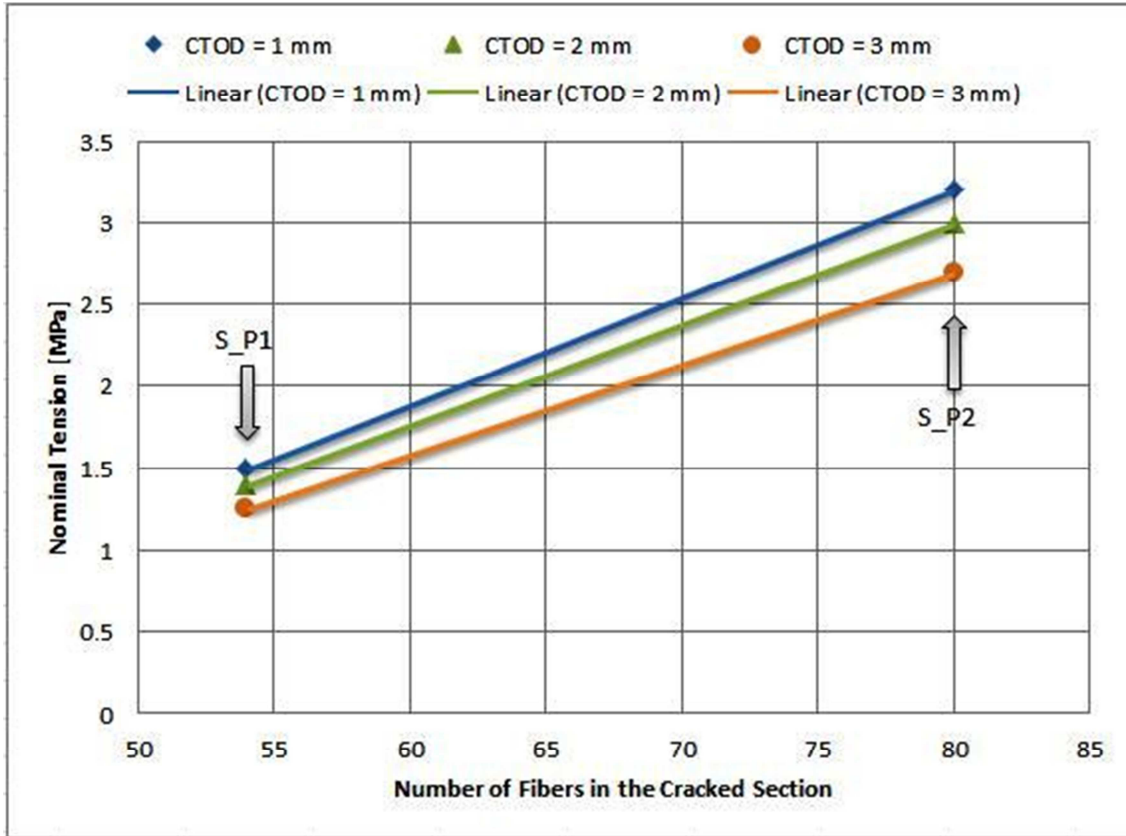


Figure 71: Influence of the total number of fiber in S

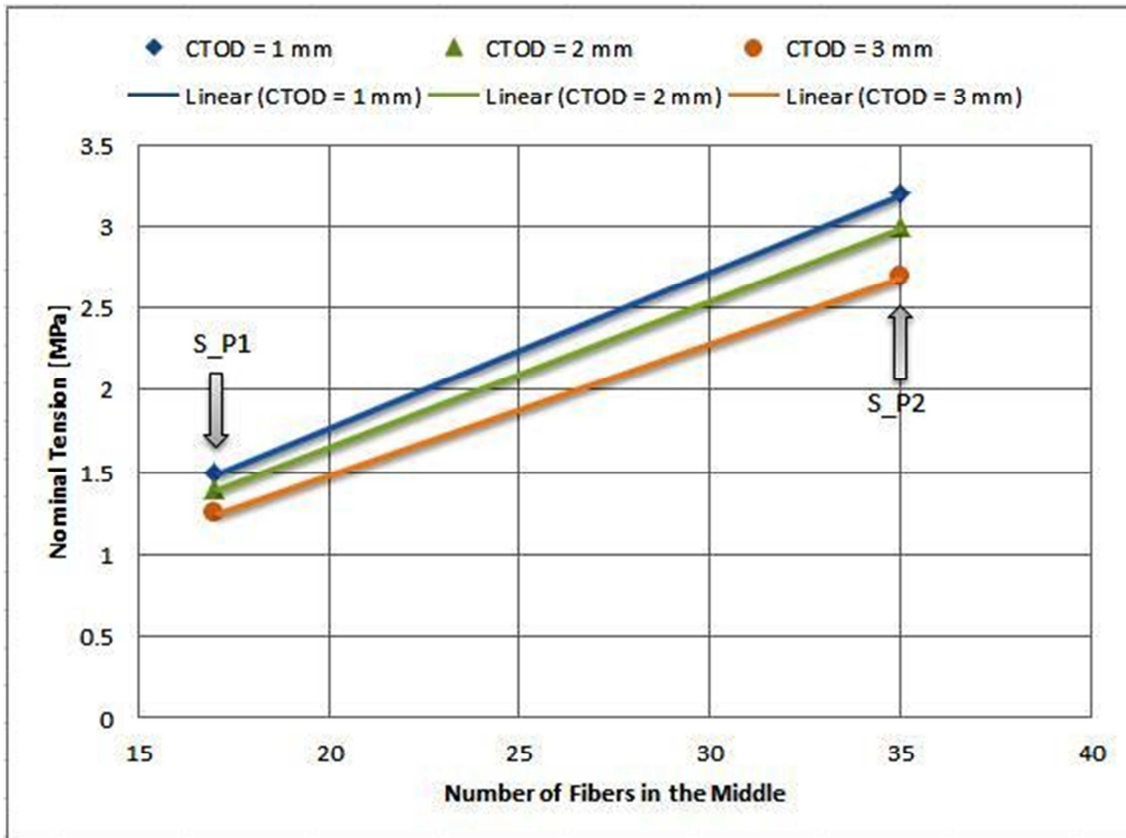


Figure 72: Influence of fiber in middle zone of S

6. Cracking Analysis of Beam Samples

6.1 Generalities

In this paragraph we have exposed and have explained the most relevant phases and results of the cracking analysis of the beams. The beams are subdivided in 3 types:

- M1 with 4 kg/mc of fibers;
- M2 with 7 kg/mc of fibers;
- B with steel reinforcement without fibers;

Before the cracking procedure the beams are cut to help the rupture in a precise point of them.

The cut is made with a width of 10 mm then the resistance section is 300 x 110 in mm.

The static scheme used is simply supported with 800 mm span.



Figure 73: Cutting operation

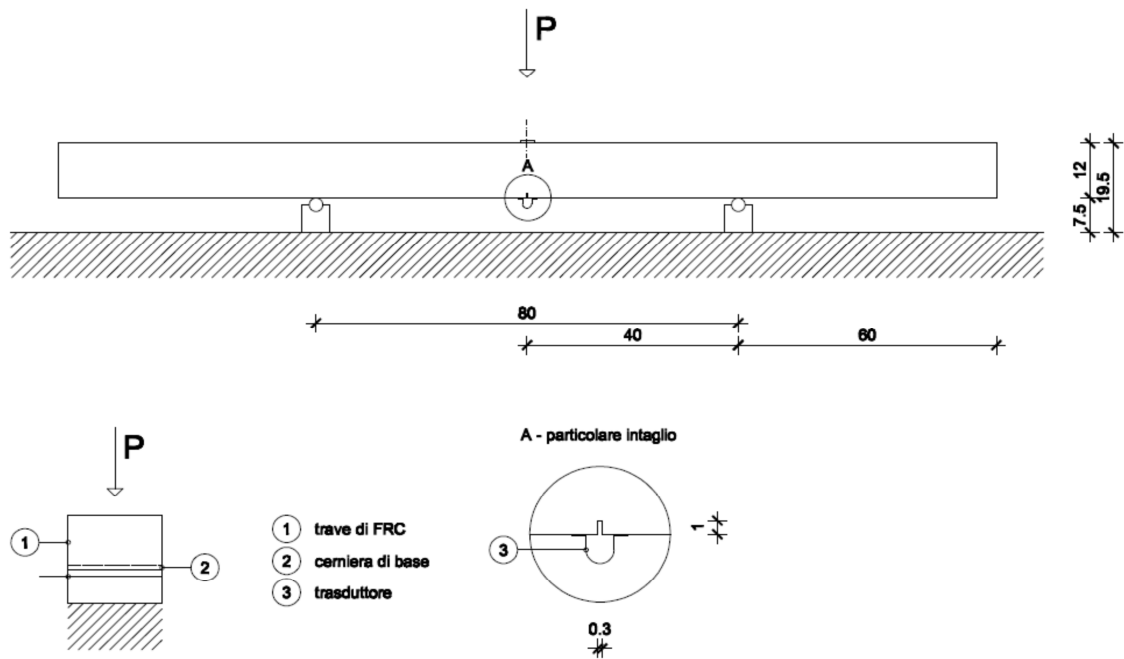


Figure 74: Static scheme for beam analysis

6.2 Speed Limits

The speed limits of the load increment are:

$$\begin{cases} 0.05 \text{ mm/ min of CMOD} \leq 0.1 \text{ mm} \\ 0.1 < 0.2 \text{ mm/ min of CMOD} \leq 4 \text{ mm} \end{cases}$$

Therefore, because we want a cyclic loading behavior, the secondary phase is repeated two times.



Figure 75: Beam cracking test

6.3 Hand Calculation

6.3.1 Maximum Bending Moment

From the theoretical scheme the maximum bending moment is:

$$M = \frac{F * l}{4}$$

Where:

- F is the concentrated load;
- l is 800 mm;

6.3.2 Tension

The tension is computed by the ratio between the moment and the resistance modulus:

$$\sigma = \frac{M}{W} = \frac{\frac{F * l}{4}}{\frac{b * h^2}{6}}$$

Where:

- b is the base of the sample = 300 mm;
- h is the height of the sample = 110 mm;
- W is the resistance modulus = 605000 mm³;

6.4 Tests Results & Diagrams

In this paragraph we have represented the behaviors of all samples referred to the code limits of crack opening. The force is expressed in kg, the Crack Opening in mm and the Nominal Tension in MPa.

	A	B	C	D	E	F	G	H	I	J	K	L	M	N	O
2	0.7504	-1	0.0002	1500.8	0.002481	0.5761	-1.001	-0.0004	1152.2	0.001904	3.3428	-1	-0.0003	6685.6	0.01105
3	0.0682	-1	0.0002	136.4	0.000225	1.842	-1.0011	-0.0005	3684	0.006089	3.7825	-0.9998	-1.00E-04	7565	0.01250
4	0.6822	-1	0.0002	1364.4	0.002255	1.1825	-1.0008	-0.0002	2365	0.003909	4.1008	-1.0001	-0.0004	8201.6	0.01355
5	0.0834	-0.9999	0.0003	166.8	0.000276	0.5988	-1.0009	-0.0003	1197.6	0.00198	2.5621	-0.9997	0	5124.2	0.0084
6	0.1668	-1.0001	1.00E-04	333.6	0.000551	1.2128	-1.0011	-0.0005	2425.6	0.004009	2.9032	-0.9996	1.00E-04	5806.4	0.00959
7	0.1364	-0.9998	0.0004	272.8	0.000451	1.8647	-1.001	-0.0004	3729.4	0.006164	3.2519	-0.9998	-1.00E-04	6503.8	0.0107
8	0.6443	-1	0.0002	1288.6	0.00213	1.7965	-1.001	-0.0004	3593	0.005939	3.0169	-0.9994	0.0003	6033.8	0.00997
9	0.6822	-0.9999	0.0003	1364.4	0.002255	2.6227	-1.0011	-0.0005	5245.4	0.00867	2.8198	-0.9996	1.00E-04	5639.6	0.00932
10	0.1213	-1	0.0002	242.6	0.000401	1.7131	-1.0013	-0.0007	3426.2	0.005663	3.2291	-0.9997	0	6458.2	0.01067
11	0.1516	-0.9998	0.0004	303.2	0.000501	2.8501	-1.001	-0.0004	5700.2	0.009422	3.5626	-0.9996	1.00E-04	7125.2	0.01177
12	0.758	-1	0.0002	1516	0.002506	2.6075	-1.0009	-0.0003	5215	0.00862	2.6758	-0.9998	-1.00E-04	5351.6	0.00884
13	0.1971	-1.0003	-1.00E-04	394.2	0.000652	2.4408	-1.0011	-0.0005	4881.6	0.008069	3.5854	-1	-0.0003	7170.8	0.01185
14	0.2198	-0.9999	0.0003	439.6	0.000727	2.1679	-1.0011	-0.0005	4335.8	0.007167	3.7597	-0.9999	-0.0002	7519.4	0.01242
15	0.6746	-1.0004	-0.0002	1349.2	0.00223	3.2291	-1.0007	-1.00E-04	6458.2	0.010675	3.8204	-0.9997	0	7640.8	0.01262
16	0.6064	-1	0.0002	1212.8	0.002005	3.0624	-1.0011	-0.0005	6124.8	0.010124	3.8355	-1.0001	-0.0004	7671	0.01267
17	0.9551	-0.9997	0.0005	1910.2	0.003157	2.653	-1.001	-0.0004	5306	0.00877	4.7679	-0.9999	-0.0002	9535.8	0.01576
18	0.8565	-1	0.0002	1713	0.002831	3.4641	-1.0011	-0.0005	6928.2	0.011452	4.0174	-0.9997	0	8034.8	0.01328

Figure 76: excel file

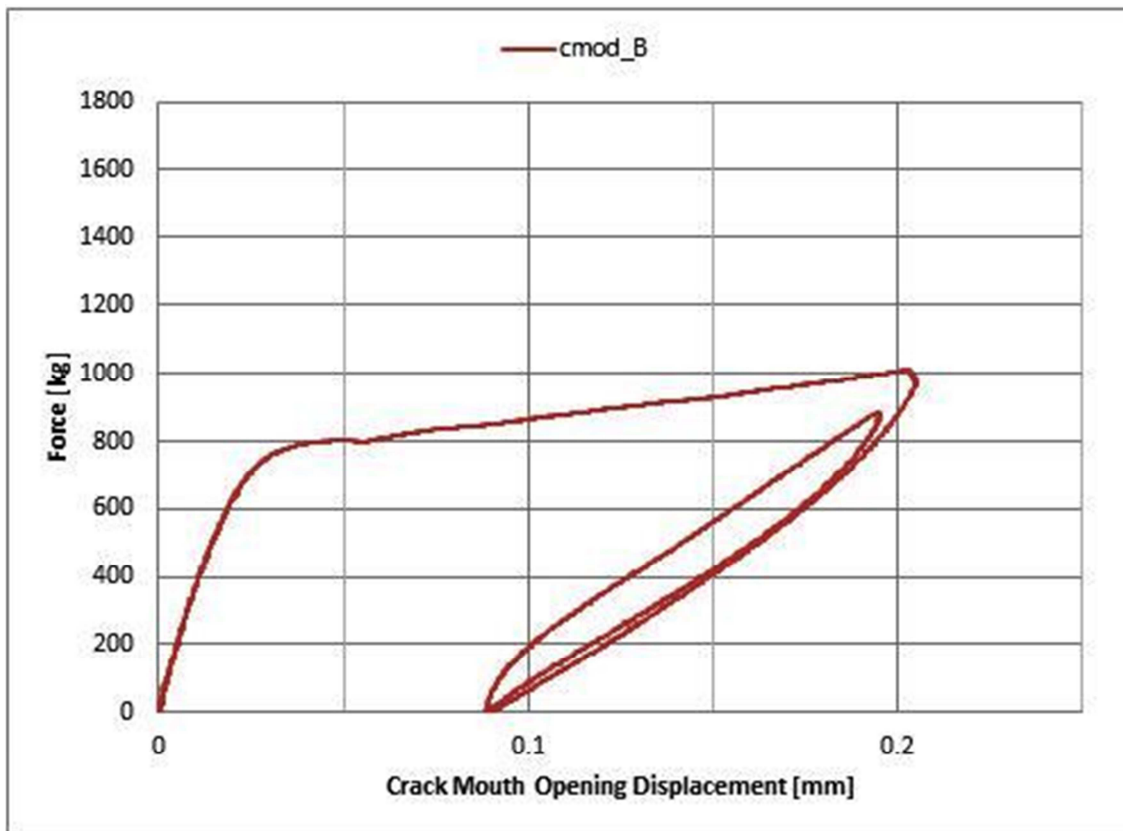


Figure 77: Force-CMOD for B beam



Figure 78: Tension-CMOD for B beam

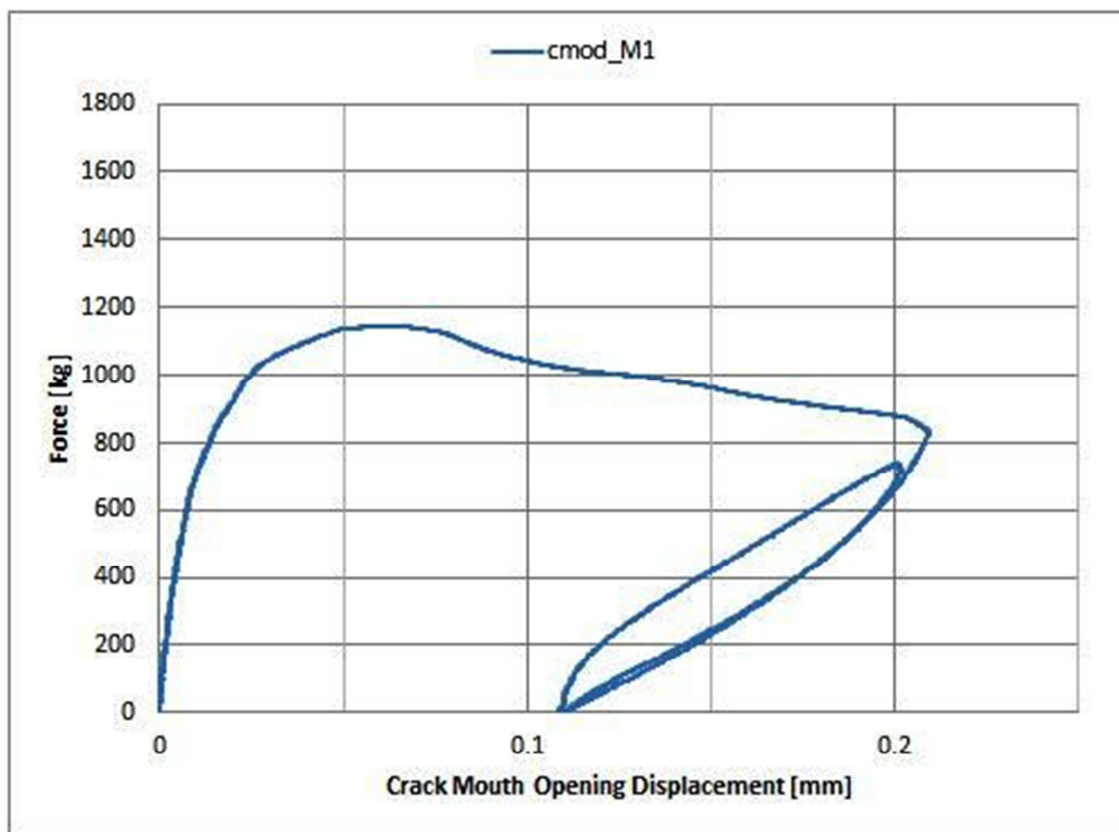


Figure 79: Force-CMOD for M1 beam

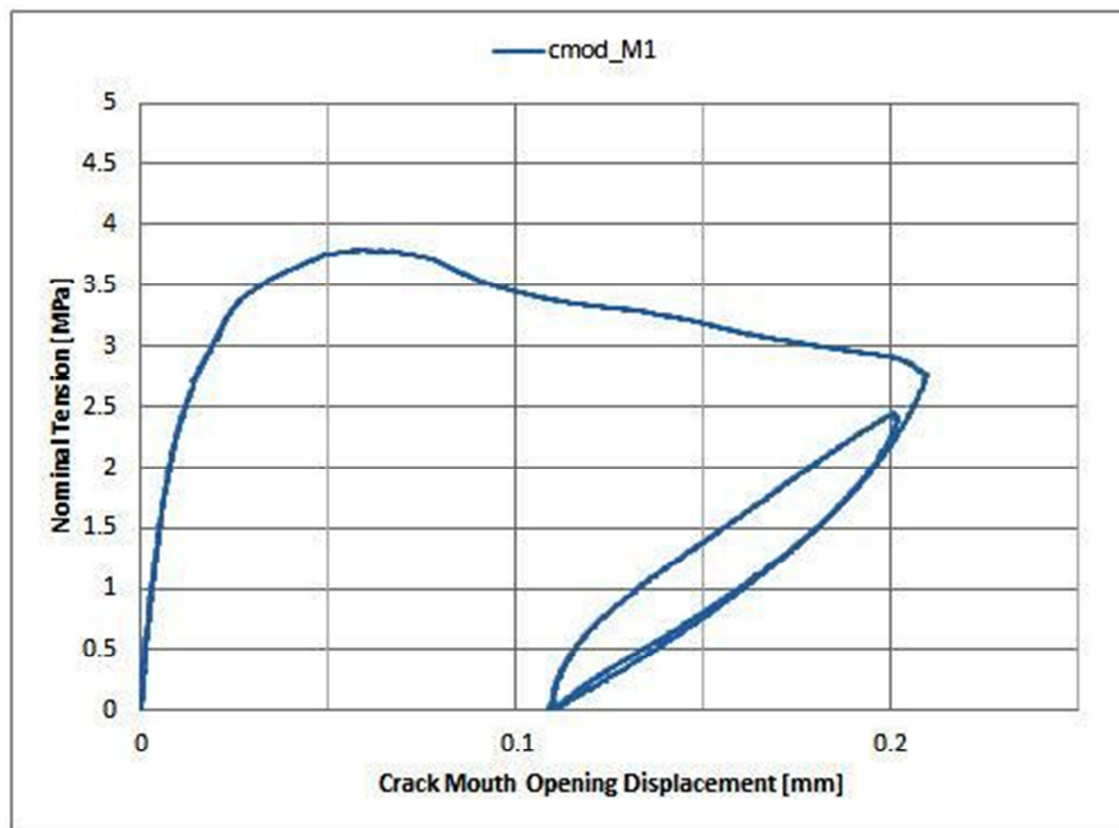


Figure 80: Tension-CMOD for M1 beam

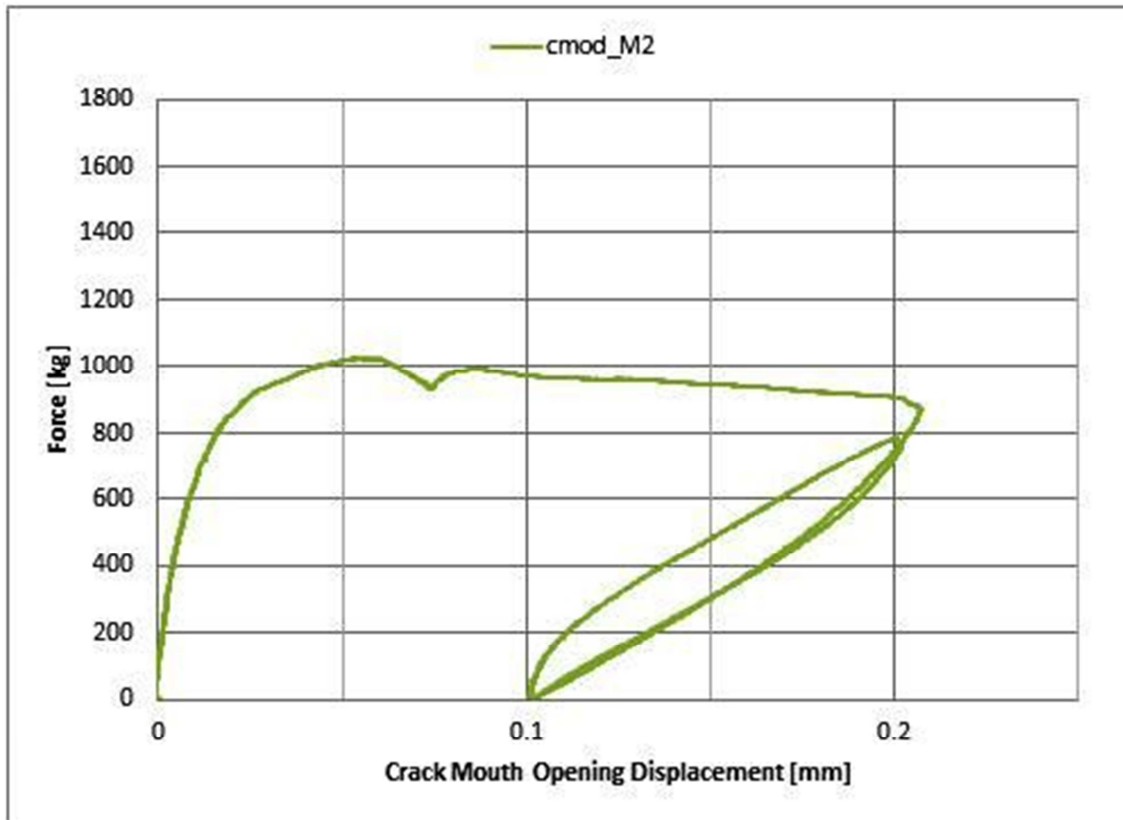


Figure 81: Force-CMOD for M2 beam



Figure 82: Tension-CMOD for M2 beam

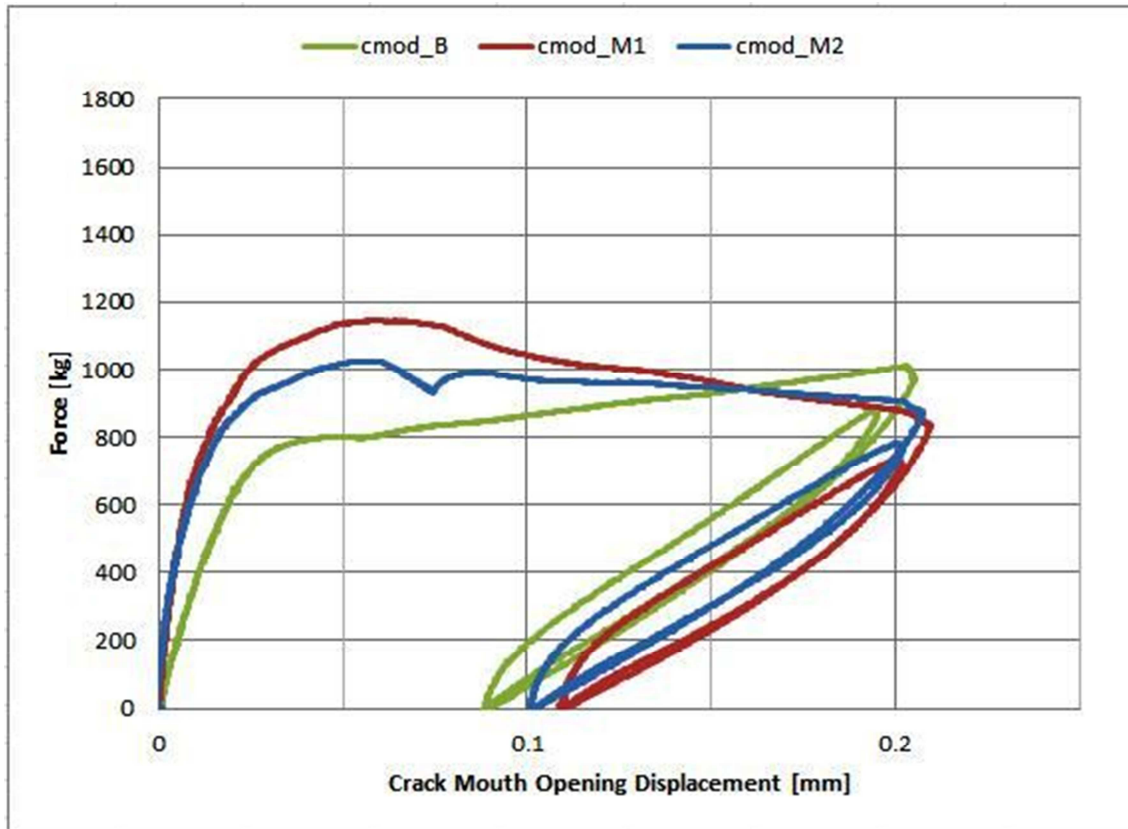


Figure 83: Force-CMOD for all beams

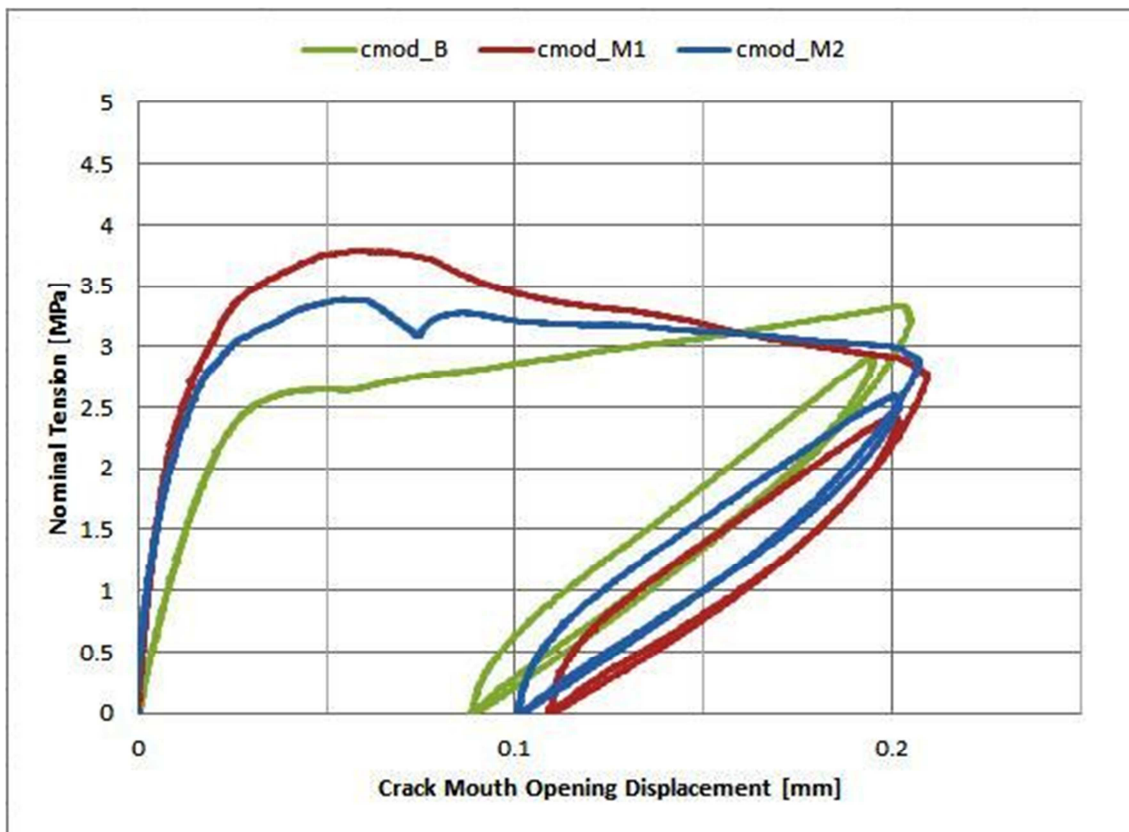


Figure 84: Tension-CMOD for all beams

6.5 Beams VS Prismatic Samples

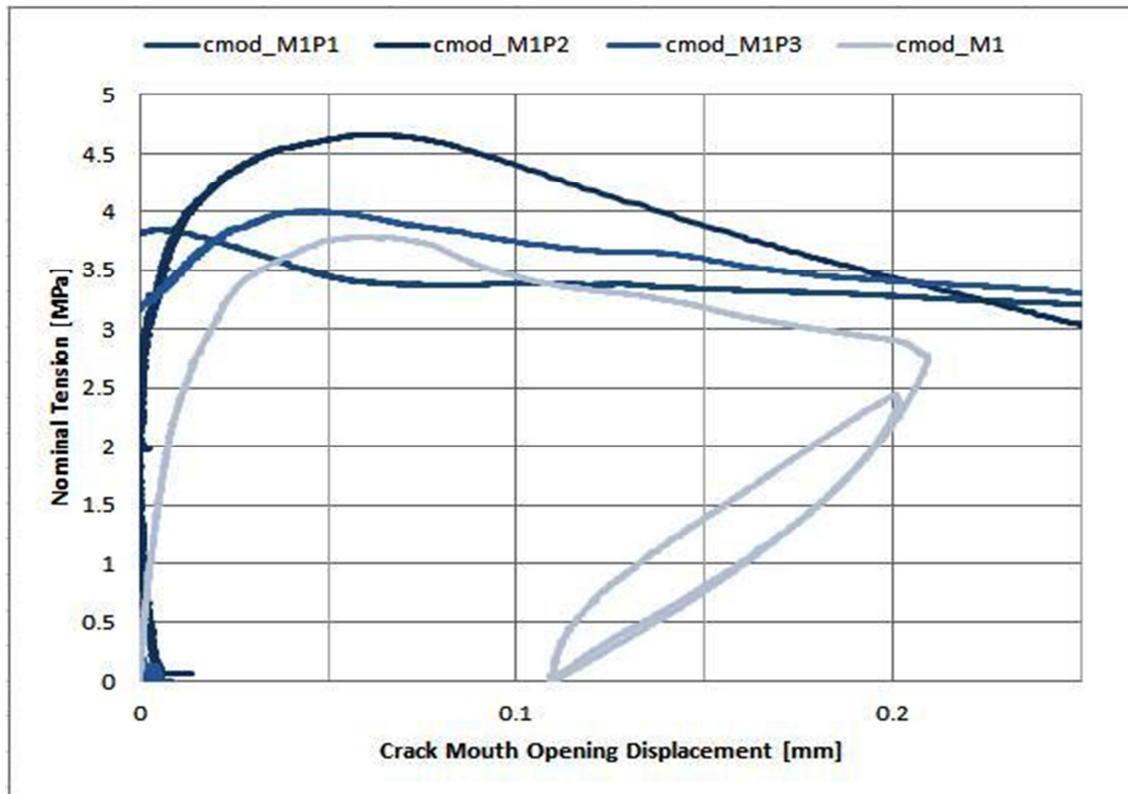


Figure 85: Tension-CMOD for M1 beams and prismatic samples

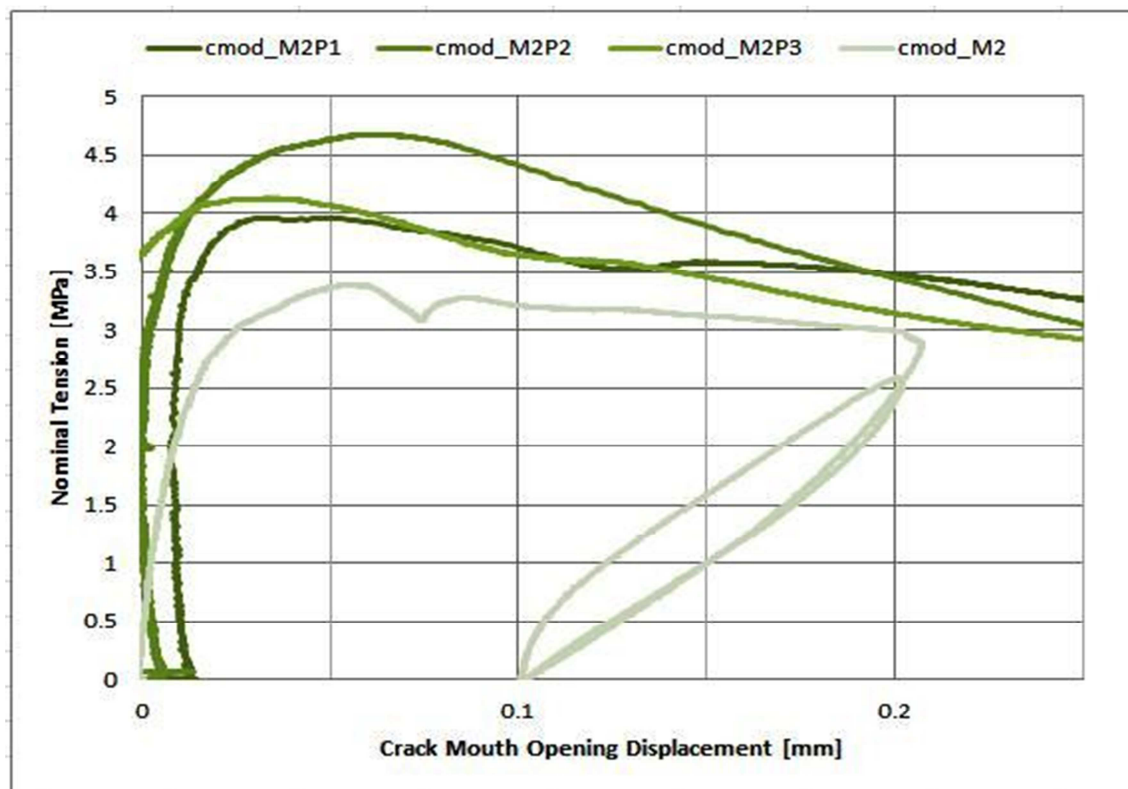


Figure 86: Tension-CMOD for M2 beams and prismatic samples

In this table you can find:

- First column: the 3 beam types;
- Second column: no cracked section at the beginning age;
- Third column: cracks obtained;

7. Shrinkage and Creep Analysis of Cylindrical and Beam Samples

7.1 Generalities

A loaded element total deformation ε at time t is equal to the sum of instantaneous deformation ε_0 , viscos deformation ε_φ and shrinkage deformation ε_{cs} :

$$\varepsilon = \varepsilon_0 + \varepsilon_\varphi + \varepsilon_{cs}$$

In the chart below there are represented all total deformation different components with constant tensional state applied at time t_0 .

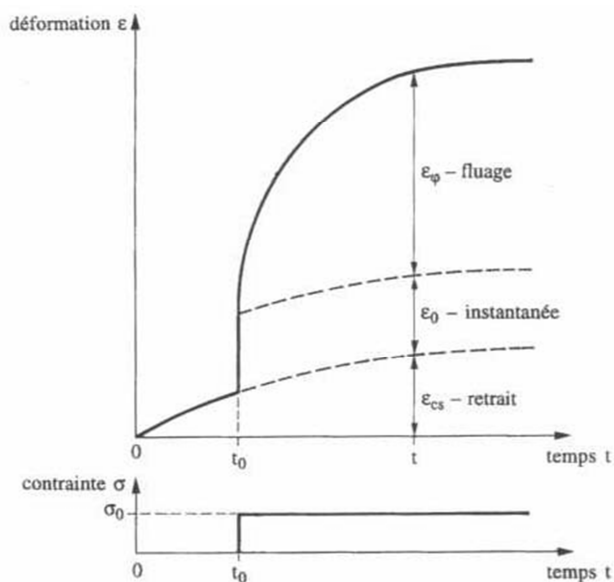


Figure 87: Different deformation components

7.2 Shrinkage Types

The shrinkage is the variation of the volume of the concrete due to chemical-physical reactions without loading. The principal variation is the water evaporation during the curing phase. However it's possible to define 5 types of shrinkage of concrete:

- *Plastic Shrinkage*

Called fresh shrinkage, is due to the free surface water evaporation when the material is still plastic. This type of variation causes a cracking zone on the surface and a decreasing in the durability property value.

- *Thermal Shrinkage*

This type of shrinkage is due to the chemical reactions inside the material at the initial time. The material expansion due to the heat decreases in time while the reaction decreases progressively. The consecutive contraction of the material due to the cooling phase is the thermal shrinkage.

- *Autogenous Shrinkage*

The autogenous shrinkage is due to the internal water consumption at the hydration time of the material. This thing leads to a volume reduction and its value increase while the water content decrease. After 28 days this shrinkage grows up 60-90%.

- *Drying Shrinkage*

Drying shrinkage is due to capillary water pores evaporation and it isn't isotropic. The phenomenon is much slower and can take several years during that the material is subjected to a volume reduction.

- *Carbonation Shrinkage*

When the calcium hydroxide Ca(OH)_2 reacts with the carbon dioxide CO_2 the product is the calcium carbonate CaCO_3 . This type of shrinkage starts from the external surface to the internal zone of the material.

All these types of shrinkage are related to the cement part but the concrete mixture contains also the aggregates. These elements aren't interested by the shrinkage phenomena and constrain the volume reduction. Then, whether the aggregates content is high the concrete deformation is lower.

For reducing the surface cracks is also important cover the material, and in particular the external surface, with humid cloth and maintain wet that for a time period directly connected to the traction resistance value.

If the wet phase continues about 7 days after the beginning point, the concrete achieves $\frac{3}{4}$ of its long term traction resistance.

7.3 Creep

The viscous deformation represents the material change, in addition to the elastic phase, when the material is loaded permanently. The creep is determined by various complex mechanisms like sliding layers, free water expulsion, micro-cracks of the ties etc.

The viscous deformation depends on ambient parameters like the relative humidity and on geometrical parameters like the surface-volume ratio:

- *Relative Humidity*

The creep is greater when the relative humidity is slower. If the load is applied after the curing phase the humidity influence is about zero.

- *Applied Load Influence*

Many test show that exist a directly proportion between the creep and the load applied. It's know that the concrete deformation starts for load greater than 40-60% of its compression resistance σ'_c . Over this proportion the creep velocity increase faster than the load and we obtain the critical point when the ratio is 80-90% of σ'_c .

- *Age Influence*

If the concrete is young the mechanical resistance is lower, then, the creep effects is higher at this time.

- *Resistance Influence*

The creep value decrease when the resistance value increase during the loading phase.

- *Aggregates Influence*

The normal aggregate hasn't a creep deformation, then the aggregates restraint the creep effects.

- *Dimensions Influence*

The creep value decrease when the dimensions of the concrete element increase because it strictly depends on the external surface. If the curing phase is without humidity exchanges the dimension influence is about zero.

- *Temperature Influence*

The creep effect increase until 50°C after that starts go down.

▪ *Cycle Load Influence*

The creep value increases after a cycle load application. Pay attention at this point because generally the experimental studies have been done with permanent load application and the cycle effects are underestimated.

7.4 Viscous Deformations Computation

When a concrete element shows viscous phenomena while is loaded under permanent load, it's assumed that the shrinkage and the creep have an additive effect and in particular the creep can be computed by the difference between total deformation and the shrinkage of a similar element in the same conditions but not loaded.

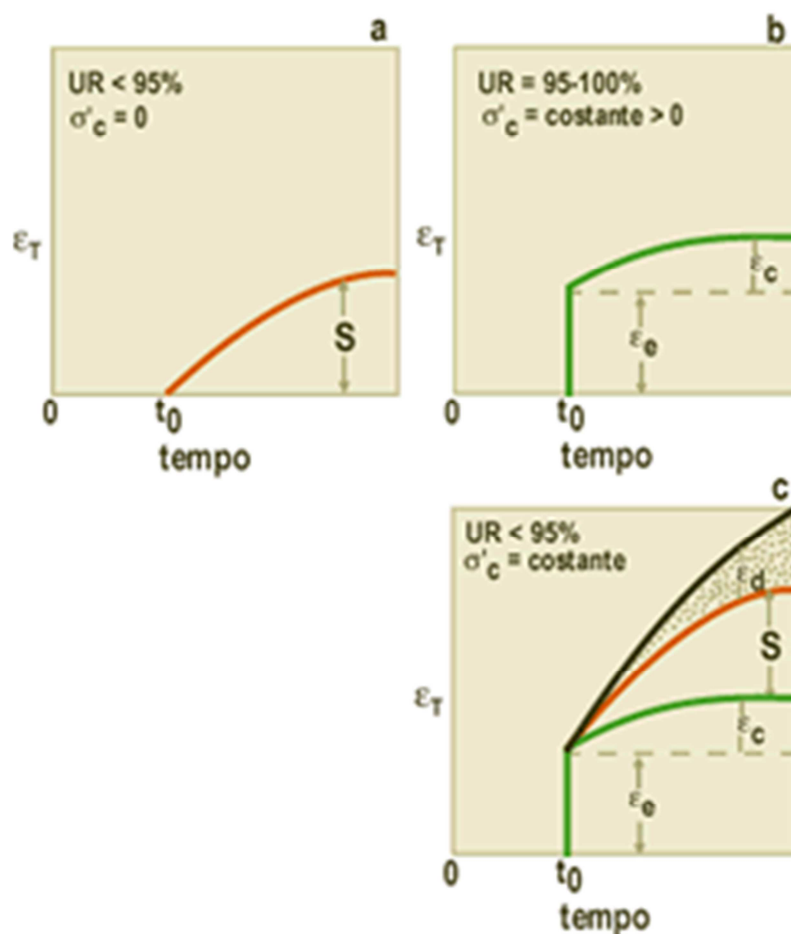


Figure 88: Contraction of shrinkage, creep, elastic phase and total.

Now we want to examine the iteration between creep and shrinkage using 3 different cases:

- Element without load, low relative humidity value, free shrinkage.
- Element with load, UR 95-100% and then without shrinkage, free basic creep.
- Element with load, low UR value, free shrinkage and creep.

In the last case the deformation is:

$$\varepsilon_T > \varepsilon_e + \varepsilon_c + S$$

The difference among the ε_T of the last case and the sum of two first cases is called “drying creep value ε_d ”.

The total deformation begins:

$$\varepsilon_T = \varepsilon_e + S + \varepsilon_c + \varepsilon_d$$

This means that, under load compression with unsaturated ambient, the evaporation is greater than the case without load, called “squeezing effect”.

In particular the total creep is obtained by the sum of drying effect plus the pure effect:

$$\varepsilon_{cc} = \varepsilon_c + \varepsilon_d$$

Then we can talk about:

$$\varepsilon_T = \varepsilon_e + S + \varepsilon_{cc}$$

When we do creep test in unsaturated ambient we evaluate the total deformations of the samples and, subtracting the shrinkage and the elastic deformations, we obtain the total creep value ε_{cc} .

Experimentally can be note that, with permanent load compression, these deformations evolve in time and for $t \rightarrow \infty$ can be assume value 3-4 times greater than the instantaneous deformations.

For a generic concrete element at the time t:

$$\varepsilon_{cc}(t) = \varepsilon_{ist}(t_0) + \varepsilon_{cc}(t, t_0)$$

$$\varepsilon_{ist}(t_0) = \frac{\sigma_c(t_0)}{E_c(t_0)}$$

$$\varepsilon_{cc}(t, t_0) = \frac{\sigma_c(t_0)}{E_{c,28}} \cdot \Phi(t, t_0)$$

The terms $\Phi(t, t_0)$ is called viscous coefficient and is obtained by:

$$\Phi(t, t_0) = \frac{\varepsilon_{cc}(t, t_0)}{\frac{\sigma_c(t_0)}{E_{c,28}}}$$

When $t = t_0$ the viscous deformations is 0 and $\Phi(t, t_0) = 0$.

We obtain:

$$\varepsilon_c(t, t_0) = \sigma_c(t_0) \frac{1}{E_c(t_0)} \left[1 + \frac{E_c(t_0)}{E_{c,28}} \Phi(t, t_0) \right]$$

Putting:

$$J(t, t_0) = \left[1 + \frac{E_c(t_0)}{E_{c,28}} \Phi(t, t_0) \right] \frac{1}{E_c(t_0)} = \frac{1}{E_c(t_0)} + \frac{\Phi(t, t_0)}{E_{c,28}}$$

We can write:

$$\varepsilon_c(t, t_0) = \sigma_c(t_0) J(t, t_0)$$

The function $J(t, t_0)$ is called “viscosity function” and its dimension is equal to the inverse of elastic modulus.

The elastic range decreases in time because the elastic modulus increases in time.

The creep value is greater if the concrete is loaded at the first time.

The creep function is a monotonic function but the developing velocity of creep is a decreasing function therefore we obtain that the curve mitigates in time.

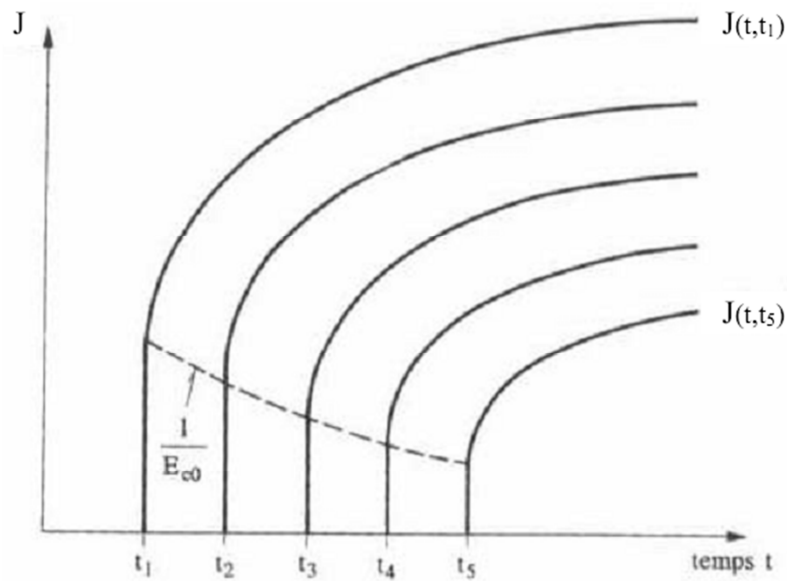


Figure 89: Creep function behavior with different time loading

In conclusion, introducing the specific viscous deformation at time t_0 like:

$$C(t, t_0) = \frac{\varepsilon_{cc}(t, t_0)}{\sigma_c(t_0)}$$

$$J(t, t_0) = \frac{\varepsilon_{ist}(t_0)}{\sigma_c(t_0)} + \frac{\varepsilon_{cc}(t, t_0)}{\sigma_c(t_0)} = \frac{1}{E_c(t_0)} + C(t, t_0)$$

And considering:

$$J(t, t_0) = \frac{1}{E_c(t_0)} + \frac{\Phi(t, t_0)}{E_{c,28}}$$

We obtain:

$$C(t, t_0) = \frac{\Phi(t, t_0)}{E_{c,28}}$$

7.5 Shrinkage and Creep Tests of Cylindrical Samples

7.5.1 Shrinkage Test

In this paragraph are explained the shrinkage results on cylindrical sample of 100 and 150 mm of diameters.

In particular we have considered:

- Mixture B without fiber;
- Mixture M1 with synthetic fibers;
- Mixture M2 with synthetic fibers;
- Mixture S with steel fibers;



Figure 90: Cylindrical samples

The cylindrical samples are tested in two different ways:

- Shrinkage test;
- Creep test;

These kinds of studies can be more important to evaluate and analyze the long term deformations of concrete structures and their viscous properties.

During the preparation phase of the mixtures, a part of them is used to realize cylindrical samples of various measures. After that we have measured all geometrical parameters of them to avoid any problems.

For measuring the quantities it was necessary to apply on the cylinder two strain gauges in opposite position.

The presence of two vertical strain gauges defines a mean value of the deformations, avoiding eventual errors.

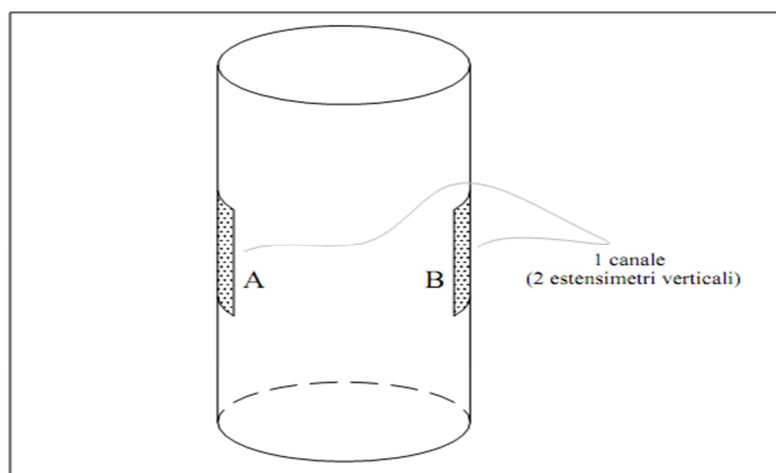


Figure 91: Shrinkage test preparation



Figure 92: Shrinkage test of cylindrical samples

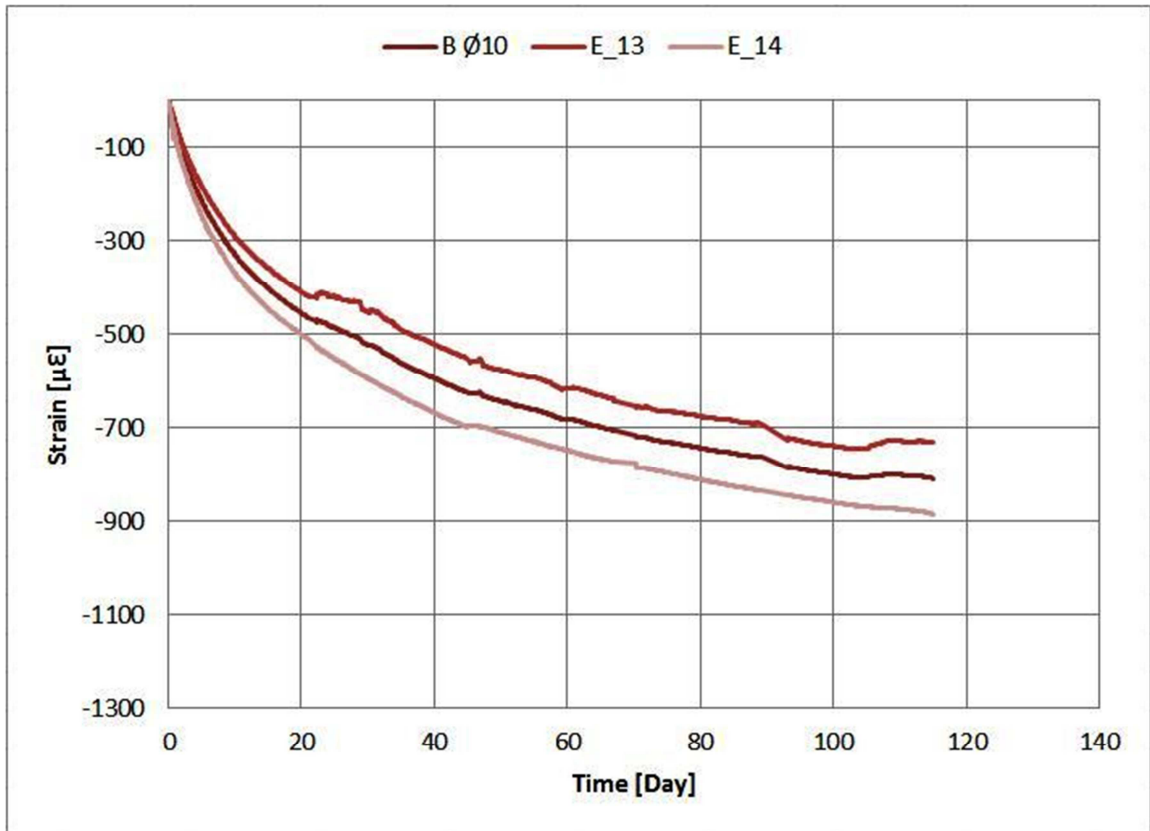


Figure 93: Mixture B and sample 100 mm of diameter

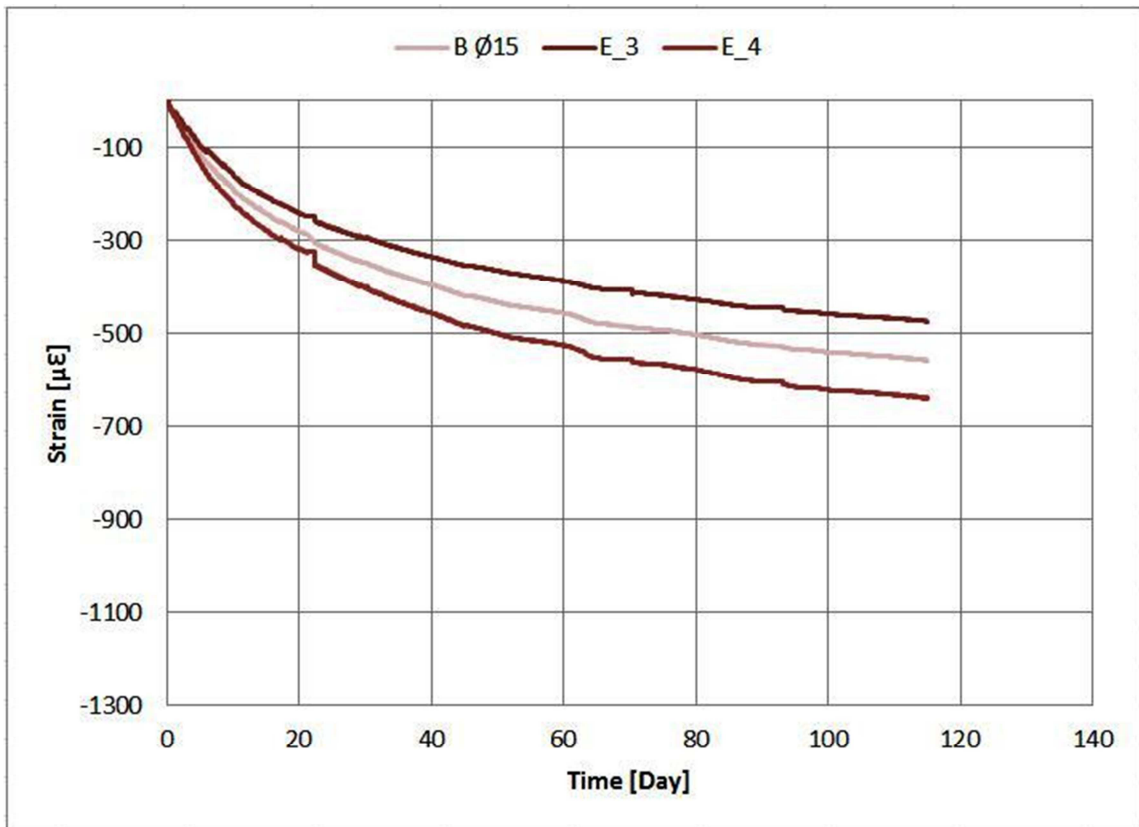


Figure 94: Mixture B and sample 150 mm of diameter

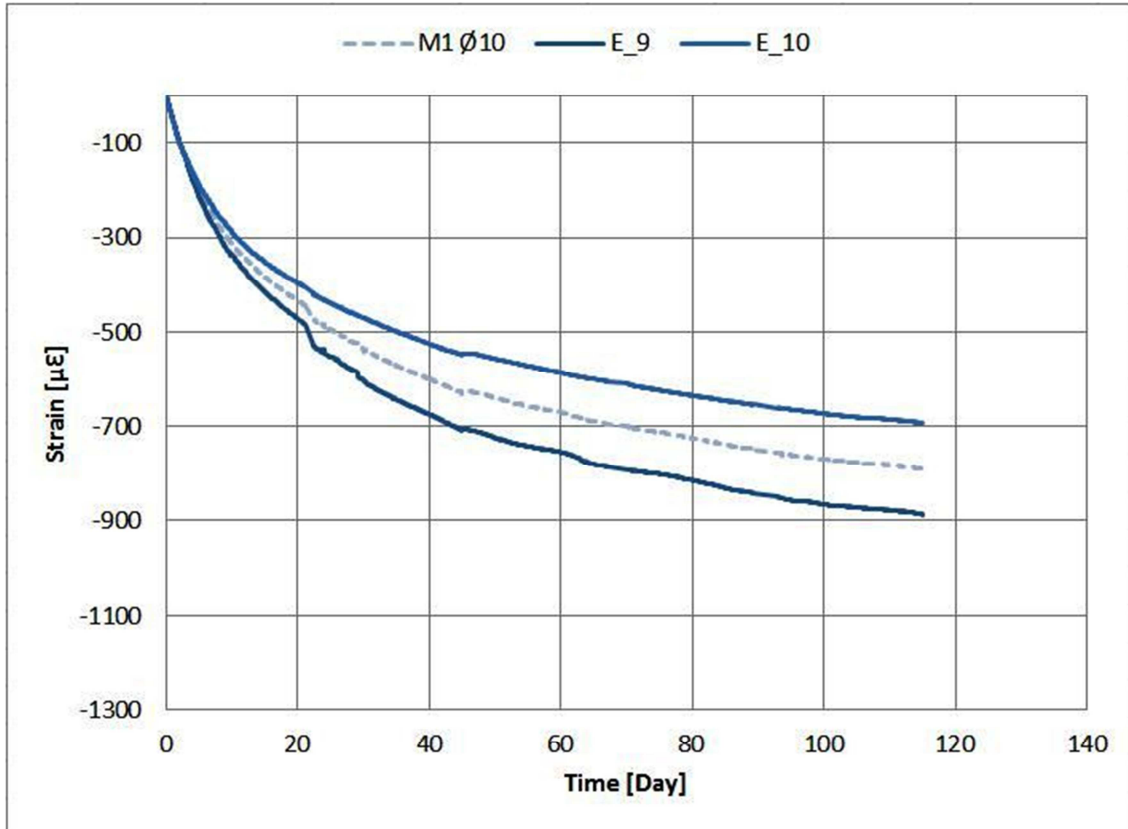


Figure 95: Mixture M1 and sample 100 mm of diameter

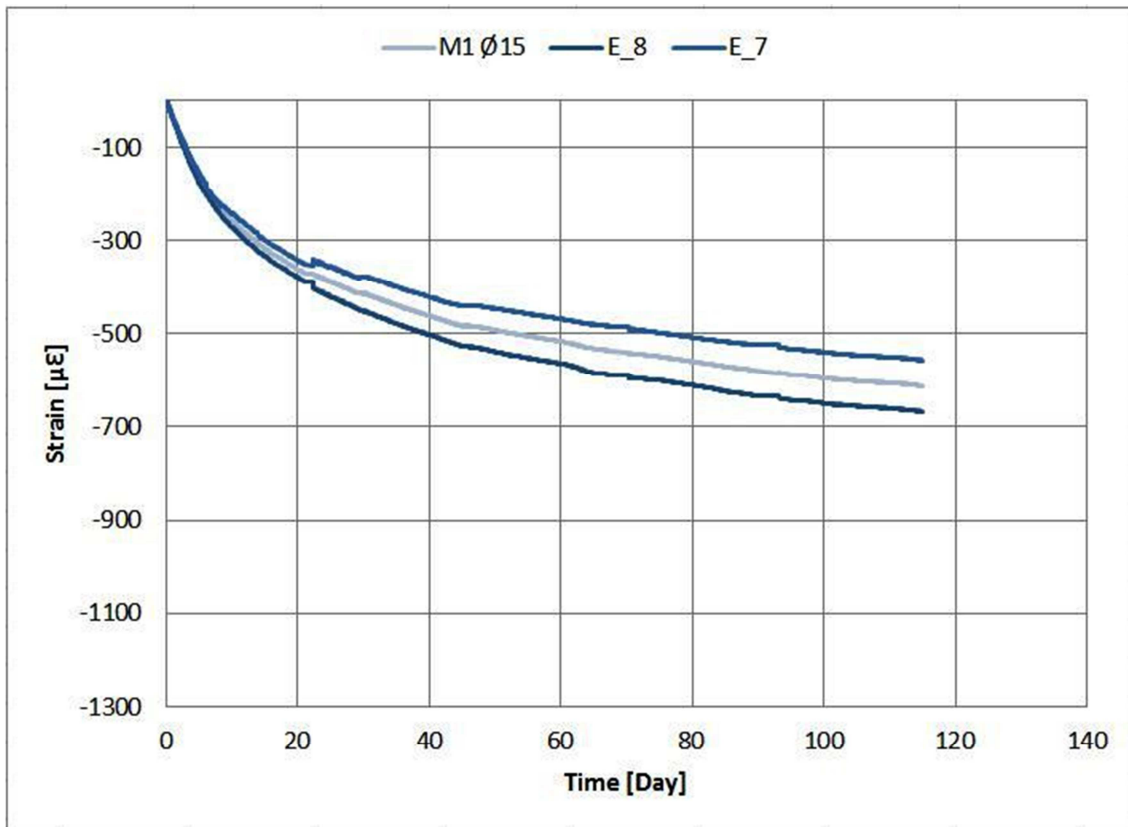


Figure 96: Mixture M1 and sample 150 mm of diameter

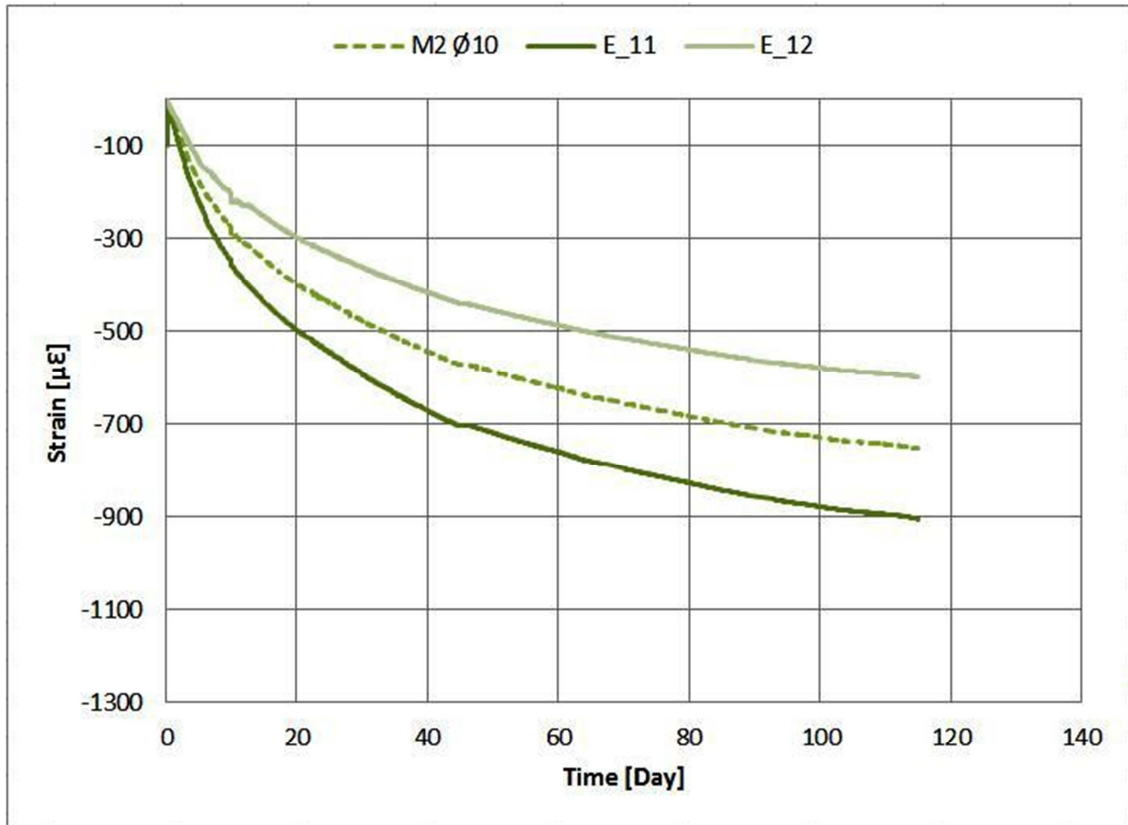


Figure 97: Mixture M2 and sample 100 mm of diameter

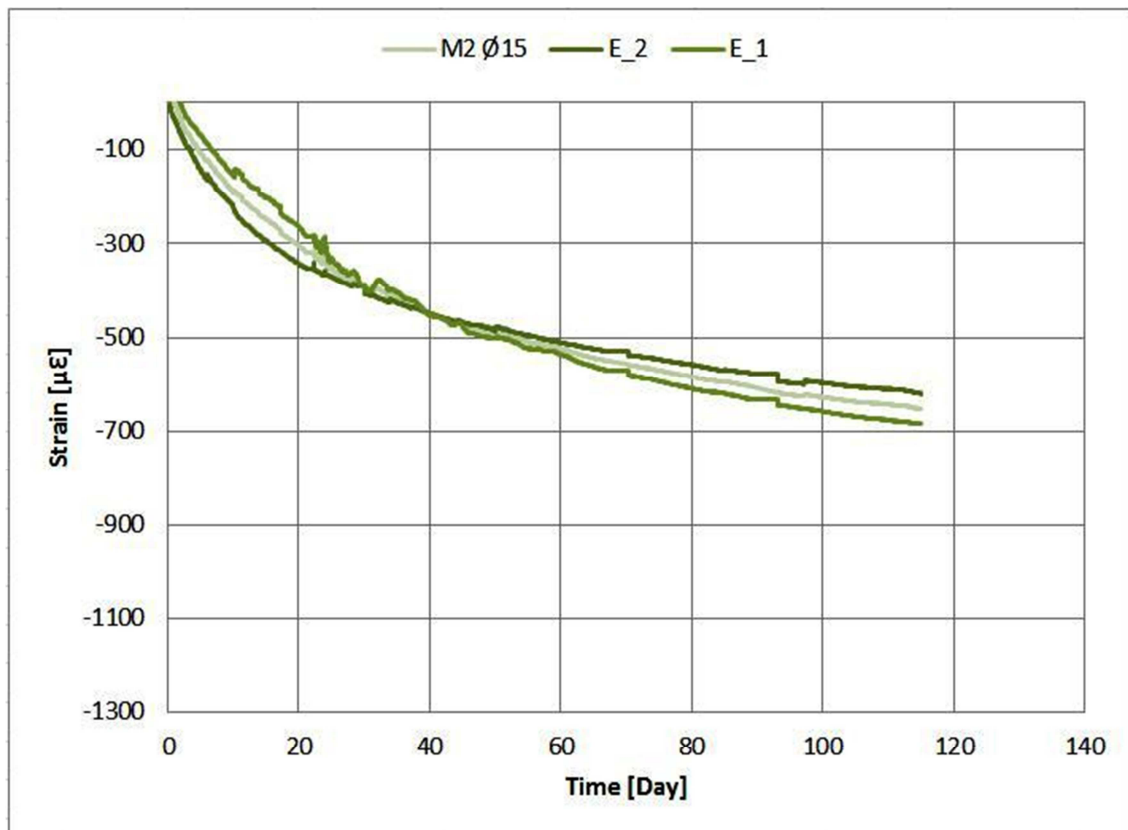


Figure 98: Mixture M2 and sample 150 mm of diameter

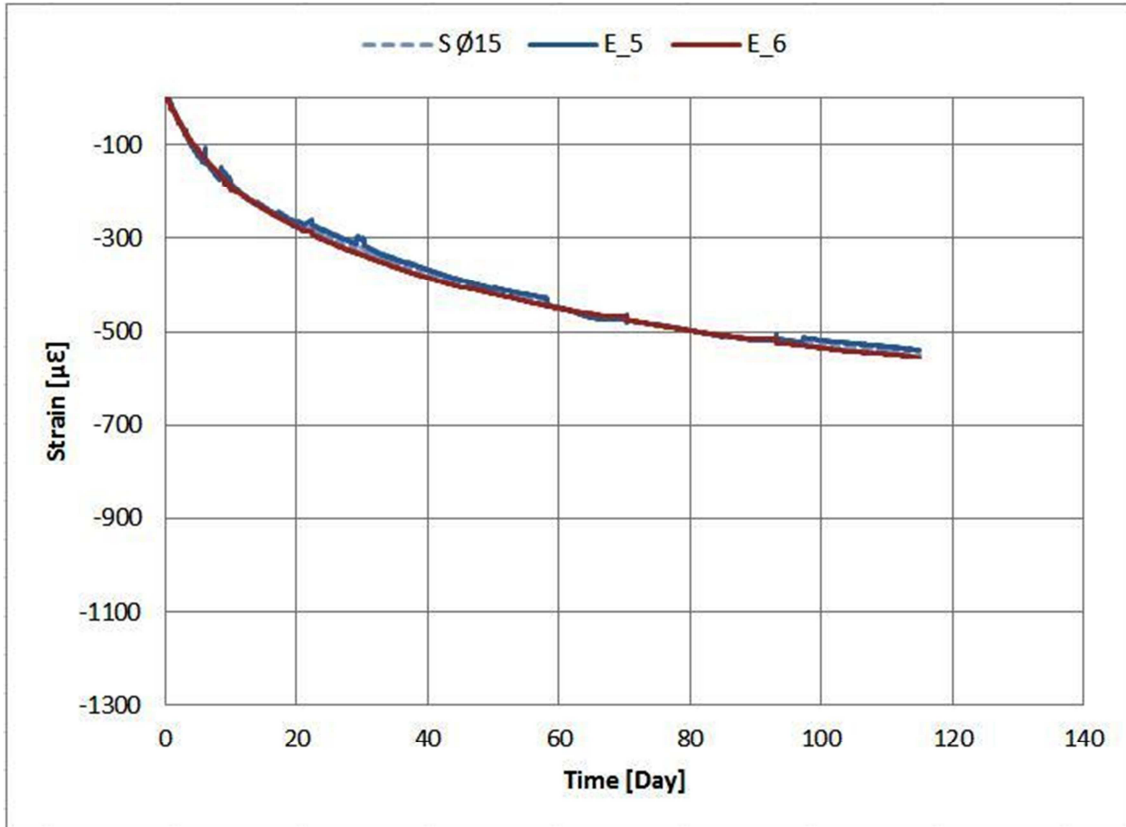


Figure 99: Mixture S and sample 150 mm of diameter

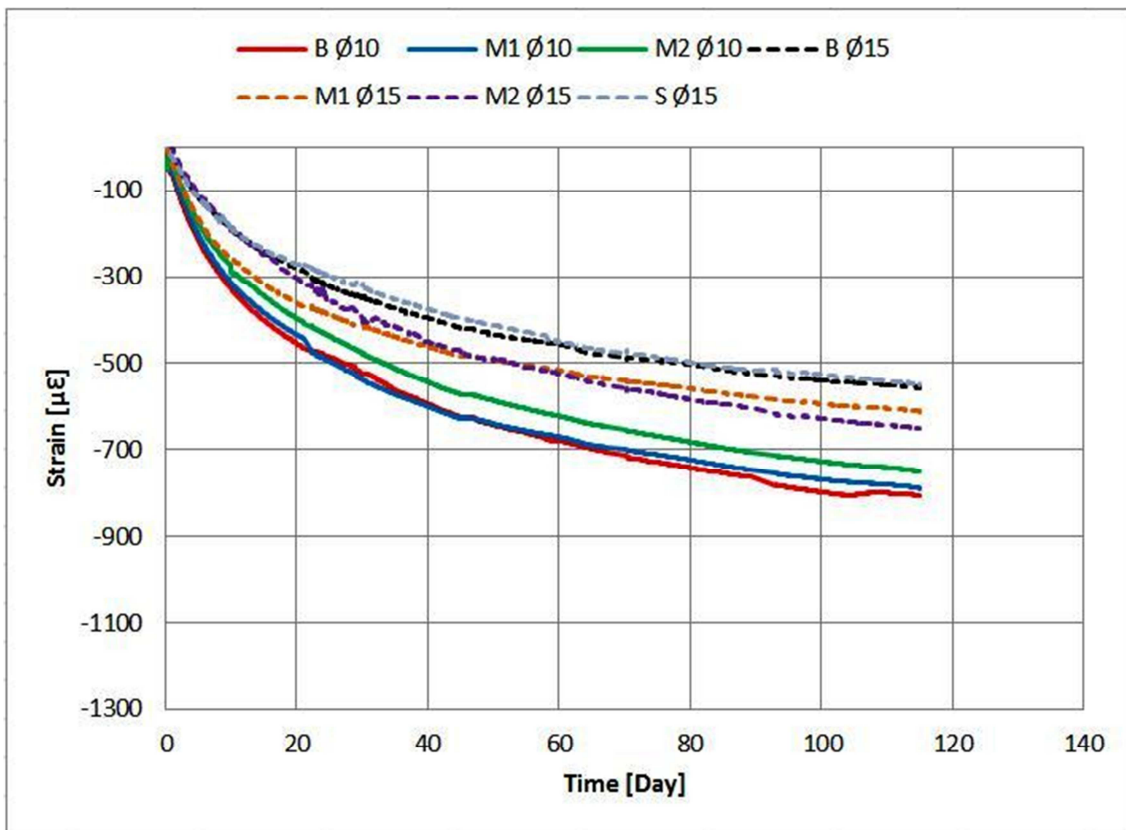


Figure 100: Generical shrinkage comparison

7.5.2 Creep Test

For testing the creep effects of the cylinder we have used a particular instrument that compresses the samples in a vertical direction with a constant pressure.

This instrument is put in a controlled climatic cell with a relative humidity of 60% and 20° C of temperature.

This instrument has very thickness plate and elements because the system must be rigid to guarantee the undeform ability during the test. Over the top plate there is a piston which loads the plate with a hydraulic oil system.

Under the top plate we have put a load cell with you can read the value of the load applied. Sometimes is necessary control the pressure level of the piston and stabilize the value of the load using an elementary pump system.

Through this system the load can follow the deformations remaining constant in time.

After this, we have positioned the cylinder in a vertical position and we put in contrast the piston.



Figure 101: Creep test of cylindrical samples

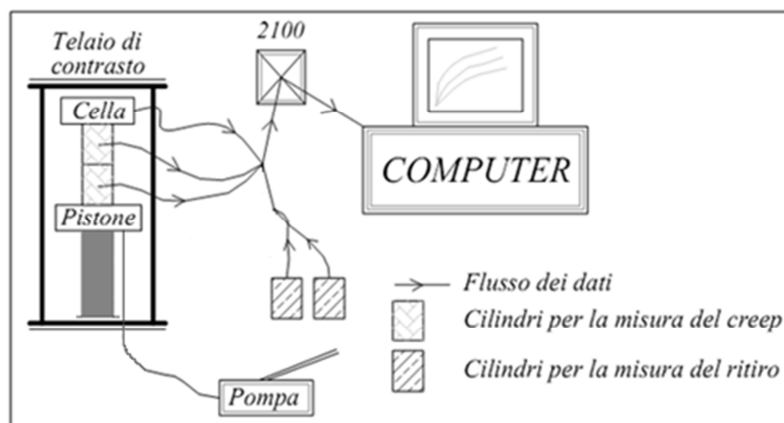


Figure 102: Acquisition data system

In order to define the value of the load applied on the piston we have measured the mean cubic compression resistance:

Lombarda Calcestruzzi [B], Mechanical Compression Resistance UNI EN 12390-3						
Day	Date	Weight after 1 day [g]	Rc1 [N/mm ²]	Weight after 2 days [g]	Rc2 [N/mm ²]	Rcm [N/mm ²]
7	16/11/2011	7813	31.6	7829	30.6	31.1
28	07/12/2011	7853	38.7	7865	40.9	39.8

Lombarda Calcestruzzi [M1], Mechanical Compression Resistance UNI EN 12390-3						
Day	Date	Weight after 1 day [g]	Rc1 [N/mm ²]	Weight after 2 days [g]	Rc2 [N/mm ²]	Rcm [N/mm ²]
7	16/11/2011	7863	31.3	7875	32.4	31.9
28	07/12/2011	7828	42.6	7842	41.8	42.2

Lombarda Calcestruzzi [M2], Mechanical Compression Resistance UNI EN 12390-3						
Day	Date	Weight after 1 day [g]	Rc1 [N/mm ²]	Weight after 2 days [g]	Rc2 [N/mm ²]	Rcm [N/mm ²]
7	16/11/2011	7850	29.1	7828	30.5	29.8
28	07/12/2011	7803	38.2	7809	39.2	38.7

Figure 103: Mean cubic compression resistance

$$R_{ckm} = 40.23 \text{ N/mm}^2$$

Then, multiplying for a coefficient we have obtained:

$$f_{cm} = 0,83 \cdot R_{ckm} = 0,83 \cdot 40.23 = 33.39 \text{ N/mm}^2$$

Knowing that the samples area is:

$$\text{Area} = \frac{\pi \cdot \Phi^2}{4} = 7853.98 \text{ mm}^2$$

$$F_r = \text{Area} \cdot f_{cm} = 262273.20 \text{ N}$$

At the end, for computing the creep load, we have reduced the force of a quantity about 75%:

$$F_{\text{creep}} = 0,25 \cdot F_r = 65568.31 \text{ N} \rightarrow 6557 \text{ Kg}$$

This reduction derives from the viscosity theory of the concrete which considers that its behavior is linear for tensional state under 40-45% of the rupture tension, where we can have nonlinear behaviors.

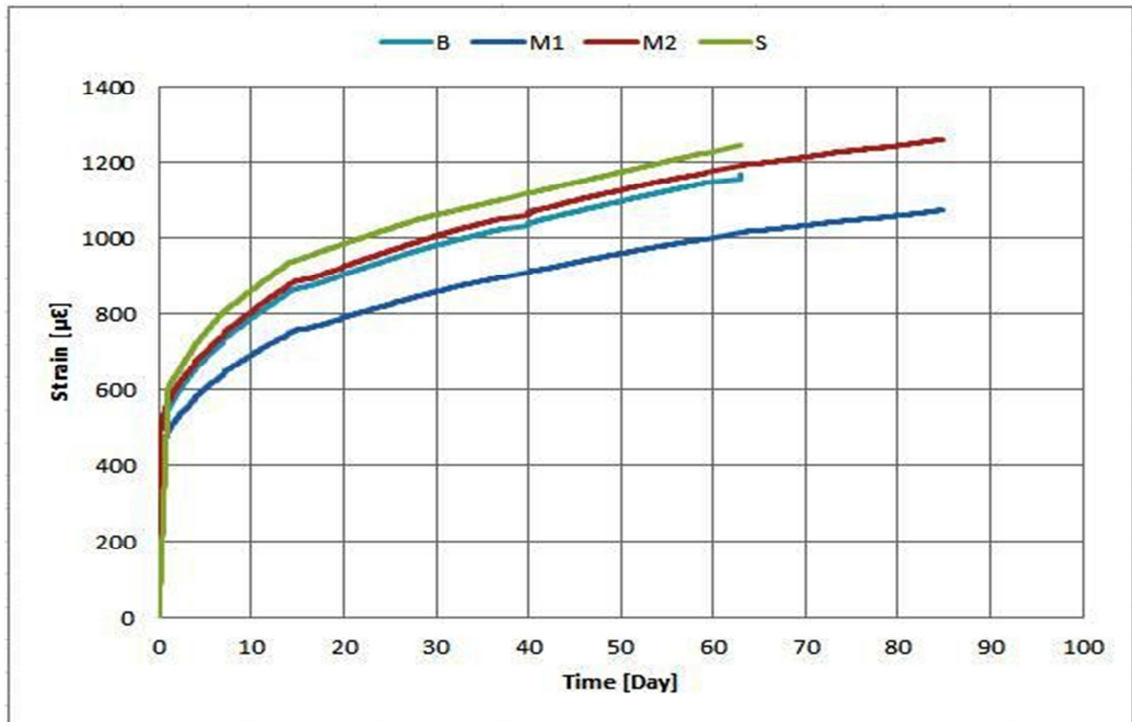


Figure 104: Creep test comparison for cylindrical samples

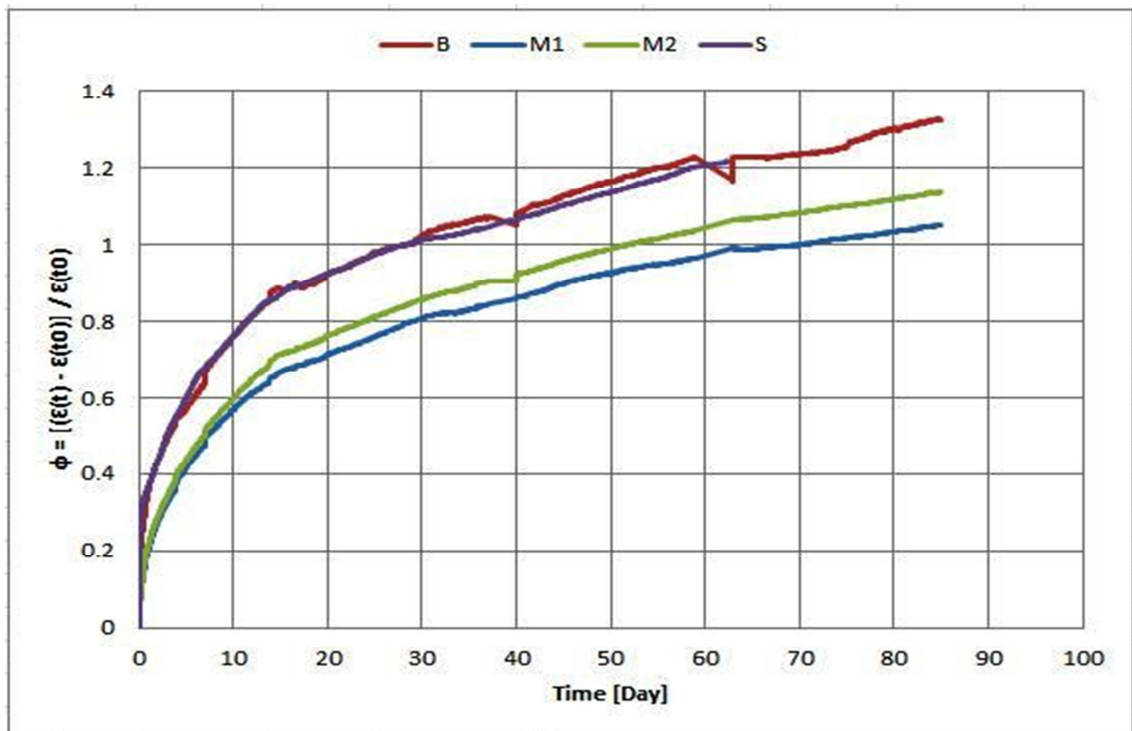


Figure 105: relative creep test comparison for cylindrical samples

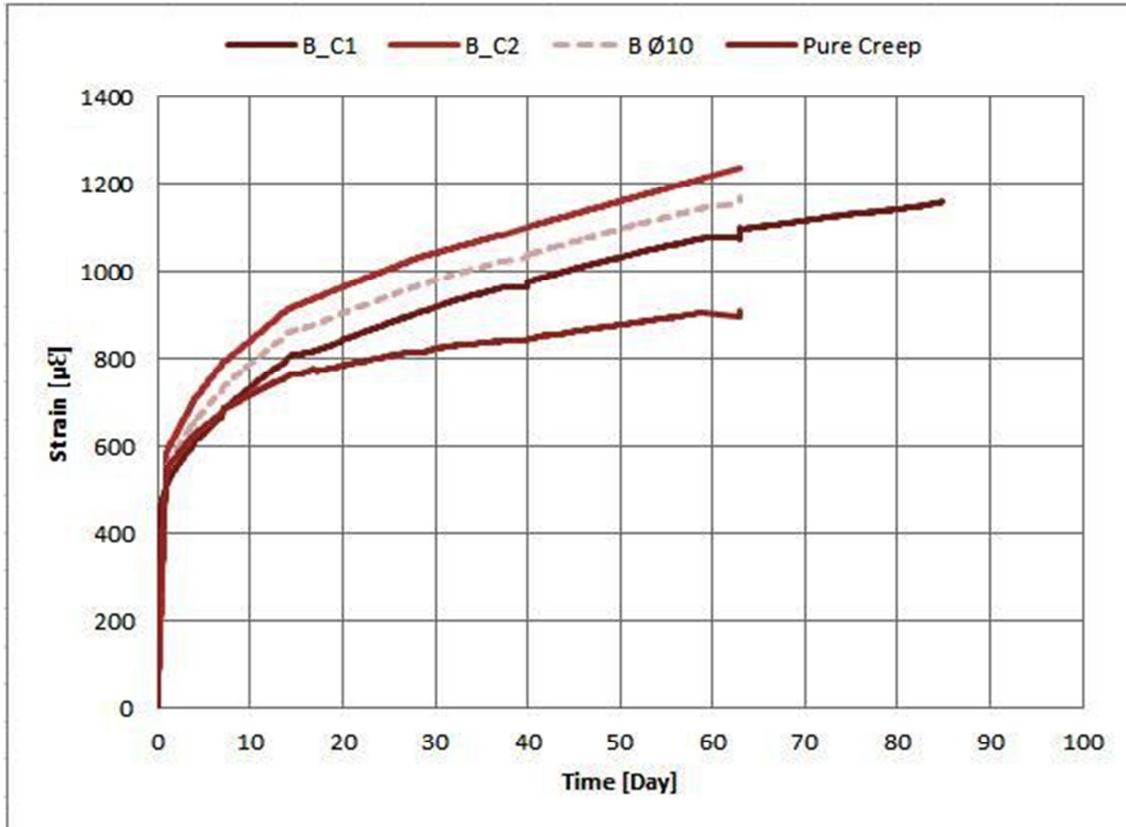


Figure 106: Creep test for samples B

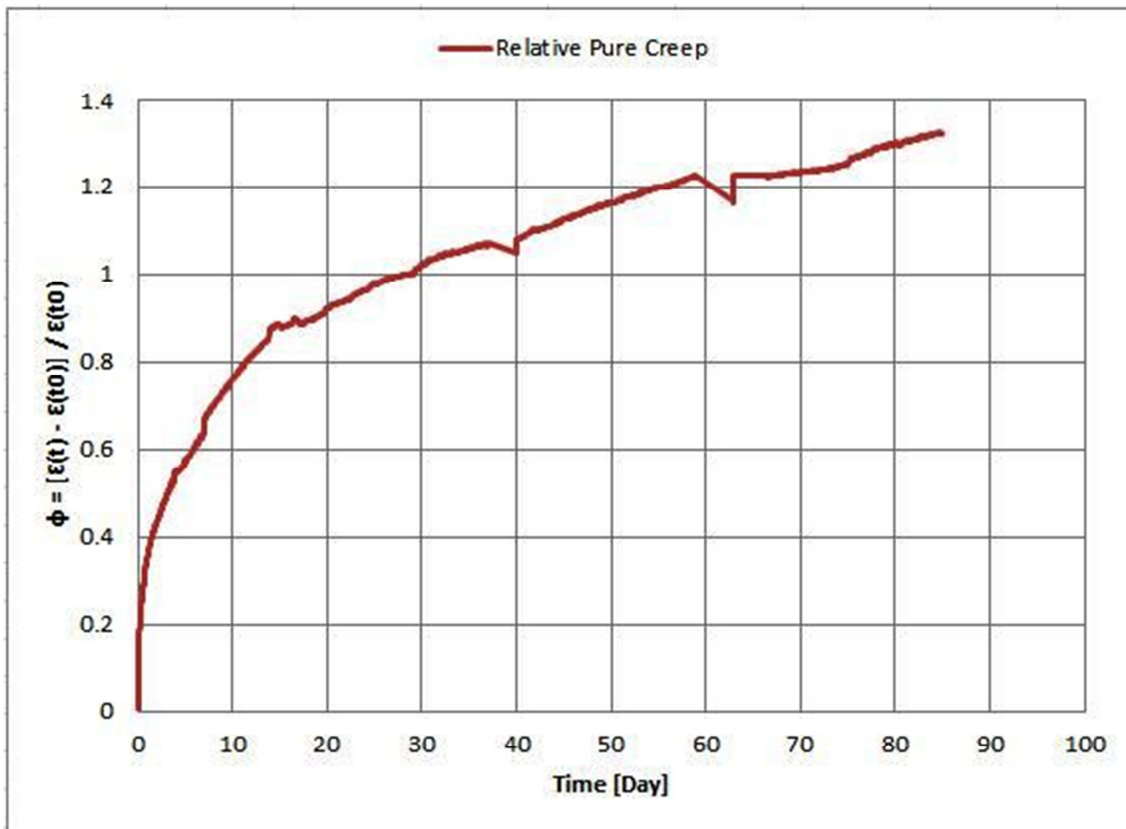


Figure 107: relative creep test for samples B

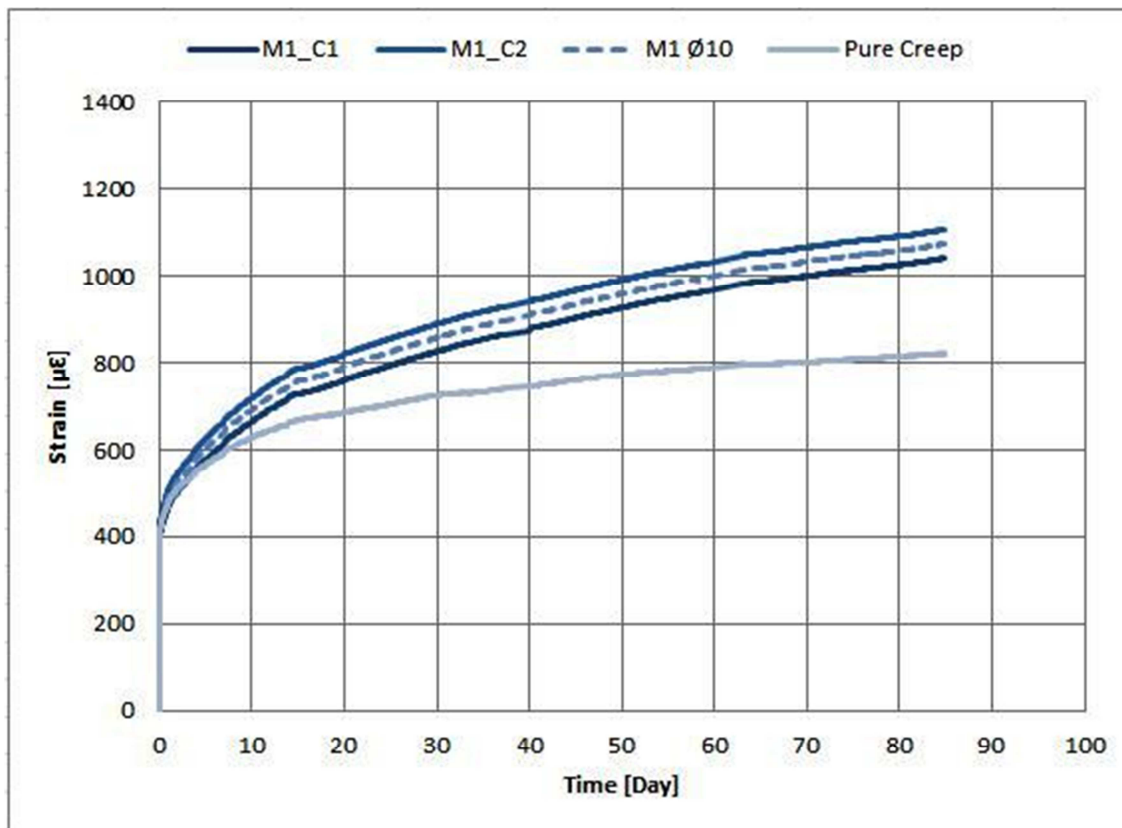


Figure 108: Creep test for samples M1

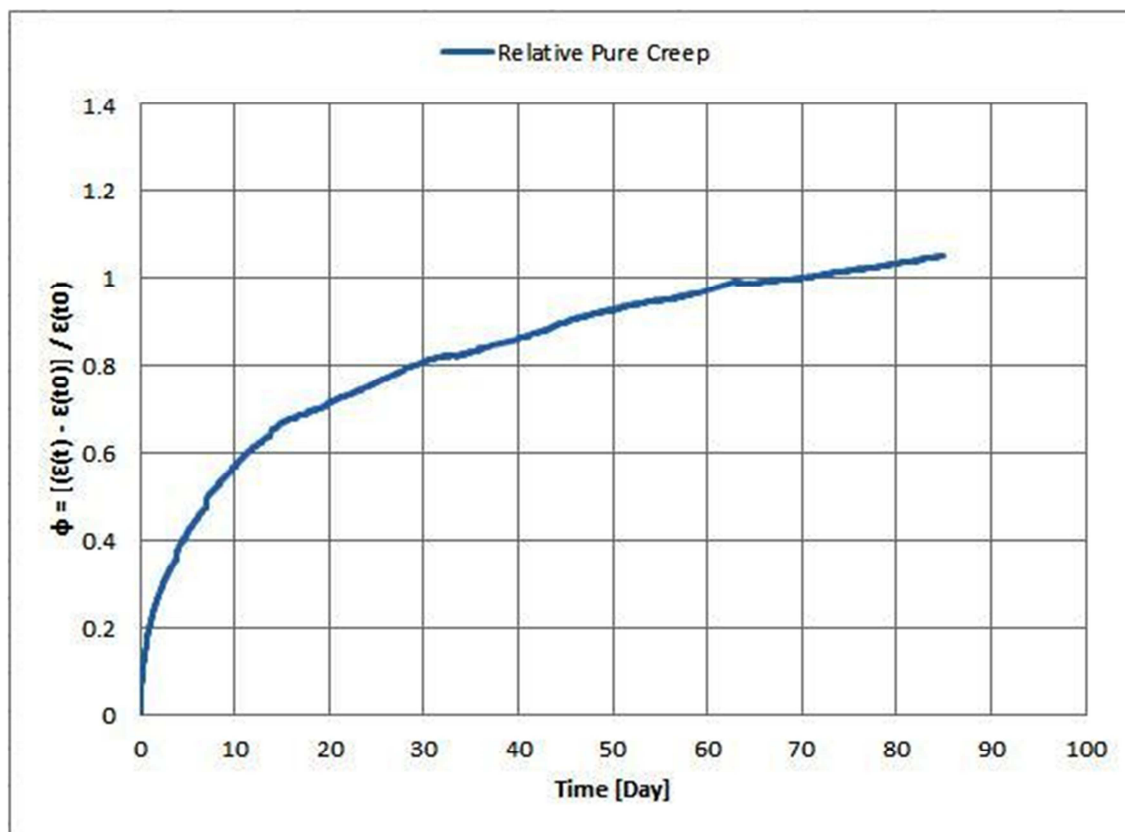


Figure 109: Relative creep test for samples M1

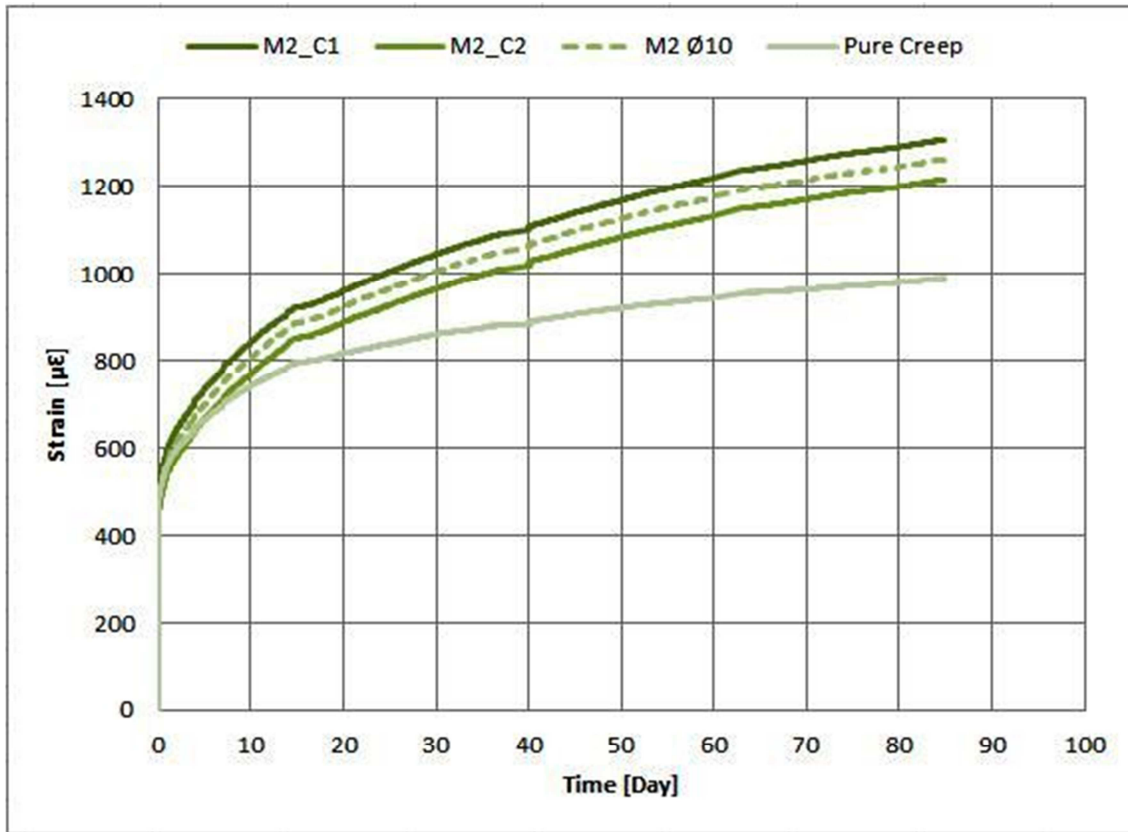


Figure 110: Creep test for samples M2

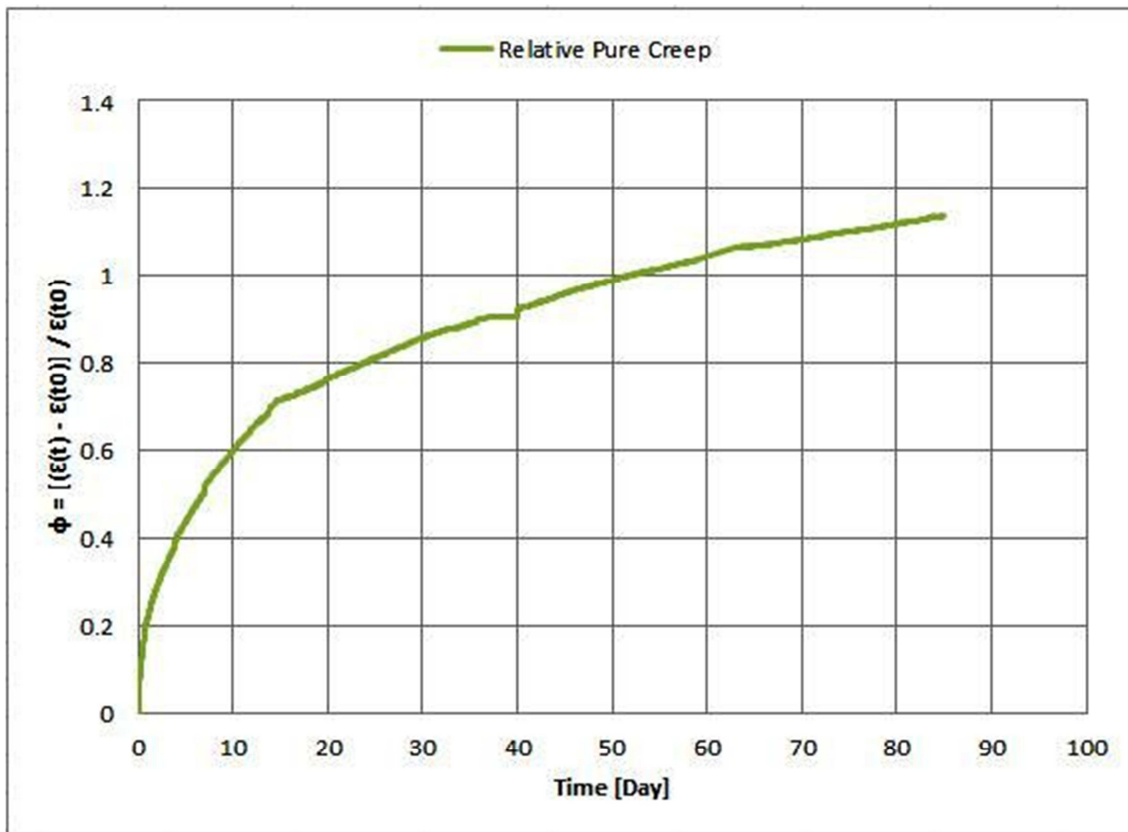


Figure 111: Relative creep test for samples M2

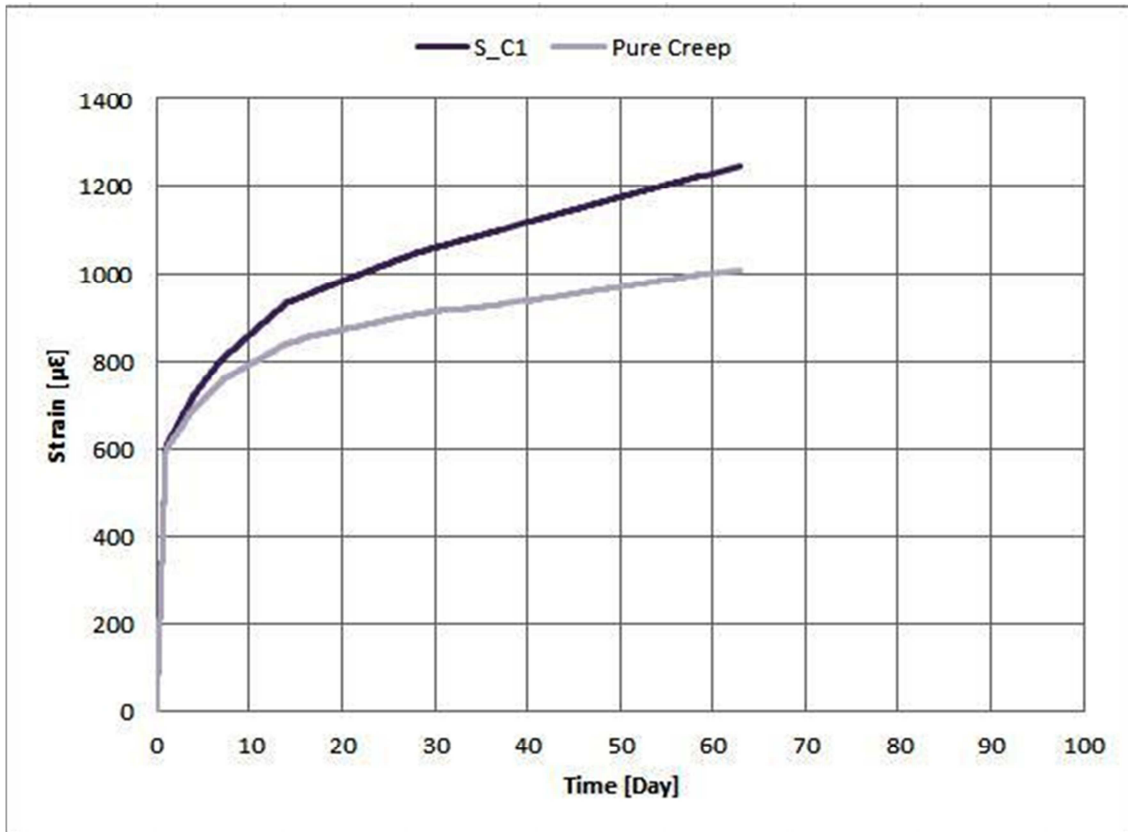


Figure 112: Creep test for sample S

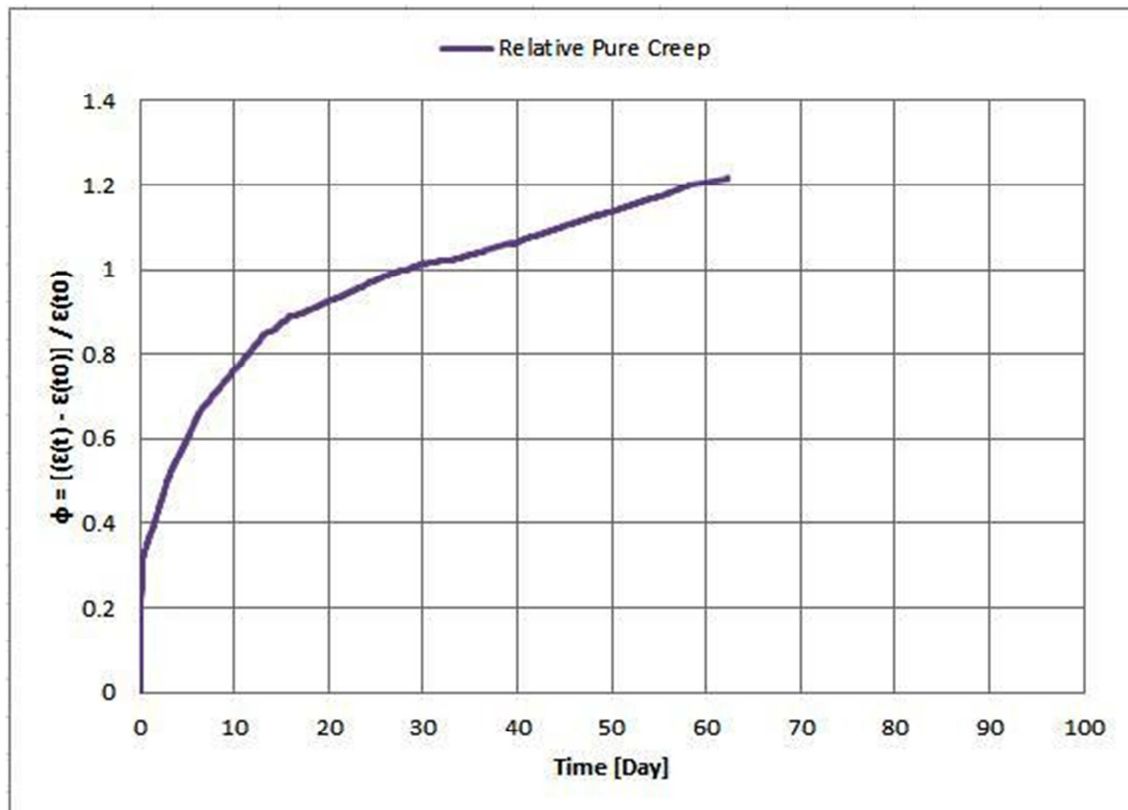


Figure 113: Relative creep test for sample S

7.6 Viscous Test of Beam Samples

7.6.1 Generalities

The viscous test of the beam samples is done using two steel supports with 75 cm of span and various weights. Each support is constituted by reinforced steel plate where we can apply the loads. At first the beam is loaded by a series of weight until the critical load computed before considering the compression resistance of the concrete with and without fibers.

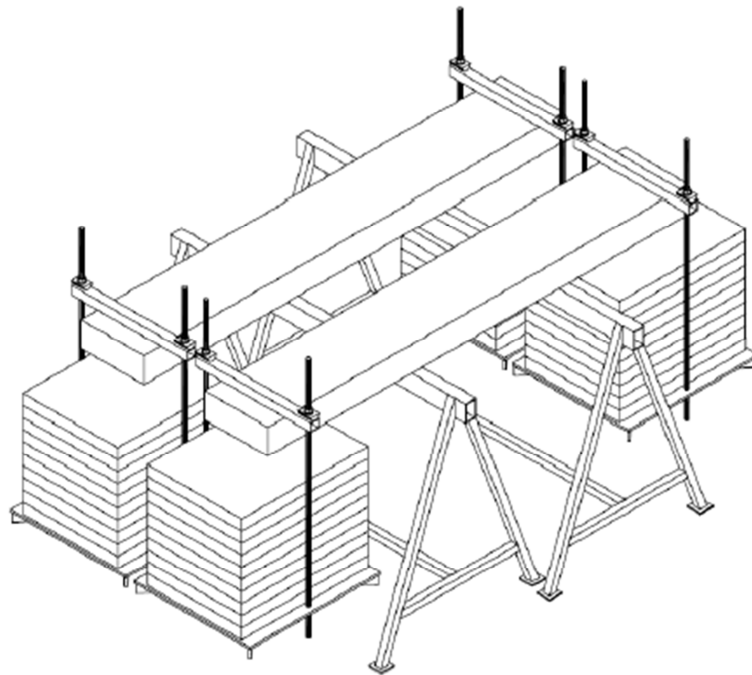


Figure 114: Beam test

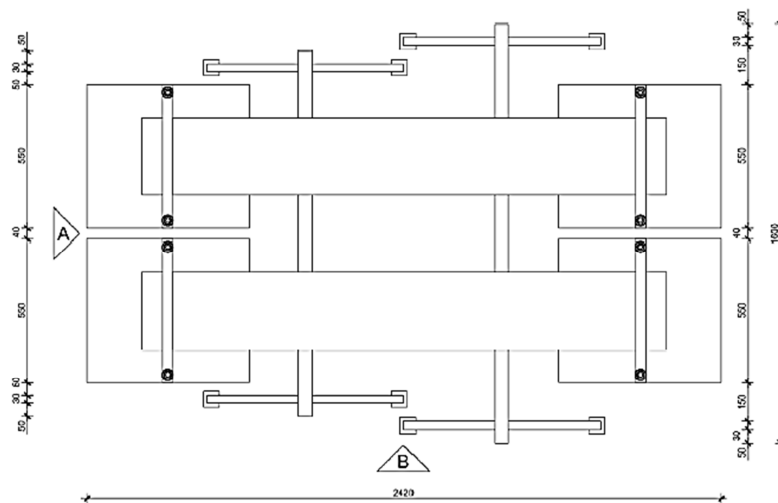


Figure 115: Beam test plan

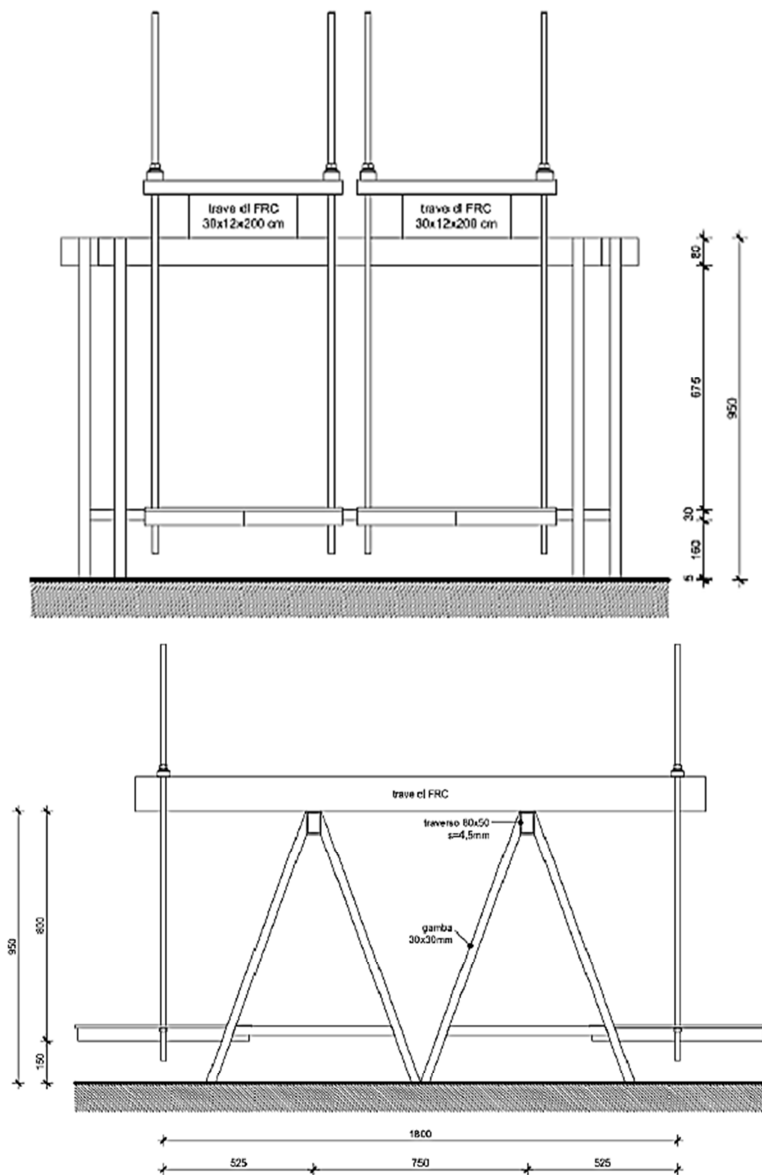


Figure 116: Lateral view of beam test

The first phase coincides with the drawing procedure to obtain a correct positioning of the supports and instruments.

In particular, the distance between the supports must be 180 cm.

For the instruments application, looks the specific chapter.

The static scheme used for this test is the following:

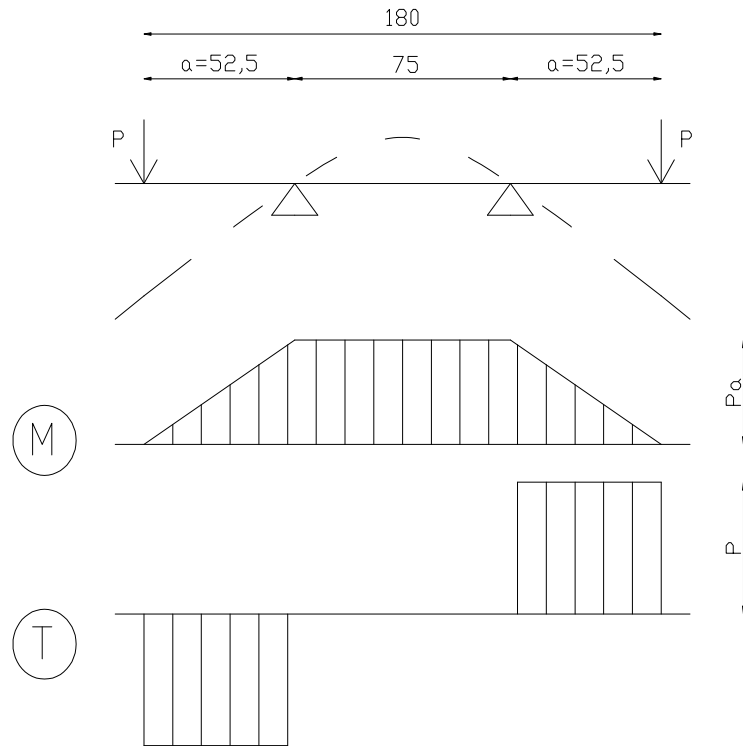


Figure 117: Static scheme



Figure 118: Instruments for viscous beam testing



Figure 119: Viscous beam test

▪ *Load Computation*

In this part the analytical procedure for the determination of the critical load are reported. The computation is obtained by the maximum opening displacements in function of the force values during the reloading phase in the cracking procedure of the samples.

The principal characteristics of the samples are shown in the table below.

Sample	SF_35	MS_4.8
Length [cm]	80	80
Creep Length [cm]	52.5	52.5
Base [cm]	30	30
Height [cm]	11	11
Inertia momentum [cm⁴]	$J = \frac{b h^3}{12} = 3328$	$J = \frac{b h^3}{12} = 3328$
Resistance modulus [cm³]	$W = \frac{b h^2}{6} = 605$	$W = \frac{b h^2}{6} = 605$

Figure 120: Beam characteristics

For evaluating the viscous phenomena of the samples in a controlled mode we have established that the creep moment is equal to the cracking moment reduced of 50%.

$$M_{cr} = M_m^{0.2} \cdot 0.5$$

This thing is finalized to avoid an instability phenomenon.

Then, from the creep moment, we have obtained the critical load:



Figure 121: Critical load

Sample	B	M1	M2
Nominal Tension [MPa]	2.89	2.39	2.61
Creep Moment [N*mm]	1748450	1445950	1500400
Critical Load [kg]	167	138	149

Figure 122: Critical loads for beam test

7.6.2 Loading Phase

The loading procedure of the beam test is done in a climatic cell where the samples stayed for all their life.

At the beginning the samples are loaded by the self-weight of the plates, then we have applied the others loads for each side in this order:

**Steel and Macro-Synthetic Self-Compacting Fiber Reinforced Concrete,
Experimental Study on the Long-Term Deformations**

Type	B	M1	M2
1° load	40 kg	40 kg	40 kg
2° load	33.10 kg	31.85 kg	34.35 kg
3° load	33.05 kg	33.10 kg	32.35 kg
4° load	31.30 kg	32.35 kg	34.40 kg
5° load	31.30 kg	0	10 kg
Total Weight for each side	168.75 kg	137.30 kg	151.10 kg

Figure 123: Beam loads



Figure 124: Loading phase examples

The loading phase results are listed below and in particular you can see:

- CMOD variation during loading phase;
- Mid-Span variation during loading phase;

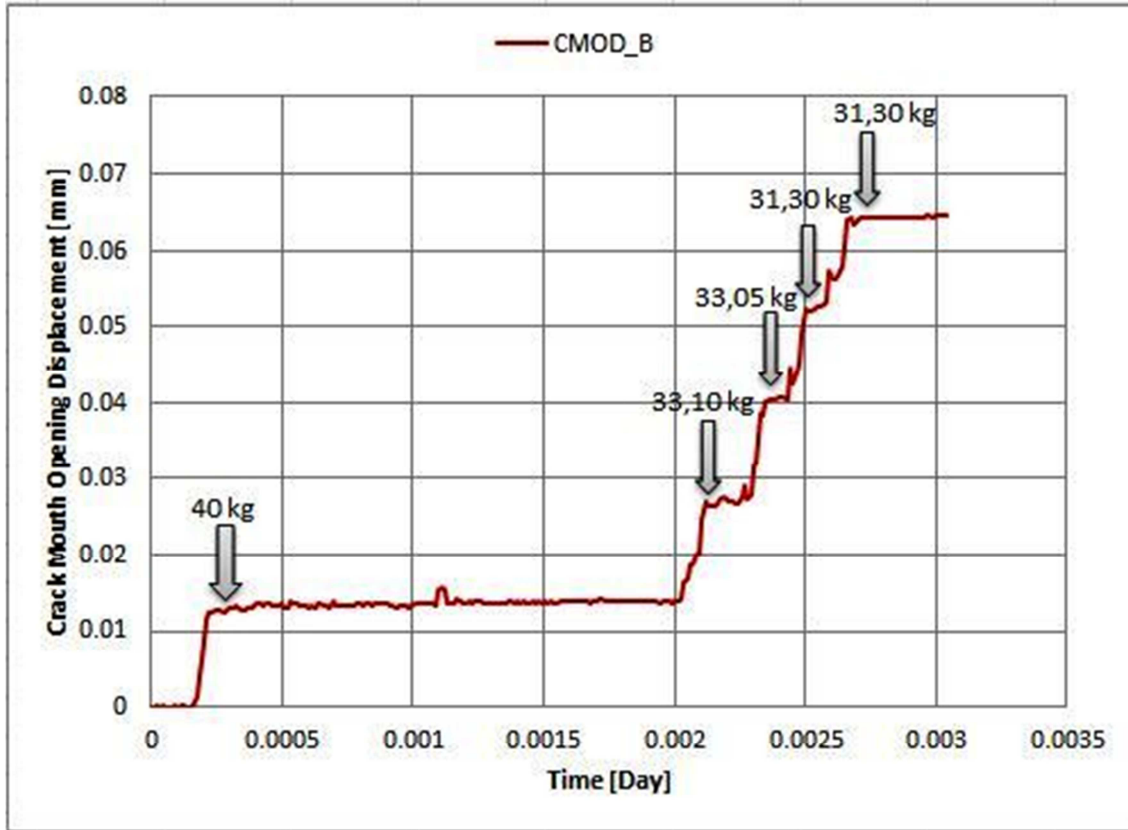


Figure 125: CMOD B during loading phase

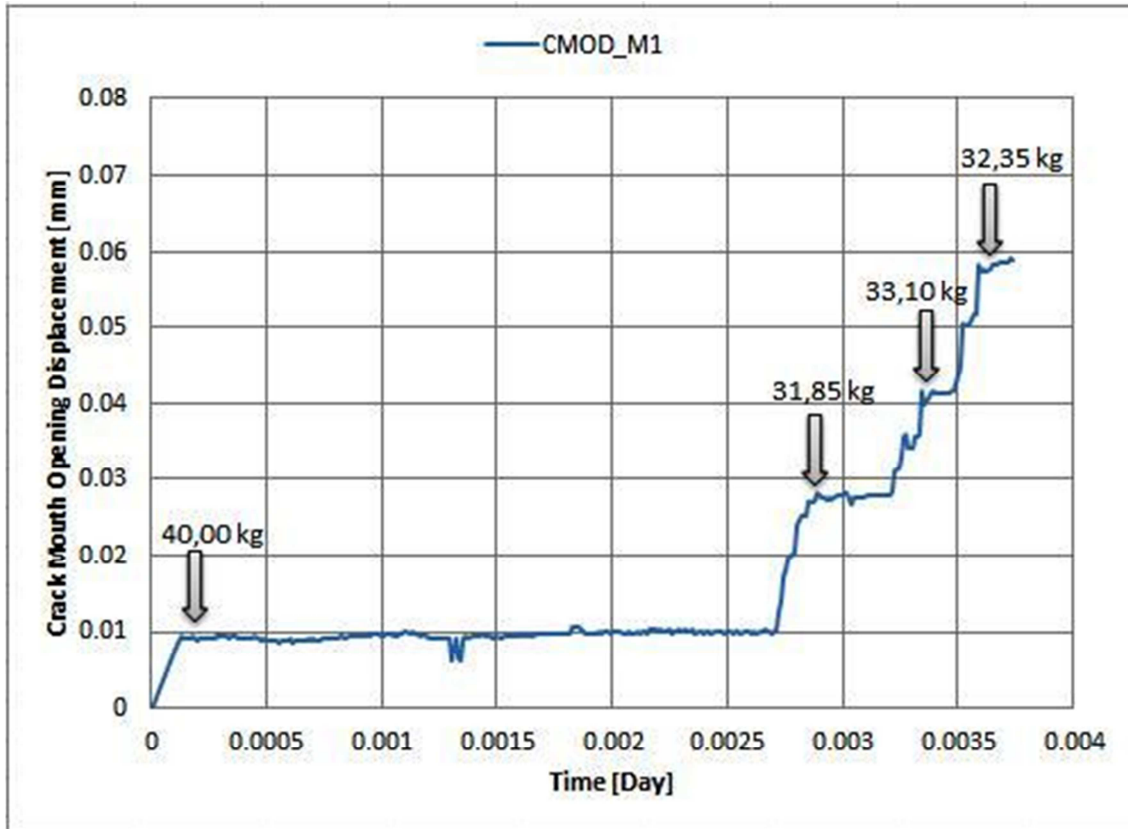


Figure 126: CMOD M1 during loading phase

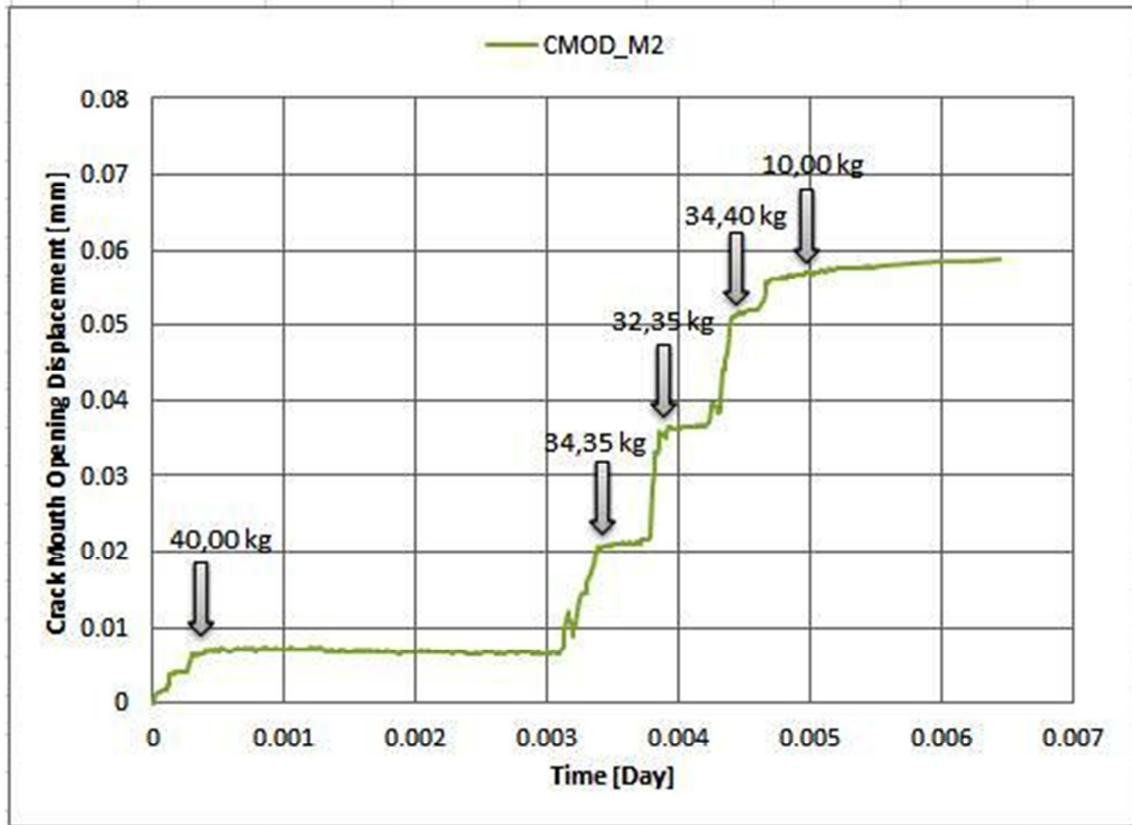


Figure 127: CMOD M2 during loading phase

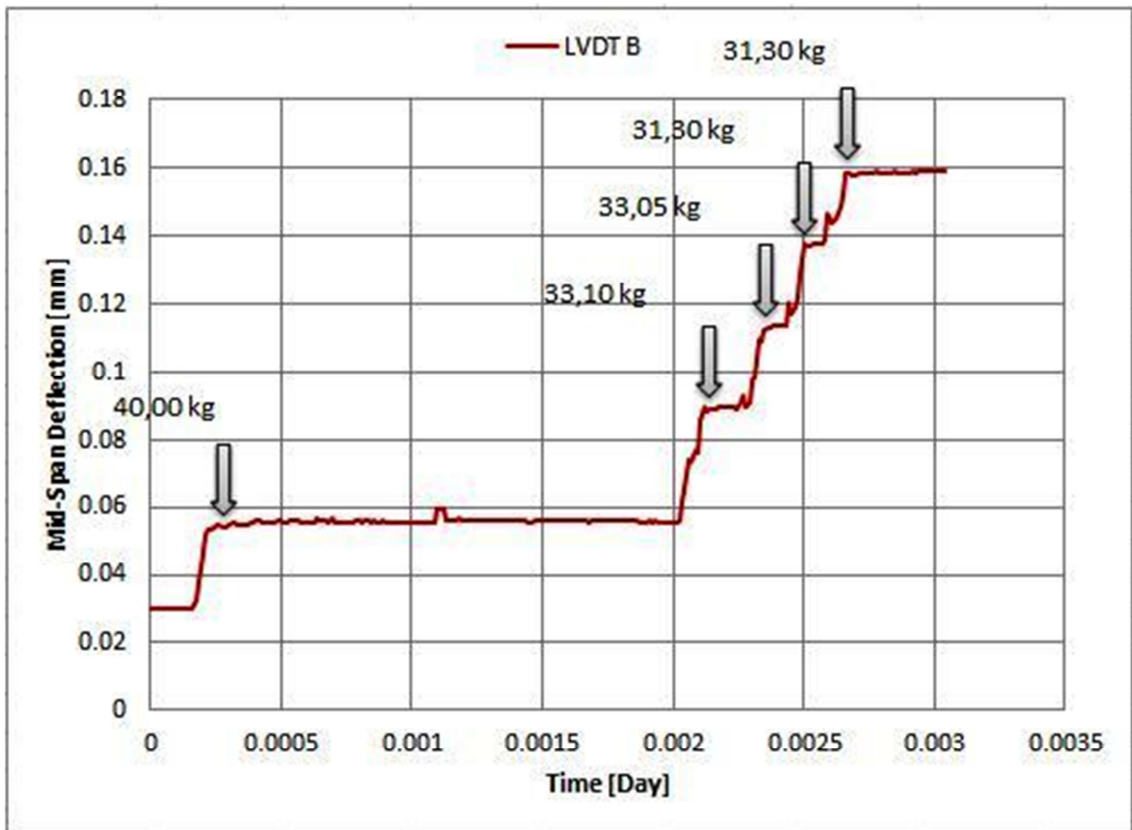


Figure 128: LVDT B during loading phase

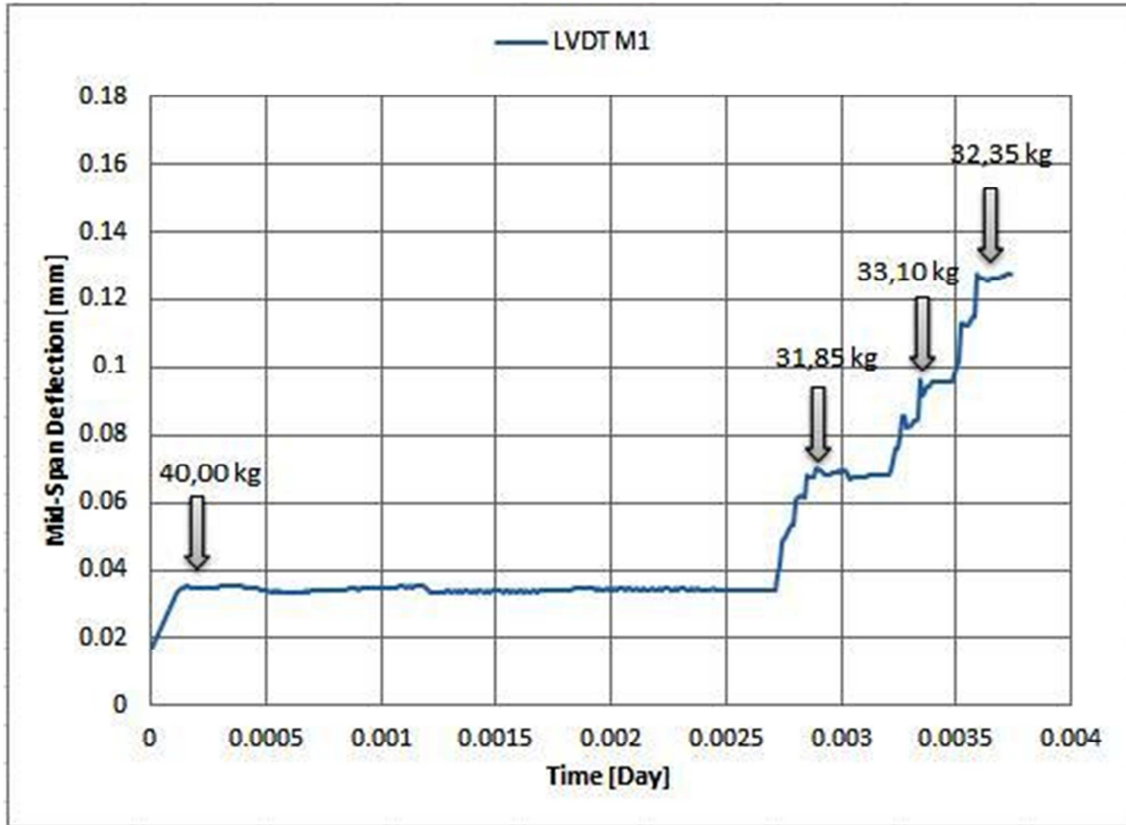


Figure 129: LVDT M1 during loading phase

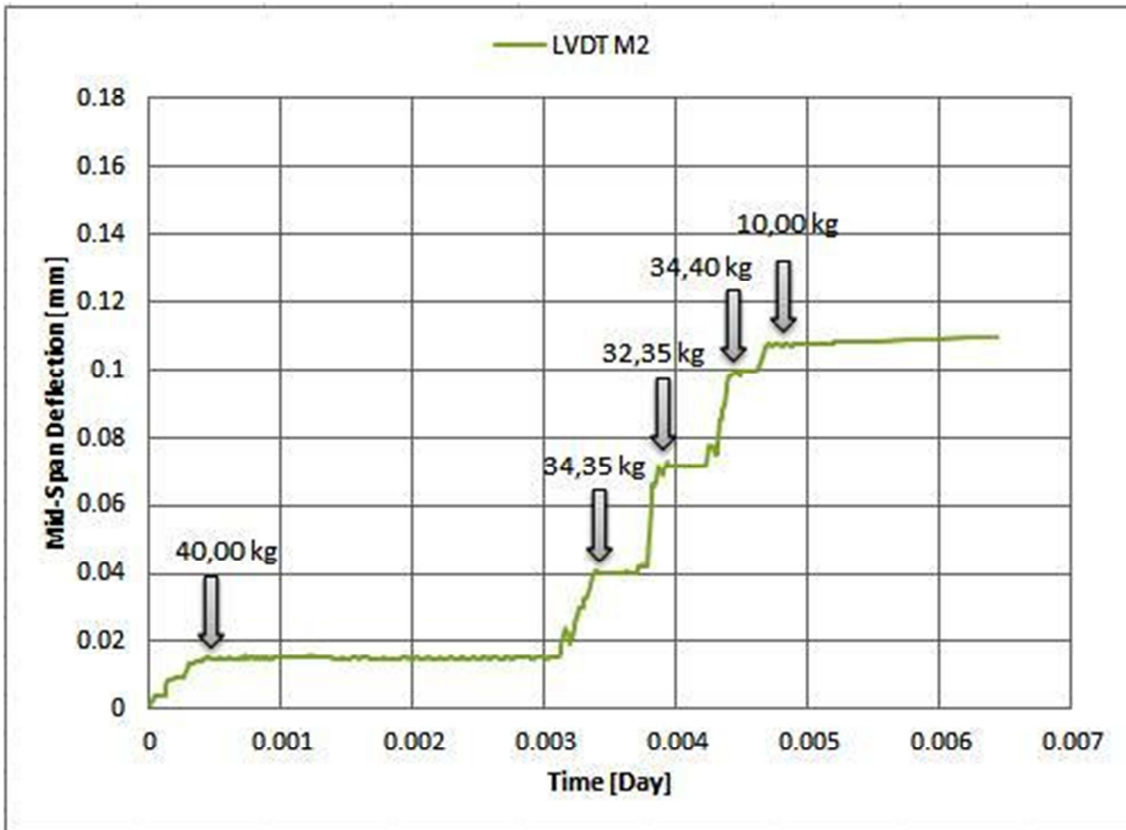


Figure 130: LVDT M2 during loading phase

7.6.3 Loading Phase Comparison

In this part you can observe the loading phase behavior of the beam samples. These three graphs explain the reload procedure in terms of CMOD and Mid-Span Deflection.

The last chart shows what the relation is between: mechanical reloading, that we've done during the cracking analysis, and the manual reloading that we have done during the viscous test. However the chart is in function of the nominal tension because the static scheme applied is different and we must do a comparison in a right mode.

As you can see before:

- $W = 605000 \text{ mm}^3$;
- F is the applied force in Kg;
- $L = 525 \text{ mm}$;

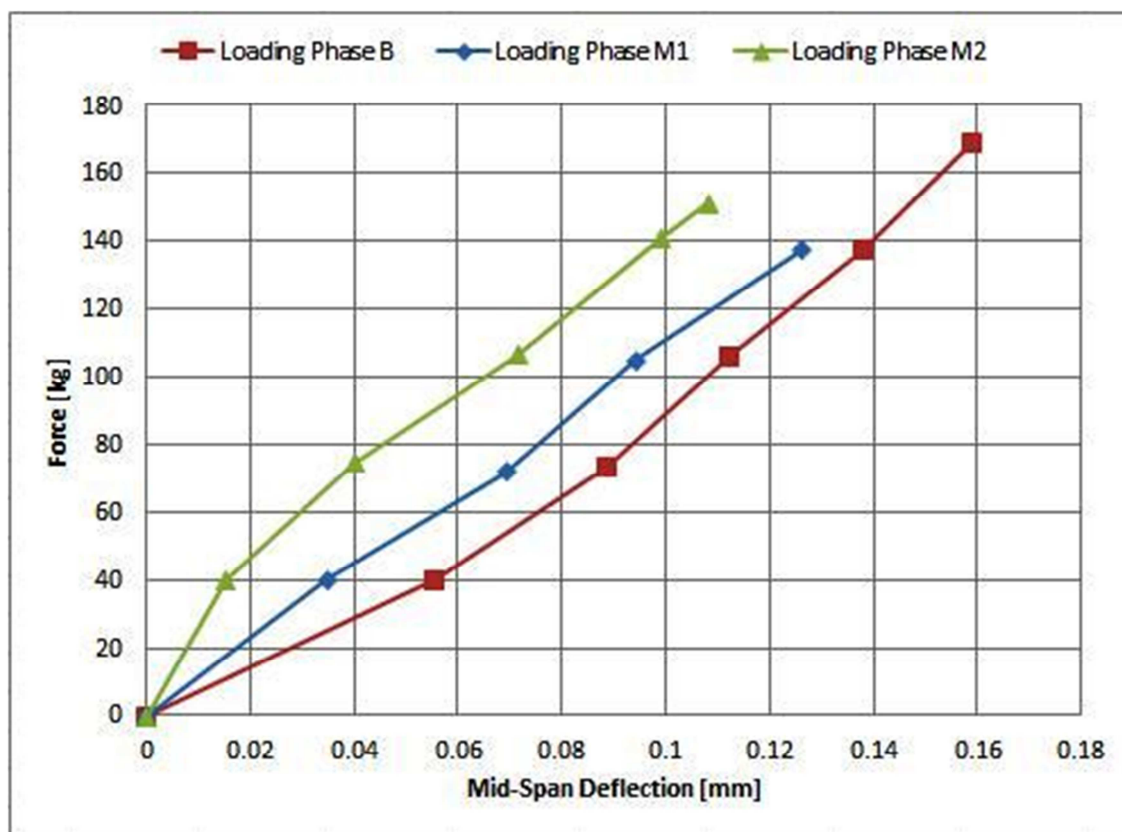


Figure 131: LVDT-Force comparison during loading phase

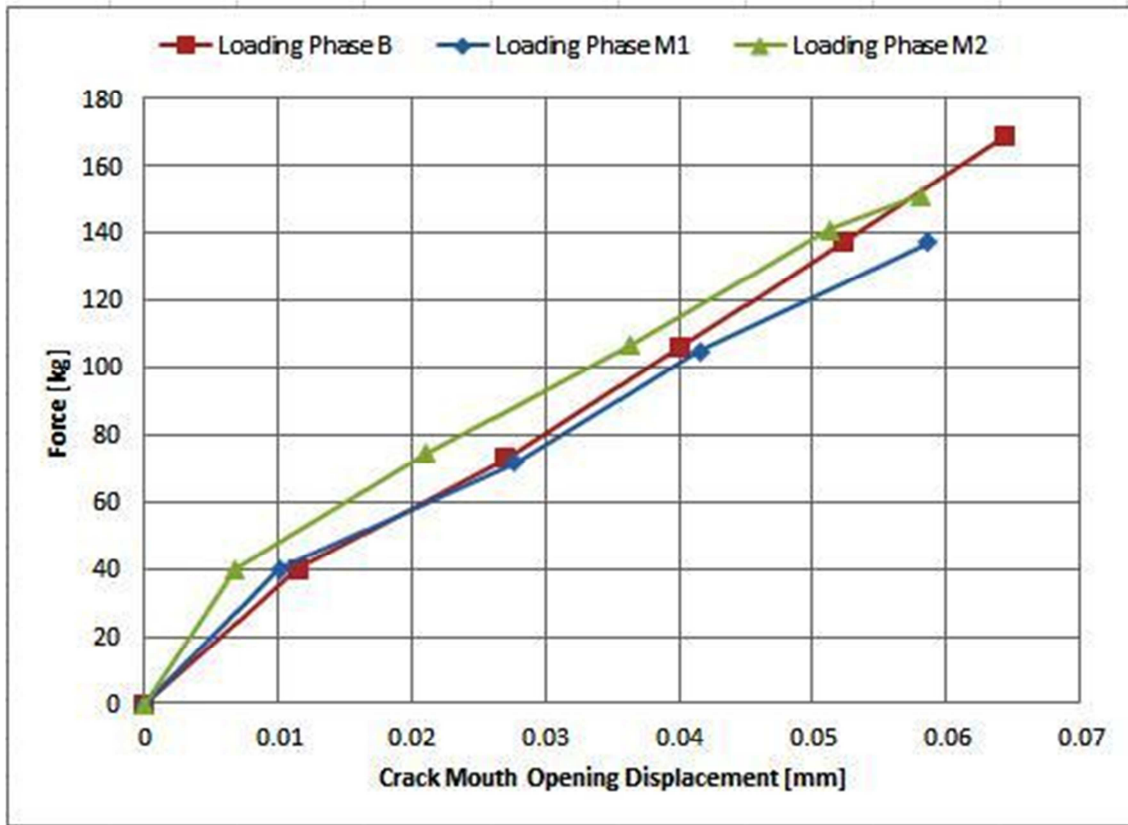


Figure 132: CMOD-Force comparison during loading phase

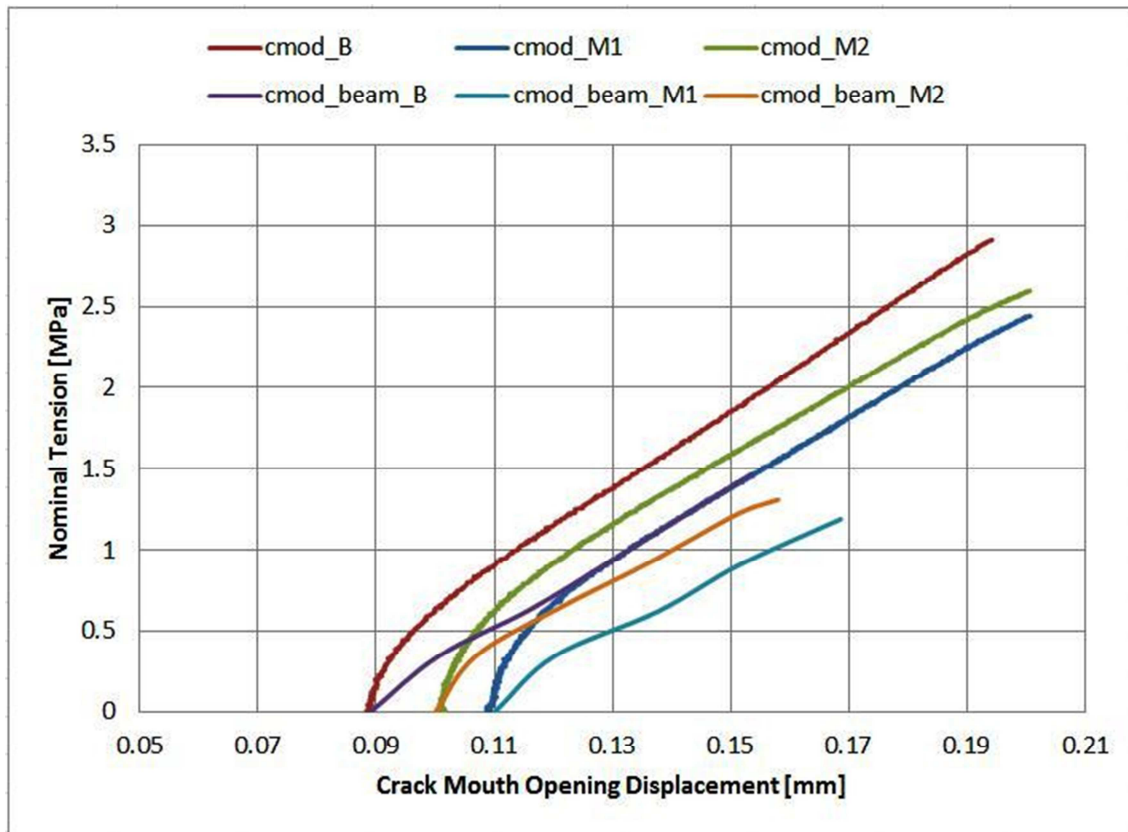


Figure 133: Loading comparison among viscous and cracking test

7.6.4 Absolute Viscous Deformations

In this paragraph you can find the data of the beam samples from the starting point of the test.

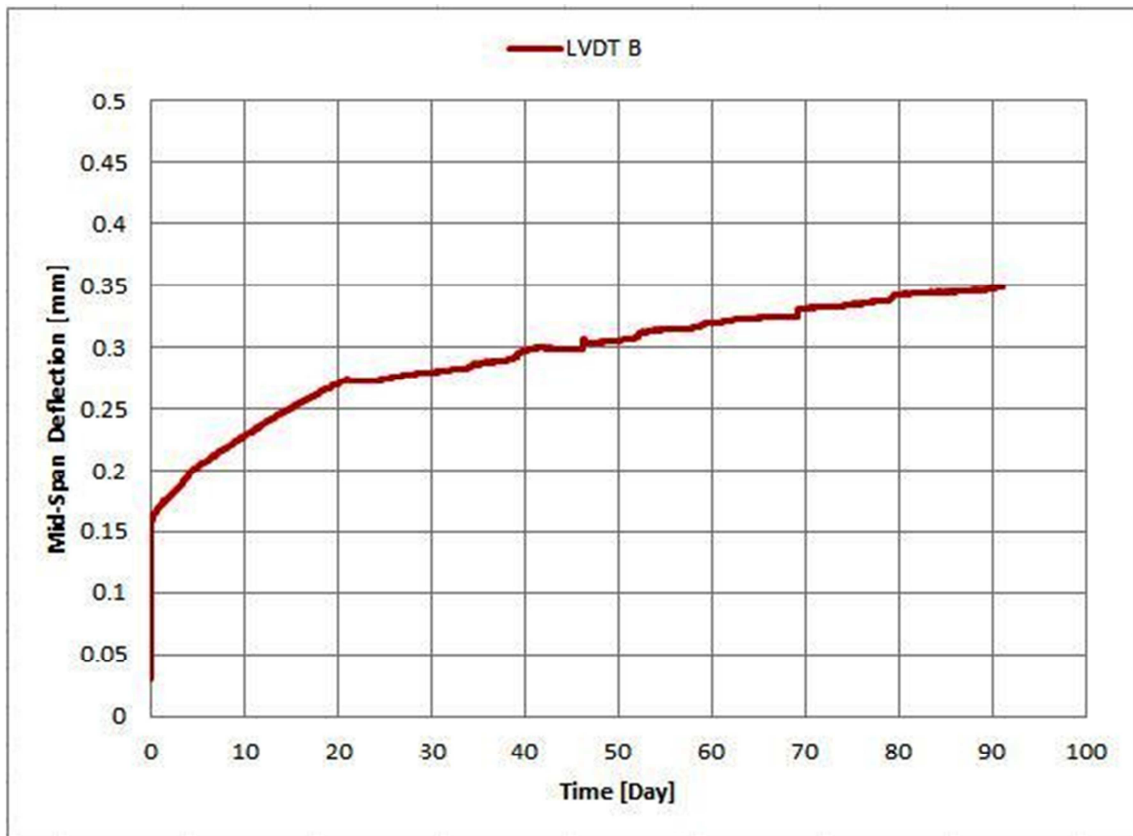
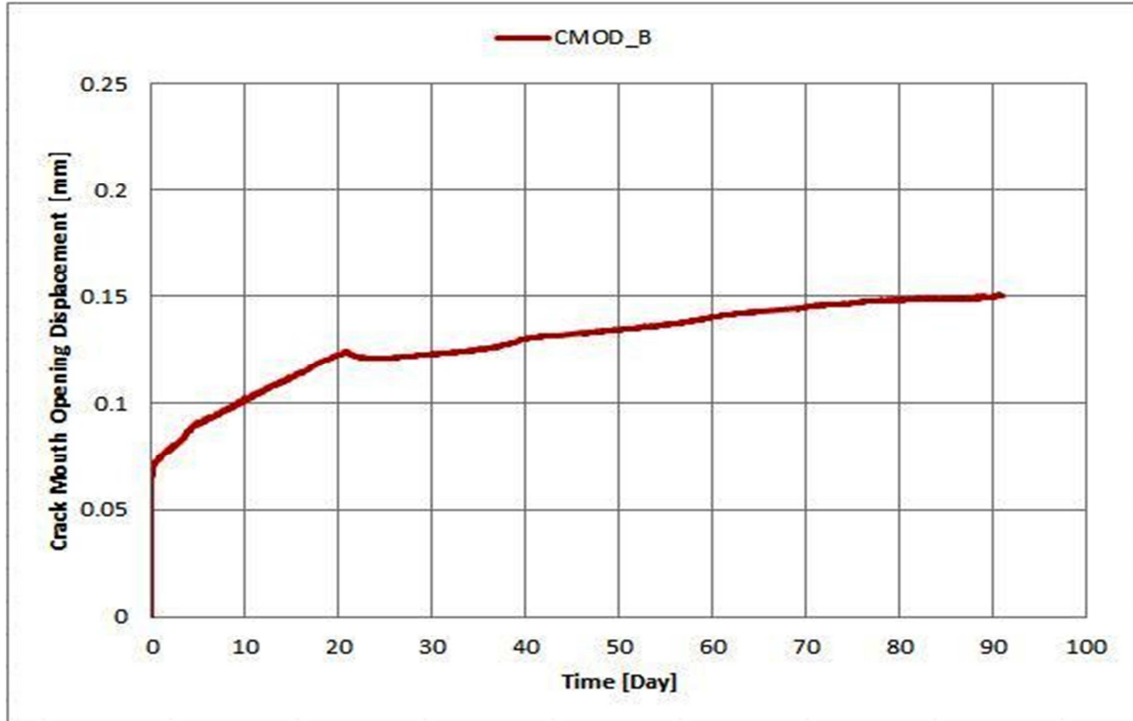


Figure 134: Absolute CMOD and Mid-Span Deflection variation of B

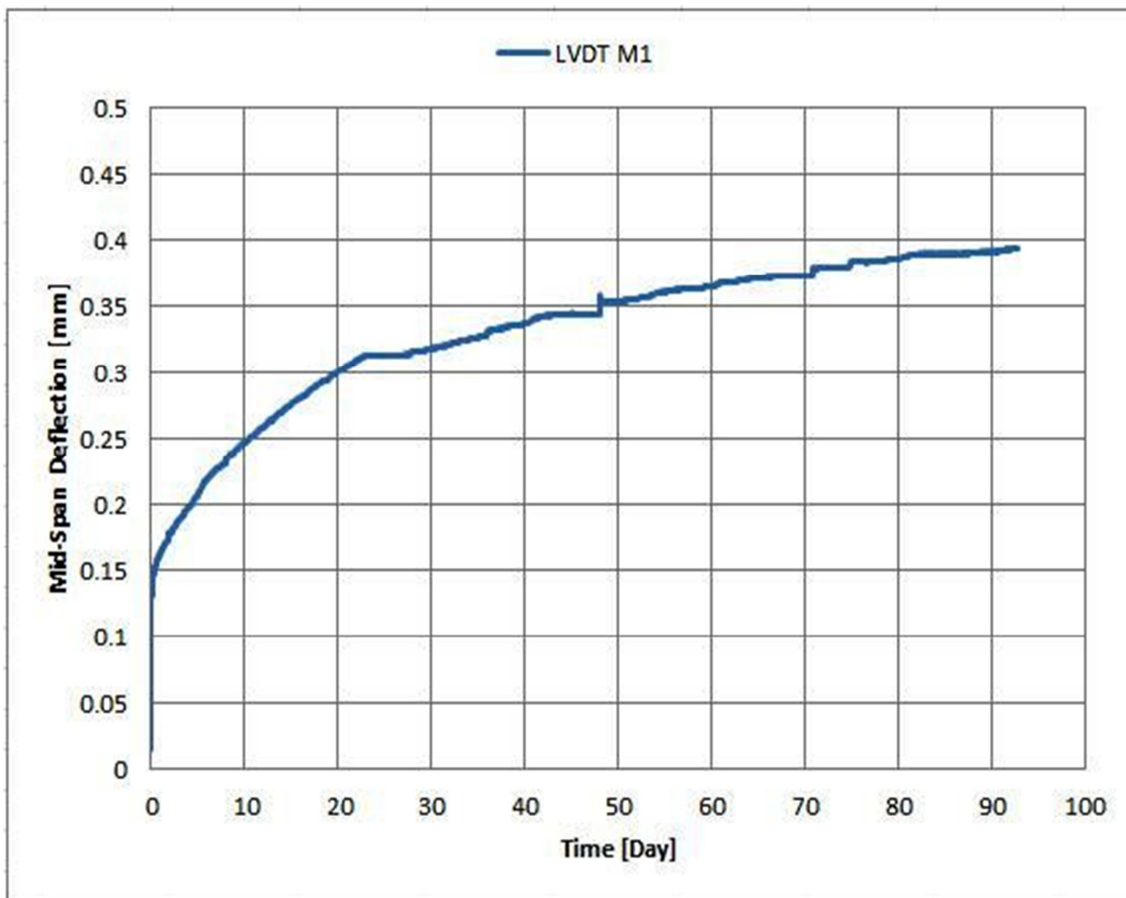
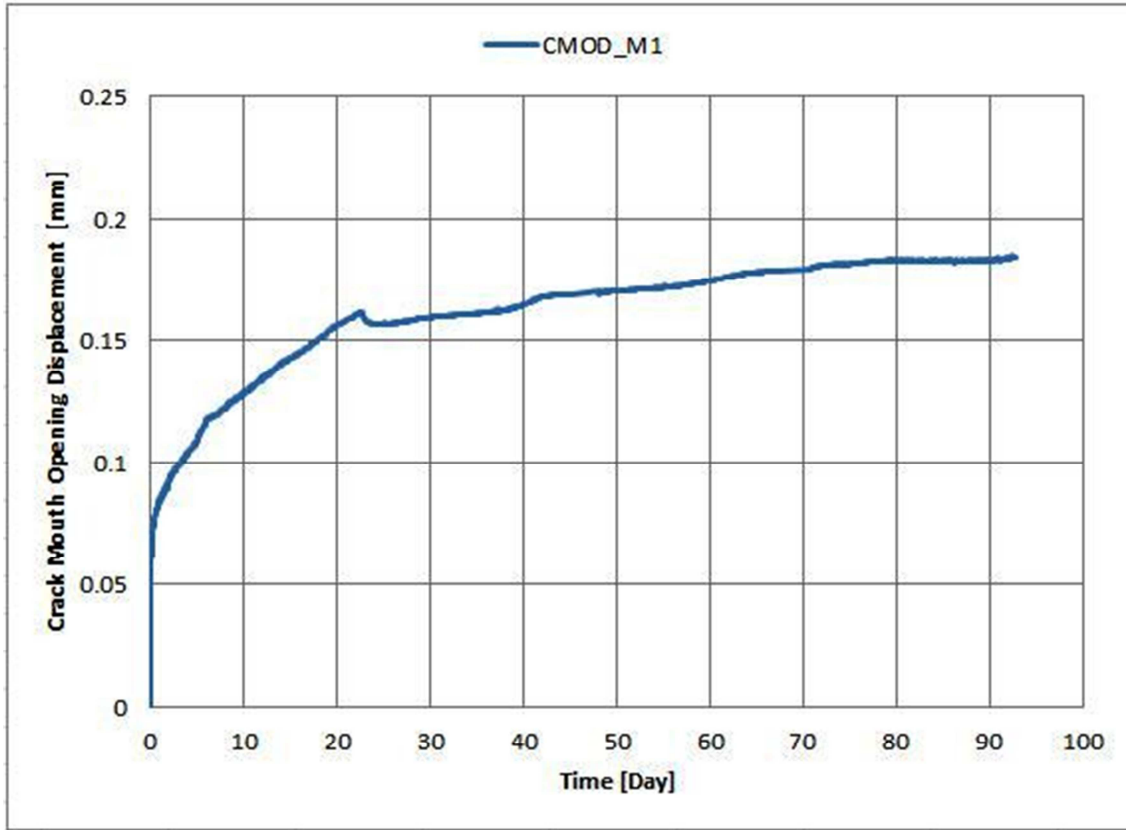


Figure 135: Absolute CMOD and Mid-Span Deflection variation of M1

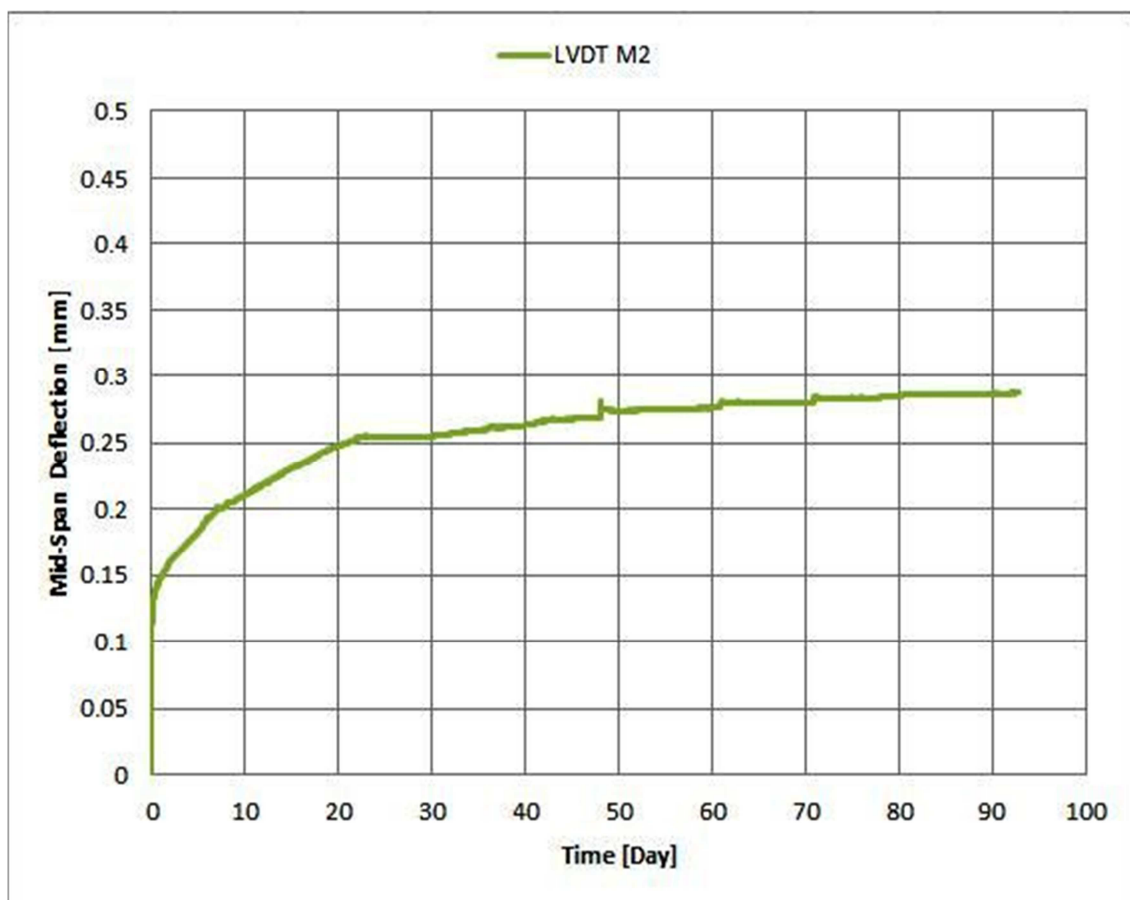
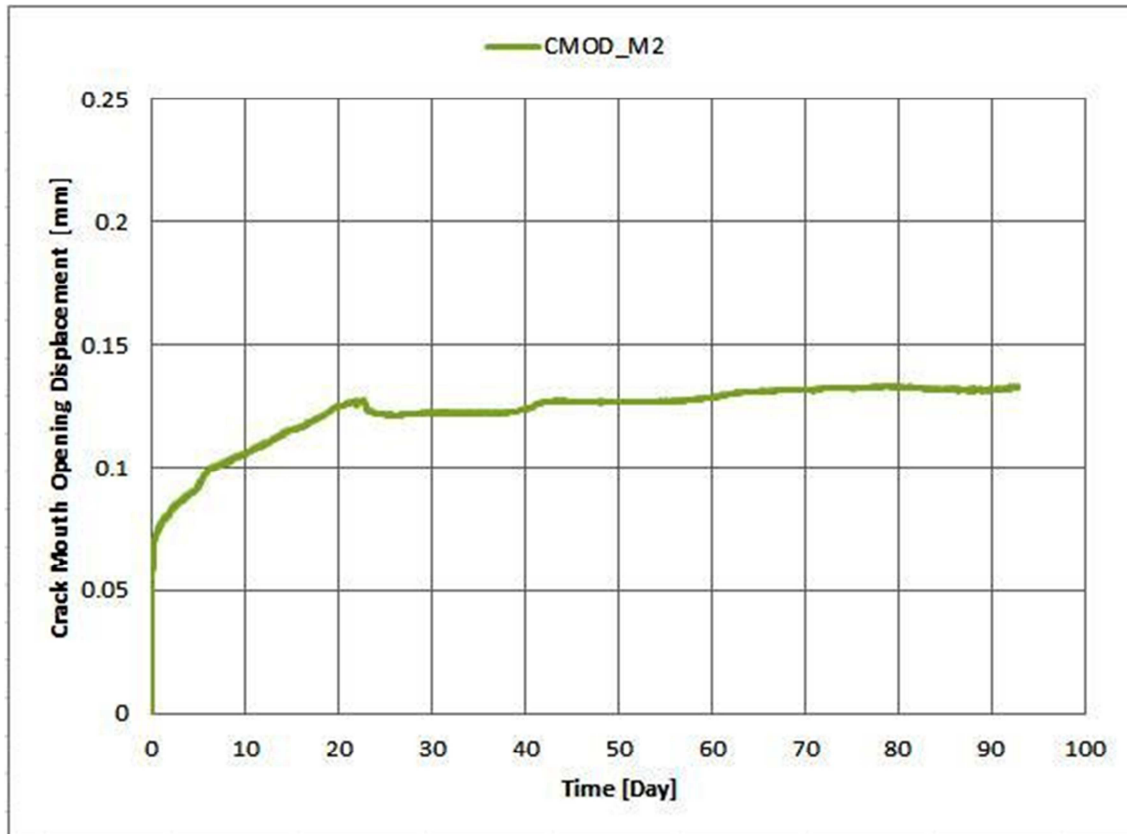


Figure 136: Absolute CMOD and Mid-Span Deflection variation of M2

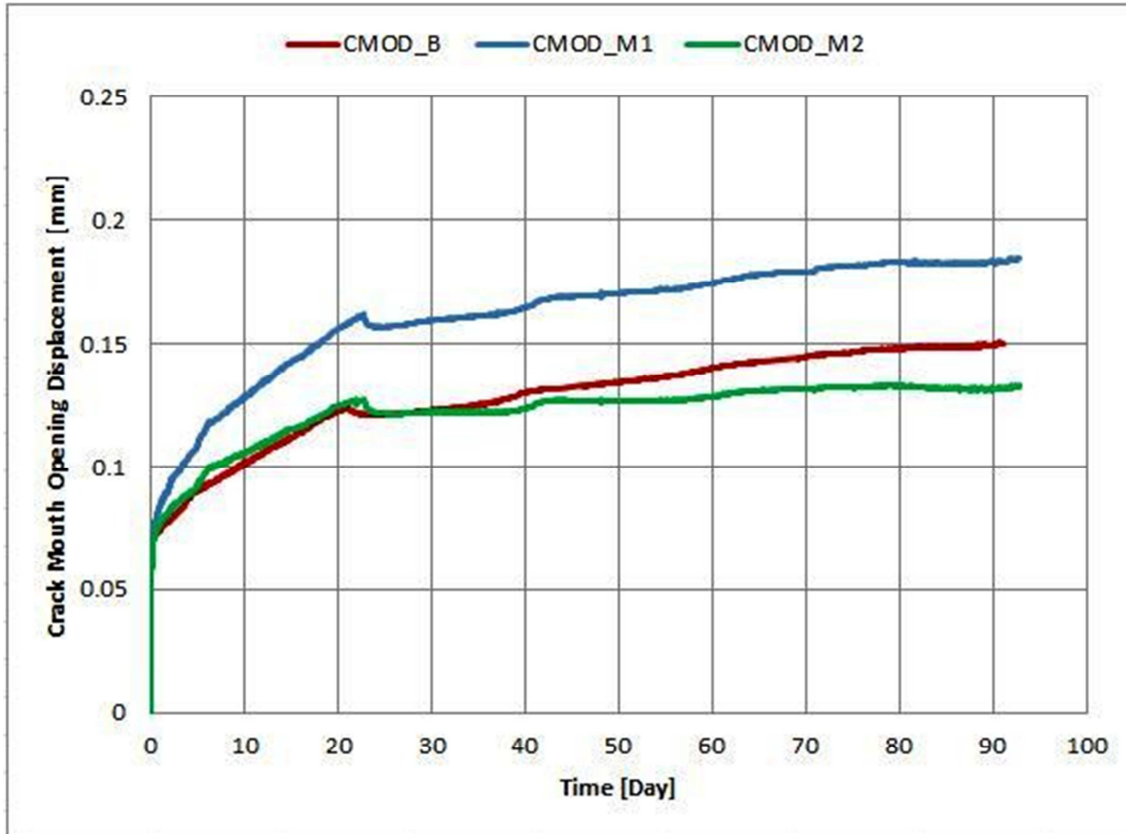


Figure 137: Absolute CMOD comparison

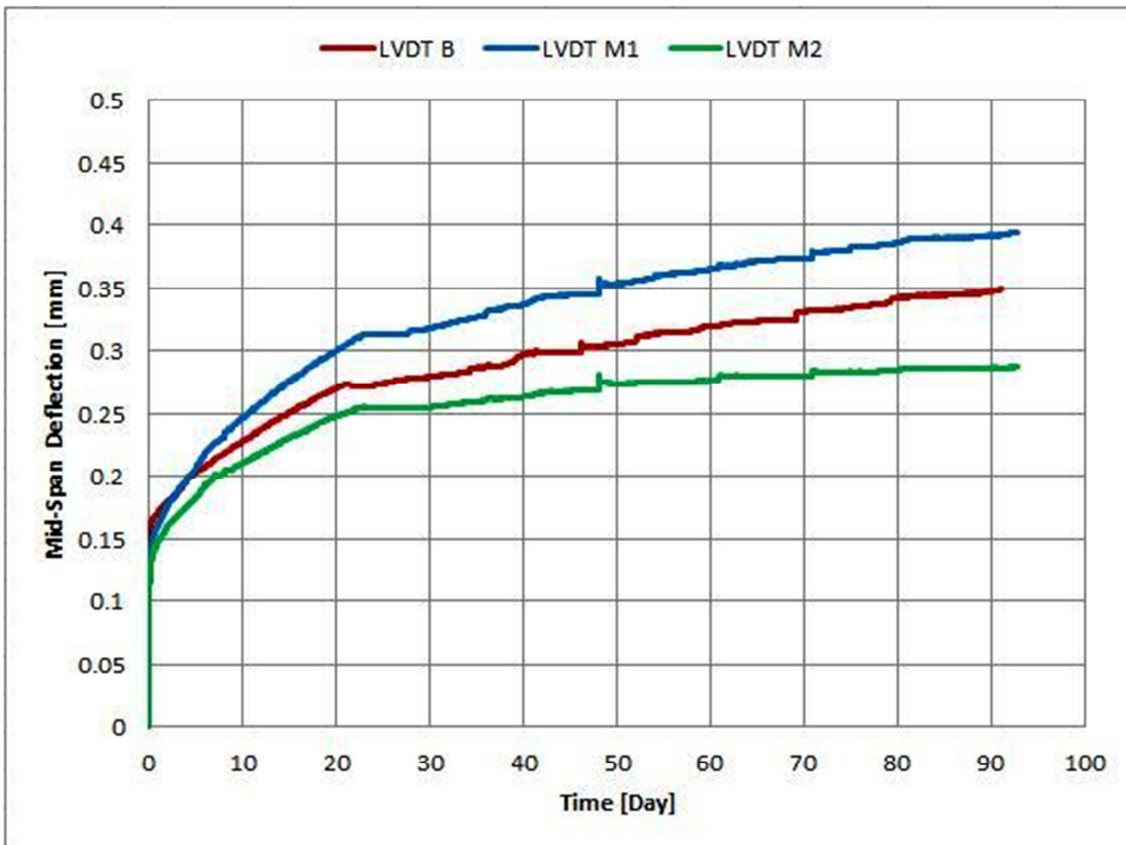


Figure 138: Absolute Mid-Span Deflection comparison

7.6.5 Relative Viscous Deformations

In this paragraph are shown data obtained during all time period of the tests. In particular you can find the relative data of the CMOD and LVDT for all samples in relation of their specific starting points. In this mode you can observe the exact deformations after the cracking and loading phase respectively.

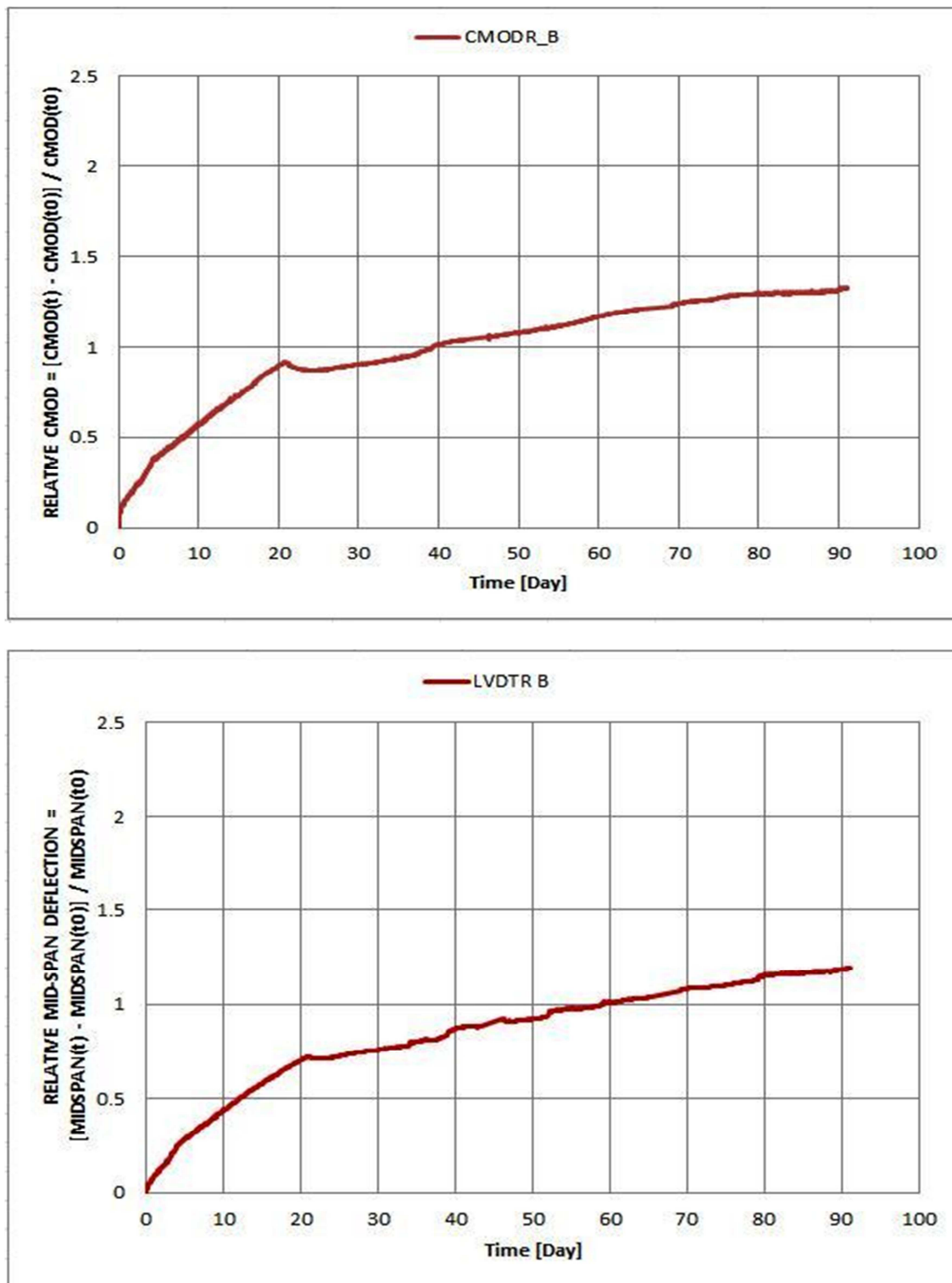


Figure 139: Relative CMOD and Mid-Span Deflection variation of B

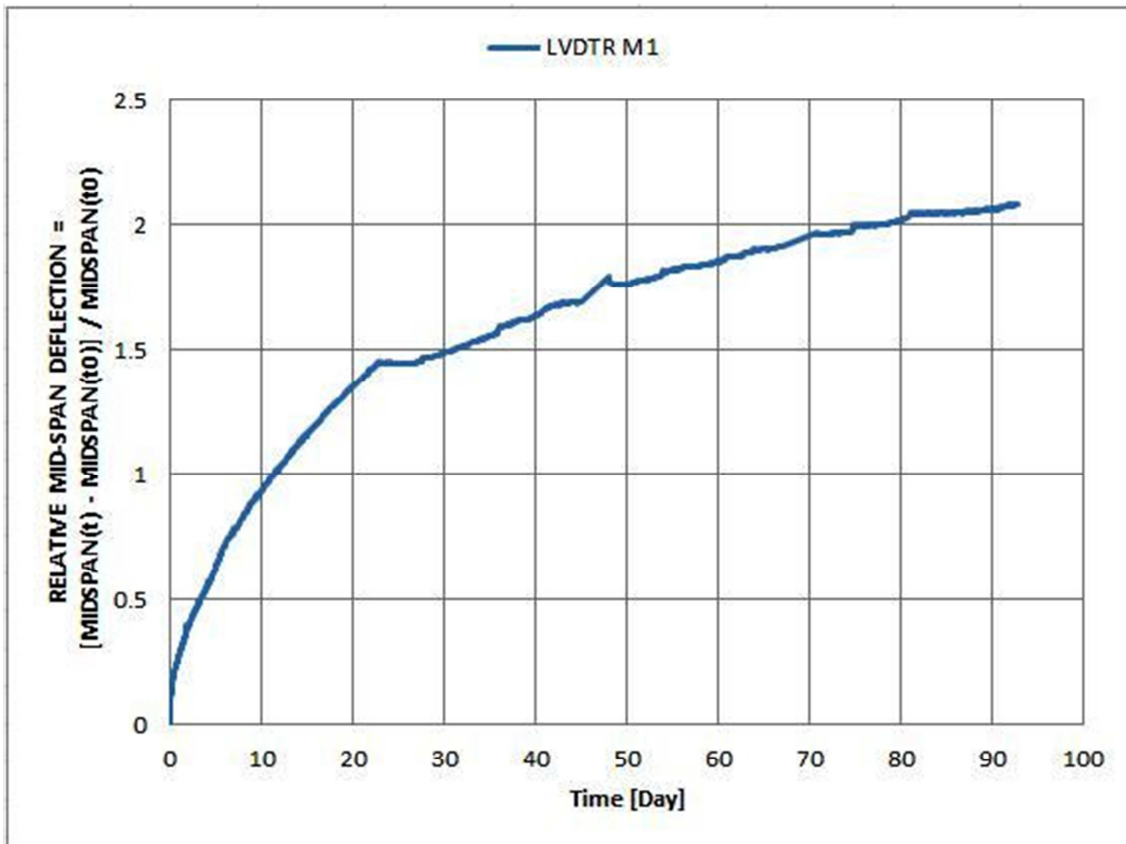
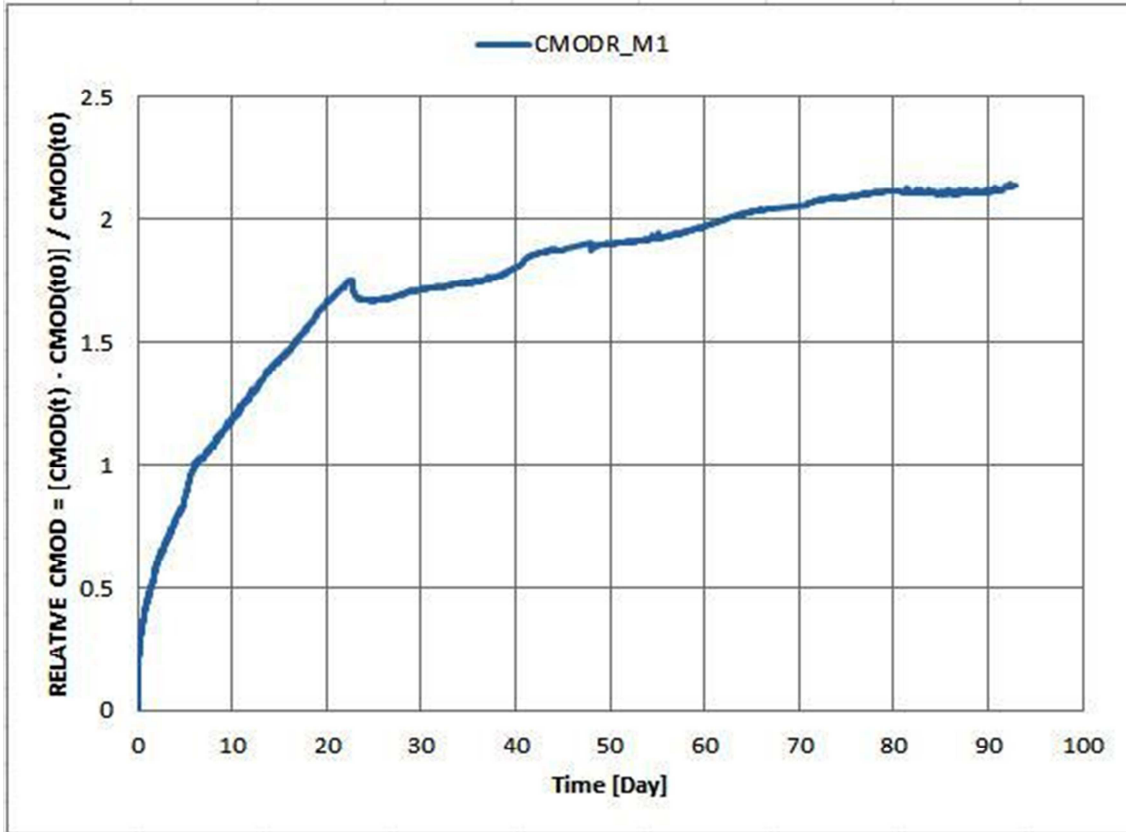


Figure 140: Relative CMOD and Mid-Span Deflection variation of M1

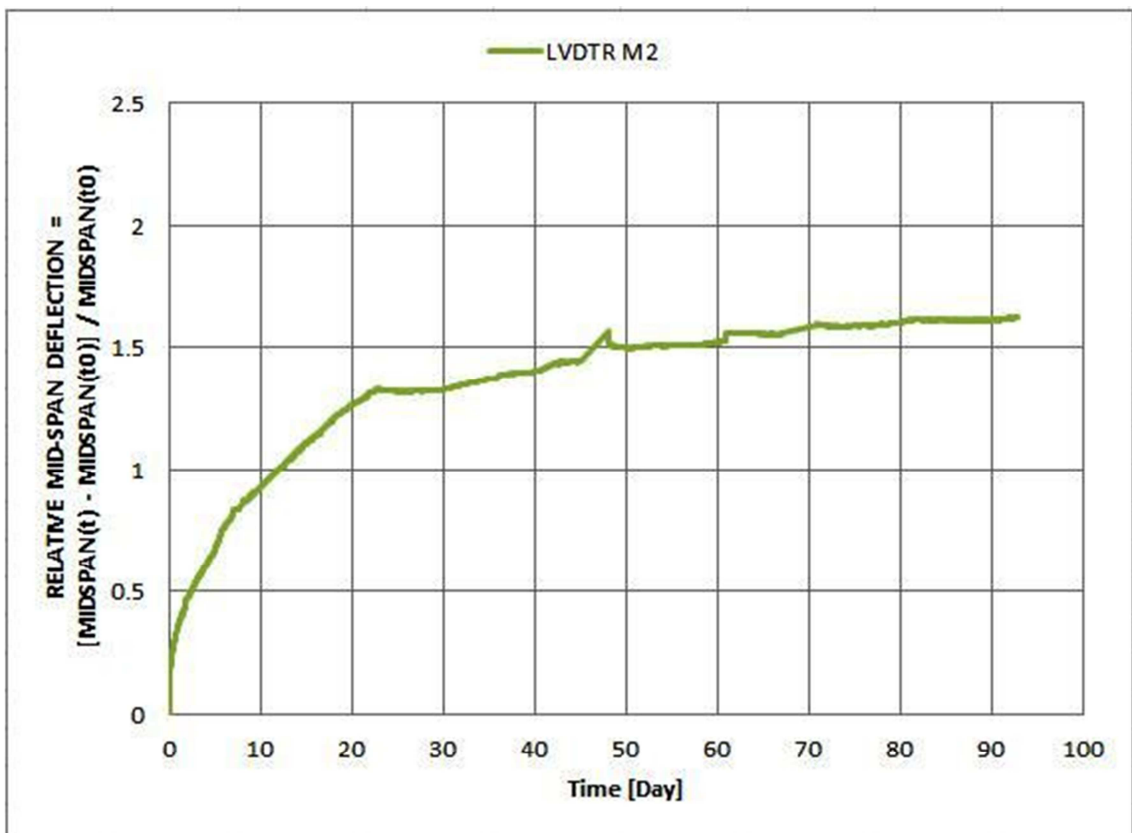
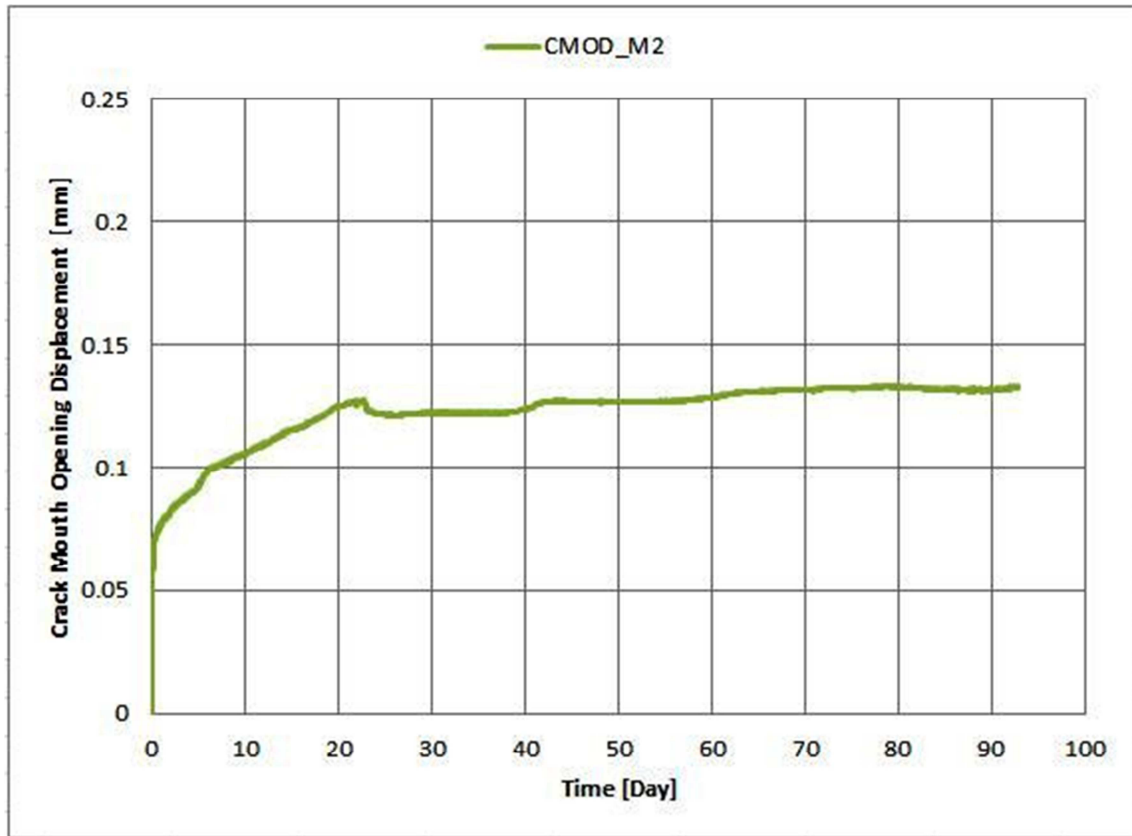


Figure 141: Relative CMOD and Mid-Span Deflection variation of M2

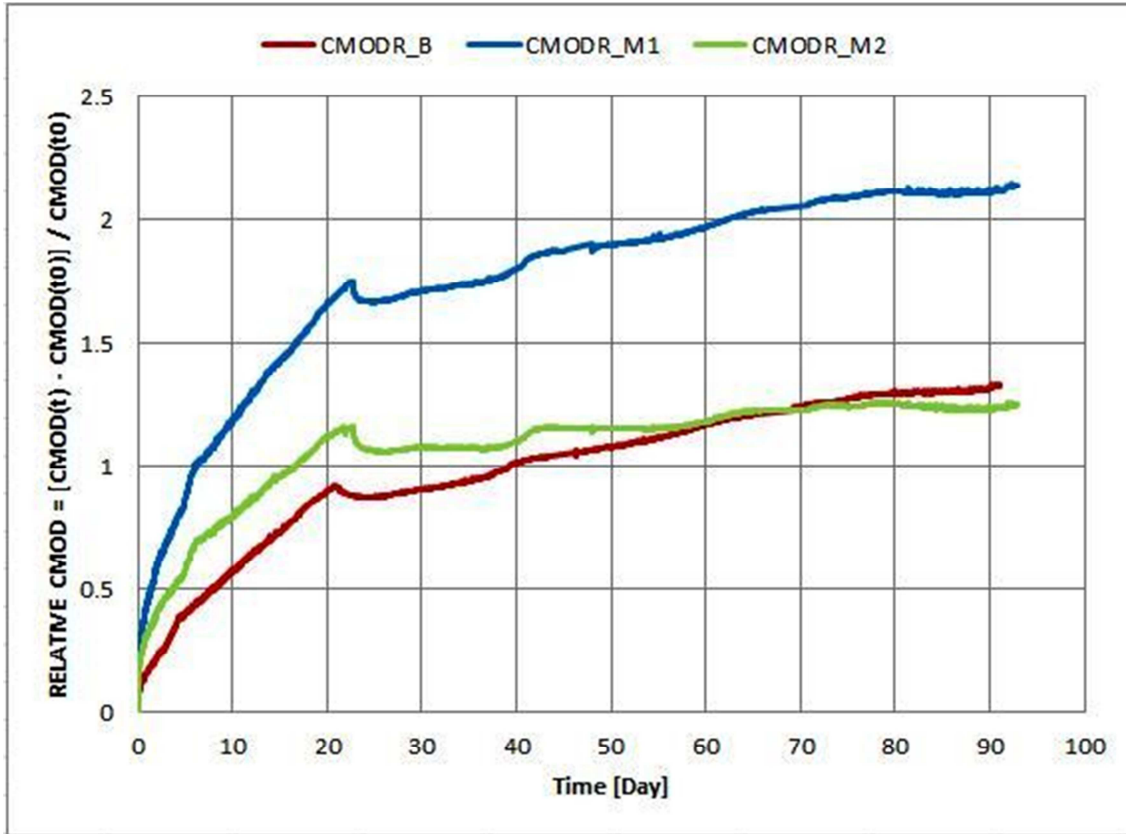


Figure 142: Relative CMOD comparison

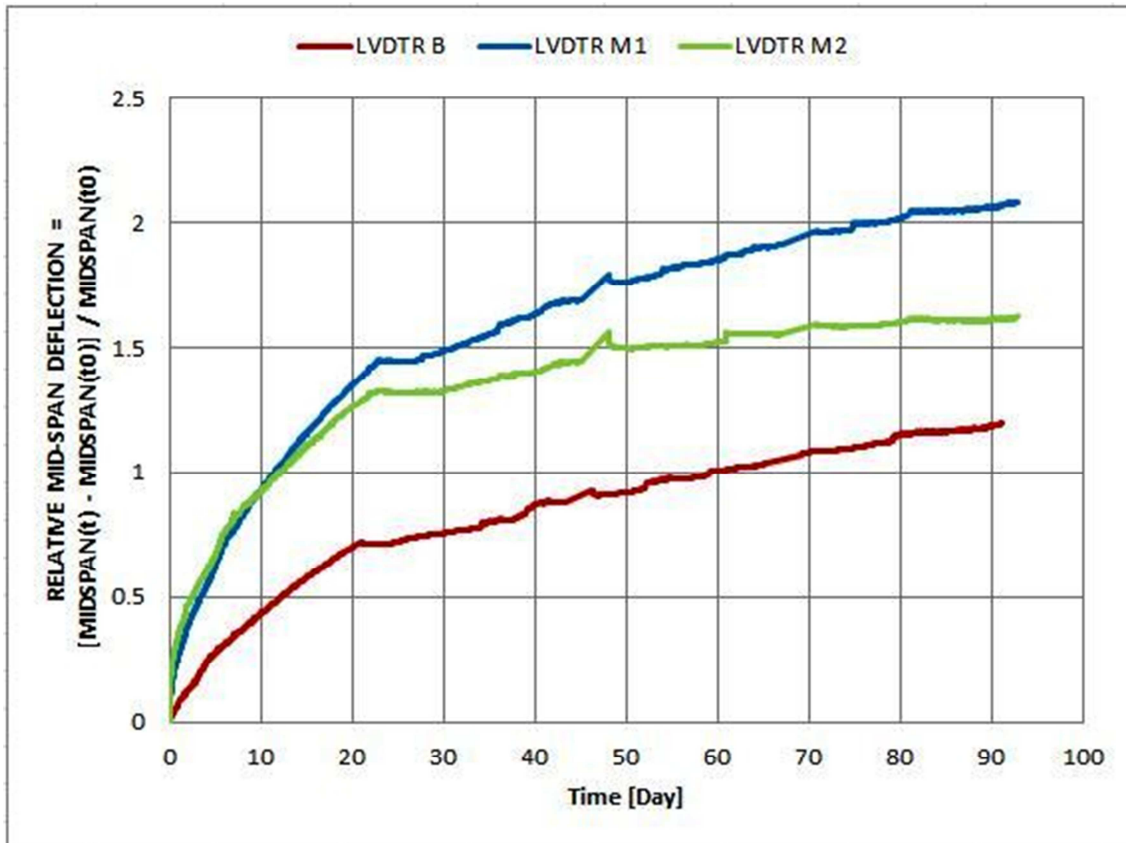


Figure 143: Relative Mid-Span Deflection comparison

7.6.6 Comparison with Old Test

In this paragraph you can analyze the behavior of our samples and other samples made in the past and analyzed in the same condition of tests. In that case the researcher used a steel fiber called FF1 variously mixed in the concrete conglomerates.

Sample	Concrete Type	Fiber Type	Fiber Dosage
R	SCC	/	/
25a	FRSCC	Maccaferri FF1	35 Kg/m ³
M	FRSCC	Mix	/
25b	FRSCC	Maccaferri FF1	25 Kg/m ³
35a	FRSCC	Maccaferri FF1	35 Kg/m ³
35b	FRSCC	Maccaferri FF1	35 Kg/m ³
B	SCC	/	/
M1	FRSCC	Mapei ST42	4 Kg/m ³
M2	FRSCC	Mapei ST42	7 Kg/m ³

Figure 144: Old test samples comparison

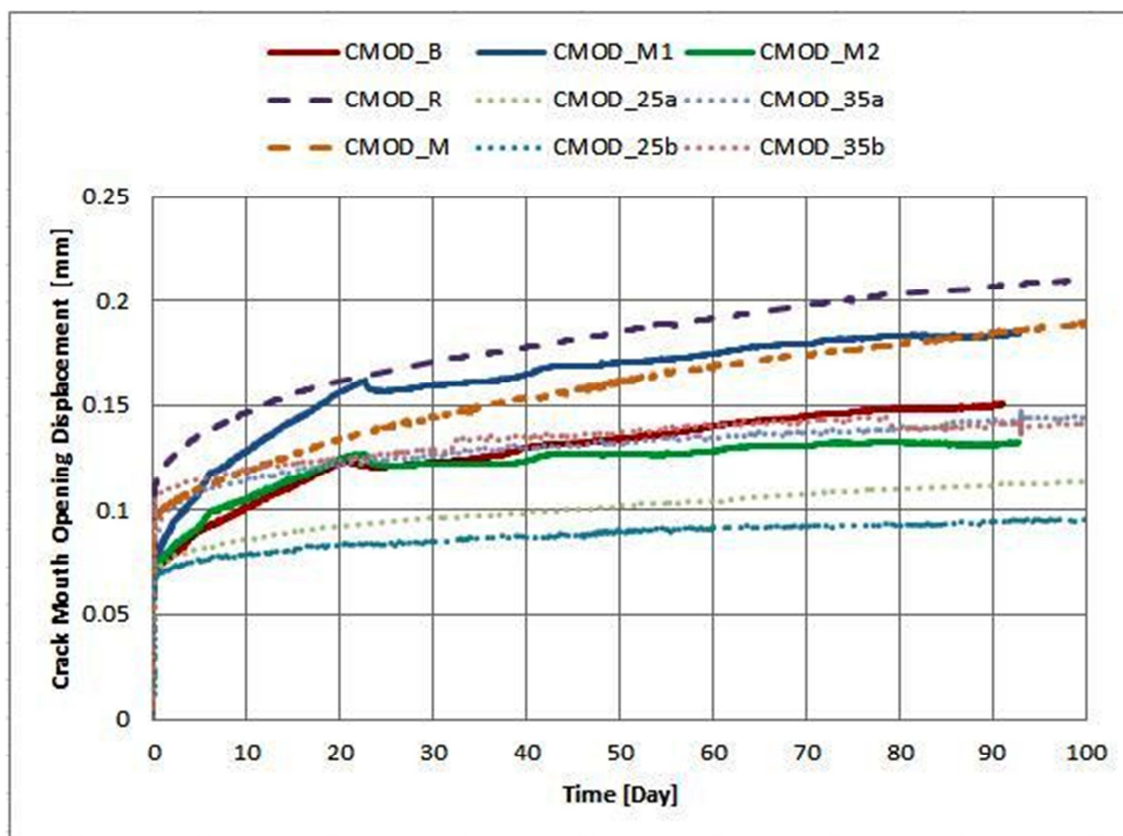


Figure 145: CMOD compared with old tests

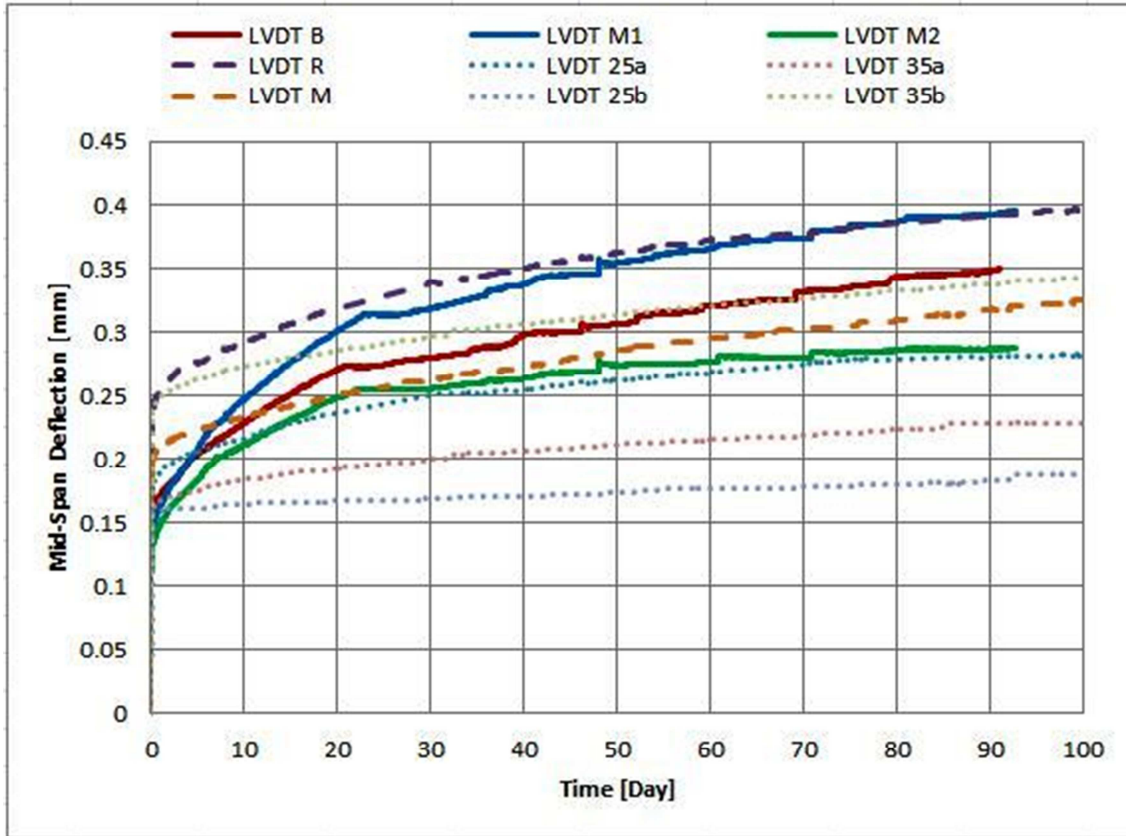


Figure 146: Mid-Span Deflection compared with old tests

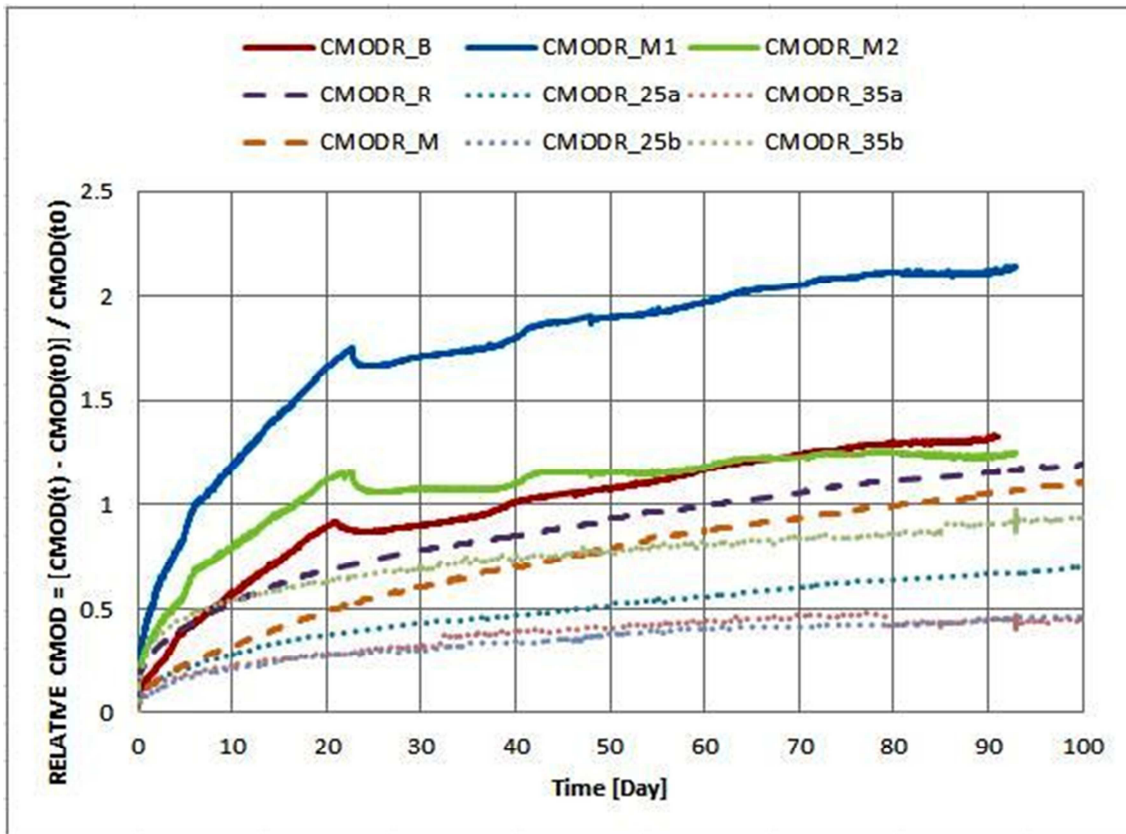


Figure 147: Relative CMOD compared with old tests

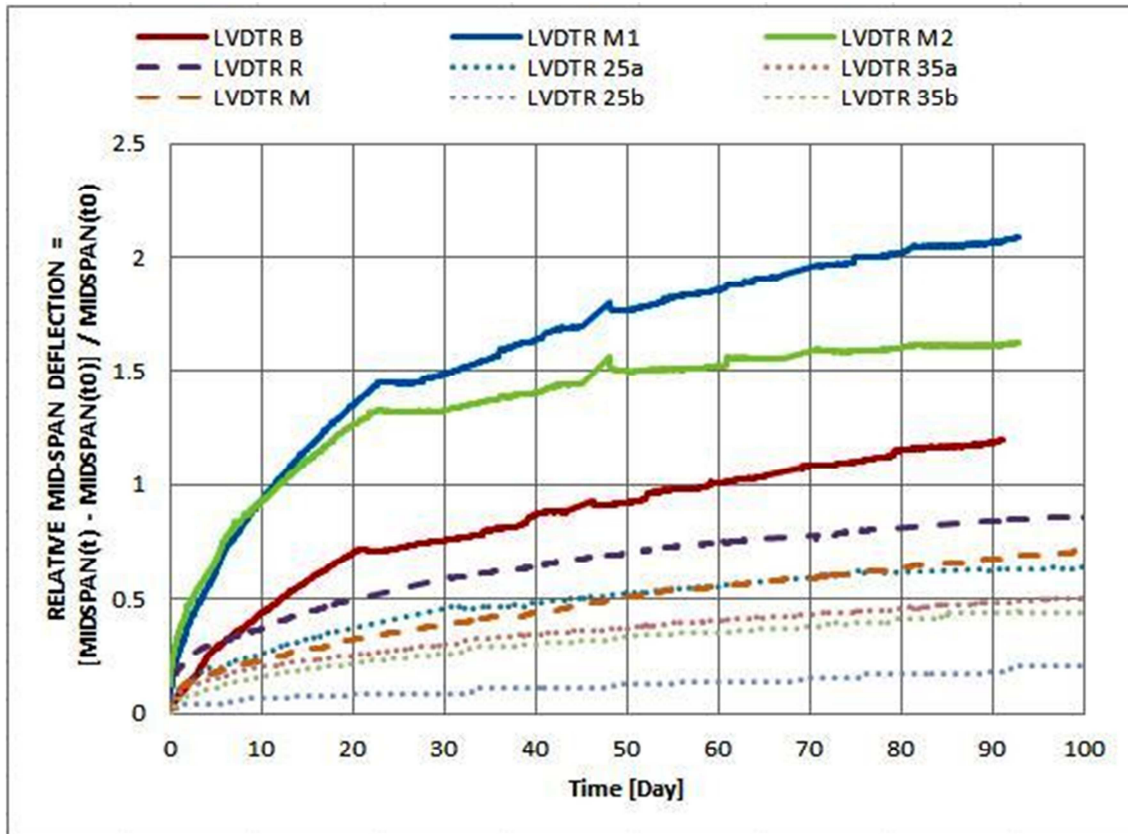


Figure 148: Relative Mid-Span Deflection compared with old tests

8. Uniaxial Tensile Test

8.1 Introduction

In this paragraph we want to discuss the experimental results of the uniaxial tensile tests which are made on particular samples of the various mixtures analyzed before in the other tests.

First of all we have done a particular shape of the samples cut in the middle line of them and connected with a steel plate at the top and at the bottom parts in order to apply the traction load.

The study is subdivided in two parts:

- Cracking analysis;
- Viscous analysis;

As you will see in the chapter, we will not able to do these because our load device isn't well designed for this end and so, because the system must be rigid than the other elements, we haven't had a good results.

8.2 Samples and Test Device

In the figure below you can see our traction sample and its preparation procedure.



Figure 149: Traction test samples

We have also had designed the system plate connections for guarantee the maximum stiffness of the test, overestimating the thickness of all elements.

After that we have applied to the samples omega transducers to measure the cracking quantities and we have connected them to the software in order to control the velocity and the CMOD values.



Figure 150: Traction test

8.3 Test Results

As you can evaluate the results from the chart below we couldn't increase the traction tension with crack control because the our device wasn't rigid and at certain point of all tests the samples were shocked by another external force due to the elastic behavior of the device.

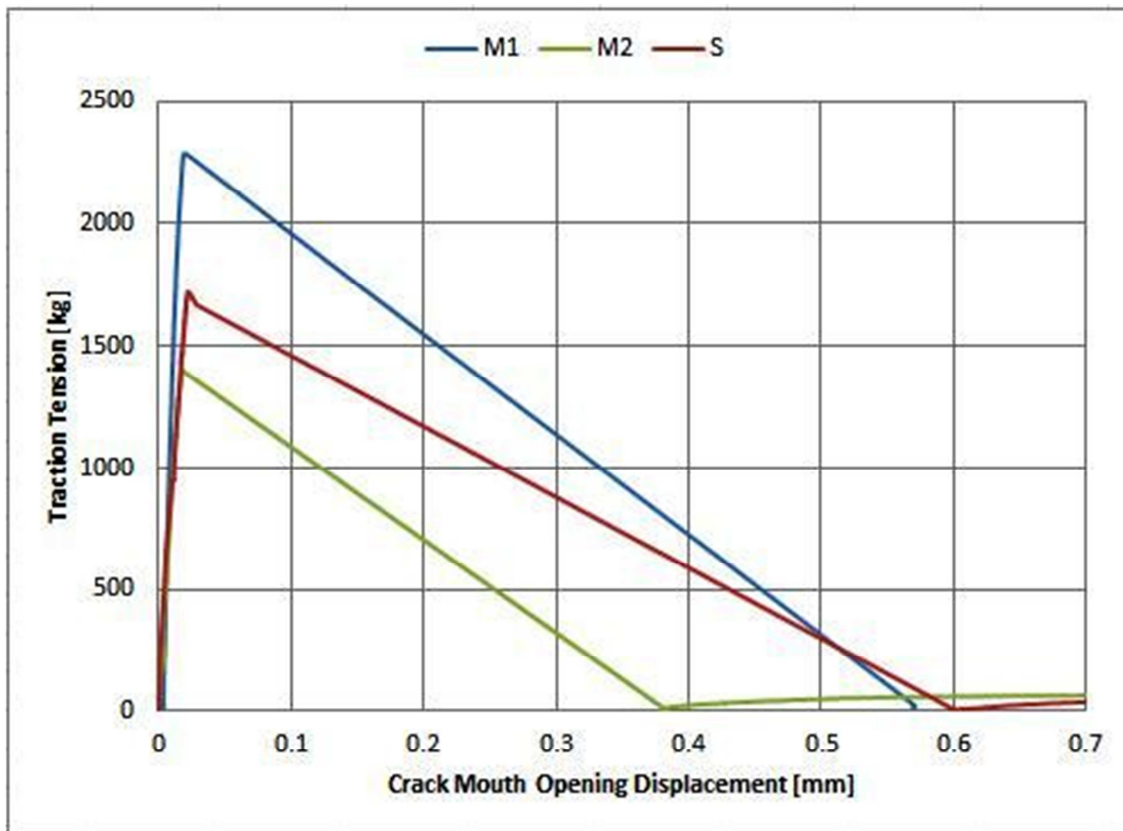


Figure 151: Traction test results

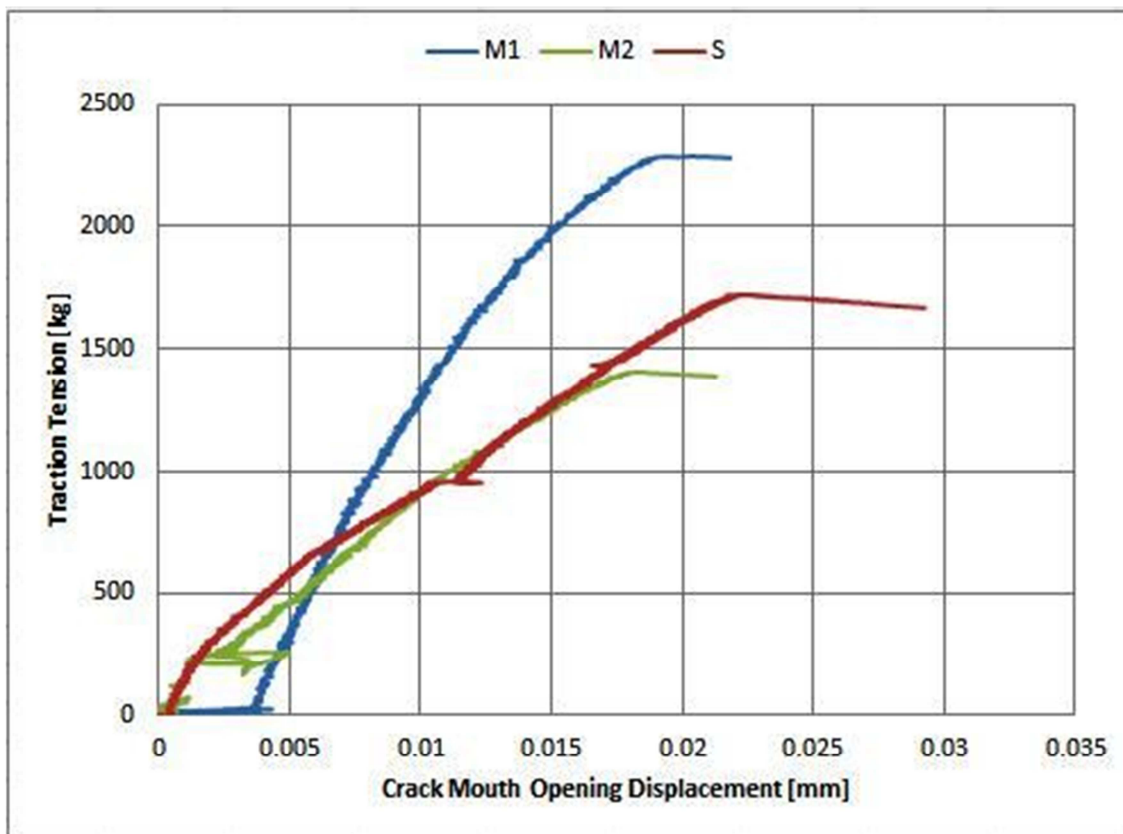


Figure 152: Traction test failure

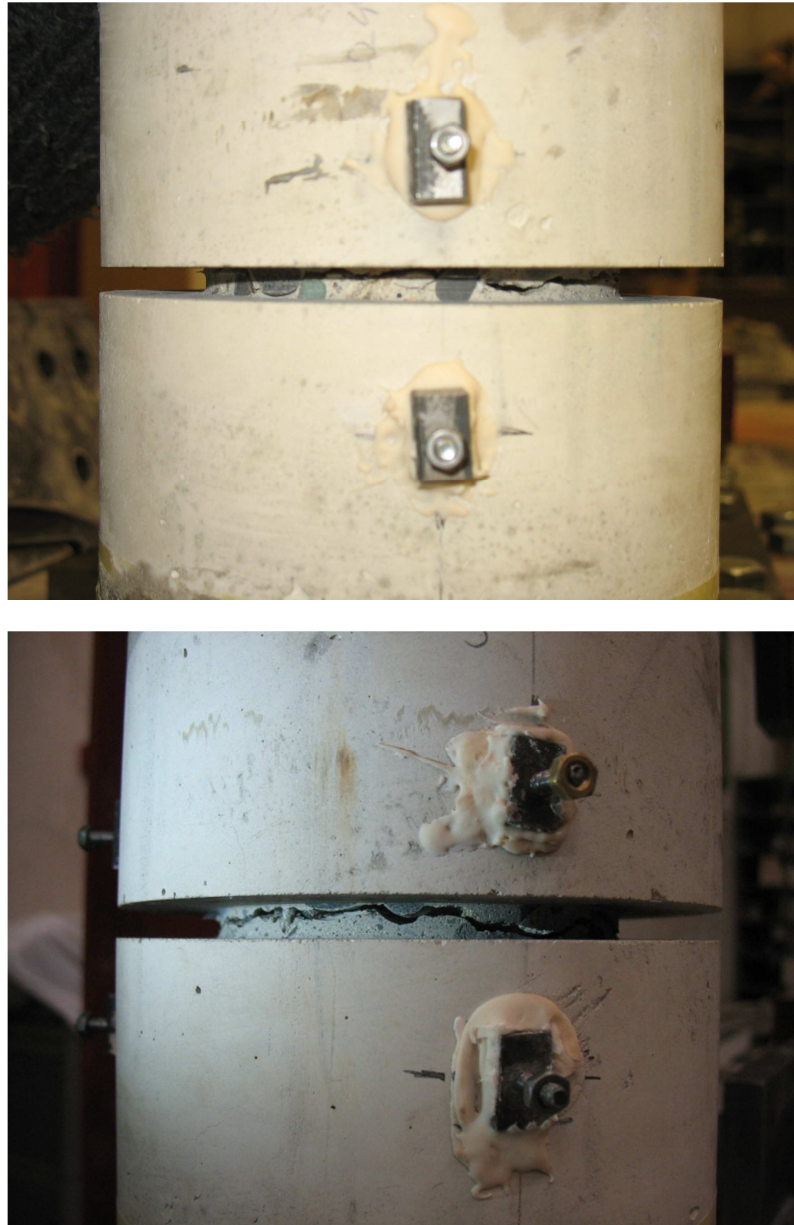


Figure 153: Traction crack failure.

9. Design Analysis

9.1 Introduction

Stresses in slabs-on-ground result from applied loads and volume changes of the soil and concrete. The magnitude of these stresses depends on factors such as the degree of slab continuity, subgrade strength and uniformity, construction method, construction quality, and magnitude and position of the loads.

In most cases, the effects of these factors are evaluated by making simplified analysis assumptions with respect to material properties and soil-structure interaction.

Two important definitions are listed below:

- *Curling or warping*: out-of-plane deformation of the corners, edges, and surface of a pavement, slab, or wall panel from its original shape.
- *Slab-on-ground*: slab, supported by ground, whose main purpose is to support the applied loads by bearing on the ground.

9.1.1 Classical Design Theories

Design methods for slabs-on-ground are based on theories originally developed for airport and highway pavements.

Westergaard developed one of the first rigorous theories of structural behavior of rigid pavement (1923, 1925, and 1926). This theory considers a homogeneous, isotropic, and elastic slab resting on an ideal subgrade that exerts, at all points, a vertical reactive pressure proportional to slab deflection; now is called Winkler subgrade (1867).

The subgrade acts as a linear spring with a proportionality constant k with units of pressure [KPa] per unit deformation [m]. The units are commonly abbreviated as KN/m^3 .

This constant is defined as the modulus of subgrade reaction.

Corrections were required only for the Westergaard corner formula to account for the effects of slab curling and loss of contact with the subgrade.

While choosing the modulus of subgrade reaction was essential for good agreement with respect to stresses, there remained ambiguity in the methods used to determine the correction coefficient.

In the 1930s, experimental information showed that the behavior of many subgrades may be close to that of an elastic and isotropic solid. Two characteristic constants, the modulus of soil deformation and Poisson's ratio, are typically used to evaluate the deformation response of such solids. Based on the concept of the subgrade as an elastic and isotropic solid, and assuming that the slab is of infinite extent but of finite thickness, Burmister proposed the layered-solid theory of structural behavior for rigid pavements (1943). He suggested basing the design on a criterion of limited deformation under load.

Design procedures for rigid pavements based on this theory are not sufficiently developed for use in engineering practice. The lack of analogous solutions for slabs of finite extent, for example, edge and corner cases, is a particular deficiency.

Other approaches based on the assumption of a thin elastic slab of infinite extent resting on an elastic, isotropic solid have been developed. The preceding theories are limited to behavior in the linear range where deflections are proportional to applied loads. Lösberg (1978) later proposed a strength theory based on the yield-line concept for ground-supported slabs, but the use of ultimate strength for slab-on-ground design is not common.

All existing design theories are grouped according to models that simulate slab and the subgrade behavior. Three models used for slab analysis are:

- Elastic-isotropic solid;
- Thin elastic slab;
- Thin elastic-plastic slab;

Two models used for subgrade are:

- Elastic-isotropic solid;
- Winkler subgrade;

The Winkler subgrade models the soil as linear springs so that the reaction is proportional to the slab deflection.

Existing design theories are based on various combinations of these models.

The elastic-isotropic model provides close prediction for the response of real soils, but the Winkler model is widely used for design and a number of investigators have reported good agreement between observed responses to the Winkler-based predictions.

9.1.2 Finite Element Method

The classical differential equation of a thin elastic plate resting on an elastic subgrade is often used to represent the slab-on-ground.

Solving the governing equations by conventional methods is feasible for simplified models where slab and subgrade are assumed to be continuous and homogeneous.

In reality, a slab-on-ground usually contains discontinuities, such as joints and cracks, and the subgrade support may not be uniform. Thus, the use of this approach is limited.

The finite-element method can be used to analyze slabs-on-ground, particularly those with discontinuities. Various models have been proposed to represent the slab (Spears and Panarese 1983). Typically, these models use combinations of elements, such as elastic blocks, rigid blocks, and torsion bars, to represent the slab. The subgrade is typically modeled by linear springs (Winkler subgrade) placed under the nodal joints.

However the finite-element method offers good potential for complex problems, graphical solutions and simplified design equations have been traditionally used for design. The evolution of modern computer software has made modeling with finite elements more feasible in the design office setting.

9.1.3 Construction Documents

Listed below is the minimum information that should be addressed in the construction documents prepared by the designer:

- Slab-on-ground design criteria;
- Base and sub-base materials, preparation requirements, and vapor retarder/barrier, when required;
- Concrete thickness;
- Concrete compressive strength, or flexural strength, or both;
- Concrete mixture proportion requirements, ultimate dry shrinkage strain, or both;
- Joint locations and details;
- Reinforcement (type, size, and location), when required;
- Surface treatment, when required;
- Surface finish;
- Tolerances (base, sub-base, slab thickness, and floor flatness and levelness);
- Concrete curing;
- Joint filling material and installation;
- Special embedment;
- Testing requirements;
- Preconstruction meeting, quality assurance, and quality control;

9.2 Slab-On-Ground Design Criteria

The design criteria should include some of the following:

- Geotechnical soil properties used for the different loading types;
- Uniform storage loading;
- Lift-truck and vehicle loadings;
- Rack loadings;
- Line loads;
- Equipment loads;
- When the slab is used to resist wind or seismic foundation uplift forces;
- When the slab is used as a horizontal diaphragm and to resist horizontal forces or both due to tilt-walls, masonry walls, tops of retaining walls, and metal building system columns;

9.2.1 Floor Flatness and Levelness Tolerance

When using slabs in offices, areas of pedestrian traffic, wide aisle warehousing, and manufacturing, where the movement is intended to be random in any direction, then a random traffic tolerance system, such as FF/FL, should be designated.

In defined traffic areas such as narrow aisle or very narrow aisle warehousing and manufacturing, where vehicle paths are restrained by rail, wire, laser, or telemetry guidance systems, a tolerance system such as F-min should be implemented.

Rack height, ft (m)	Longitudinal* F-min	Transverse† F-min
0 to 25 (0 to 7.6)	50	60
26 to 30 (7.9 to 9.1)	55	65
31 to 35 (9.4 to 10.7)	60	70
36 to 40 (11 to 12.2)	65	75
41 to 45 (12.5 to 13.7)	70	80
46 to 50 (14 to 15.2)	75	85
51 to 65 (15.5 to 19.8)	90	100
66 to 90 (20.1 to 27.4)	100	125

*Longitudinal value between the front and rear axle.

†Transverse value between loaded wheel tracks.

Figure 154: Example of Designed Traffic Value

9.3 Slab Types

The term “slab-on-ground” is preferred but “slab-on-grade” is often used. Slab-on-ground includes interior slabs subject to loadings. These include industrial, commercial, residential, and related applications. Although might include parking lot and roadway pavements.

Some of the more important expectations that should be discussed for the prospective slab type are:

- Cracking potential;
- Crack widths for slabs designed with reinforcement to limit crack widths;
- Use of doweled joints versus aggregate interlock;
- Possible future repairs including joint deterioration;
- Joint maintenance requirements and the owner's responsibility for this maintenance;
- Floor flatness and levelness requirements to meet the owner's needs;
- Changes to the flatness and levelness over time, especially in low-humidity environments;
- Advantages and disadvantages of slab placement with the watertight roofing system in place versus placing the slab in the open;
- Level of moisture vapor resistance required;
- Advantages and disadvantages of using the building floor slab for tilt-wall constructions form and temporary bracing;

9.3.1 Basic Design for Slab-On-Ground

There are four basic design choices for slab-on-ground construction:

- Unreinforced concrete slabs;
- Slabs reinforced to limit crack widths due to shrinkage and temperature restraint and applied loads. These slabs consist of:
 - Non prestressed steel bar, wire reinforcement, or fiber reinforcement, all with closely spaced joints;
 - Continuously reinforced, free-of-sawcut, contraction joints;
- Slabs reinforced to prevent cracking due to shrinkage and temperature restraint and applied loads. These slabs consist of:
 - Shrinkage-compensating concrete;
 - Post-tensioned;
- Structural slabs designed in accordance with ACI 318:
 - Plain concrete;
 - Reinforced concrete;

▪ *Unreinforced Concrete Slabs*

The thickness is determined as a concrete slab without reinforcement; however, it may have joints strengthened with steel dowels. It is designed to remain uncracked between joints when loaded and restraint to concrete volumetric changes.

Unreinforced concrete slabs do not contain macro synthetic fibers, wire reinforcement, steel fibers, plain or deformed bars, post-tensioning, or any other type of steel reinforcement.

Type I or II Portland cement is normally used.

Drying shrinkage effects and uniform subgrade support on slab cracking are critical to the performance of unreinforced concrete slabs.

- *Slabs Reinforced for Crack-Width Control*

Thickness design can be the same as for unreinforced concrete slabs, and they are designed to remain uncracked when loaded. For slabs constructed with Portland cement, shrinkage crack widths (when cracking occurs) between joints are controlled by a nominal quantity of distributed reinforcement.

Slabs reinforcement can consist of bars, welded wire reinforcement sheets, steel fibers, or macro synthetic fibers.

Bar and wire reinforcement should be stiff enough to be accurately located in the upper 1/3 of the slab. Bars or welded wire reinforcement are used to provide flexural strength at a cracked section. In this case, and for slabs of insufficient thickness to carry the applied loads as an unreinforced slab, the reinforcement required for flexural strength should be sized by reinforced concrete theory. Using the methods with high steel reinforcement stresses, however, may lead to unacceptable crack widths.

Building codes do not support the use of fiber reinforcement to provide flexural strength in cracked sections for vertical or lateral forces from other portions of a structure.

Other than post-tensioning or the reinforcement in a shrinkage-compensating slab, reinforcement does not prevent concrete cracking.

Typically, the most economical way to increase flexural strength is to increase the slab thickness.

- *Slabs Reinforced to Prevent Cracking*

Post-tensioned slabs and shrinkage-compensating slabs are typically designed not to crack, but some incidental minor cracking may occur. For shrinkage-compensating slabs, the slab is designed unreinforced, and the reinforcement is designed to pre-stress the expanding slab to offset the stresses caused by the shrinkage and temperature restraint.

For post-tensioned slabs, the reinforcement is typically designed to compensate for shrinkage and temperature restraint stress and applied loads.

Shrinkage-compensating concrete slabs are produced either with a separate component admixture or with special expansive cement. This concrete does shrink, but first expands to an amount intended to be slightly greater than its drying shrinkage. To limit the initial slab expansion and to pre-stress the concrete, reinforcement is distributed in the upper 1/3 of the slab. Such reinforcement should be rigid and positively positioned.

The slab should be isolated from fixed portions of the structure, such as columns and perimeter foundations, with a compressible material that allows the initial slab expansion.

▪ *Structural Slabs*

Structural plain and reinforced slabs that transmit vertical loads or lateral forces from other portions of the structure to the soil should be designed in accordance with codes.

Using the methods with high steel reinforcement stresses, however, may lead to unacceptable crack widths.

9.3.2 General Comparison of Slab Types

To assist with selecting the most appropriate slab type for the particular project, the table below provides general advantages and disadvantages for the slab types discussed before.

Slab Type	Advantages	Disadvantages
Unreinforced Concrete.	Simple to construct. Generally is less expensive to install than slabs designed by other methods.	Requires relatively closely spaced sawcut contraction joints. More opportunity for slab curl and joint deterioration. Large number of joints to maintain. Positive load transfer may be required at joints. Flatness and levelness may decrease over time.
Reinforced with deformed bars or welded-wire reinforcement sheets for crack-width control.	Reinforcement is used to limit crack width.	May be more expensive than an unreinforced slab. Reinforcement can actually increase the number of random cracks, particularly at wider joint spacings. More opportunity for slab curl and joint deterioration. Positive load transfer may be required at joints.
Continuously reinforced with deformed bars or welded-wire reinforcement mats.	Sawcut contract joints can be eliminated where sufficient reinforcement is used. Eliminates sawcut contraction joint maintenance. Curling is reduced when high amounts of reinforcement are used. Less changes in flatness and levelness with time.	Requires relatively high amounts (at least 0.5%) of continuous reinforcement placed near the top of the slab to eliminate joints. Typically produces numerous, closely spaced, fine cracks (approximately 0.9 to 1.8 m) throughout slab.
Shrinkage-compensating concrete.	Allows construction joint spacings of 12 to 46 m. Sawcut contraction joints are normally not required. Reduces joint maintenance cost due to increased spacing of the joints reducing the total amount of joints. Negligible curl at the joints. Increases surface durability and abrasion resistance.	Requires reinforcement to develop shrinkage compensation. Window of finishability is reduced. Allowance should be made for concrete to expand before drying shrinkage begins. Construction sequencing of adjacent slab panels should be considered, or joints should be detailed for expansion. Contractor should have experience with this type of concrete.
Post-tensioned.	Construction spacings 30 to 150 m. Most shrinkage and flexural cracks can be avoided.	More demanding installation. Contractor should have experience with post-tensioning or employ a consultant

	<p>Eliminates sawcut contraction joints and their maintenance.</p> <p>Negligible slab curl when tendons are draped near joint ends.</p> <p>Improved long-term flatness and levelness.</p> <p>Decreased slab thickness or increased flexural strength.</p> <p>Resilient when overloaded.</p> <p>Advantages in poor soil conditions.</p>	<p>with post-tensioning experience.</p> <p>Inspection essential to ensure proper placement and stressing of tendons.</p> <p>Uneconomical for small areas.</p> <p>Need to detail floor penetrations and perimeter for slab movement.</p> <p>Impact of cutting tendons should be evaluated for post-construction slab penetrations.</p>
Steel fiber-reinforced concrete.	<p>Increased resistance to impact and fatigue loadings when compared to slabs reinforced with bars or mesh.</p> <p>Simple to construct.</p>	<p>May require adjustments to standard concrete mixing, placement, and finishing procedures.</p> <p>Fibers may be exposed on the surface of slab.</p> <p>Floors subjected to wet conditions may not be suitable for steel fiber because fibers close to the surface and in water-permeable cracks will rust.</p>
Synthetic fiber-reinforced Concrete.	<p>Helps reduce plastic shrinkage cracking.</p> <p>Simple to construct.</p> <p>Macro synthetic fibers provide increased resistance to impact and fatigue loadings, similar to steel fibers.</p> <p>Synthetic fibers do not corrode.</p>	<p>Micro synthetic fibers do not help in controlling drying shrinkage cracks.</p> <p>Joint spacing for micro synthetic fiber-reinforced slabs is the same as unreinforced slabs.</p>
Structural slabs reinforced for Building code requirements.	<p>Slabs can carry structural loads such as mezzanines.</p> <p>Reduces or eliminates sawcut contraction joints where sufficient reinforcement is used.</p>	<p>Slab may have numerous fine or hairline cracks if reinforcement stresses are sufficiently low.</p>

Figure 155: Table of Slab Types Comparison

9.3.3 Construction Variables

Design and construction of slabs-on-ground involves both technical and human factors.

Technical factors include loadings, soil-support systems, joint types and spacings, design method, slab type, concrete mixture, development of maintenance procedures, and the construction process.

Human factors include the workers' abilities, feedback to evaluate the construction process, and conformance with proper maintenance procedures for cracking, curling, and shrinkage.

These and other factors should be considered when designing a slab (Westergaard 1926).

9.3.4 Conclusion

No single slab design method is recommended for all applications.

Rather, from the number of identifiable construction concepts and design methods, a combination should be selected based on the requirements of the specific application.

9.4 Loads

9.4.1 Introduction

This paragraph describes loadings, the variables that control load effects, and provides guidance for factors of safety for concrete slabs-on-ground.

Concrete slabs are typically subjected to some combinations of the following loads and effects:

- Vehicle wheel loads;
- Concentrated loads;
- Distributed loads;
- Line and strip loads;
- Unusual loads;
- Construction loads;
- Environmental effects;

Slabs should be designed for the most critical combination of these loadings, considering variables that produce the maximum stress.

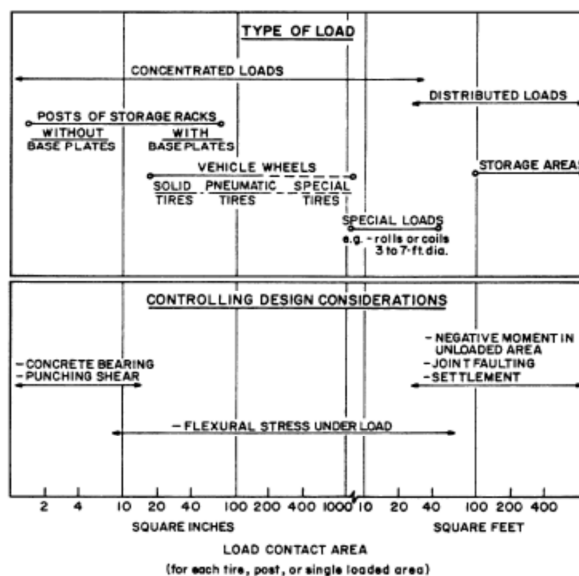


Figure 156: Controlling Design Consideration for Various Types of Slab-On-Ground (1 in.² = 645.2 mm²; 1 ft² = 0.0929 m²)

Because a number of factors, such as slab thickness, concrete strength, subgrade stiffness, and loading are relevant, cases where several design considerations that may control should be investigated carefully. Other potential load conditions, such as loadings that change during the life of the structure and those encountered during construction should also be considered.

For example, material-handling systems today make improved use of the building's volume. Stacked pallets, once considered uniform loads, may now be stored in narrow

aisle pallet racks that produce concentrated loads. The environmental exposure of the slab-on-ground is also a concern.

These effects include subgrade volume changes (shrink and swell soils), buildings with equipment to reduce humidity, and temperature changes. Thermal effects may be minimized by constructing the slab after the building is enclosed, but many slabs are placed before building enclosure. Therefore, construction sequence is important in determining whether transient environmental factors should be considered in the design.

Finally, thermal effects due to in-service conditions should be considered.

9.4.2 Load Types

- *Vehicular Loads*

Most vehicular traffic on industrial floors consists of lift trucks and distribution trucks with payload capacities as high as 310 kN. The payload and much of a truck's weight are generally carried by the wheels of the loaded axle for the standard (counterbalanced) lift truck. Vehicle variables affecting the thickness selection and design of slabs-on-ground include:

- Maximum axle load;
- Distance between loaded wheels;
- Tire contact area;
- Load repetitions during service life;

The axle load, wheel spacing, and contact area are functions of the lift truck or vehicle specifications.

The number of load repetitions, which may be used to help establish a factor of safety, is a function of the facility's usage. Knowledge of load repetitions and traffic patterns helps the designer to quantify fatigue. Consider whether these values are predictable or constant during the slab's service life. Often, the slab is designed for an unlimited number of repetitions.

The contact area between tire and slab is used in the analysis for lift truck with pneumatic or composition tires (Wray 1986). The contact area of a single tire can be approximated by dividing the tire load by the tire pressure (Packard 1976). This calculation is somewhat conservative because the effect of tension in the tire wall is not included.

An important consideration for the serviceability of a slab subject to vehicular loads is the design of construction and sawcut contraction joints. Joints should be stiff enough and have sufficient shear transferability to limit differential movement such that the joint filler can perform properly and resists edge spalling as a vehicle travels across the joint.

▪ *Concentrated Loads*

Warehousing improvements in efficiency and storage densities have trended toward increased rack post loads. These changes include narrower aisles, higher pallet or material stacking, and using automated stacking equipment. Pallet storage racks may be higher than 24 m and may produce concentrated post loads of 180 KN or more. For the higher rack loads, racks that cover a large plan area (which affects deeper soil layers), and racks with long-term loading, consider the effect of the long-term soil settlement in the design of the slab. Cracking can also be caused by early installation of rack systems that may restrain the slab's shrinkage and thermal movement and prevent joint activation.

The racks may restrain the slab with the rack system bracing or by the increase in base friction from additional storage loads.

The concentrated load variables that affect slab-on-ground design include:

- Maximum or representative post load;
- Duration of load;
- Spacings between posts and aisle width;
- Location of the concentrated load relative to slab joint location and the amount of shear transfer across the slab joint;
- Area of contact between post base plate and slab.

Material-handling systems are major parts of the building layout and should be well defined early in the project. Rack data can be obtained from the manufacturer. It is not uncommon to specify a larger base plate than is normally supplied to reduce the flexural stress caused by the concentrated load.

The base plate should be sized to distribute the load nearly uniformly over the plate area.

▪ *Distributed Loads*

In many industrial buildings, materials are stored directly on the slab-on-ground.

Flexural stresses in the slab are usually less than those produced by concentrated loads.

The design should prevent negative moment cracks or limit crack widths for the reinforced slabs in the aisles and prevent excessive settlement. For higher load intensities, distributed loads that cover a large plan area (which affect deeper soil layers) and long-term uniform loads, consider the effect of the differential soil settlement in the slab design.

The effect of a lift truck operating in aisles between uniformly loaded areas is not normally combined with the uniform load into one loading case, as the moments produced generally offset one another. The individual cases are always considered in the design.

For distributed loads, the variables affecting the design of slabs-on-ground are:

- Maximum load intensity;
- Load duration;
- Width and length of loaded area;
- Aisle width;
- Presence of a joint located in and parallel to an aisle;

▪ *Line and Strip Loads*

A line or strip load is a uniform load distributed over a relatively narrow area.

Consider a load to be a line or strip load when its width is less than 1/3 of the radius of relative slab stiffness.

When the width approximates this limit, review the slab for stresses produced by line loading and uniform load. When the results are within 15% of one another, consider the load as uniform.

Partition loads, bearing walls, and roll storage are examples of this load type.

For higher load intensities and long-term loading, consider the effect of differential soil settlement in the design of the slab.

The variables for line and strip loads are similar to those for distributed loadings and include:

- Maximum load intensity;
- Load duration;
- Width, length of loaded area, and when the line or strip loads intersect;
- Aisle width;
- Presence of a joint in and parallel to an aisle;
- Presence of parallel joints on each side of an aisle;
- The amount of shear transfer across the slab joint, which is especially important when the line load crosses perpendicular to a joint or is directly adjacent and parallel to a joint.

▪ *Unusual Loads*

Loading conditions that do not conform to the previously discussed load types may also occur. They may differ in the following manner:

- Configuration of loaded area;
- Load distributed to more than one axle;
- More than two or four wheels per axle;

▪ *Construction Loads*

During the building construction, various equipment types may be located on the newly placed slab-on-ground. The most common construction loads are:

- Pickup trucks;
- Scissor lifts;
- Concrete trucks;
- Dump trucks;
- Hoisting equipment and cranes used for steel erection;
- Tilt wall erection and bracing loads;
- Setting equipment;

In addition, the slab may be subjected to loads such as scaffolding and material pallets. Because these loads can exceed design limits, anticipate the construction load case, particularly relative to early-age concrete strength. Also, consider limiting construction loads near the free edges or slab corners. The controlling load variables for construction loads are the same as for vehicle loads, concentrated loads, and uniform loads.

9.4.3 Environmental Factors

Overall slab design should consider flexural stresses produced by thermal changes, reduction in humidity, expansive soils, and moisture changes in the slab, which will affect curling due to the different shrinkage rates between the top and bottom of the slab. These effects are of particular importance for exterior slabs and for slabs constructed before the building is enclosed. Curling caused by these changes produces flexural stresses due to the slab lifting off the subgrade. Generally, the restraint stresses can be ignored in short slabs because a smooth, planar subgrade does not significantly restrain the short slab movement due to uniform thermal expansion, contraction, or drying shrinkage. When the joint spacing recommendations given in the figure below are followed, then these stresses will be sufficiently low.

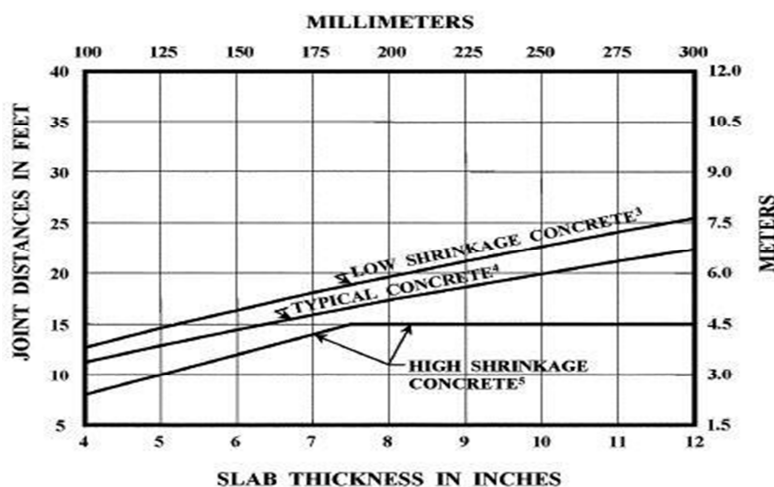


Figure 157: Joint distance in function of thickness

9.4.4 Safety Factors

Unique serviceability requirements distinguish slabs-on-ground from other structural elements. Some of these serviceability requirements can:

- Minimize cracking and curling;
- Increase surface durability;
- Optimize joint locations and joint types for joint stability, which is the differential deflection of the adjacent slab panels edges as wheel loads cross the joint;
- Maximize long-term flatness and levelness;

Because building codes primarily provide guidance to prevent catastrophic failures that affect public safety, the factors of safety for serviceability, inherent in building codes, are not directly addressed as are those for strength.

The designer selects the factor of safety to minimize the likelihood of serviceability failure. Some items the designer should consider in selecting the factor of safety are:

- Consequences of serviceability failure, including lost productivity, lost beneficial use, and the costs for repairing areas in an active facility. For example, minimizing cracking and limiting crack widths for facilities such as pharmaceutical and food processing;
- Concrete mixture proportion and its shrinkage characteristics (test and minimize shrinkage to reduce linear drying shrinkage and curling);
- Humidity-controlled environment that increases linear drying shrinkage and slab curling;
- Subgrade smoothness and planeness to minimize restraint during linear drying shrinkage;
- Spacing and joint types;
- Geotechnical investigation to determine the shallow and deep properties of the soil;
- Number of load repetitions and traffic patterns to allow consideration of fatigue cracking;
- Impact effects;
- Storage racks installed at an early stage, which restrain linear drying shrinkage;
- Compounding factors of safety that may produce an overly conservative design.

Inclusion of cumulative factors of safety in the modulus of subgrade reaction, applied loads, compressive or flexural strength of the concrete, or number of load repetitions, may produce a very conservative and, consequently, expensive construction.

The factor of safety is normally accounted for only in the allowable flexural stress in the concrete slab.

Load type	Commonly used factors of safety	Occasionally used factors of safety
Moving wheel loads	1.7 to 2.0	1.4 to 2.0 and greater
Concentrated (rack and post) loads	1.7 to 2.0	Higher under special circumstances
Uniform loads	1.7 to 2.0	1.4 is lower limit
Line and strip loads	1.7	2.0 is conservative upper limit
Construction loads	1.4 to 2.0	—

Figure 158: Load type safety factor

This table shows some commonly used factors of safety for various types of slab loadings. Most range from 1.7 to 2.0, but some loading conditions use factors as low as 1.4. A moving vehicle subjects the slab-on-ground to the effect of fatigue.

Fatigue strength is expressed as the percentage of the static tensile strength that can be supported for a given number of load repetitions.

As the ratio of the actual flexural stress to the modulus of rupture decreases, the slab can with stand more load repetitions before failure. For stress ratios less than 0.45, concrete can be subjected to unlimited load repetitions.

The table below shows various load repetitions for a range of stress ratios. The factor of safety is the inverse of the stress ratio.

Stress ratio	Allowable load repetitions	Stress ratio	Allowable load repetitions
<0.45	Unlimited	0.73	832
0.45	62,790,761	0.74	630
0.46	14,335,236	0.75	477
0.47	5,202,474	0.76	361
0.48	2,402,754	0.77	274
0.49	1,286,914	0.78	207
0.50	762,043	0.79	157
0.51	485,184	0.80	119
0.52	326,334	0.81	90
0.53	229,127	0.82	68
0.54	166,533	0.83	52
0.55	124,523	0.84	39
0.56	94,065	0.85	30
0.57	71,229	0.86	22
0.58	53,937	0.87	17
0.59	40,842	0.88	13
0.60	30,927	0.89	10
0.61	23,419	0.90	7
0.62	17,733	0.91	6
0.63	13,428	0.92	4
0.64	10,168	0.93	3
0.65	7700	0.94	2
0.66	5830	0.95	2
0.67	4415	0.96	1
0.68	3343	0.97	1
0.69	2532	0.98	1
0.70	1917	0.99	1
0.71	1452	1.00	0
0.72	1099	>1.00	0

Figure 159: Stress ratio versus allowable repetitions

9.5 Joints

9.5.1 Generalities

Joints are used in slab-on-ground construction to limit the frequency and width of random cracks caused by concrete volume changes.

Generally, when limiting the number of joints or increasing the joint spacing can be accomplished without increasing the number of random cracks, floor maintenance will be reduced.

Every effort should be made to avoid connecting the slab to any other element of the structure. Restraint from any source, whether internal or external, will increase the potential for random cracking.

Three types of joints are commonly used in concrete slabs-on-ground and are discussed in detail in this paragraph:

- Isolation joints;
- Sawcut contraction joints;
- Construction joints;

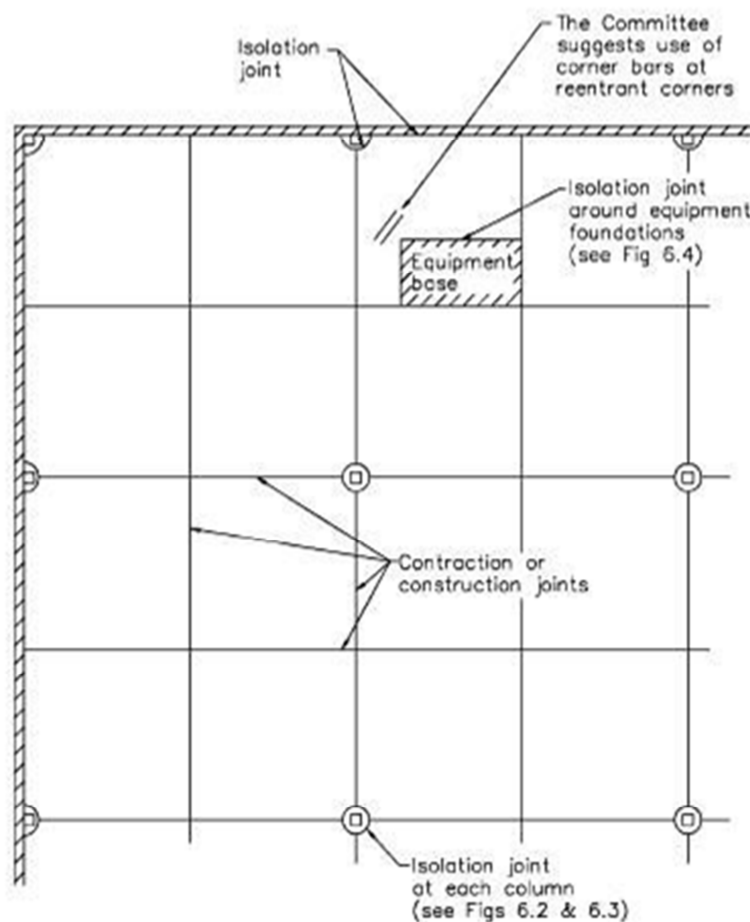


Figure 160: Appropriate locations for joints

Joints in topping slabs should be located directly over joints in the base slab and, when the topping is bonded, no additional joints are required.

The bonded topping slab should be designed for the shrinkage restraint due to the bond to the existing slab, and the bond should be sufficient to resist the upward tension force due to curling. For a thin, unreinforced, unbonded topping slab, consider additional joints between the existing joints in the bottom slab to help minimize the curling stress in the topping slab.

The topping slab can have high curling stresses due to the bottom slab being a hard base for the topping slab. Also, any cracks in the base slab that are not stable should be repaired to ensure they will not reflect through into the topping slab.

9.5.2 Isolation Joints

Isolation joints should be used wherever complete freedom of vertical and horizontal movement is required between the floor and adjoining building elements. Isolation joints should be used at junctions with walls (not requiring lateral restraint from the slab), columns, equipment foundations, footings, or other points of restraint such as drains, manholes, sumps, and stairways.

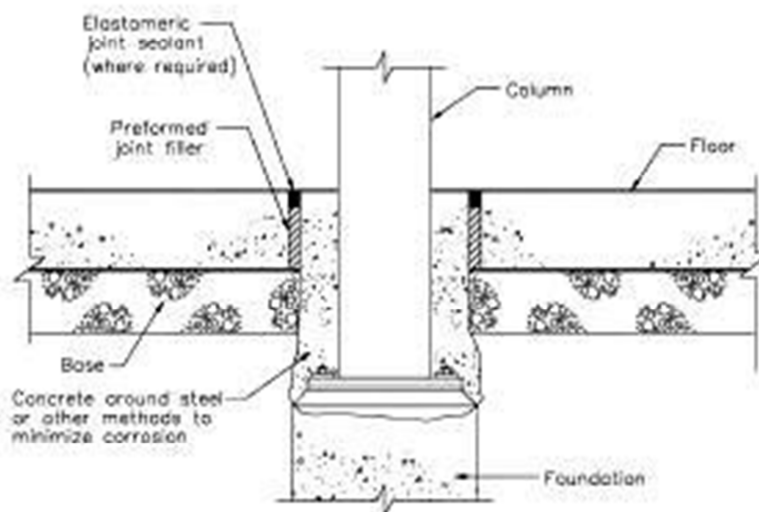
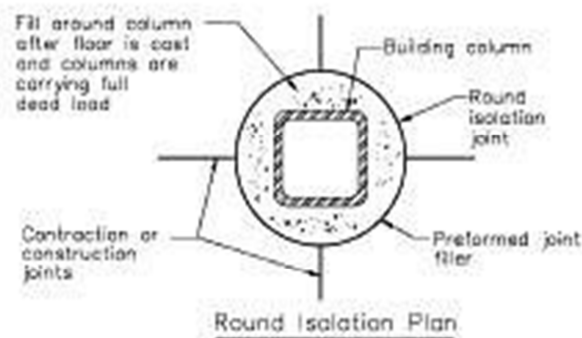
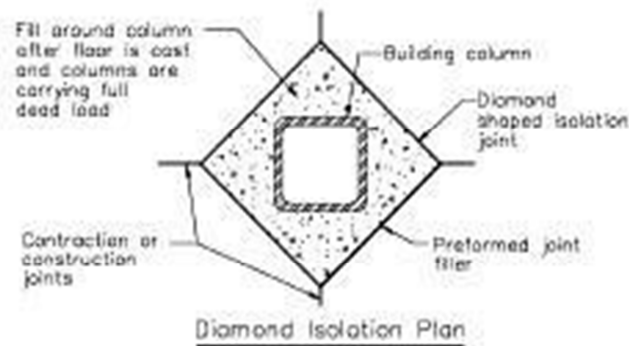
Isolation joints are formed by inserting preformed joint filler between the floor and the adjacent element. Where the isolation joint will restrain shrinkage, flexible closed cell foam plank should be used with a thickness that accommodates the anticipated shrinkage movement.

The joint material should extend the full depth or slightly below the bottom of the slab to ensure complete separation and not protrude above it. Where the joint filler will be objectionably visible, or where there are wet conditions or hygienic or dust control requirements, the top of the preformed filler can be removed and the joint caulked with an elastomeric sealant.

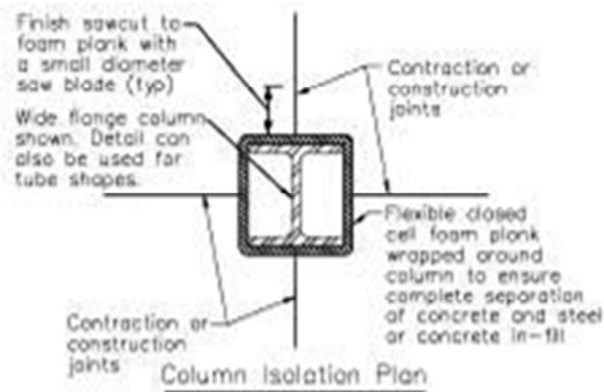
Listed as follows are three methods of producing a relatively uniform joint sealant depth:

- Use a saw to score both sides of the preformed filler at the depth to be removed. Insert the scored filler in the proper location. After the concrete hardens, use a screwdriver or similar tool to remove the top section.
- Cut a strip of wood equal to the desired depth of the joint sealant. Nail the wood strip to the preformed filler and install the assembly in the proper location. Remove the wood strip after the concrete has hardened.
- Use premolded joint filler with a removable top portion.

See the figure below for typical isolation joints around columns.



Section at Column Diamond or Round Isolation Joint



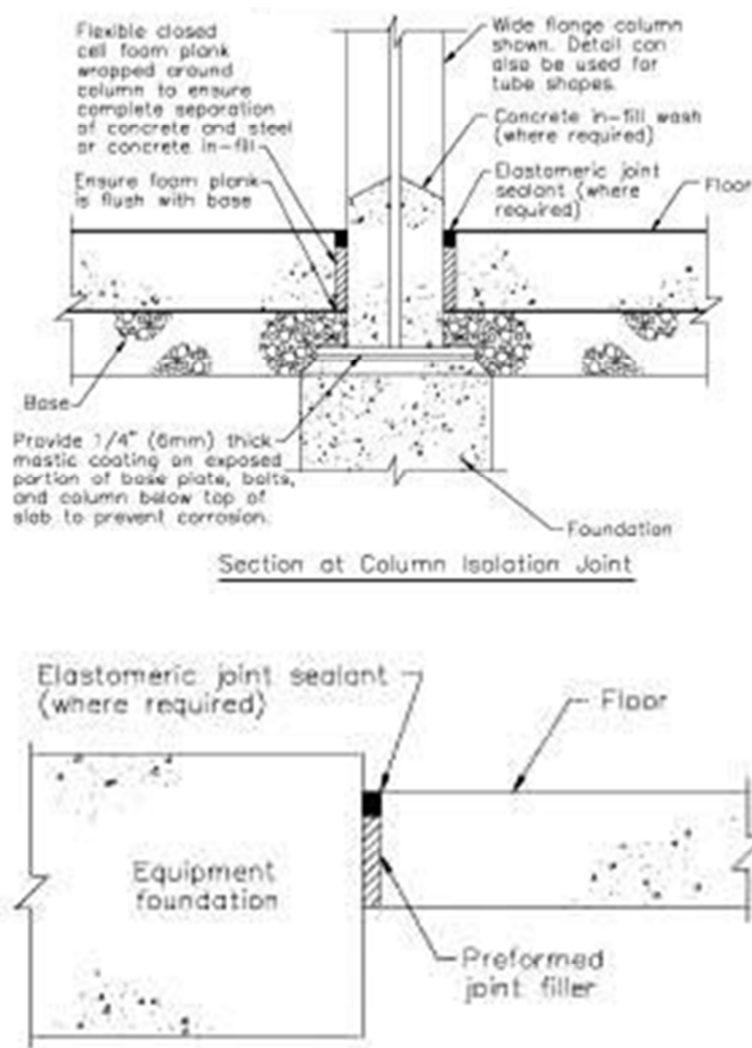


Figure 161: Isolation joint details

Then, the last figure above shows an isolation joint at an equipment foundation.

9.5.3 Construction Joints

Construction joints are placed in a slab to define the extent of the individual placements, generally in conformity with a predetermined joint design.

For specialty floors such as defined traffic slabs, *unplanned* joints can have a significant effect on the long-term floor flatness and levelness when not detailed appropriately.

In areas not subjected to wheel traffic or when differential curling movement is not a concern, a *butt* joint or *keyed* joint may be adequate. In areas subjected to wheeled traffic, heavy loads, or both, joints with load transfer devices are recommended.

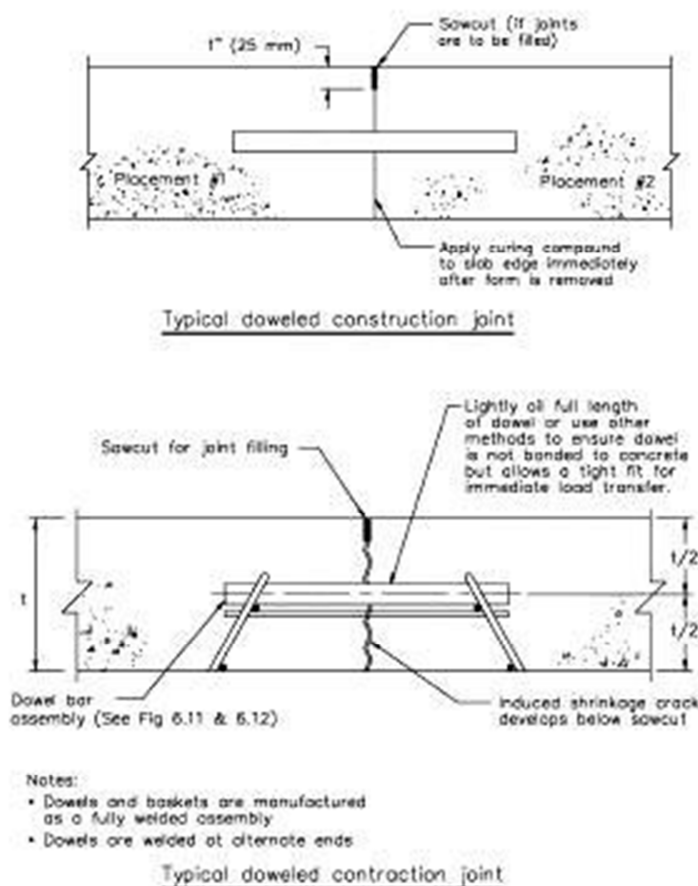


Figure 162: Typical doweled joints

A *keyed* joint is not recommended for load transfer in areas subjected to wheel traffic because the male and female key components lose contact when the joint opens due to drying shrinkage. This can eventually cause a breakdown of the concrete joint edges and failure of the top side portion of the key.

Construction joints are commonly formed using *bulkheads*. These bulkheads should be placed to ensure specified concrete slab thickness and elevation at the slab edge. Provide the necessary support to keep the bulkheads straight, true, and rigid during the entire placing and finishing operations. When positive load transfer is required, provisions should be made along the bulkhead to ensure proper alignment of the load-transfer device during placing and finishing operations.

Proper alignment can be achieved by rigidly attaching alignment devices to the bulkhead or by accurately slotting or drilling the bulkhead to accept a load-transfer device.

These methods should allow the load-transfer device to be installed at the joint face while maintaining proper alignment during placing and finishing operations. The load-transfer devices should be parallel to the top surface, each other, and perpendicular to the joint face. Depending on the method used, the load-transfer device can be inserted before or after the bulkhead is removed. When incorporating alignment or installation devices into

the bulkhead, which remain in the slab, the device should be manufactured with a thin rigid material that is a tight fit with the load-transfer device to minimize vertical deflection due to load. Load-transfer devices in direct contact with the concrete will be the most effective load-transfer mechanism for controlling vertical joint deflection.

All construction joints should be internally vibrated at frequent intervals to properly consolidate the concrete at the joint and around the load-transfer devices. Vibratory screeds, laserguided screeds, and hand-rodding techniques do not provide sufficient internal vibration around the load-transfer devices.

9.5.4 Sawcut Contraction Joints

Sawcut contraction joints are used to limit random, out-of-joint floor slab cracking.

Joints are usually located on column lines, with intermediate joints located at equal spaces between column lines.

Consider the following when selecting spacing of sawcut contraction joints:

- Slab design method;
- Slab thickness;
- Type, amount, and location of reinforcement;
- Shrinkage potential of the concrete, including cement type and quantity; aggregate type, size, gradation, quantity, and quality; water-cementitious material ratio; type of admixtures; and concrete temperature;
- Base friction;
- Floor slab restraints;
- Layout of foundations, racks, pits, equipment pads, trenches, and similar floor discontinuities;
- Environmental factors such as temperature, wind, and humidity.

Establishing slab joint spacing, thickness, and reinforcement requirements is the responsibility of the designer. The specified joint spacing will be a principal factor dictating both the amount and the character of random cracking to be experienced, so joint spacing should always be carefully selected.

For unreinforced slabs-on-ground and for slabs reinforced only for limiting crack widths, other than continuously reinforced with more than 0.5% of steel by cross-sectional area.

The spacings are based on shrinkage values for specimens that have been moist-cured 7 days and then placed in air storage. Use the appropriate prism size for the concrete mixture being placed.

Sawcut contraction joints should be continuous across *intersecting* joints, not staggered or offset. The aspect ratio of slab panels that are unreinforced, reinforced only for crack-width control, or made with shrinkage-compensating concrete should be a maximum of 1.5 to 1; however, a ratio of 1 to 1 is preferred. L- and T-shaped panels should be

avoided. Floors around loading docks have a tendency to crack due to their configuration and restraints.

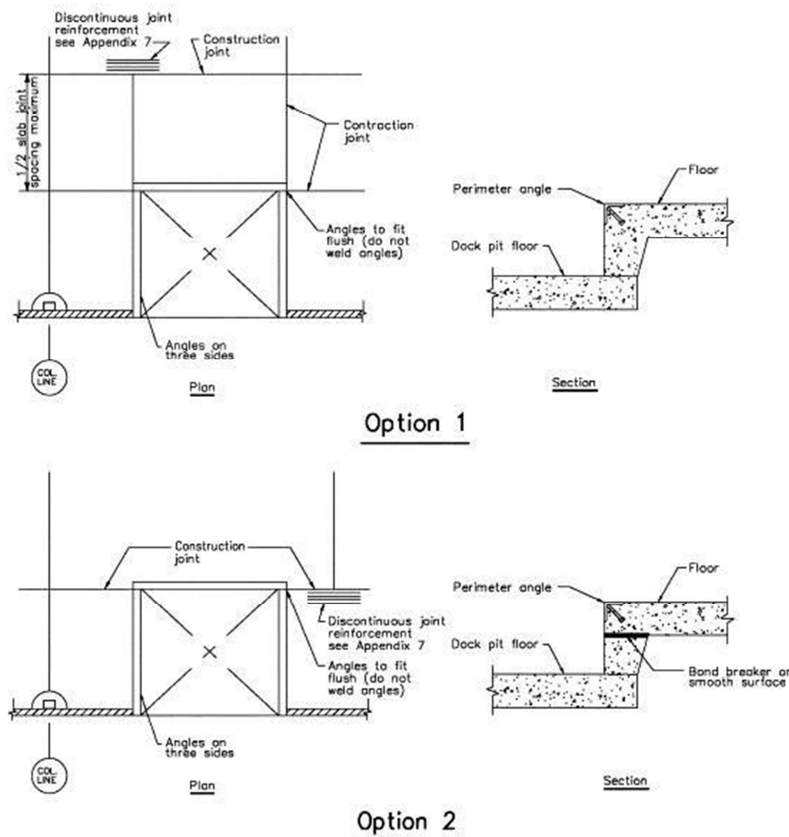


Figure 163: Joint details at loading dock

The figure above shows two options that minimize slab cracking at reentrant corners of loading docks. In Option 1, the loading dock pit wall is placed integral with the slab and, therefore, most of the shrinkage movement is forced to the construction joint shown in the figure. To minimize the opening width of this construction joint, place the joint at 1/2 of the typical slab joint spacing. In Option 2, create a slip surface at the top of the pit wall that will help equalize the shrinkage movement on each side of the slab panel so the typical slab joint spacing can be used. By using a construction joint as shown in Option 2, there is less likelihood of cracking at the dock pit corners.

Plastic or metal inserts are not recommended for creating a contraction joint in any exposed floor surface subject to wheel traffic.

Contraction joints in industrial and commercial floors are usually formed by sawing a continuous slot in the slab to form a weakened plane so a crack will form below as you can see in the next figure.

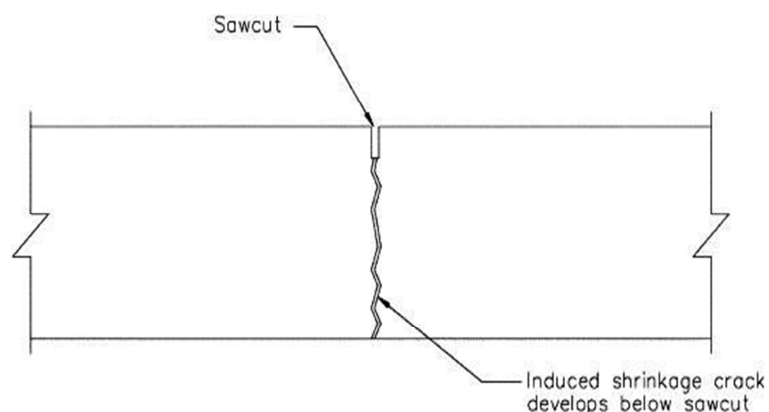


Figure 164: Sawcut contraction joint

When using load-transfer assemblies at sawcut contraction joints, the concrete around these assemblies should be internally vibrated. This properly consolidates the concrete around the load-transfer assemblies.

9.5.5 Load-Transfer Mechanism

Use load-transfer devices at construction and contraction joints when positive load transfer is required, unless a sufficient amount of post-tensioning force is provided across the construction joint to transfer the shear.

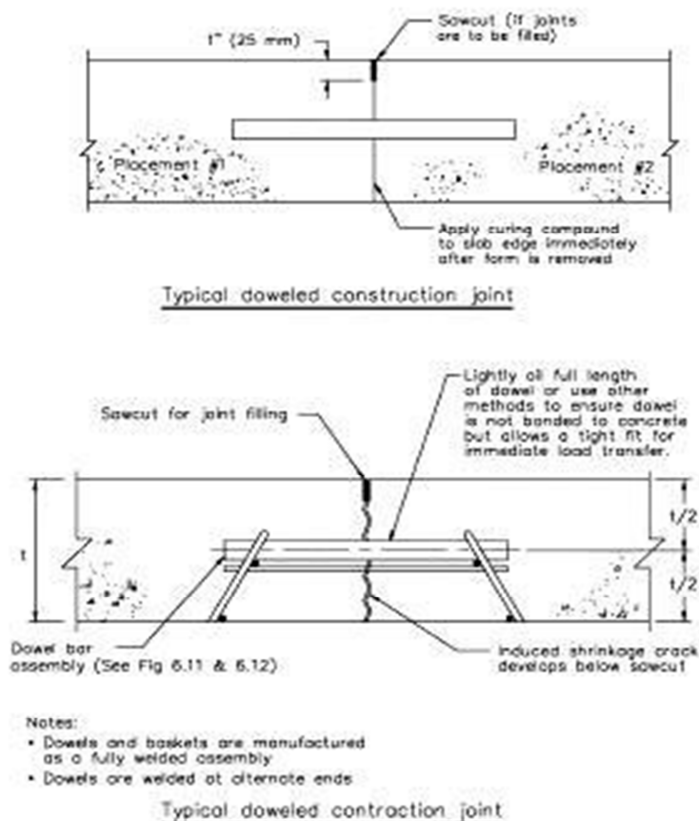


Figure 165: Typical doweled joint

Load-transfer devices force concrete on both sides of a joint to deflect approximately equally when subjected to a load. This can help prevent damage to an exposed edge when subjecting the joint to wheel traffic.

For dowels to be effective, they should be smooth, aligned, and supported so they remain parallel in both the horizontal and vertical planes during the placing and finishing operation. Plate dowels are now commonly used in construction and contraction joints.

Manufacturers offer various plate dowel geometries and associated installation devices. Plate dowels can minimize shrinkage restraint by using a tapered shape, formed void, or by having compressible material on the vertical faces with a thin bond breaker on the top and bottom dowel surfaces.

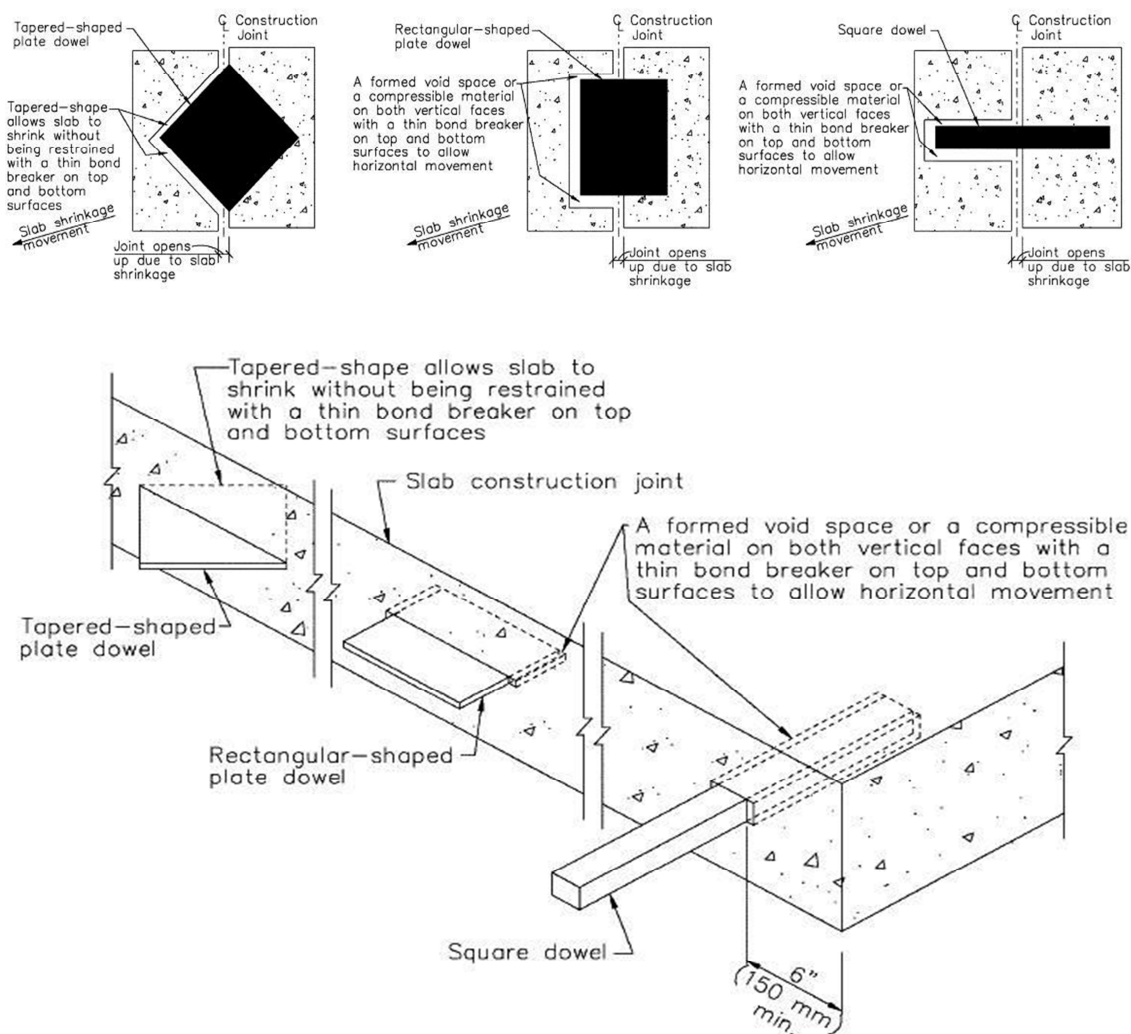


Figure 166: Indicating and movements for doweled construction joint

When a formed void on the vertical sides is constructed by a stay-in-place device, then that stay-in-place device should be of a rigid material and fit tightly with the dowel surface to minimize vertical deflection at the joint.

Dowel baskets should be used to maintain alignment of dowels in sawcut contraction joints, and alignment installation devices should be used in construction joints.

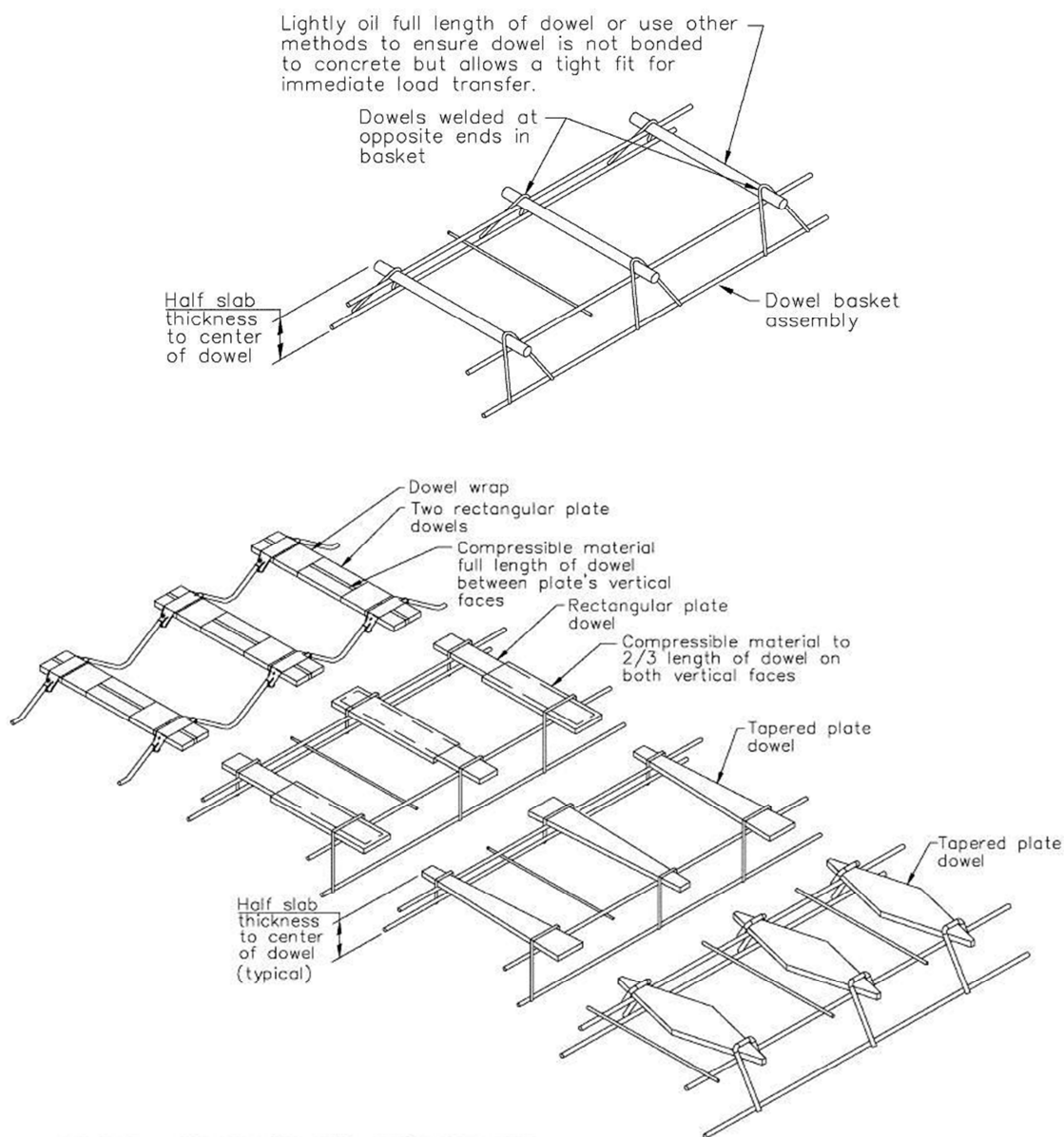


Figure 167: Dowel basket

In corrosive environments, the designer should consider corrosion protection for the dowels. Plate and square dowel systems that minimize horizontal restraint as shown in the figure showed before can be placed close to the intersection of joints, but no closer than 150 mm. Other dowels should be placed no closer than 300 mm from the intersection of any joints because the maximum movement caused by horizontal dry shrinkage occurs at this point, and the corner of the slab may consequently crack.

Slab depth, in. (mm)	Dowel dimensions, in. (mm)				Plate dowel	Dowel spacing center-to-center, [†] in. (mm)		
	Construction joint		Contraction joint			Round [‡]	Square [§]	Plate dowel
	Round [‡]	Square [§]	Round [‡]	Square [§]				
5 to 6 (130 to 150)	3/4 x 10 (19 to 250)	3/4 x 10 (19 x 250)	3/4 x 13 (19 x 330)	3/4 x 13 (19 x 330)	M/R [#]	12 (300)	14 (360)	18 (460)
7 to 8 (180 to 200)	1 x 13 (25 x 330)	1 x 13 (25 x 330)	1 x 16 (25 x 410)	1 x 16 (25 x 410)	M/R [#]	12 (300)	14 (360)	18 (460)
9 to 11 (230 to 280)	1-1/4 x 15 (32 x 380)	1-1/4 x 15 (32 x 380)	1-1/4 x 18 (32 x 460)	1-14 x 18 (32 x 460)	M/R [#]	12 (300)	12 (300)	18 (460)

Figure 168: Dowel size and spacing

This table provides recommended dowel sizes and spacing for round and square shapes. A less effective load-transfer mechanism than those just discussed is aggregate interlock.

Aggregate interlock depends on the irregular face of the cracked concrete at joints for load transfer.

Not all joints activate uniformly. This result in some joint opening widths that are larger than might normally be anticipated. These wide joints are often called the “*dominant joints*.” The dominant joint behavior is made worse by the ever-increasing use of vapor retarders/barriers placed below the floor slab, which reduces base friction and makes the dominant joints more noticeable and problematic.

A more reliable and definable method to evaluate the performance of a joint having a load-transfer mechanism, a joint using aggregate interlock, or a crack that has developed, is by measuring the joint or crack stability. The joint or crack stability is the differential deflection of the adjacent slab panel or crack edges when a service load crosses the joint or crack.

Joint or crack stability can be easily measured. It is commonly done by using a leveled straightedge and gauge for example, a tri-square or dial indicator to measure the vertical distance from the upper straightedge to slab surface 300 mm spacing 150 mm each side of the joint to determine the amount of vertical movement under the bottom of the straightedge as it occurs or by using a device with an inclinometer having 300 mm contact point spacing located 150 mm on each side of the joint that gives a visual readout of the vertical movement as it occurs.

Joint or crack stability measurements below 0.25 mm for joints or cracks subjected to lift truck wheel traffic with small hard wheels will have good service life. For lift truck traffic with large, cushioned rubber wheels, a joint or crack stability measurement of 0.51 mm should have good service life. These joint stability values assume the joint is properly filled full depth with semi-rigid joint filler and that the joint filler is properly maintained.

For joint or crack stability values above 1.5 mm, the joint or crack would be considered unstable, have a much reduced service life, and most likely should be repaired.

Another load-transfer mechanism is enhanced aggregate interlock. Enhanced aggregate interlock depends on a combination of the effect of a small amount of deformed reinforcement continued through the joint and the irregular face of the cracked concrete at joints for load transfer. The continuation of a small percentage of deformed reinforcement (0.1% of the slab cross-sectional area) through sawcut contraction joints in combination with joint spacings, has been used successfully by some designers to provide load-transfer capability without using dowels.

A slab design that uses this small amount of deformed reinforcement to enhance aggregate interlock at the joints should conform to the following:

- Space joints from table showed before;
- Place the reinforcement above mid-depth but low enough that the sawcut will not cut the reinforcement;
- Place a construction or sawcut contraction joint with a load-transfer device at a maximum of 38 m. This forces activation at these joints when the other joints with the deformed reinforcement do not activate;
- Use an early-entry saw to cut all sawcut contraction joints;
- The slab should be a uniform thickness.

9.6 Design of Unreinforced Concrete Slabs

9.6.1 Introduction

The thickness of unreinforced concrete slabs is determined using an allowable concrete flexural tensile stress.

Although the effects of any welded wire reinforcement, plain or deformed bars, post tensioning, fibers, or any other type of reinforcement are not considered, joints may be reinforced for load transfer across the joint.

Slabs are normally designed to remain un-cracked due to applied loads with a factor of safety of 1.4 to 2.0 relative to the modulus of rupture.

It is important to note that, slabs-on-ground are not considered structural members unless they are used to transmit vertical or horizontal loads from other elements of the building's structure.

Consequently, cracking, joint instability, and surface character problems are considered slab serviceability issues and not relevant to the general integrity of the building structure.

Concrete floor slabs employing portland cement, regardless of slump, will begin to experience a reduction in volume as soon as they are placed. This continues as long as water, heat, or both, are released into the surroundings. Because the drying and cooling

rates at the top and bottom of the slab are dissimilar, the shrinkage will vary with the depth.

This distorts the as-cast shape and reduces volume. Resistance to this distortion introduces internal concrete stresses that, when unrelieved, may cause cracks.

Controlling the effects of drying shrinkage is critical to the performance of unreinforced concrete slabs.

Two principal objectives of unreinforced slab-on-ground design are to avoid the formation of random, out-of-joint cracks and to maintain adequate joint stability.

The slab's anticipated live loading governs its thickness and cross-joint shear transfer requirements, whereas shrinkage considerations dictate the maximum joint spacing.

Current design and construction procedures are based upon limiting cracking and curling, due to restrained shrinkage, to acceptable levels, but not eliminating them.

In jointed, unreinforced slabs-on-ground, the design intends to cause shrinkage cracks to occur beneath sawcut contraction joints.

In industrial construction, this can result in a floor slab that is susceptible to relative movement of the joint edges and joint maintenance problems when exposed to wheel traffic. When the designer cannot be sure of positive long-term shear transfer at the joints through aggregate interlock, then positive load-transfer devices should be used at all joints subject to wheel traffic.

9.6.2 Thickness Design Methods

When the slab is loaded uniformly over its entire area and supported by uniform subgrade, stresses will be due solely to restrained volumetric changes; however, most slabs are subjected to non-uniform loading.

In warehouses, the necessity for maintaining clear aisles for access to stored materials results in alternating loaded and unloaded areas. Rack post and lift truck wheel loads present a more complex loading pattern.

Three separate cases, differentiated on the basis of the location of the load with respect to the edge of the slab, might be considered (Winter et al. 1964). These cases are provided to illustrate the effect of load location, particularly at free corners or edges.

Most of the generally used structural design methods discussed do not provide for loading at free edges and corners. The designer should carefully consider such loading.

▪ *Wheel load close to corner of large slab*

With a load applied at the corner of a slab, the critical stress in the concrete is tension at the top surface of the slab. An approximate solution assumes a point load acting at the corner of the slab.

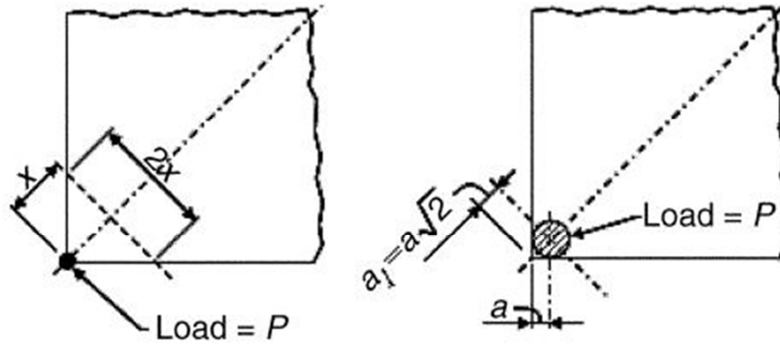


Figure 169: Corner load

At short distances from the corner, the upward reaction of the soil has little effect, and the slab is considered to act as a cantilever. At a distance x from the corner, the bending moment is Px ; it is assumed to be uniformly distributed across the slab section width at right angles to the bisector of the corner angle. For a 90-degree corner, the section width is $2x$, and the bending moment per unit width of slab is:

$$\frac{Px}{2x} = \frac{P}{2}$$

When h is the thickness of the slab, the tensile stress at the top surface is:

$$f_t = \frac{M}{S} = \frac{\frac{P}{2}}{\frac{h^2}{6}} = \frac{3P}{h^2}$$

This equation provides reasonably close results only in the immediate vicinity of the slab corner, and only when the load is applied over a small contact area.

In an analysis that considers the reaction of the subgrade, and that considers the load to be applied over a contact area of radius a , Westergaard derives the expression for critical tension at the top of the slab, occurring at a distance $2(a_1L)^{0.5}$ from the corner of the slab:

$$f_t = \frac{3P}{h^2} \left[1 - \left(\frac{a\sqrt{2}}{L} \right)^{0.6} \right]$$

Where:

- f_t is concrete tensile stress, Pa;
- a is the radius of load contact area, m;

- P is the load on the slab-on-ground, N;
- h is the slab thickness, m;
- L is the radius of relative stiffness, m, equal to:

$$L = \sqrt[4]{\frac{Eh^3}{12(1-\nu^2)k}}$$

Where:

- E is elastic modulus of concrete, Pa;
- ν is Poisson's ratio for concrete, approximately 0.15;
- k is modulus of subgrade reaction, N/m³.

The value of L reflects the relative stiffness of the slab and the subgrade. It will be large for a stiff slab on a soft base, and small for a flexible slab on a stiff base.

- *Wheel load considerable distance from edges of slab*

When the load is applied some distance from the edges of the slab at approximately four times the relative stiffness ($4L$), the critical stress in the concrete will be in tension at the bottom surface. This tension is greatest directly under the center of the loaded area.

- *Wheel load at edge of slab, but removed considerable distance from corner*

When the load is applied at a point along an edge of the slab, the critical tensile stress is at the bottom of the concrete, directly under the load. If the flexural tensile stress f_b exceeds the allowable concrete flexural tensile stress, it is necessary to increase slab thickness, increase concrete flexural strength, or provide reinforcement. Such reinforcement is usually designed to provide for all the tension indicated by the analysis of the assumed homogeneous, elastic slab.

- *Loads distributed over partial areas*

In addition to concentrated loads, uniform loads distributed over partial areas of slabs may produce the critical design condition.

Again, in warehouses, heavy loads alternate with clear aisles. With such a loading pattern, cracking is likely to occur along the centerline of the aisles.

In an analysis based on such loading, Rice (1957) derived an expression for the critical negative moment in the slab M_c that occurs at the center of the aisle:

$$M_c = \frac{w}{2\lambda^2} e^{-\lambda a} [\sin(\lambda a)]$$

Where:

- M_c = slab moment at the center of the aisle, m-N/m;

- $\lambda = (k/4EI)^{1/4}$, m⁻¹;
- E = elastic modulus of concrete, Pa;
- I = moment of inertia, m⁴;
- a = half-aisle width, m;
- k = modulus of subgrade reaction, N/m³;
- w = uniform load, N/m²;
- e = base of natural logarithms.

Recognizing that the aisle width cannot always be predicted exactly, Rice suggests that a “critical aisle width” be used. This width is such as to maximize the above for bending moment (Westergaard 1926). Generally accepted thickness design methods for unreinforced slabs-on-ground are the:

- PCA method;
- WRI method;
- COE method;

Each of these methods, seek to avoid live load-induced cracks through the provision of adequate slab cross section by using an adequate factor of safety against rupture. The PCA and WRI methods only address live loads imposed on the slab’s interior, whereas the COE method only considers live loads imposed on the slab’s edges or joints. All three methods assume that the slab remains in full contact with the ground at all locations. Curl-induced stresses are not considered.

9.6.3 Portland Cement Association Design Method

The PCA method is based on Pickett’s analysis (Ringo 1986).

The variables used are flexural strength, working stress, wheel contact area, spacing, and the subgrade modulus. Assumed values are Poisson’s ratio (0.15) and the concrete modulus of elasticity (28,000 MPa). The PCA method is for interior loadings only; that is, loadings are not adjacent to free edges.

- *Wheel loads*

Slabs-on-ground are subjected to various types, sizes, and magnitudes of wheel loads. Lift truck loading is a common example of wheel loads.

- *Concentrated loads*

Concentrated loads can be more severe than wheel loads. Design for concentrated loads is the same as for wheel loads. Consider also the proximity of rack posts to joints. Generally, flexure controls the concrete slab thickness.

- *Uniform loads*

Uniform loads do not stress the concrete slab as highly as concentrated loads. The two main design objectives are to prevent top cracks in the unloaded aisles and to avoid excessive settlement due to consolidation of the subgrade. Top cracks are caused by tension in the top of the slab and depend largely on slab thickness, load placement, and short- and long-term subgrade deflections.

- *Construction loads*

The PCA method does not directly address construction loading. If, however, such loading can be determined as equivalent wheel loads, concentrated loads, or uniform loads, the same charts and tables can be used.

9.6.4 Wire Reinforcement Institute Design Method

The WRI design charts, for interior loadings only, are based on a discrete element computer model. The slab is represented by rigid bars, torsion bars for plate twisting, and elastic joints for plate bending. Variables are slab stiffness factors, modulus of elasticity, subgrade modulus, and trial slab thickness; diameter of equivalent loaded area; distance between wheels; flexural strength; and working stress.

- *Wheel loads*

The WRI thickness selection method starts with an assumption of slab thickness so that the stiffness of slab relative to the subgrade is determined. The moment in the slab caused by the wheel loads and the slab's required thickness are then determined.

- *Concentrated loads*

The WRI charts do not address concentrated loads directly. Because it is possible, however, to determine a wheel load that represents an equivalent concentrated loading, the charts can be used.

- *Uniform loads*

The WRI provides other charts for design of slab thickness where the loading is uniformly distributed on either side of an aisle.

- *Construction loads*

Construction loads such as equipment, cranes, concrete trucks, and pickup trucks may affect slab thickness design. As with the PCA design method, these are not directly addressed by WRI. Thickness design, however, may be based on an equivalent load expressed in terms of wheel loads or uniform loads.

9.6.5 The COE Design Method

The COE design charts are intended for wheel and axle loadings applied at an edge or joint only. The variables inherent in the axle configuration are built into the design index category. Concentrated loads, uniform loads, construction loads, and line and strip loads are not addressed.

The COE method is based on Westergaard's formula for edge stresses in a concrete slab-on-ground. The edge effect is reduced by a joint transfer coefficient of 0.75 to account for load transfer across the joint. Variables are concrete flexural strength, subgrade modulus, and the design index category.

The design index is used to simplify and standardize design for the lighter-weight lift trucks, generally having less than 110 kN axle load. The traffic volumes and daily operations of various sizes of lift truck for each design index are considered representative of normal warehouse activity and are built into the design method. Assumed values are an impact factor of 25%, concrete modulus of elasticity of 28,000 MPa, Poisson's ratio of 0.20, the wheel contact area, and the wheel spacings.

The latter two values are fixed internally for each index category.

Additional design charts for pavements with protected and unprotected corners have been developed by the COE for pavements, although they may be applied to slabs-on-ground in general.

9.6.6 Shear Transfer at Joints

A principal concern governing the spacing of sawcut contraction joints is edge curl (Walker and Holland 1999). Effective shear transfer at both construction and intermediate sawcut contraction joints is required to avoid a loaded free edge. Also, curl and shrinkage can reduce joint stability by disengaging aggregate interlock or keyed joints, allowing the free edges to deflect independently under wheel traffic.

Excessive curling and shrinking can also reduce the joint stability of doweled joints. Positive load-transfer devices, such as dowels, should be used for joints subjected to wheel traffic where the joint is expected to open more than 0.6 to 0.9 mm.

The PCA (2001) provides considerations for the effectiveness of shear transfer at joints.

- *Steel dowels*

Steel dowels are the most effective means to provide effective load transfer and to ensure adjacent curled joint edges deflect together.

When dowels are installed across a joint, the slab edges abutting the joint may still curl and deflect when loaded, but they do so in unison.

When the wheel reaches the joint, no significant relative vertical displacement between the panels is encountered, and the impact loads imposed on the edges are greatly reduced.

9.6.7 Maximum Joint Spacing

Assuming the subgrade is relatively free from abrupt changes in elevation, such as that caused by uncorrected wheel rutting, the tensile stresses created in the shrinking panel by subgrade frictional restraint are relatively minor in comparison to curling-induced stresses.

These higher curling stresses are likely the principal cause of shrinkage cracking in most unreinforced concrete floor slabs (Walker and Holland 1999).

9.7 FRC Design

This chapter presents synthetic and steel fiber-reinforced concrete, FRC, material properties and design methods for FRC slabs-on-ground. The performance of FRC slabs-on-ground depends on the mixture proportions and all mixture constituents, including fiber type and quantity.

9.7.1 Steel Fiber Reinforcement

Steel fibers are used to reinforce concrete slabs-on-ground to provide increased strain strength, impact resistance, flexural toughness, fatigue endurance, crack-width control, and tensile strength. Steel fibers are smooth or deformed. Deformations provide mechanical anchorage in the concrete. The matrix bond and anchorage allows steel fibers to bridge cracks that develop in the hardened state and redistribute the accumulated stress caused by applied loads and shrinkage stresses. The length of steel fibers used for slab-on-ground applications can range from 19 to 64 mm.

Steel fibers for concrete reinforcement are short, discrete lengths of steel having an aspect ratio, or ratio of length-to-diameter, from about 20 to 100, with several types of cross sections. They are sufficiently small to be randomly dispersed in an unhardened concrete mixture using common mixing procedures.

Steel fibers are made of low-carbon, high-carbon, or stainless steel.

Carbon steel fibers are either uncoated or galvanized.

High-carbon fibers are typically used with concrete mixtures of 55 MPa compressive strength and higher.

Stainless steel fibers may be used when the concrete will be exposed to extremely high temperatures.

Steel fiber bond to the matrix is enhanced by mechanical anchorage, surface area, alloying, surface roughness, or a combination of these.

- *Random Crack Control*

Steel fibers are commonly used for random crack control. As in the case with conventional reinforcement, the fibers do not prevent cracking, but serve to hold cracks tight such that the slab performs as intended during its service life. The degree of random crack control by the fibers is directly related to the fiber type and quantity.

- *Crack Width Opening*

As with conventional reinforcement, steel fibers at volumes of 0.25 to 0.5% (20 to 39 kg/m³) can increase the number of cracks and thus, reduce crack widths. Using steel FRC with conventional, deformed, or smooth continuous reinforcement has synergistic effects, and can be designed to share the applied tensile forces with the continuous reinforcement, thereby adding to crack-width control. The degree of crack width control is directly related to the fiber type and quantity.

- *Flexural Toughness*

Flexural toughness of steel FRC is determined by testing beams or panels in a laboratory. It is generally accepted that the presence of steel fibers in quantities less than 0.5% by volume, as expected in most slabs-on-ground, does not affect the concrete's modulus of rupture. Toughness is a measure of the post cracking energy-absorbing strength of steel FRC, and is defined as the area under the test beam load-deflection curve. Use residual strength factors $R_{e,3}$ and average residual strength (ARS), in slab-on-ground design. These factors represent an average value of load-carrying strength of the test beam over a deflection interval. The ARS is reported in MPa and represents a portion of the modulus of rupture. $R_{e,3}$ is reported as a percentage of the modulus of rupture. The residual strength factor $R_{e,3}$ represents the post-crack characteristics of steel FRC. The degree of flexural toughness is directly related to the mixture proportion and all mixture constituents, including fiber type and quantity.

- *Impact Resistance*

The impact resistance of steel FRC is three to 10 times greater than plain concrete when subjected to explosive charges, dropped weights, and dynamic flexural, tensile, and compressive loads (Williamson 1965; Robins and Calderwood 1978; Suaris and Shah 1981). The degree of impact resistance is directly related to the mixture proportion and all mixture constituents, including fiber type and quantity.

- *Flexural Fatigue Resistance*

The flexural fatigue resistance at two million cycles for plain concrete is approximately 50% of the static rupture modulus. This is the basis for the well-known factor of safety of

2.0 shown in the PCA design document (Spears and Panarese 1983). Steel FRC mixtures have shown fatigue strengths of 65 to 90% of the static rupture modulus at two million cycles when non reversed loading is used (Ramakrishnan and Josifek 1987; Ramakrishnan et al. 1987). The fatigue strength is slightly less when full reversal of loads is used (Batson et al. 1972). The degree of fatigue resistance relates directly to the mixture proportions and all mixture constituents, including fiber type and quantity.

- *Shear Resistance*

Steel FRC can provide higher punching shear strength and anchor bolt pullout strength compared with plain concrete (Concrete Society 2003). Shear strength is directly related to the mixture proportion and all mixture constituents, including fiber type and quantity.

- *Freezing and Thawing Resistance*

Steel fibers do not inherently increase freezing-and-thawing resistance of concrete.

- *Durability in Corrosive Environments*

Plain carbon steel fibers are protected from corrosion by the alkaline environment of the cementitious matrix and their electrical discontinuity. Laboratory and field testing of intact steel FRC shows that in the long term, the corrosion of steel fiber exposed at the surface is limited to a concrete depth of 2.5 mm. Laboratory and field testing of cracked steel FRC in an environment containing chlorides indicates that fibers passing across the crack can corrode similarly to conventional reinforcement but without causing spalling (Hoff 1987). Previous studies show that crack widths less than 0.1 mm do not allow corrosion of steel fibers passing the crack (Morse and Williamson 1977). Studies that are more recent show that crack widths up to 0.5 mm have no adverse effect on corrosion of steel fibers (Lambrechts et al. 2003). When cracks wider than 0.5 mm are limited in depth, the consequences of this localized corrosion may not be structurally significant.

9.7.2 Synthetic Fiber Reinforcement

Synthetic fibers are used to reinforce concrete against plastic shrinkage and drying shrinkage stresses. Fine micro monofilament (diameters less than 0.30 mm) or fibrillated synthetic fibers are typically added at low volume addition (LVA) rates of 0.1% or less of concrete volume for plastic shrinkage crack control. Macro-synthetic fibers (diameters equal or greater than 0.30 mm) are typically added at high volume addition (HVA) rates of 0.25 to 1% by volume for drying shrinkage crack control. The length of fibers used for slab-on-ground applications can range between 13 to 64 mm.

Micro-synthetic fibers are normally used in the range of 0.05 volume percent to 0.20 volume percent. These volume percentages equate to 0.44 to 1.8 kg/m³. Some micro-synthetic fibers can increase the fracture toughness of concrete slabs-on-ground in the hardened state. Use macro-synthetic fibers in the range of 0.20 to 1.0% by volume, which

equates to 1.8 to 8.9 kg/m³. Macro-synthetic fibers provide increased post-cracking residual strength to slabs-on-ground.

Adding micro-synthetic fibers at quantity rates of 1% by volume or less does not significantly alter the ultimate compressive, flexural, and tensile strength of concrete. Adding macro-synthetic fibers at quantities between 0.20 to 1.0% by volume significantly increases the flexural toughness of concrete.

▪ *Design Principles*

The design principles for micro-synthetic FRC are the same as those used for *unreinforced concrete*, including using the joint spacing recommendations. Macro-synthetic fibers provide increased post-cracking residual strength to concrete slabs-on-ground. The same design principles for steel FRC can be used for macro-synthetic FRC.

▪ *Joints Details*

Construction and sawcut contraction joint details and spacing for micro-synthetic FRC are the same as those used for unreinforced concrete. Macro-synthetic fibers at quantities between 0.2 to 1% by volume increase the post-cracking residual strength of the concrete. This material behavior permits longer sawcut contraction joint spacing; however, load transfer stability may be reduced at sawn contraction joints and should be considered carefully at the longer joint spacing.

9.7.3 Thickness Design Methods

Five methods available for determining the thickness of steel FRC slabs-on-ground are described in this section:

- The PCA, WRI, and COE thickness design methods;
- Elastic method;
- Yield line method;
- Nonlinear finite modeling;
- Combined steel FRC and bar reinforcement.

These design methods depend on steel FRC attaining a minimum level of residual strength. In addition, the table below provides suggested performance levels for various floor loading conditions. These values represent a compilation of performance values obtained from trade literature.

Fiber concentration, lb/yd ³ (kg/m ³)	Application (typical residual strength factors)	Anticipated type of traffic
Over 33 (over 20)	Random crack-width control (20 to 40%)	Commercial and light industrial with foot traffic or infrequent lift trucks with pneumatic tires
33 to 50 (20 to 30)	Light dynamic loading (30 to 50%)	Industrial vehicular traffic with pneumatic wheels or moderately soft solid wheels
40 to 60 (24 to 36)	Medium dynamic loading (40 to 60%)	Heavy-duty industrial traffic with hard wheels or heavy wheel loads
60 to 125 (36 to 74)	Severe dynamic loading, extending joint spacing design (60% or higher)	Industrial and heavy-duty industrial traffic

Figure 170: Comparative design table

▪ *PCA/WRI/COE Method*

The PCA/WRI/COE methods described before may all be applied to the design of steel FRC slabs-on-ground. With this approach, use steel fiber reinforcement for serviceability design issues such as temperature and shrinkage crack control, enhanced joint stability, and impact and fatigue resistance. Consult fiber manufacturers for specific designs or steel fiber quantities.

▪ *Elastic Method*

The thickness of slabs-on-ground with steel fibers should be selected to prevent cracking due to external loading as discussed before with the following modifications: Account for steel fibers by setting the allowable stress equal to the equivalent flexural strength of the composite steel FRC:

$$f_b = R_{e,3}/100 \times f_r$$

where:

- f_b is allowable flexural tensile stress, MPa;
- f_r is the modulus of rupture of concrete, MPa;
- $R_{e,3}$ is the residual strength factor determined using JSCE SF4, %.

For example, using a $R_{e,3} = 55$ and modulus of rupture = 570 MPa, the allowable bending stress is $F_b = 55/100 \times \text{modulus of rupture} = 0.55 \times 570 \text{ psi} = 314 \text{ MPa}$.

Compare this with an unreinforced slab that has an allowable flexural strength of $0.50 \times 570 \text{ MPa} = 285 \text{ MPa}$.

▪ *Yield Line Method*

Yield line analysis accounts for the redistribution of moments and formation of plastic

hinges in the slab. These plastic hinge regions develop at points of maximum moment and cause a shift in the elastic moment diagram. Using plastic hinges permits the use of the full moment strength of the slab and an accurate determination of its ultimate load strength. Because the formation of plastic hinges depends on toughness, the minimum $R_{e,3}$ residual strength should be greater than 30%. The results of tests (Beckett 1995) led to the adoption of yield-line design methods based on the work of Meyerhof (1962) and Lösberg (1961).

The work of Meyerhof (1962) presents three separate cases, differentiated on the basis of load location with respect to the edges of the slab, which may be considered.

Central load on large slab

$$P_0 = 6\left[1 + \frac{2a}{L}\right]M_0$$

For this case, express the value of M_0 as

$$M_0 = M_n + M_p = \left[1 + \frac{R_{e,3}}{100}\right] \times \left(\frac{f_r \times b \times h^2}{6}\right)$$

Edge load

$$P_0 = 3.5\left[1 + \frac{3a}{L}\right]M_0$$

For this case, express the value of M_0 as

$$M_0 = M_n + M_p = \left[1 + \frac{R_{e,3}}{100}\right] \times \left(\frac{f_r \times b \times h^2}{6}\right)$$

Corner load

$$P_0 = 2\left[1 + \frac{4a}{L}\right]M_0$$

For this case, express the value of M_0 as

$$M_0 = M_n = \left(\frac{f_r \times b \times h^2}{6}\right)$$

In the previous formulas:

- a = radius of circle with area equal to that of the post base plate, mm;
- b = unit width (1 mm);
- f_r = concrete modulus of rupture, MPa;
- h = slab thickness, mm;

- L = radius of relative stiffness, mm;
- M_n = negative moment strength of the slab, tension at top slab surface, N-mm;
- M_p = positive moment strength of the slab, tension at bottom slab surface, N-mm;
- P_o = ultimate load strength of the slab, N;
- $R_{e,3}$ = residual strength factor determined by JSCE SF4, %.

The term $f_r[1 + R_{e,3}/100]$ is an enhancement factor that accounts for the toughness of steel FRC slabs-on-ground.

- *Nonlinear Finite Element Computer Modeling*

Proprietary finite-element modeling techniques can be used to model nonlinear material behavior. Such designs may include linear shrinkage, curling, and applied loads and are typically iterative. Once final stresses are determined, calculate a residual strength factor $R_{e,3}$ to determine the steel fiber quantity.

- *Steel Fibers Combined with Bar Reinforcement*

Serviceability requirements often control over strength considerations in fluid-tight slabs-on-ground. Equations presented estimate the reduction in reinforcing bar stress due to the presence of steel fibers.

9.7.4 Joint Details

Three joint types commonly used are isolation joints, sawcut contraction joints, and construction joints. Isolation and construction joints for SFRC floors should be designed as discussed before.

Steel fibers may offer additional shear load transfer through fiber-enhanced aggregate interlock compared with unreinforced concrete where the joint opening width remains small enough to not impair the bond between concrete and fiber. The performance of fibers at sawn contraction joints depends on slab thickness, contraction joint spacing, joint opening width, sawcut depth, and mixture constituents, including fiber type and quantity.

As mentioned, sawcut contraction joints are usually located on column lines, and locate intermediate joints at predetermined spacings. In addition to the amount of steel fibers added to the mixture, when selecting sawcut contraction joint spacing. Sawcut contraction joint spacings for steel FRC slabs-on-ground with quantities less than 0.25% by volume (20 kg/m^3) should follow the same guidelines as those for plain concrete or slabs with minimum conventional reinforcement. Joint spacings greater than those shown in the joint's paragraph require higher quantities of steel fiber reinforcement to ensure proper crack control and shear load transfer across the sawn joints. When increased sawcut contraction joint spacings are required, consider: blended aggregate gradation optimization, water-reducing admixtures, adequate curing, a choker run base material,

and a slip membrane. For case studies, refer to Shashanni et al. (2000) and Destree (2000).

9.8 Design Example

9.8.1 Introduction

These examples show the design of a slab-on-ground containing steel FRC. This design procedure is iterative and involves assumption of a slab thickness, determination of a residual strength factor, and determination of the reasonableness of the residual strength factor. Select an appropriate fiber type and quantity rate to meet the residual strength factor.

- a = radius of circle with area equal to that of the base plate, mm;
- E = elastic modulus of concrete, MPa;
- f_c = concrete cylinder compressive strength, MPa;
- f_r = concrete modulus of rupture, MPa;
- h = slab thickness, mm;
- k = modulus of subgrade reaction, N/mm^3 ;
- L = radius of effective stiffness, mm;
- M_n = negative bending moment strength of the slab, tension at top slab surface, N-mm;
- M_p = positive bending moment strength of the slab, tension at bottom slab surface, N-mm;
- P_{ult} = ultimate load strength of the slab, $kip \times 4.448222 E+03 = N$;
- $R_{e,3}$ = residual strength factor (JSCE SF4);
- S = slab section modulus, mm^3/mm ;
- ν = Poisson's ratio for concrete (approximately 0.15);

9.8.2 Assumption and Design Criteria

- Slab thickness $h = 150$ mm;
- Concrete compressive strength (cylinder) $f_c = 27.5$ MPa;
- Concrete rupture modulus $f_r = 3.79$ MPa;
- Concrete elastic modulus $E = 25,000$ MPa;
- Poisson's ratio = 0.15;
- Modulus of subgrade reaction, $k = 0.027$ N/mm^3 ;
- Storage rack load = 67 KN;
- Base plate = 10 x 15 cm;

9.8.3 Calculations for Concentrated Load

The radius of relative stiffness is given by:

$$L = \left[\frac{E \times h^3}{12(1 - \nu^2)k} \right]^{0.25} = \left[\frac{3600000 \times 63^3}{12(1 - 0.15^2)100} \right]^{0.25} = 28.5 \text{ in.}$$

The section modulus of the slab is:

$$S = 1 \text{ in.} \times \left(\frac{h^2}{6} \right) = \frac{6 \text{ in.}^3}{\text{in.}}$$

The equivalent contact radius of the concentrated load is the radius of a circle with area equal to the base plate.

$$a = (\text{base plate area}/3.14)^{0.5} = (24/3.14)^{0.5} = 2.8 \text{ in.}$$

A concentrated load applied a considerable distance away from slab edges should not exceed the ultimate load strength of the slab:

$$P_{\text{ult}} = 6 \left(1 + \left(\frac{2a}{L} \right) \right) \times (M_p + M_n)$$

Where:

- $M_p = f_r \times R_{e,3}/100 \times S$;
- $M_n = f_r \times S$

Combining M_p and M_n :

$$M_p + M_n = f_r \times S \times (1 + R_{e,3}/100)$$

Select a factor of safety of 1.5 for this example:

$$M_p + M_n = f_r \times S \times (1 + R_{e,3}/100)/1.5$$

Solving:

$$15 = 6 (1 + 2 \times 2.8/28.5) \times (M_p + M_n)/1.5$$

The minimum required bending moment strength of the slab for the applied load is:

$$3.13 \text{ in.-k/in.} = M_p + M_n$$

The stresses due to shrinkage and curling can be substantial.

For the purpose of this example, select 200 psi. This translates into an additional moment of 1.2 in.-k/in. (6.0 in.³/in. × 200 psi) to account for shrinkage and curling stresses. This stress varies depending on the factor of safety and other issues, including mixture proportion, joint spacing, and drying environment.

$$3.13 \text{ in.-k/in.} + 1.2 \text{ in.-k/in.} = f_r \times S \times (1 + R_{e,3}/100)$$

- $R_{e,3} \geq [(4.33 \times 1000/550/6.0) - 1.0]100$;

- $R_{e,3} \geq 31$;

Residual load factors for various fiber types and quantities are available from steel fiber manufacturers' literature. Use laboratory testing for quality control to verify residual strength factors on a project basis. The quantity of steel fibers to provide the residual strength factor shown in this example ranges from 20 to 30 kg/m³, depending on the properties (length, aspect ratio, tensile strength, and anchorage) of the fiber.

9.8.4 Calculations for Post Load

Assuming 20% of the load is transferred across the joint (Meyerhof 1962), the load for a concentrated load applied adjacent to a sawcut contraction joint should not exceed

$$0.80 \times P_{ult} = 3.5(1 + (3a/L)) \times (M_p + M_n)/1.5$$

Solving:

$$0.80 \times 15 = 3.5(1 + 3 \times 2.8/28.5) \times (M_p + M_n)/1.5$$

The minimum required bending moment strength of the slab for the applied load is:

$$3.97 \text{ in.-k/in.} = M_p + M_n.$$

As in the previous example, use an additional moment of 1.2 in.-k/in. to account for shrinkage. No curling stress exists at the edge.

$$3.97 \text{ in.-k/in.} + 1.2 \text{ in.-k/in.} = f_r \times S \times (1 + R_{e,3}/100)$$

- $R_{e,3} \geq [(5.17 \times 1000/550/6.0) - 1.0] \times 100$;
- $R_{e,3} \geq 57$

The quantity of steel fibers to provide the residual strength factor shown in this example ranges from 25 to 35 kg/m³, depending on the mixture proportion and all mixture constituents, including fiber type and quantity.

10. Final Considerations

The present study was conducted in order to analyze the different behavior of a new type of concrete that contains a certain amount of fibers.

Many types of test were done to evaluate different parameters like CMOD/CTOD variations, Mid-Span Deflection, but also shrinkage, creep and tensile strength.

These studies were done in about 100 days, but the samples will be analyzed until 2013.

This, in accordance with the title of the research, is going to check the long term deformations in a better mode.

From the results, the main topics that were evaluated are:

- Steel and Macro-synthetic fibers increase the traction resistance of the concrete in both prism and beam samples;
- The cyclic loading resistance is higher than the resistance of common concrete;
- The amount of fibers is a very important parameter: the higher the quantity of fibers, the better the properties of the concrete;
- Shrinkage doesn't directly depend on the presence of fibers, whereas the creep coefficient does, but these results should be change during time;
- Regarding the uniaxial tensile test, it is necessary to use another frame with velocity control in order to avoid the elastic response.

Thus, the knowledge of the behavior of this type of concrete after more days can increase very much the use of this structural material, because the unique disadvantage of it it's the higher cost than the common concrete.

At the end, I will hope that some other researchers will study the influence of the fibers in other environmental condition, with other devices and how the fibers work with the concrete because, in my case, it's was a really interesting and innovative experience.

11. Reference

- S. Collepari, L. Coppola, R. Troli, *Pavimentazioni industriali in calcestruzzo*, ed. Tintoretto, 2006.
- R. Aicardi, *Progettazione, costruzione e calcolo delle pavimentazioni industriali*, ed. Se Sistemi Editoriali, 2006.
- L. Di Domenico, *Comportamento del calcestruzzo fibrorinforzato alle medie temperature*, 2011.
- ACI 360-92, *Design of slab on grade*, 1997.
- ACI 504R-90, *Guide to sealing joint in concrete construction*, 1997.
- ACI 544.4R-88, *Design consideration for steel fiber reinforced concrete*, 1999.
- ACI 224.3R-95, *Joints in concrete construction*, 2001.
- ACI 302.1R-04, *Guide for concrete floor and slab construction*, 2004.
- ACI 360R-10, *Guide to design of slab-on-ground*, 2010.
- ACI 318
- CNR 204, *Istruzioni per la progettazione, l'esecuzione ed il controllo di strutture di calcestruzzo fibrorinforzato*, 2006.
- NTC 2008, *Norme tecniche per le costruzioni*, 2008.
- UNI EN 206-1, *Calcestruzzo, specificazione, prestazione, produzione e conformità*, 2001.
- UNI EN 11104, *Istruzioni complementari per l'applicazione della EN 206-1*, 2004.
- UNI 11037, *Fibre d'acciaio da impiegare nel confezionamento di conglomerato cementizio rinforzato*.
- UNI 11039-1, *Calcestruzzo rinforzato con fibre d'acciaio. Definizioni, classificazione e designazione*.
- UNI 11039-2, *Calcestruzzo rinforzato con fibre d'acciaio. Metodi di prova per la determinazione della resistenza di prima fessurazione e degli indici di duttilità*.
- UNI 11146, *Pavimenti di calcestruzzo a uso industriale. Criteri per la progettazione esecuzione e collaudo*, 2005.
- UNI EN 13670, *Posa e Maturazione dei getti*.
- UNI EN 14615, *Metodi di prova per calcestruzzi rinforzati con fibre metalliche*.
- UNI U73041440, *Progettazione, esecuzione e controllo degli elementi strutturali in calcestruzzo rinforzato con fibre d'acciaio*, 2004.